CHARACTERISATION AND EFFICACY TESTING OF MULTIFUNCTIONAL COTTON FABRICS BASED ON NANOPARTICLES GREEN-SYNTHESIZED WITH *SOLANUM TUBEROSUM* POTATO PEELS

BY
NONSIKELELO SHERON MPOFU

A Thesis Submitted to the Department of Manufacturing, Industrial and Textile Engineering, School of Engineering in Partial Fulfilment of the Requirements for the Award of the Doctor of Philosophy in Materials and Textiles Engineering

Moi University

2023

DECLARATION

Declaration by Student

This thesis is my original work and has not been presented for a degree in any other university. No part of this thesis may be reproduced without prior written permission of the author and/or Moi University.

Signature:_____ Date:_____

Nonsikelelo Sheron Mpofu

ENG/DPHIL/MT/3973/20

DECLARATION BY SUPERVISORS:

We declare that this thesis has been submitted for examination with our approval as university supervisors.

Signature:_____ Date:_____

Prof. Josphat Igadwa Mwasiagi

Moi University, Eldoret, Kenya

Signature:_____ Date:_____

Dr. Cleophas Achisa Mecha

Moi University, Eldoret, Kenya

Signature:_____ Date:_____

Dr. Eric Oyondi Nganyi

Moi University, Eldoret, Kenya

DEDICATION

This thesis is dedicated to my wonderful family. I appreciate your support in helping me achieve my goals. I would not have progressed this far without your love, encouragement and sacrifices.

ACKNOWLEDGEMENTS

My heartfelt gratitude goes to the Lord God almighty for the guidance through my PhD journey and for granting me sufficient grace and wisdom to complete this work. To Him be the glory.

I would like to thank the Africa Centre of Excellence in Phytochemicals, Textiles and Renewable Energy (ACEII-PTRE) for the scholarship which enabled me to study towards this PhD. A special thank you goes the coordinators, administrators and all staff in the ACEII-PTRE office for the support and for ensuring smooth operation of this scholarship. I would also like to extend my gratitude to the African German Network of Excellence (AGNES) through the "Programme Advocating Women in Science, Technology, Engineering and Mathematics", for the grant awarded for my PhD research in Busitema University.

I would like to express my deepest gratitude and appreciation to my supervisors Prof. Josphat Igadwa Mwasiagi, Dr. Cleophas Achisa Mecha and Dr. Eric Oyondi Nganyi. Their expertise, insights, and unwavering encouragement have been instrumental in shaping this research project and ultimately, its successful completion. I am indebted to them for the countless hours they spent reviewing my work, providing constructive feedback, and pushing me to expand the boundaries of my research. I am also grateful for the mentorship and support received from Prof. Martin Onani of The University of the Western Cape and for his guidance and advice throughout this research.

I would like to extend my gratitude to my lecturers in the Department of Manufacturing, Industrial and Textile Engineering (MIT) at Moi University for their valuable inputs and insightful suggestions. I am also thankful to the technicians in the MIT, Chemistry and Biology laboratories of Moi University for their practical assistance during my

experiments. I am also grateful for the technical assistance received from staff in laboratories in Busitema University and University of the Western Cape.

Last but not least, I would like to express my sincere appreciation to my fellow students, family and friends who have inspired me throughout this journey. Their continuous support has been invaluable, and I am truly grateful for having them in my life. I appreciate the friendship, motivation and encouragement.

ABSTRACT

The demand for antimicrobial cotton fabrics in hospitals is increasing due to exposure to microbes and susceptibility of cotton to microbial attack. Silver nanoparticles (AgNPs) offer antimicrobial properties, but their production is expensive and chemical intensive; necessitating environmentally friendly sustainable nanoparticle synthesis techniques. Therefore, the main objective of this research was to investigate the use of potato peel extracts in the synthesis of silver nanoparticles for the production of antibacterial finishes for textile fabrics. The specific objectives were: to characterise the phytochemical constituents and antibacterial properties of potato peel extracts, to investigate the green synthesis of silver nanoparticles using potato peel extracts and the characteristics of the nanoparticles, to evaluate the synergy of silver nanoparticles and potato peel extracts applied on cotton fabrics against bacteria and to characterise the physical and chemical properties of the treated fabrics. Potato peel extracts were characterized using classical phytochemical screening, Fourier Transform Infrared (FTIR) Spectroscopy and antibacterial agar well diffusion assay against staphylococcus aureus (S.aureus) and escherichia coli (E.coli). AgNPs were synthesized using the reduction method and characterised using the scanning electron microscope, X-Ray diffractometer, FTIR, zeta-sizer, UV-Visible spectroscopy (UV-vis) and the agar well diffusion assay. In-situ synthesis of AgNPs onto cotton fabrics was optimised using a Central Composite Design with synthesis time, incubation time and curing temperature as variables. The responses were bacterial reduction(%) of the AgNP-treated fabrics and loss in antibacterial activity(%) after washing. Developed models were statistically analysed using two-way ANOVA. In-situ synthesis was then performed using the optimised parameters. The treated fabrics were assessed for their antibacterial properties against S. aureus and E.coli using ISO-20743:2021, their morphology, tensile strength, elongation and air permeability. The results showed that potato peel extracts contain several phytochemicals including phenols and flavonoids; this was also observed in the FTIR spectra. The extracts displayed good antibacterial efficacy against S. aureus and E.coli. AgNP synthesis was confirmed by the formation of a golden-brown solution and a UV-vis peak at 418 nm. The nanoparticles were spherical in shape, crystalline in nature, moderately stable, with an average size of 50.18 nm and antibacterial efficacy against both E.coli and S.aureus. Regression models for the in-situ synthesis were significant with p-values less than 0.005 and R^2 values of 90.28% and 87.99% for E.coli and S. aureus respectively. The optimum values were found to be: 42.18 hours incubation time, 3 hours synthesis time and 180 ℃ curing temperature. AgNP-treated fabrics demonstrated a 99.52 % and 99.01 % bacterial reduction after 20 washes for E.coli and S. aureus respectively. The AgNP-treated fabrics had a rougher surface, less air permeability, higher tensile strength and less percentage elongation than the untreated fabrics. In conclusion, potato peel extracts contain the necessary phytochemicals and can be utilized in the green synthesis of silver nanoparticles. The results of the research also showed that potato peel extracts and green synthesized silver nanoparticles can be employed as durable antibacterial finishes for cotton fabrics. The study's findings recommend using the optimised parameters for in-situ synthesis of AgNPs onto cotton fabric to achieve a higher percentage bacterial reduction and improved antibacterial finish durability.

TABLE OF CONTENTS

LIST OF TABLES

LIST OF FIGURES

ACRONYMS AND ABBREVIATIONS

Ag	Silver
$AgNO_3$	Silver nitrate
AgNPs	Silver nanoparticles
ANOVA	Analysis of Variance
DLS	Dynamic Light Scattering
E. Coli	*Escherichia Coli*
FTIR	Fourier Transform Infrared Spectroscopy
GAE	Gallic Acid Equivalent
MIC	Minimum inhibitory concentration
MRSA	*Methicillin Resistant Staphylococcus Aureus*
PDI	Poly dispersive index
PPE	Potato peel extracts
QE	Quercetin Equivalent
S. Aureus	*Staphylococcus Aureus*
SEM	Scanning Electron Microscopy
SPR	Surface Plasmon Resonance
TEM	Transmission Electron Microscopy
TFC	Total flavonoid content
TGA	Thermogravimetric Analysis
TPC	Total phenolic content
UV-Vis	UV-Visible Spectroscopy
VIF	Variance Inflation Factor
XRD	X-Ray Diffractometer

CHAPTER ONE: INTRODUCTION

1.1 Background to the Study

Consumer's attitudes towards hygiene and comfort have created an increasing market for textiles possessing more functions than those of traditional textile fabrics. Cotton, like other natural fibre-based textile materials is highly susceptible to microbial attack. This is due to its porous hydrophilic nature, which holds nutrients, oxygen and water, creating ideal conditions for bacterial growth (Boryo, 2013). According to a previous study, microbes such as *methicillin-resistant staphylococcus aureus* can contaminate the gowns or uniforms of health care workers as they administer treatment to patients. These microbes have the capacity to live on the fabric surface and then be transmitted to another person (Neely & Maley, 2000). The microbes can also continue to grow on the fabric and possibly convert human perspiration into foul smelling substances resulting in an unpleasant odour. Heavy microbe infestation can cause the fabric to rot and break down, resulting in physical changes such as loss of strength, less flexibility and ultimately reduce the performance of the fabric (Boryo, 2013). These challenges can be mitigated by the production of multifunctional fabrics.

Multifunctional fabrics have properties and applications such as antibacterial, antiviral, antifungal, water repellence, flammability, easy clean and anti-odour. Antibacterial and antifungal finishes are used in textiles to control bacteria, moulds and fungi on the textile substrate. These properties have been very useful in the health sector particularly in the production of hospital products such as linen, towels, gowns, scrubs, and masks. Socks with antimicrobial finishes have also been created for use by diabetes patients and also for the treatment of ulcers. These finishes may contact the skin of an individual and also affect their surroundings. As a result, it is critical to ensure that the finishes are environmentally friendly and have no detrimental effects on human health.

Inorganic finishing agents such as metal oxides, gold, silver, copper, titanium, zinc and magnesium have been used for durable antimicrobial and antifungal finishes on natural, regenerated and synthetic textile materials (Afraz et al., 2019). They have been used in nanoparticle form due to their durability to textile fabrics, their higher antimicrobial properties and their lower environmental risks. Nanoparticles are defined as materials with all dimensions in the nanometre range (less than 100 nm). Silver, zinc, titanium and silicon are the most commonly utilised nanoparticles in textiles. Silver nanoparticles (AgNPs) and iron nanoparticles have displayed antiviral properties against viruses like H1N1 influenza, HIV-1 and African swine fever (Dung et al., 2019; Lara et al., 2010; Mori et al., 2013) and could potentially be used to incorporate antiviral properties in textiles. These finishes have exhibited good durability for protein, cellulose, regenerated and synthetic materials.

Silver is the most commonly used inorganic antimicrobial finish because of its high thermal and electrical conductivity, lower contact resistance and also because it occurs in several oxidation states. Silver kills microorganisms by blocking and disengaging the intracellular proteins (Afraz et al., 2019). Silver nanoparticle has been shown to exhibit antibacterial properties against *Escherichia coli* when applied on cotton and viscose fabrics; the treated fabrics showed good results even after washing (Mirjalili et al., 2013). The application of silver nanoparticles and cotton fabric with protein capping has resulted in fabrics displaying antimicrobial activities against *Candida albicans, candida parapsilosis* and *xanthomonas axonopodis* (Ballottin et al., 2017).

The efficacy of silver nanoparticles against *staphylococcus aureus (S. aureus)* and *escherichia coli (E. coli)* has been reported by other researchers who applied silver nanoparticles onto cotton fabrics (Y. N. Gao et al., 2021). The antibacterial efficacy of chitosan-silver nanoparticles against *S. aureus* and *E. coli* was observed when applied

as a coating onto linen fabric. The silver nanoparticle/chitosan composites were also shown to have antiviral activity against influenza A virus. The antiviral activity of the composites increased as the amount of silver nanoparticles increased. Chitosan alone did not exhibit antiviral activity suggesting that silver nanoparticles are essential for the antiviral activity (Mori et al., 2013). Another study also showed the capability of silver nanoparticles to inhibit non-envelop viruses at low concentrations, particularly poliovirus (Huy et al., 2017).

Numerous studies have agreed that silver nanoparticles possess antimicrobial and antiviral properties. However, environmental concerns have been raised on the use of metal particles for multifunctional finishes as they tend to be toxic to human organs including the brain, the lungs, the liver and the reproductive organs (Ahamed et al., 2010). They may also be detrimental to the environment during and after use (Uddin, 2014). The issue of toxicity of metal oxide nanoparticles has been the subject of much systematic investigation with many studies highlighting the challenge of the silver particles being released into the washing or rinsing effluent and subsequently into waste water disposal sites (Lorenz et al., 2012; Reed et al., 2016).

These silver particles can inhibit the nitrification of waste water and hence reduce the effectiveness of water treatment (Tan et al., 2014). Another challenge is that if they make their way to the aquatic systems they result in oxidative stresses in marine organisms from the dissolution of the metal ions thus leading to chronic health impacts (Baker et al., 2013). It has also been observed that silver nanoparticles can be transferred to the skin through sweat and this can be harmful to the user especially when in close contact to the skin. There is a chance of the nanoparticles being absorbed into the body through skin pores and any other openings (Kulthong et al., 2010). It is

therefore important to curb the toxicity challenges associated with the use of these metal oxide nanoparticles.

Recent trends have seen the production of greener AgNPs by eco-friendly chemical reduction of silver nitrate ($AgNO_3$) using chemical and biological routes such as biodegradable polymers, sugars, plant extracts and food waste (N. A. Ibrahim, 2015). The synthesis of nanoparticles using plants is enhanced by the presence of different functional groups in plants such as phenols, ketones, amines, hydroxyl groups, carbonyl groups and flavonoids that enable the synthesis by reduction. Several parts of plants can be explored in the synthesis of nanoparticles such as the stem bark, seeds, leaves, fruits, flowers and roots. Although plant extracts have numerous merits such as being environmentally green, cost effectiveness, good synthesis rate and improved stability of the nanoparticles; careful consideration should be taken in the use of plant extracts as it could lead to further degradation of the environment through deforestation (Mathew, 2020). Studies have explored the use of food and agro-industrial waste as multifunctional finishing agents as well as reducing agents in the production of nanoparticles. The presence of carboxyl, amine and hydroxyl groups in banana peels has enabled the reduction of silver nitrate in the production of silver nanoparticles (Bankar et al., 2010). Extracts from garlic cloves have also been used in the synthesis of silver nanoparticles due to the bioactive compounds found in the plant (Ahamed et al., 2011). Lemon peel extracts, potato peel extracts and tea extracts have also been studied and have shown that the nanoparticles synthesized using green methods are more stable and can replace the toxic nanoparticles (Almadiy & Nenaah, 2018; Bhuvaneswari, Subashini, & Subramaniyam, 2017; Ibrahim, 2015; Sun et al., 2014; Wolela, 2020). Green synthesized silver nanoparticles have been used not only to impart antibacterial properties but also for colouration of the textile substrate.

Colouration of polyester fabric was achieved with green synthesized silver nanoparticles using chitosan as a natural eco-friendly reducing agent. Improved colouration and fastness properties were observed due to the surface plasmon resonance of the nanoparticles. Antibacterial properties of fabric were found to be excellent as more than 80 % bacterial reduction was noticed even after 10 washing cycles (Hasan et al., 2019).

Potatoes (*Solanum tuberosum*) are the second most consumed starch in Kenya and are widely used globally resulting in considerable amounts of peels that end up in waste. In 2019, approximately 376,626,967 metric tonnes of potatoes were produced globally (Pieter, 2020). In Kenya, potatoes are supplied from the farmers to the consumers in several ways; through county markets, supermarkets, restaurants and for processing into products such as crisps, flakes and other snacks. One of the most commonly grown potato varieties in Kenya is the *Shangi* potato due to its high yield, strong market demand and early maturity. Other advantages of the *Shangi* potato are the fast-cooking time and the versatile uses (Sophie, 2018), making it popular for processing into crisps and chips as well for domestic use. The percentage of potatoes sold to the different sectors is shown in Table 1:1.

Table 1:1. Estimated Proportion of Potatoes Sold to Different Sectors in Kenya

Sector	**Estimated Percentage Sold**
Open County Markets	80%
Supermarkets	1%
Institutions/ Restaurants	10%
Processing (Crisps, Flakes, Snacks, Potato Flour etc.)	9%

Source: (Kaguongo et al., 2014)

In urban centres the major consumption of potatoes is in restaurants that serve the potatoes as chips, chips *bhajia* (spiced potato slices) and as mashed potatoes (Kaguongo et al., 2014). These processed potatoes all require the need for peeling either by hand

or machine before cooking. The creation of waste from potato peels is therefore inevitable. The use of potatoes generates approximately 70000 to 140000 tonnes of potato peels globally every year. These potato peels generate waste which is among the highest contributors to the global waste streams (see Table 1:2); in the year 2018 they contributed 70 % to the total waste streams together with other by-products such as slivers and grey starch.

Table 1:2. Breakdown of Waste Streams in 2018

Type of Waste Stream	**Percentage contribution to waste**
By-products : slivers, **potato peels**, grey starch	70 %
Clean (tare) soil	12 %
Struvite : natural fertilizer	0.8 %
Organic : composted externally	4 %
Organic : fermented on-site	7 %
Used cooking oil	0.4 %
Native potato starch	3 %
Water treatment sludge	2.6 %
Metals	0.0 %
Mixed company waste	0.1 %
Plastics	0.1 %
Paper	0.3 %

Source: (Hintzen et al., 2018)

To reduce the possible problems associated with the disposal of potato peels, they could be converted into useful products. Results from several studies have shown that potato peel extracts have bioactive compounds that exhibit antimicrobial, antiviral, antioxidant and antifungal properties (Friedman et al., 2018; Salawu et al., 2015; Silva-Beltrán et al., 2017). These properties have been utilized and found to be very useful in industries such as the pharmaceutical industry and the food industry. Studies on edible biofilm from potato peel extract showed that the extract has high antibacterial activity against both gram negative and gram positive bacteria (Gebrechristos et al., 2020). They have also been used for the production of biogas, lactic acid, enzymes, biochar, bio-oil and bio fertilizer (Daimary et al., 2022). However, there is still very little utilisation of the

bioactive compounds in potato peels for their value addition and for use as antibacterial agents. These extracts can therefore be explored in the textile industry by applying them directly onto textiles or by using them for the synthesis of nanoparticles that can be incorporated into textile fabrics. Although the use of potato peels in the synthesis of nanoparticles and in the textile industry is likely to contribute a small percentage in the reduction of potato peel waste; it will be useful in the value addition of the waste and will provide background information for further utilization of the waste. The application of potato peel extracts on the fabrics will result in the production of environmentally friendly multifunctional textiles. Furthermore, the application of green-synthesized silver nanoparticles onto the fabric will encourage the use of environmentally friendly techniques in the production of silver nanoparticles for multifunctional textiles. The use of the green nanoparticles reduces the use of chemicals in nanoparticle synthesis while promoting the value addition of agro -waste.

1.2 Statement of the Problem

The increasing demand for multifunctional textiles with enhanced properties such as antibacterial activity and durability has led to a growing interest in incorporating silver nanoparticle finishes onto fabrics. However; current silver nanoparticle finishes for textile substrates are synthesized using chemicals which are poisonous and can degrade in the environment. Furthermore, chemically synthesized nanoparticles require the use of additional capping agents to improve the stability of the nanoparticles, resulting in the use of even more chemicals. By exploring the green synthesis approach using potato peels and comprehensively evaluating the multifunctional cotton fabrics, this research seeks to reduce the use of toxic chemicals in the synthesis of silver nanoparticles.

1.3 Justification of the Study

The study addresses the important issues of environmentally friendly production of antibacterial finishes for textile substrates. Green synthesis of nanoparticles reduces the use of chemicals through the use of plant extracts (Shafey, 2020). *Solanum Tuberosum* potato peels are biodegradable and are therefore not harmful to the environment. Their use in the synthesis of nanoparticles will result in the production of greener and more stable nanoparticles for textile finishes due to the presence of bioactive compounds in the peels (Bhuvaneswari et al., 2017; Rodríguez-Martínez et al., 2021). The combination of the functional properties of silver and extracts of potato peels will result in nanoparticles with higher efficacy against bacteria, fungi and viruses. Also, the use of potato peels will create additional alternatives for the valorisation of waste and address challenges of waste disposal.

1.4 Objectives of the Study

The main objective of the study was to investigate the use of plant extracts (potato peels) in the green synthesis of silver nanoparticles for the production of antibacterial finishes for textile fabrics. The specific objectives were:

1. To characterise the phytochemical constituents and antibacterial properties of potato peel extracts.
2. To investigate the green synthesis of silver nanoparticles using potato peel extracts and the characteristics of the nanoparticles.
3. To evaluate the efficacy and synergy of silver nanoparticles and potato peel extracts applied on cotton fabrics against bacteria.
4. To characterise the physical and chemical properties of cotton fabrics treated with silver nanoparticles.

1.5 Significance of the Study

There are many challenges in multifunctional textiles related to toxicity of the fabric as well as the effects of the washing effluent on the environment. The use of greener nanoparticles will reduce the amount of toxic waste in the environment. Potato peels are easily accessible, require a simpler synthesis process and possess numerous functional groups that can be utilized in several fields. This study of the potato peels will not only lead to a wider variety of greener nanoparticles for textile finishes but will also create knowledge for future research. It will also result in value addition of potato peels and utilization of the functional properties that they possess.

1.6 Scope of the Study

This study focuses on the synthesis of silver nanoparticles from potato peel extracts as well as the application of the extracts and nanoparticles onto cotton fabric for the incorporation of antibacterial properties. The potato peels used were from the *Shangi* potatoes and these potatoes were collected from a local farm in Tulwop village, Uasin Gishu County Kenya. Another set of potatoes was purchased from the market in Eldoret town. The potatoes were peeled using the mechanical peeling method, which is the most used peeling method; it also preserves the Potato peels were extracted using two different solvents: ethanol through solvent extraction and distilled water through ultrasound-assisted extraction. The fabric used was 100 % plain woven bleached, mercerized and scoured cotton fabric and was purchased from Rivatex East Africa Limited. These parameters were selected because these fabrics have been shown to increase fixation and durability of nanoparticles on fabrics. The fabric had the following characteristics: 72 ends/inch, 34 picks/inch, 28 tex warp count, 128 g/m^2 and a thickness of 0.002 mm. Antibacterial tests were performed against gram - negative *Escherichia Coli* and gram - positive *Staphylococcus Aureus* because these strains of bacteria are

the most common causes of various infections. Green synthesis of the nanoparticles was done through the reduction method using potato peel extracts to reduce silver nitrate to silver nanoparticles. The following properties of the treated fabrics were assessed to determine their properties after treatment as well as their suitability for their intended end-use: morphology using the scanning electron microscope, chemical bonding using the FTIR, thermal analysis using the TGA analyser, air permeability using the air permeability tester and tensile strength using the universal tensile tester. Optimization and characterisation were done using multiple regression analysis using Design expert and Minitab statistical software.

1.7 Thesis Outline

The thesis contains five chapters organised as follows:

Chapter 1 provides a background of the study area, the problem statement as well as the justification for doing the research. The chapter also gives the objectives and significance of the study.

Chapter 2 gives a survey of reviewed literature on potato peels and their bioactive components as well as their antibacterial properties. It outlines the use of plant extracts and agro-waste in the green synthesis of silver nanoparticles, the effect of process parameters as well as the characterisation techniques for these nanoparticles. It provides information on the different antibacterial assays used to investigate the efficacy of nanoparticles and plant extracts against different strains of bacteria. Methods of application of plant extracts and nanoparticles onto fabric are presented and a comparison is made to determine the most suitable method. The chapter also gives literature on the different characterisation tests for treated fabrics and their suitability for different end-uses of the treated fabrics. Finally, a summary of the research gaps is provided.

Chapter 3 gives the different methods used to achieve the objectives of the study. It provides the methods used for the extraction, phytochemical screening, functional group analysis and antibacterial testing of the potato peel extracts. A description of the method used in the green synthesis of silver nanoparticles using potato peel extracts is given as well as the characterisation techniques for the nanoparticles. The chapter also describes the methods for application of potato peel extracts and nanoparticles onto cotton fabric, their antibacterial properties and the characteristics of the treated fabric. It also gives details of the optimisation parameters for the in-situ synthesis of the silver nanoparticles onto cotton fabric.

Chapter 4 presents the discussion of results. It gives the phytochemical constituents, antibacterial properties and characteristics of the potato peel extracts. The effect of process parameters in the green synthesis of nanoparticles is given as well as their characteristics and antibacterial properties. Results for the antibacterial efficacy of fabrics treated with potato peels and silver nanoparticles are also given. It also gives the effect of process parameters on the antibacterial properties of fabrics treated with silver nanoparticles using in-situ synthesis. The properties of the treated fabrics in comparison with untreated fabrics are also given.

Chapter 5 provides the conclusions of the study; that is the main findings as well as the limitations of the study. It also provides recommendations based on the study and also recommendations for further study.

CHAPTER TWO: LITERATURE REVIEW

2.1 Overview

This chapter presents an extensive review of the existing body of literature pertinent to this research and is organized into four distinct sections aligning with the specific objectives of the study. The objective of this comprehensive literature review is to establish a strong foundation for the research by not only understanding the relevant background but also identifying the gaps in knowledge that form the rationale for this study. The first section of this chapter undertakes an in-depth exploration of the composition of potato peels and their antibacterial potential. Through an extensive review of scientific literature, the section aims to elucidate the chemical composition of potato peels, focusing on the compounds responsible for their antimicrobial properties. This section also discusses the mechanisms by which these compounds exert their antibacterial effects, shedding light on their potential applications in various contexts. The second section gives an overview of the green synthesis of nanoparticles. This entails a detailed examination of the methods employed in the environmentally friendly production of nanoparticles, with particular attention to the factors that influence the synthesis process. Additionally, the section delves into the characterisation techniques employed for assessing the properties and qualities of green synthesized nanoparticles. The section also explores the antibacterial properties of nanoparticles, discerning their mechanisms of action and relevance to the study.

The third section discusses the impartation of antibacterial properties onto textile fabrics and assessment of antibacterial properties of the treated fabrics; a vital component of this study. The various antibacterial agents used to treat fabrics are investigated, analysing their mechanism and efficacy in inhibiting antibacterial growth. Furthermore, the section delves into the durability of the antibacterial treatments,

exploring their ability to withstand repeated washing and wear. In the final section of this chapter, an overview of the characterisation methods used to assess the fabrics treated with antibacterial agents is provided. The techniques play a pivotal role in this study, enabling the comprehensive evaluation of the performance and properties of the treated fabrics. The conclusion of the chapter summarises the literature review findings and identifies gaps in existing knowledge, highlighting the importance of the research in bridging these gaps. In general, the chapter provides a comprehensive understanding of the relevant background, the intricacies of green synthesized nanoparticles, the antibacterial properties of treated fabrics, and the expected outcomes of the research.

2.2 Valorisation of Potato Peel Waste

The ever-increasing consumption of potatoes and their processed products has resulted in the upsurge of potato peel production. According to data published by the United Nations' Food and Agriculture Organization (FAO), global potato output has increased in recent years with data from 2000 to 2019 predicting that the production will continue to increase in the coming years (Rodríguez-Martínez et al., 2021). The potato peel is the outermost tissue of the fruit and is usually removed or peeled before cooking or processing. It is the outer skin or covering of the potato and its colour may vary depending on the potato variety. The peel functions to safeguard the inner potato flesh, providing resilience against microbial infections and mechanical harm, while also contributing to freshness preservation(Junwei et al., 2018). The potato peel is a useful and functional material that can be utilized as a low-cost raw material because of its availability as agro-industrial waste. Potato peels have been identified as a valuable resource in the production of building materials. The potato peel waste provides an environmentally friendly and cost free material for the fabrication of medium-density fibre board (Miller, 2019). Potato peels contain high levels of starch which have made

them useful in the production of ethanol by acid and enzymatic hydrolysis followed by fermentation (Arapoglou et al., 2010). The production of bioplastics from potato peels has been reported by (Arikan & Bilgen, 2019). In their study they concluded that potato peel bioplastic can be produced and has higher water absorption capacity than commercial bioplastic with potential applications in the food industry.

Potato peel waste has also been used for the production of activated carbon and carbon nanotubes for use in heavy metal removal with a potential to get rid of approximately 84% of lead ions (Pb^{2+}) in just one hour of operation (Osman et al., 2019). Additionally, potato peels have been utilized as animal feed as well as manure in the agricultural sector. However, although these potato peel disposal methods have benefited some industries and have also reduced the challenges of potato peel waste, some of these methods have low added value and do not fully utilise the active compounds that are present in potato peels. Furthermore, there are large quantities of potato peels that still remain underutilized and end up being disposed of, thus resulting in environmental pollution due to decomposition (Javed et al., 2019). Hence there is need for exploring other potential uses of potato peels that get the full benefit out of their active compounds and add value to the peels.

2.2.1 Composition of Potato Peels

Potatoes are composed of several compounds which can be utilized in different ways when extracted. Potato peels and the core of potatoes differ in their composition. Potato peels exhibit significantly higher levels of protein, fibre, ash and minerals (excluding magnesium) compared to the flesh. However, the flesh contains the highest concentrations of dry matter and total soluble solids. In both the peel and flesh, potassium has the highest content followed by phosphorus, magnesium, calcium, iron, zinc, boron, manganese and copper (Vaitkevičienė, 2019). The composition of potatoes

and hence those of potato peels may differ based on their geographical location. The different planting and cultivating areas have diverse breeds, varieties and colours of potatoes resulting in variations in the compositions and morphology of the potato peels produced (Escuredo et al., 2020).

Another factor that affects the chemical and physical composition of potato peels as well as the yield of bioactive components in potato peel is the peeling procedure. The methods that have been used for peeling potatoes are the steam, lye, manual and abrasion peeling. These methods also affect the suitability of the potato peel for further exploitation (Javed et al., 2019). In wet lye peeling, the peel is softened by immersing into a hot concentrated solution of alkali for a predetermined time. The peel of the chemically treated potato peel can then be removed by washing off with water spray or by abrasive drums. The most commonly used lye solution is caustic soda due to its low cost. The main challenge of this method is that it is not environmentally friendly due to the discarding of the lye solution to the environment. Another challenge is that the peel may not be reusable after peeling due to the immersion in lye solution (Kohli et al., 2021). Steaming produces more dietary fibre and less starch than abrasion which is used in potato chip manufacturing. Steam peels have increased lignin and dietary fibre content with decreased starch. Potato peels from manual peeling produce about 63 % of fibre on a dry weight basis, which is further categorised into hemicellulose, lignin, cellulose and pectic substances (Javed et al., 2019). The abrasive and manual peeling techniques are time and labour consuming but have the advantage that the peel can be re-utilized in another value addition process. Generally, potato peels contain beneficial compounds mainly composed of carbohydrates, starch, dietary fibre and protein (See Table 2:1), that affect the subsequent properties as well as their use in several applications.

Table 2:1. Chemical Composition of Raw Potato Peel

Compound	Range (grams per 100grams)
Water	83.3 – 85.1
Protein	1.2 – 2.3
Total lipids	0.1 – 0.4
Total carbohydrate	8.7 – 12.4
Starch	7.8
Total dietary fibre	2.5
Ash	0.9 – 1.6
Total phenolic content	1.02 -2.92
Total flavonoids	0.51 – 0.96

Source: (Javed et al., 2019)

2.2.2 Bioactive Properties of Potato Peels

Potatoes have phenolic compounds that provide their antioxidant, anti-inflammatory, antifungal and antibacterial properties. Phenolic compounds are secondary plant metabolites and their main function is to defend the plant against invading pathogens such as fungi, bacteria and viruses (Friedman & Levin, 2009). Their main defence function in plants is what gives them the antimicrobial properties. The peels of potatoes have a higher phenolic content than the flesh (Joly et al., 2020; Kim et al., 2019). The phenolic compounds that are present in potato peels are flavonoids and phenolic acids. The main phenolic acids found in potato peels are chlorogenic acid, gallic acid, protocatechuic acid, caffeic acids, ferulic acids, vanillic acid and salicylic acids (Gebrechristos et al., 2020; Kim et al., 2019; Susarla, 2019; Torres & Domínguez, 2020). These compounds have been shown to have antibacterial activities against *Escherichia coli*, Salmonella typhimurium and Bacillus cereus. Caffeic acid is an antioxidant that has also shown anti-inflammatory and immunomodulatory activity while chlorogenic acid also has anti-inflammatory activity (Susarla, 2019).

Potato peels contain the following flavonoids; quercetin, naringenin, catechin and epicatechin. Quercetin possesses anti-inflammatory and antioxidant properties while catechin has properties that prevent type II diabetes, cancer and cardiovascular

complications (Susarla, 2019). Quercetin has also displayed antifungal properties against candida *parapsilosis* species complex and can be considered as an alternative for the control of fungal biofilms (Rocha et al., 2019). Research has also shown that quercetin, catechin and epicatechin have enhanced antifungal activity when used as a co-treatment with fluconazole (C. R. Da Silva et al., 2014; M. Gao et al., 2016).

Phenolic compounds have also been reported as possessing antimicrobial properties against gram-negative bacteria. In a study carried out by (Puupponen-Pimiä et al., 2001) myricetin had the highest antimicrobial activity against most bacterial strains. Other phenolic compounds that inhibited bacterial activity were quercetin, pelargonidin chloride, delphinidin chloride, cyanidin glucose, caffeic acid, ferulic acid and chlorogenic acid. (Sotillo & Hadley, 1998) reported that the extracts of potato peels inhibited the growth of *E. coli, S. typhimurium* and *B. cereus* for up to 72 hours. According to the authors, the presence of caffeic acid in the potato peels may have contributed to the antibacterial action. Potato peel extracts have demonstrated antiviral properties against human enteric viruses. In a study carried out by (Silva-Beltrán et al., 2017), the human enteric viral surrogates of MS2 and Av-05 are successfully inhibited by the potato peel extracts thus suggesting that these extracts can effectively be used against human enteric viruses. The study also indicated that potato peels have a strong antioxidant activity.

Although potato peels have been shown to contain the necessary bioactive compounds for antibacterial, antiviral, antioxidant and antifungal properties. The yield and efficacy of these compounds may differ from one potato plant to the other based on the planting conditions, soil type, geographical location, post-harvesting as well as processing conditions (Ezekiel et al., 2013; Samaniego et al., 2020). When comparing Colorado potato tubers to those grown in Texas, researchers discovered that Colorado tubers

contained higher levels of anthocyanins; hence showing that the location of the potato growing has an impact on phytochemical content. Colorado's colder temperatures and longer days were hypothesized to be the reason for these disparities (Reyes et al., 2004). A study was conducted in the Czech Republic on the total phenolic content of different potato cultivars in relation to environmental and fertilizing conditions. The geographical location with a greater altitude, the lowest average annual temperature and the highest quantity of precipitation had a higher total phenolic content (Hamouz et al., 2007). It is therefore important to consider these factors while deciding which potato peels to use for optimal phytochemical output.

2.2.3 Determining the Bioactive Compounds of Plants and Plant By-Products

Due to the differing properties of potatoes and potato peels based on their geographical location and other factors; it is important to determine the bioactive compounds of potato peels before exploiting their antimicrobial activity. There are several stages in the attaining of bioactive components of plants and plant by-products. These stages are shown in Figure 2:1 and can also be applied in acquiring the bioactive components of potato peels.

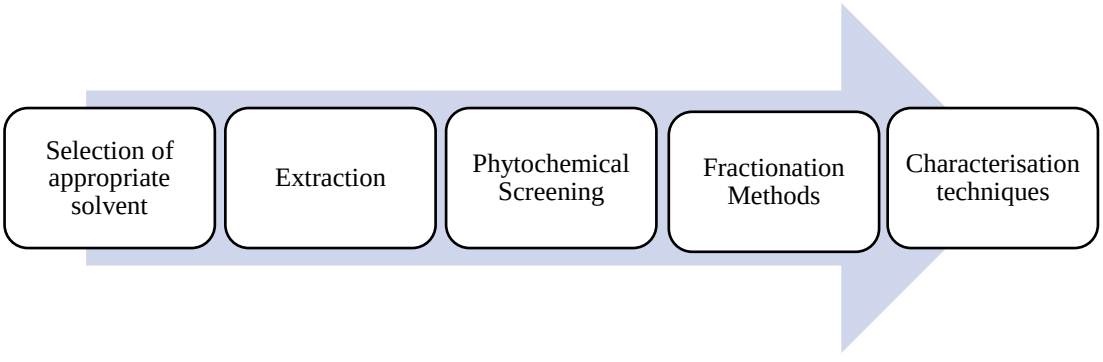

Figure 2:1. Stages Involved in Attaining Bioactive Molecules from Plants and Plant By-Products (*Source*: Author Elucidation based on Abubakar & Haque).

2.2.3.1 Selection of Appropriate Solvent

The extraction solvent is a significant parameter because it has an impact on the yield of bioactive chemicals, as well as the extraction time and other features. It is therefore vital to consider several important factors when choosing a solvent. The factors include safety, viscosity, polarity, reactivity and the boiling temperature of the solvent (Pandey et al., 2014). The chosen solvent should be non-flammable, non-toxic and should have the ability to extract the required bioactive compounds while leaving out the inert material. To allow for easy penetration, it is vital for the solvent to have a low viscosity and it should not react with the extract. Where boiling is necessary for extraction, the solvent ought to have a boiling temperature that is as low as possible so that sample degradation by heat is prevented (Abubakar & Haque, 2020).

Polar solvents such as alcohols and water, intermediate polar solvents such as dichloromethane and acetone as well as nonpolar solvents such as chloroform, n-hexane and ether; are often utilized in plant extraction (Akyol et al., 2016; Dorta et al., 2012; Fu et al., 2016). The polarity of the solvent determines the suitability of a solvent for the extraction of different compounds from a sample. The influence of different polarity of solvents on the recovery and antioxidant activity of polyphenols from sweet potato leaves was investigated. The highest total flavonoid content was found in the 70 percent ethanol extract, while the highest total phenolic content was found in the 50 percent acetone extract (Fu et al., 2016). Some commonly used solvents and their properties are shown in Table 2:2.

Water and ethanol have gained popularity as solvents because they are environmentally friendly and can be used in applications where safety is of great concern. The efficiency of the two solvents differs based on the extraction technique used as well as the compound being extracted. Although water has been frequently employed in effective

extraction, the extract contains a considerable quantity of water-soluble contaminants, which might reduce the extract's efficacy for further exploitation (Q. W. Zhang et al., 2018).

Table 2:2. Properties of Extraction Solvent

SOLVENT	PROPERTIES	ADVANTAGES	DISADVANTAGES
Alcohol	-Polar -Used for extraction of polar secondary metabolites - Miscible with water	- Does not require special preservation at concentrations above 20% -Extraction can be done at low temperatures. -Non-toxic at low concentrations.	-It is volatile and flammable. -It cannot dissolve wax, gums and fats.
Water	-Polar -Used for extracting several polar compounds.	- Cheap, non-flammable and non-toxic - Highly polar and can therefore dissolve many substances.	- May require high heat for extraction. - Promotes the growth of bacteria and moulds. - May cause hydrolysis.
Ether	-Non-polar - Mainly used for the extraction of terpenoids, fatty acids, alkaloids and coumarins.	-Very stable compound and therefore does not react with bases, acids and metals. - Miscible with water. - Low boiling point.	- Flammable - Highly volatile
Chloroform	-Non-polar -Used for extracting compounds such as flavonoids, terpenoids, oils and fats. -Sweet smelling and colourless	-Soluble in alcohols. - Well absorbed and broken down in the body.	- Carcinogenic - Sedative

Source: (Abubakar & Haque, 2020)

In the extraction of antioxidants, ethanol extracts outperformed water extracts in terms of antiradical, reducing and chelating activities (Samotyja, 2019). Ethanol extracts also showed superior properties in the extraction of phenols from potato peels attaining the

highest total phenolic content when compared with methanol extracts and petroleum extracts (Gebrechristos et al., 2020; Joly et al., 2020). Furthermore, in a study carried out by (Silva-Beltrán et al., 2017) total phenolics and flavonoids were found to be greater in the acidified ethanol extract than in the water extract. However, when different solvents were used in the extraction of bioactive compounds from potato peels, extraction using water resulted in a higher yield of the extract as well as a higher phenolic content as compared to the ethanolic extracts. Moreover, the use of water as an extract has proven to be a non-toxic and efficient option. Water is the most environmentally friendly solvent available; it dissolves a variety of bioactive substances and can be used as a solvent in various extraction techniques, whether they are traditional or modern (Mihaylova & Lante, 2019).

2.2.3.2 Commonly Used Extraction Methods

Several procedures are used for the extraction of bioactive compounds in plants and plant products. These procedures differ and can affect the properties of the resultant extract. Different factors need to be considered in the selection of the extraction technique to be used; such as the intended use, the nature of the solvent, the final volume required, the duration of the extraction process as well as stability to heat (Abubakar & Haque, 2020). Maceration, Soxhlet extraction, ultrasound-assisted extraction and microwave-assisted extractions are all examples of extraction processes.

i. Maceration

This is a method of extraction in which a powdered sample, such as leaves, root bark or any other plant material is placed in a container and the extraction solvent is poured over it until the powder is entirely covered. The container is covered and stored for 48 to 72 hours while periodically stirring or shaking it occasionally to guarantee complete extraction. Once the extraction is complete, the solution is filtered and then evaporated

(Bandar et al., 2013). This is a very convenient method particularly for thermolabile plant materials that are easily deactivated or destroyed by heat (Q. W. Zhang et al., 2018). This technique has produced extracts with superior phenolic compounds in comparison with other techniques when used for the extraction of chlorogenic acid as reported in an earlier study. In that study, maceration, heating, reflux, ultrasound, percolation and Soxhlet techniques were used for extraction of potato peels with methanol. The best technique was heating-assisted extraction, which was followed by maceration and then the ultrasound-assisted technique (Joly et al., 2020). However, despite its simplicity, this technique has the drawbacks of a long extraction time and low extraction effectiveness.

ii. Soxhlet Extraction

Soxhlet extraction, also known as hot continuous extraction, ensures thorough extraction while using the least quantity of solvent possible (Gopalasatheeskumar, 2018). In this method, a powdered sample is placed in an extraction thimble , covered with glass wool and then placed in the Soxhlet extractor for extraction with the appropriate solvent (Redfern et al., 2014). This is a continuous process that can take several hours or days for complete extraction to take place. It works on the basis of backflow and siphoning of the solvent, and extracts the required bioactive components from the liquid and solid mixture (Kumar, 2020).

This approach is beneficial when the desired compound’s solubility in a solvent is limited and the impurities are insoluble in the solvent. This technique was used in comparison with other techniques and was shown to be less effective in the extraction of chlorogenic acid from potato peels (Joly et al., 2020). The main advantage of this method of extraction is that it results in efficient extraction of the bioactive compounds,

however, the process is very lengthy as it can take several hours or days for complete extraction.

iii. Microwave-Assisted Extraction

Microwave-assisted extraction includes heating a solvent that is in contact with a sample by use of microwave energy in order to extract bioactive compounds from the sample into the solvent (I. Akhtar et al., 2019). Because of its increased extraction efficiency, shorter extraction time, less labour and high extraction selectivity, this technique is often preferred for extraction (Bandar et al., 2013).

This approach has so far been utilized by (Singh et al., 2011) in the extraction of potato peel components. In their study, microwave-assisted extraction was shown to be more efficient than the conventional solid-liquid extraction techniques in extracting phenolic compounds from potato peels. Additionally, a higher yield of phenolic compounds was extracted using less solvent and at a reduced extraction time than in earlier investigations. This approach, however, is restricted to compounds that are stable under high heating conditions of the microwave such as small-molecule phenolic acids, isoflavone and quercetin (Trusheva et al., 2007). Secondary metabolites such as anthocyanins and tannins may not be suited for microwave-assisted extraction since they are susceptible to temperature degradation (Altemimi et al., 2017; Azwanida, 2015; Doughari, 2012). In order to examine the applicability of microwave assisted extraction in recovering different biomolecules from potato by-products, more study effort focusing on the utilization of this technique is required.

iv. Ultrasound-Assisted Extraction

Ultrasound extraction involves the application of ultrasonic waves at a very high frequency higher than 20 KHz causing the solute to diffuse swiftly from the solid to the

liquid phase (Abubakar & Haque, 2020; Akyol et al., 2016). The main advantage of this technique is that it is an economical method with reduced extraction time and reduced quantities of solvent used. It also reduces energy expenditure while resulting in an increased yield of the bioactive compounds. The ultrasound-assisted extraction has been shown to preserve the secondary metabolites and extracted compounds with greater efficiency and effective functional activities (Quiroz et al., 2019). While using this technique, it is important to find the best position for the container holding the sample and solvent inside the bath since the effect of the ultrasound waves differs based on the position. This is a disadvantage because it affects consistency of the extraction (Carreira-Casais et al., 2021).

The use of methanol in the extraction of potato peel components has been described, and two alternative extraction procedures, that is, ultrasound assisted extraction and traditional solvent extraction, were utilized. The ultrasonic extraction method yielded extracts with a greater total phenolic content (Samarin et al., 2012). In the extraction of potato peels using different solvents, such as ethanol/water mixtures and glycerol/water mixtures, ultrasound assisted extraction was used. The study's findings demonstrated that high yields of polyphenolic phytochemicals were successfully recovered from the extracts. This was attributed to the fact that ultrasonic energy speeds up diffusion by increasing the permeability of solid particles to the solvent, allowing for easier polyphenol release (Paleologou et al., 2016).

The efficacy of this technique in the extraction of phenolic compounds from potato peel powder has also been assessed in a study comparing the direct ultrasound assisted extraction, indirect ultrasound extraction and conventional shaking extraction. The results showed that ultrasound approaches provided a larger yield of phenolic compounds in less time, ranging from 1 to 5 minutes compared to 60 minutes with

conventional shaking extraction (Wang et al., 2020). It has also been reported that ultrasound-assisted extraction yielded a much higher recovery rate of phenolics from potato peels in comparison to the solid-liquid extraction procedure alone (Kumari et al., 2017).

The major challenge with this technique is that a very high ultrasound energy may affect the active phytochemicals by forming free radicals (Azwanida, 2015). It is therefore important to take note of the ultrasound energy used in the extraction process. Overall, these studies suggest that the ultrasound assisted extraction technique is a reliable technique for the extraction of phenolic compounds as it saves on extraction time while increasing the yield.

2.2.3.3 Phytochemical Screening Procedures

Preliminary procedures to detect the presence of primary and secondary metabolites in an extract are known as phytochemical screenings. Phytochemical screening aids in the discovery of plant extract constituents and the ones that are more abundant than the others, as well as the search for bioactive compounds that can be employed in the development of therapeutic medications (Pant et al., 2017). Flavonoids, alkaloids, saponins, tannins, terpenes, flavones, cardiac glycosides, sterols, carbohydrate, proteins and fats were detected using the qualitative analyses shown in Table 2:3.

Table 2:3. Techniques for Phytochemical Screening of Extracts

Phytochemical	**Test Methods**	**Reagents Used**	**Observation Indicating Presence of Phytochemical**
Alkaloids	Dragendorff's Test	Solution of Potassium Bismuth Iodide	Red precipitate
	Wagner's Test	Iodine in Potassium Iodide	Brown/reddish precipitate
	Mayer's Test	Potassium Mercuric Iodide	Yellow coloured Precipitate
	Hager's Test	Saturated Picric Acid Solution	Yellow coloured Precipitate
Glycosides	Bontrager's Test	Ferric Chloride Solution and then ammonia solution	Rose-pink colour in the ammoniacal layer
	Legal's Test	Sodium Nitroprussidein in sodium hydroxide and pyridine	Pink to a blood red colour
	Keller-Kiliani Test	Ferric chloride then concentrated sulphuric acid	Brown or red layer at the interface and blue to green at the upper acetic layer
	Kedde's Reaction	3,5-dinitrobenzoic acid in methanol and sodium hydroxide	Violet colour
Saponins	Froth Test	Distilled water with shaking	Formation of one centimetre of foam.
	Foam Test	Distilled water with shaking	Foam persisting for ten minutes.
	Blood hemolysis Test	Erythrocites in saline solution	Hemolysis
Phytosterols	Salkowski's Test	Concentrated Sulphuric Acid	Golden yellow colour
	Liebermann Burchard Test	Chloroform then acetic anhydride and finally sulphuric acid	Brown ring at the junction
Phenols	Ferric Chloride Test	Ferric Chloride Solution	Bluish-black Colour
Tannins	Gelatin Test	Gelatin Solution (1%) containing sodium chloride	White precipitate
Flavonoids	Alkaline Reagent Test	Sodium hydroxide solution	Intense yellow colour that turns to colourless when a dilute acid is added.
	Lead Acetate Test	Lead acetate solution	Yellow precipitates
Proteins and Amino Acids	Xanthoproteic Test	Concentrated Nitric Acid	Yellow colour
	Ninhydrin Test	Ninhydrin Reagent	Blue colour
Quinones			
Terpenoids	Test for Terpenoids	Chloroform and then concentrated sulphuric acid.	Grey colour
Steroids	Test for Steroids	Chloroform and concentrated sulphuric acid	Red colour in the lower chloroform layer
Anthraquinones	Test for Anthraquinones	Benzene then ammonia	Pink, violet or red colour.

Source: (Alam & El-Nuby, 2019; Gul et al., 2017; Pandey et al., 2014)

Plant wastes from eight plants, including potato peels, were subjected to preliminary phytochemical screening. The researchers were able to determine the presence of many secondary metabolites such as flavonoids, tannins, alkaloids and anthraquinones, demonstrating the value of the assays (Alam & El-Nuby, 2019). Results from phytochemical screening often predict the extracts' efficacy against bacteria, fungi and viruses as well as their antioxidant properties and are an important step in the preliminary testing of these properties.

2.2.3.4 Fractionation Techniques

Various chromatographic techniques, such as thin-layer chromatography, paper chromatography, high-performance liquid chromatography and gas chromatography are used to fractionate and purify phytochemical compounds (Abubakar & Haque, 2020). The Folin-Ciocalteu method is often used to determine the total phenolic components in potato peel extracts. However, techniques such as the High-Performance Liquid Chromatography, Diode array Detector (DAD), Electrospray Ionization and Mass Spectrometer can be used to identify and quantify particular phenolic chemicals found in potato peel extracts (Al-Weshahy & Venket Rao, 2009; Benavides-guerrero et al., 2020; Martinez et al., 2020; Poulikakos et al., 2017).

Potato peel phenolic acids have been purified using microporous membrane filtration, and their content was evaluated using high-performance liquid chromatography (HPLC) and reference compounds such as chlorogenic acid, caffeic acid and neochlorogenic acid. According to the study, the main constituents detected in potato peel extracts are chlorogenic, caffeic, and neochlorogenic acids which are responsible for the antimicrobial capabilities (Gebrechristos et al., 2020). HPLC and proton nuclear magnetic resonance (^{1}H NMR) studies conducted by (Devi et al., 2018) also confirmed the presence of phenolic compounds in potato peels such as gallic acid, chlorogenic

acid and caffeic acid. A previous study also reported the use of fractionation techniques to identify and quantify phenolic components in ethanolic extracts of five potato by-products and twelve different compounds were detected in the extracts (Riciputi et al., 2018). The importance of these techniques is that they ensure the purity of the compound and also aid in isolating the specific phytochemical compounds present in the extract.

2.2.3.5 Characterisation Techniques of Plant Extracts

Several identification techniques, including mass spectroscopy, nuclear magnetic resonance spectroscopy, ultraviolet spectroscopy and infrared spectroscopy, are used to characterise the compounds produced. The approaches are primarily used to detect functional groups, numerous bonds and rings, carbon and hydrogen arrangement, and complete structural elucidation (Abubakar & Haque, 2020). The Fourier Transform Infrared Spectroscopy (FTIR) has been used to assess the functional groups present in potato peels and their potential use in subsequent studies and the main characteristics observed are due to the presence of cellulose, lignin and protein (Aschale et al., 2021; Attia et al., 2020; Liang & McDonald, 2014). X-ray diffraction analysis has also been used for characterisation of potato peel extracts and has revealed that they are more amorphous in nature and only semi-crystalline (Aschale et al., 2021; Devi et al., 2018; Osman et al., 2019). The morphological analysis of potato peels using the Scanning Electron Microscope and the Transmission Electron Microscope showed that the structure consisted of a rough surface with a long-range pore system and are useful in the modification of potato peels (Aschale et al., 2021; Devi et al., 2018; Wang et al., 2020). Thermal analysis has also been done on potato peels using the thermal gravimetric analysis (TGA) to determine the purity, composition and stability temperatures of the extract (Bouhadjra et al., 2021; Liang & McDonald, 2014; Osman

et al., 2019). These characterisation are not only useful for determining the properties of the raw potato peel extract but can also be used to show the change in the properties of the extracts after modification and treatment with other substances.

2.2.4 Antibacterial Assessment of Plant Extracts

Antibiotic – resistant bacteria are on the rise, posing a threat to global health. Due to the loss of effectiveness of traditional bacteria over time; there has been a need to develop novel antibiotics to address these issues. Plants possess bioactive compounds with extensive therapeutic potential. Flavonoids, terpenes, flavanols and alkaloids have been shown in studies to have promising antimicrobial activity when isolated or as part of extracts (Álvarez-Martínez et al., 2021). The antimicrobial activity of plant extracts can be evaluated and screened using a variety of bioassay techniques, including diffusion methods, thin-layer chromatography, dilution methods, time-kill tests, ATP bioluminescence, and the flow cytofluorometric method (Balouiri et al., 2016). The most common and fundamental antimicrobial testing methods are diffusion and dilution techniques.

The disk-diffusion testing method is one diffusion method that is used for antimicrobial susceptibility testing in many clinical microbiology laboratories. This method is used to test different bacterial pathogens by using specific culture media, incubation conditions and by measuring the inhibition zones. Several researchers have used this method for the efficacy testing of various plant extracts such as cumin, clove, pomegranate, ginger, thyme, guava, olive, sage and mulberry against gram-negative and gram-positive bacterial strains. The tested bacterial strains include *bacillus cereus, escherichia coli, staphylococcus aureus, pseudomonas aeruginosa, salmonella typhi, pasteurella multocida, salmonella enteritidis* and *mycoplasma gallisepticum* (Hemeg et al., 2020; Mohamed et al., 2020; Mostafa et al., 2018). In this method, agar plates are

inoculated with a standardized inoculum of the test microorganism, as shown in the schematic diagram in Figure 2:2.

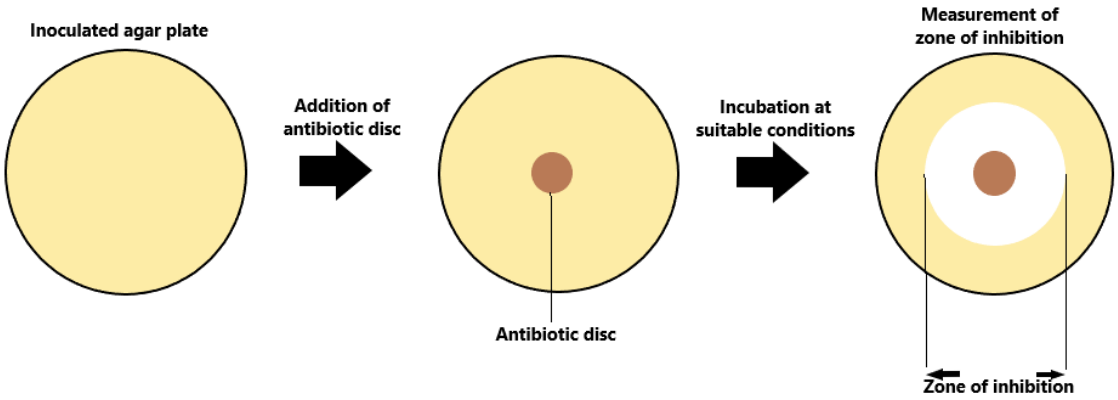

Figure 2:2. Disc Diffusion Assay for Antimicrobial Susceptibility Testing (*Source*: Author elucidation)

Filter paper discs (about 6 mm in diameter) containing the test antimicrobial compound at the desired concentration are placed on the agar surface. The petri dishes are then incubated at the suitable conditions; the antimicrobial agent diffuses into the agar and inhibits the growth of the test bacteria. The diameters of zones of inhibition that appear around the antimicrobial discs are measured.

Another diffusion technique that has been used in the antimicrobial testing of plant extracts is the agar well diffusion method (Gebrechristos et al., 2020; Gonelimali et al., 2018; Helal et al., 2020). This method uses similar culture media and incubation conditions as the disc diffusion technique. The difference between the two methods is that the agar well diffusion method involves creating a hole or a well on the solid medium and then adding the plant extract to the well, whereas the disc diffusion method involves adding the extract to a filter paper disc then placing it on the agar surface (Balouiri et al., 2016). Both methods measure the zone of inhibition around the antimicrobial agent to determine its efficacy against the test bacteria. The agar well and disc diffusion methods have various advantages, including ease of use, simple and

quick interpretation of data, and the ability to test a large number of antibiotics per test. The main disadvantages of these assays are that some antibiotics cannot be examined and that the test does not determine the minimum inhibitory concentration (Gajic et al., 2022). As a result, while establishing the efficacy of the bacterium, extra quantitative tests may be required.

A fundamental and commonly used quantitative antimicrobial susceptibility testing method is broth macro or micro dilution and has been used in the antimicrobial testing of various plant extracts (Gebrechristos et al., 2020; Helal et al., 2020; Hemeg et al., 2020). This method is used to determine the minimum inhibitory concentration of the antimicrobial agent, that is, the minimum concentration of the antimicrobial agent required to completely inhibit the growth of bacteria. The technique involves the preparation of two-fold dilutions of antimicrobial agent in 96 well plates, inoculating the wells with microbial inoculum, and incubating them under suitable conditions depending on the test microorganism (Balouiri et al., 2016; Qidwai et al., 2018).

The antimicrobial activity of potato peels has been assessed against gram-negative *E. coli, salmonella typhumurium* and *salmonella enterica* as well as gram-positive *bacillus subtilis* and *staphylococcus aureus*. A study on the antimicrobial properties of potato peel extracts using the agar well diffusion showed a distinct zone of inhibition against all tested bacteria except *klebsiella pneumonia* and *listeria monocytogenes*. The MIC was found to be 7.5 ± 2, 5.8 ± 2, 4.7 ± 1 mg/ml for *E. coli, S. enterica* and *S. aureus* respectively (Gebrechristos et al., 2020). In another earlier study the zone of inhibition was found to be suitable with a range of 2.5 mm to 7 mm for the different bacterial strains and was higher than that of ampicillin (positive control) which had a zone of inhibition in the range of 2.2 mm to 5 mm for the different bacteria (Helal et al., 2020). The disc diffusion assay has also been used together with the MIC to determine the

antibacterial effects of potato peels extracts and the results are in agreement with other studies and show that the peels have antibacterial properties against several bacterial strains but have no effect against *klebsiella pneumonia* (Amanpour et al., 2015). These studies confirm the antimicrobial activity of potato peels; however, tests need to be done on different potato varieties because the presence of the bioactive compounds responsible for the antimicrobial activity is dependent on the variety and geographical location of the potatoes.

2.3 Synthesis of Nanoparticles

Nanoparticles are synthesised using different approaches, namely, top-down, bottom-up and self-assembly methods. The bottom-up method involves the generation of nanoparticles by the arrangement of the molecular components into more complex assemblies' molecule by molecule, cluster by cluster from the bottom. In the top-down method, the size of the bulk participate materials is diminished into smaller and smaller particles. The self-assembly method is one that allows structures to organise themselves into configuration of the lowest-energy using local forces (Daraio & Jin, 2011). In the green synthesis of nanoparticles, they are formed from the oxidation/reduction process of the metallic ions by biomolecules. This is a bottom-up nanoparticle synthesis approach (Prabhu & Poulose, 2012).

Additionally, nanoparticle synthesis can be classified using a variety of methods, including chemical, physical and green synthesis. These different techniques can further be categorised based on the physical, chemical and biological components employed in the process. Physical methods include the vapour condensation method, the laser ablation method and the arc discharge method. Chemical methods include the microemulsion method, the chemical reduction method, the tollens' method and the polyol process (Harish et al., 2022). The physical and chemical methods that have been

used in the synthesis of metal and metal oxide nanoparticles have some drawbacks in that they are costly and hazardous due to the use of toxic ingredients, high production costs and the generation of hazardous by-products (Bhardwaj et al., 2020). Greener methods have therefore been considered as they are safe, inexpensive and environmentally friendly.

2.3.1 Green Synthesis of Nanoparticles

Green approaches have been shown to be beneficial for the production of nanoparticles, with the benefits of lower failure rates, lower costs and easier characterisation. Different techniques are used in the green synthesis of nanoparticles such as chemical reduction, electro-chemical methods, green synthesis from enzymes, green synthesis from vitamins, microwave-assisted synthesis and utilization of environmentally friendly solvents . Other techniques include bio-based methods such as bacteria and actinomycetes, yeasts and fungi, algae as well as plants and phytochemicals (Gour & Jain, 2019; N. A. Ibrahim, 2015).

In the green synthesis of nanoparticles plants are gaining more attention than other agents. The phytochemicals in plants such as phenols, and flavonoids act as reducing as well as stabilizing agents in the synthesis procedure (Mathew, 2020). The plants can be washed, dried and then powdered prior to use. Plants with known medicinal properties have been used in order to incorporate the properties onto the textile fabrics and have exhibited superior antibacterial properties with potential for use in medical textiles (B. S. Kumar, 2016). Food wastes have also been used such as banana peels (H. M. M. Ibrahim, 2015), potato peels (Bhuvaneswari et al., 2017) and orange peels (Skiba & Vorobyova, 2019) and have been effective in the production of nanoparticles.

2.3.2 Factors Affecting the Green Synthesis of Nanoparticles

In the synthesis of nanoparticles using green methods challenges were still observed in the stability, size, shape and subsequently the performance of the nanoparticles. This was attributed to the different factors affecting the synthesis of the nanoparticles. Earlier researchers found that synthesis of nanoparticles with varying operating parameters such as silver metal salt concentration, incubation and reaction time, pH as well as temperature were found to be more stable and uniformly dispersed (Patra & Baek, 2014). This section goes over some of the key physical and chemical reaction parameters that determine silver nanoparticle size, shape and stability.

2.3.2.1 Capping Agents

Silver nanoparticles are not normally stable in solution under typical conditions and have a tendency to agglomerate. In the synthesis of nanoparticles capping agents are used to prevent silver nanoparticle aggregation. They also regulate the size and the shape of the silver nanoparticles and also affect their physicochemical properties (Restrepo & Villa, 2021). Four capping agents were tested in a study to investigate the influence of capping agents on the synthesis of silver nanoparticles, namely; polyethylene glycol (PEG), ethylenediaminetetraacetic acid (EDTA), polyvinylpyrrolidone (PVP) and polyvinyl alcohol (PVA). The study showed that the size of the nanoparticles, their stability and their antibacterial activity were affected by the capping agent used (Ajitha et al., 2016).

It is therefore important to select the appropriate capping agent for stabilizing the nanoparticles during synthesis. In the green synthesis of nanoparticles plant extracts such as neem leaves, *ligustrum ovalifolium* fruits and banana peels not only act as the reducing agents but also as the capping agents and aid in stabilizing the nanoparticles (H. M. M. Ibrahim, 2015; Moldovan et al., 2018; Verma & Mehata, 2016). The

presence of functional groups in plant extracts that can be useful as reducing and capping agents can be detected by use of characterisation techniques such as the FTIR (Sithara et al., 2017). The results will serve as proof that the extracts can act as capping agents thus eliminating the need for any additional capping agents.

2.3.2.2 Precursor-Extract Volume Ratio

The volume ratio of the extract to the silver nitrate solution influences the nanoparticle production rate and size. The size of the nanoparticles produced increases as the volume ratio of the extract increases, as evidenced by the shape and placements of the surface plasmon resonance peaks (Asif et al., 2022; Kaur et al., 2021). Several studies agree that the volume of the silver nitrate solution should be higher than that of the plant extract for effective nanoparticle synthesis to be achieved. The rate of the nanoparticle synthesis reaction depends on the availability of reactants. When the silver nitrate concentration is higher than that of the plant extract, there are more Ag^{+} ions available for reduction by the phytochemicals present in the plant extract. This can lead to a faster and more efficient synthesis process (Bamsaoud et al., 2021). Different optimum volume ratios have been recorded based on the different plant extracts used in the green synthesis procedure. In a research conducted by (Azarbani & Shiravand, 2020) different volume ratios of *ferulago macrocarpa* flower extract to the silver nitrate solution, that is; 1:1, 1:2, 1:4, 3:4 and 3:2 were used in the green synthesis of silver nanoparticles. The absorption peak changed towards a lower wavelength as the silver nitrate volume ratio was increased, indicating a reduction in particle size. The study concluded that a ratio of 3:4 produced smaller nanoparticles. In another study, the optimum volume ratio of *ligustrum ovalifolium* fruit extract to the silver nitrate solution was found to be 1:3 (Moldovan et al., 2018).

Other researchers also got different optimum volume ratios such as 1:10 (Sithara et al., 2017), 2:5 (Seifipour et al., 2020), and 0.06:1 (Sharma et al., 2020). Although the volume ratios differed for all studies, in all the results the silver nitrate volume ratio was higher than the extract ratio. Other parameters, for instance the concentration of the precursor, such as silver nitrate solution, and the extract employed are expected to influence the effect of the precursor-extract volume ratio on nanoparticles formation, explaining the large variances in the volume ratios used by different researchers. It is therefore necessary to determine the combined effect of these different parameters to achieve the optimum conditions for the synthesis of nanoparticles.

2.3.2.3 The pH of the Solution

The pH of the solution has a big impact on the synthesis of silver nanoparticles because it changes the electrical charge of the biomolecules, which affects their capping and reducing properties (Liaqat et al., 2022). A higher pH has been shown to increase the synthesis rate of nanoparticles, reduce their size and also produce more stable nanoparticles in comparison with acidic pH (Phongtongpasuk & Poadang, 2015). In a previous study on the effect of pH on silver nanoparticle green synthesis; on the tenth day of the experiment, nanoparticles generated in low pH (2, 4 and 6) solutions began to lose their stability. The nanoparticles generated in higher pH (8 and 10) solutions, on the other hand, were more stable (Velgosová et al., 2016). A study carried out by (Kredy, 2018) found that a higher pH resulted in a higher nanoparticle synthesis rate. In their research, the impact of pH was investigated in three separate scenarios: acidic (4.0), neutral (7.0) and basic (9.0). The reaction's colour intensity was highest at a basic pH of 9, and there was no response at an acidic pH of 4.

At higher pH increases the amount of OH^- ions in the solution which can connect with the silver ions resulting in enhanced nanoparticle synthesis as well as smaller nanoparticles (Kaur et al., 2021; Mahiuddin et al., 2020). However, if the pH is too high it may lead to agglomeration and the formation of larger nanoparticles. Another study carried out by (Verma & Mehata, 2016) reported that higher pH promotes the synthesis of nanoparticles while lower pH suppresses synthesis. The study also revealed that at a very high pH above 13 the nanoparticles become unstable and agglomerate thus making pH 13 the most suitable for synthesis. Several other researchers have reported that alkaline conditions are the most conducive in the synthesis of nanoparticles with optimum pH being recorded at 9 (Sharma et al., 2020), 10 (Moldovan et al., 2018; Seifipour et al., 2020), and 11 (Azarbani & Shiravand, 2020; Sana & Dogiparthi, 2018).

Other researchers, however, have contradicted these findings and reported that acidic pH is more suitable for the synthesis of nanoparticles than alkaline pH. In the green synthesis of nanoparticles using *pistiastratiotes* extract, the researchers found that an acidic medium gave smaller size nanoparticles than in a basic medium (Traiwatcharanon et al., 2015). Similar results were reported by Ibrahim who discovered that the creation of silver nanoparticles with banana peel extract was best done at an acidic pH of 4.5 (H. M. M. Ibrahim, 2015). It has been suggested that the effect of the pH can also be based on the degradation properties of the extract; some extracts may be denatured or degraded by acidic conditions thus resulting in a reduced rate of nanoparticle synthesis (Melkamu & Bitew, 2021). It is also important to understand the reason for these disparities and to determine the most suitable pH for a particular synthesis reaction.

2.3.2.4 Silver Nitrate Concentration

The concentration of silver ions has a significant impact on the size, shape and extent of production of silver nanoparticles. A modification in the concentration of metal salt employed in the synthesis of nanoparticles has been proven in several investigations to alter the synthesis result. In most biological synthesis processes, and the rate at which the surface plasmon resonance is attained rises with increasing silver ion intensity (Dada et al., 2018). In a previous study, silver nanoparticles were produced utilizing silver nitrate as the metallic salt and banana peel extract as the reductant and capping agent. Results of the study showed that at lower concentrations of silver nitrate, yellowish brown and light reddish colours were observed. Darker shades of reddish brown were detected as the concentration increased. The surface plasmon resonance absorption peak also increased and became more distinct at higher concentrations of silver nitrate (Ibrahim, 2015).

There is a positive correlation between initial metal ion concentration and the average nanoparticle size; an increase in silver nitrate concentration results in the formation of larger nanoparticles (Htwe et al., 2019). Synthesis of nanoparticles has mostly been conducted with silver nitrate concentrations varying from 0.25 mM up to 1 mM with some studies using concentrations up to 300 mM. However, the results have revealed that at concentrations below 0.5 mM, the silver concentration is too low for synthesis (Kaur et al., 2021). Furthermore, synthesis at extremely high silver nitrate concentrations may result in the development of particles that are larger than the requisite nanoparticle sizes, eventually leading to the formation of bulk silver. This was observed in a research where concentrations of 300 mM resulted in the formation of particles with a size of 630 nm (Janardhanan et al., 2009).

When establishing the optimum concentration of silver nitrate in the synthesis of silver nanoparticles, it is critical to take into account both the nanoparticle size and the heterogeneity of the sample depending on size, that is, the polydispersity index (Rao & Tang, 2017). Another factor to consider is the relationship between the volume of the extract and the silver nitrate concentration. According to one investigation, the strength of the SPR peak stabilized beyond 2.0 mM due to a lack of plant extract needed for the reaction with the silver ions. As a result, they recommended that smaller concentrations of silver nitrate should be utilized to get better quality and quantity of silver nanoparticles (Mahiuddin et al., 2020).

2.3.2.5 Synthesis Temperature

Another reaction parameter that has a significant impact on the synthesis rate, shape and size of silver nanoparticles is reaction temperature. The majority of research has been carried out at room temperature so that the procedure is simple, non-toxic and low cost (J. M. Ashraf et al., 2016; Y. Gao et al., 2014; T. Liu et al., 2020). Other researchers, on the other hand, have looked into the effect of temperature on the synthesis of silver nanoparticles in order to speed up the process and ensure that all silver ions are converted into silver nanoparticles. The synthesis of silver nanoparticles using *lawsonia inermis* leaf extract was investigated at three distinct temperature: 25 ℃, 35 ℃ and 45 ℃. With increasing temperature, the rate of production of silver nanoparticles increased and it also resulted in the formation of smaller nanoparticles this is due to the rapid consumption of the reactants and particle growth kinetics (Kredy, 2018).

In a study on the influence of temperature on the green synthesis of silver nanoparticles using neem leaves at temperatures ranging from 10 ℃ to 50 ℃, the reduction of silver

salt accelerated as the temperature increased with an optimum temperature of 50 ℃, as evidenced by a quick change in the colour of the solution. (Verma & Mehata, 2016). Similarly, an optimum reaction temperature of 50 ℃ was inferred by (Sithara et al., 2017) when synthesis temperature was varied from 30 ℃ to 70 ℃. Additionally, (Azarbani & Shiravand, 2020) investigated a temperature set with slightly higher values, that is, 30 ℃, 60 ℃ and 80 ℃ for *ferulago macrocarpa* flower extract - mediated silver nanoparticles and found a positive correlation between temperature and the rate of synthesis of silver nanoparticles with optimum conditions observed at 80 ℃. A higher temperature results in an increase in the kinetic energy of the molecules resulting in an increased rate of silver ion consumption therefore reducing the chances of further nanoparticle size growth (Azarbani & Shiravand, 2020).

A recent research however showed that there was no discernible rise in peak intensity at higher temperatures from 60 ℃ to 80 ℃ suggesting that the nanoparticle size or shape had not changed. As a result, 40 ℃ was chosen as the optimum temperature for nanoparticle synthesis (Seifipour et al., 2020). The differences in the optimum temperatures could be affected by the degradation temperatures of the bioactive components of some of the extracts used in synthesis. In a previous study on the effect of temperature on the synthesis of silver nanoparticles using *acalypha hispida* leaf extract; a decrease in rate of synthesis was observed at temperatures higher than 50 ℃. This could have been attributed to the breakdown of metabolites found in the leaf extract at higher temperatures (Sithara et al., 2017).

2.3.2.6 Reaction Time

Reaction time is an important factor in the synthesis of silver nanoparticles. It is critical for ensuring total silver ion consumption. By adjusting the reaction time, the form and size of the nanoparticles may also be adjusted. In most synthesis, the formation of the

nanoparticles becomes more visible as time increases until it reaches a point where complete nanoparticle synthesis takes place. This time of complete synthesis is different for every synthesis reaction based on other conditions of synthesis. When neem leaves were used in the green synthesis of silver nanoparticles, complete colour change which indicated complete synthesis of nanoparticles, occurred in 30 minutes (Verma & Mehata, 2016). Likewise, (Kaur et al., 2021) reported complete nanoparticle formation after 30 minutes of reaction time and an extension of the synthesis time had no further influence on the production of nanoparticles as evidenced by the lack of change in the surface plasmon resonance peaks. Other researchers reported longer synthesis times where complete synthesis took 60 minutes (Rao & Tang, 2017), 90 minutes (Melkamu & Bitew, 2021) and between 1 and 6 hours (Mahiuddin et al., 2020). These all used different extracts and different synthesis conditions which greatly affect the time. These studies further show the importance of optimising the nanoparticle synthesis because every procedure differs based on the extract used and the synthesis conditions employed.

2.3.3 Characterisation of Nanoparticles

Nanoparticles have different properties which influence their efficacy, bio-distribution and behaviour. Nanoparticle characterisation is therefore important to determine the size, shape and other functional aspects of the synthesized nanoparticles. Analytical techniques such as Fourier Transform Infrared Spectroscopy (FTIR), X-ray diffraction (XRD), UV-visible spectroscopy (UV-vis), Dynamic Light Scattering (DLS), Scanning Electron Microscopy (SEM), and Transmission Electron Microscopy (TEM) are used to characterise nanoparticles (Mourdikoudis et al., 2018).

2.3.3.1 UV-Visible Spectroscopy (UV-Vis)

The extinction (scatter and absorption) of light flowing through a material is measured using UV-Vis. This is a useful technique for recognizing, characterizing and analysing nanomaterials because nanoparticles have unique optical properties that are sensitive to shape, size, refractive index, aggregation sate, and concentration near the nanoparticle surface (X. F. Zhang et al., 2016). In the synthesis of silver nanoparticles, the biosynthesis and reduction of silver ions is measured by analysing the surface plasmon resonance using the UV-vis usually in the scanning range of either 200 nm to 800 nm (Melkamu & Bitew, 2021; Rao & Tang, 2017). The appearance of a characteristic surface plasmon resonance (SPR) peak between 400 nm to 500 nm confirms the formation of silver nanoparticles. The SPR peak is based on the nanoparticles' size and shape as well as the nature and composition of the dispersion medium (Jana et al., 2016). The SPR peak also shows the concentration of the nanoparticles in the solution which is directly proportional to the absorbance (Elbagory et al., 2016; Tyavambiza et al., 2021). As a result, process parameters such as pH, synthesis time, synthesis temperature and precursor volume ratio influence the position and intensity of the peak. The observation of this peak in the characterisation of green synthesised silver nanoparticles has been documented by several researchers with SPR peaks ranging from 417 to 424 nm (Htwe et al., 2019), 419 nm (Asif et al., 2022) and 440 nm (Rautela et al., 2019); with all of them falling within the required range of 400 nm to 500 nm.

2.3.3.2 Fourier Transform Infrared Spectroscopy (FTIR)

The Fourier Transform Infrared Spectroscopy (FTIR) technique is used to obtain the infrared spectrum of emission, absorption and photoconductivity of gases, liquids and solids. It is a cost effective, non-invasive and simple technique and is used to identify the different functional groups in compounds (X. F. Zhang et al., 2016). The FTIR

analysis method scans test samples with infrared light to observe the chemical properties. The instrument passes infrared radiation ranging through a sample and the resulting signal at the detector appears as a spectrum typically ranging from 4000 cm^{-1} and 400 cm^{-1}. The observed intense bands in the spectrum are compared with standard values to identify the functional groups (Karthik et al., 2020). The technique has been used in nanoparticle synthesis studies to determine whether biomolecules are involved in the formation of nanoparticles. The identified characteristic functional groups from spectral bands allow for the determination of the conjugation between the nanomaterial and the adsorbed biomolecules (Lin et al., 2014).

FTIR is suitable for the identification of the role of bioactive molecules in the reduction of silver nitrate to silver. In the green synthesis of silver nanoparticles using *litchi chinensis* leaf extract, FTIR was used to identify the presence of phenols, flavonoids, amides and hydroxyl groups responsible for the reduction of silver nitrate to silver (Kaur et al., 2021). Many other studies are reported in which FTIR has been used to successfully identify the biomolecules responsible for silver nanoparticle synthesis (Jyoti et al., 2016; Mahiuddin et al., 2020; Rao & Tang, 2017). Because each molecule or chemical structure produces a distinct spectral fingerprint, FTIR analysis is an excellent tool for chemical identification.

2.3.3.3 X-Ray Diffractometer (XRD)

The XRD is a non-destructive analytical technique that uses X-rays to penetrate deeply into a material to observe its crystallinity. The crystallinity of nanoparticles is a fundamental aspect that influences their properties such as hardness, melting point, density and chemical reactivity; their behaviour and suitability for various applications (L. Lin et al., 2023). When X-ray radiation reflects on a crystal, many diffraction patterns are formed. These diffraction patterns confirm the formation of crystalline

nanoparticles and also reflects the physicochemical properties of the crystal structures (Holder & Schaak, 2019; Varberg & Skakuj, 2015). The formation of diffraction patterns is crucial in the analysis of these materials. Each material has a distinct diffraction beam that can be defined and identified by comparing diffracted beams to reference standards. The diffracted patterns reveal whether the sample materials are pure or contaminated (X. F. Zhang et al., 2016). As a result, XRD can be used to investigate the structural properties of various materials such as polymers, biomolecules, forensic samples and industrial materials. Furthermore, XRD is an effective method for studying nanomaterials. The Debye-Scherrer equation is used to calculate crystalline size from XRD data by determining the width of the Bragg reflection law according to Equation 1 (Almatroudi, 2020).

$$d = K\lambda / \beta \cos \theta \qquad \text{Equation 2.1}$$

where:

d is the crystalline size (nm),

K is the Scherrer constant,

λ is the wavelength of X-ray,

β is the full width half maximum

θ is the diffraction angle (half of Bragg angle) that corresponds to the lattice plane

XRD analysis of green synthesized nanoparticles has confirmed the crystallinity of the nanoparticles and has shown them to have a face centred cubic structure. The technique has also been able to detect additional compounds through the presence of unassigned peaks in the diffraction pattern. The size of the nanoparticles obtained is also in agreement with those attained using other analytical techniques (Kaur et al., 2021; Melkamu & Bitew, 2021; Rao & Tang, 2017). This is therefore a useful analytical technique in the characterisation of nanoparticles.

2.3.3.4 Scanning Electron Microscopy (SEM)

The Scanning Electron Microscope creates detailed magnified images of materials by scanning their surfaces to generate a high-resolution image. It accomplishes this by focusing a beam of electrons at the surface of the sample material and the secondary electrons produced provide information about the sample's topography, morphology and the size at the nano and micro scales (K. Akhtar et al., 2018). These properties have been detected in several studies of green synthesized silver nanoparticles. The nanoparticles were found to be mostly spherical in shape with a homogeneous morphology and a narrow size distribution (Kaur et al., 2021; Mahiuddin et al., 2020; Rao & Tang, 2017).

SEM can be used together with the Energy-Dispersive X-ray spectroscopy (EDX) to examine the chemical composition of the nanoparticles. All elements have distinct atomic structures, resulting in a distinct set of peaks in the x-ray spectrum, which can be used to investigate the elemental composition of any nanoparticle (Scimeca et al., 2018). EDX of silver nanoparticles shows a very strong signal for silver atoms and may also detect adjacent elements such as carbon (C) and oxygen (O). C and O are associated with organic compounds adsorbed on the surface of the nanoparticles. These play an important role in the reduction and stability of the nanoparticles (Rao & Tang, 2017). SEM and EDX are therefore essential characterisation techniques in confirming the complete synthesis of nanoparticles. SEM however, does not provide information about the internal composition. To do so, characterisation with a transmission electron microscope is required (Akhtar et al., 2018).

2.3.3.5 Transmission Electron Microscopy (TEM)

The Transmission Electron Microscope is an extremely powerful tool for characterizing nanoparticles. It is used to obtain quantitative measurements of materials such as size

distribution, particle size and morphology. In this technique an electron beam is transmitted through an ultra-thin sample and then forms an image on a photographic plate showing the characteristics of the test sample (Subramanian et al., 2013). Using this technique, the electronic and chemical structure of individual nanoparticles can be detected and quantified. TEM has advantages over SEM in that it has a much higher resolution and magnifying power. TEM also has the ability to give details about the internal composition of materials and thus illustrate several material properties such as crystallization, morphology and stress (K. Akhtar et al., 2018). TEM studies of green synthesized nanoparticles also showed their spherical shape which is in agreement with the results attained in SEM (Kaur et al., 2021; Mahiuddin et al., 2020). Furthermore, the images revealed selected area diffraction patterns with circular spots, confirming the nanoparticles' crystalline nature (Ibrahim, 2015).

2.3.3.6 Dynamic Light Scattering (DLS)

The most versatile and useful set of techniques for measuring the size, size distribution and zeta potential of nanoparticles in liquids is dynamic light scattering (Pecora, 2000). Using a monochromatic light source, DLS can probe the size distribution ranging in size from a few nanometres to several micrometres in solution or suspension. By analysing the fluctuating scattered intensity from the nanoparticles in the solution, the DLS technique determines the diffusion coefficient of suspended nanoparticles in a solution undergoing Brownian motion. The scattered light from a nanoparticle suspension fluctuates on a specific time scale, which is inversely proportional to the particle diffusion coefficient (Elamawi et al., 2018). The dynamic light scattering is also used to assess the zeta potential, which is the stability of a suspension over time. The zeta potential is used to characterise the surface charge of nanoparticles in order to learn about their stability and surface interactions with other molecules (Carvalho et al.,

2018). High zeta potential particles are highly charged, which prevents particle aggregation due to electric repulsion. Table 2:4 gives summary of the different zeta potential values and the corresponding levels of stability of the nanoparticles.

Table 2:1. Guideline for Zeta Potential Analysis

Zeta Potential (mV)	Stability behaviour of the particles
0 to ±5	Rapid coagulation or flocculation
±10 to ±30	Incipient instability
±31 to ±40	Moderate stability
±41 to ±60	Good stability
More than ±60	Excellent stability

Source : (Raja & Barron, 2022)

When the zeta potential is low, attraction overcomes repulsion and the mixture coagulates. A zeta potential of +/- 30 mV is thought to be optimal for good stability of the nanoparticles (Samimi et al., 2018). Although the DLS technique produces more robust data on the polydispersity index and size distribution, it has the disadvantage that the measurements are insufficient to evaluate the real size of nanoparticles. This is because they measure a hydrodynamic size rather than a physical size (Bhattacharjee, 2016; Carvalho et al., 2018). The size obtained is also different, often larger than that of other characterisation techniques that measure the physical size (Anand et al., 2017; Mahiuddin et al., 2020; Mollick et al., 2019). Therefore, to get the physical size of the dry nanoparticles and the shape, it is necessary to also use other characterisation techniques such as the SEM and the TEM.

2.3.4 Antibacterial Action of Silver Nanoparticles

Green synthesized silver nanoparticles have been reported to be potential antibacterial agents against a variety of gram-negative and gram-positive bacteria, including, *E. coli, S. aureus, Asiatic cholera, proteus vulgaris, enterococcus faecalis, salmonella typhi, Citrobacter, bacillus cereus, salmonella enteritidis* and *klebsiella pneumoniae* (Labulo

et al., 2022; Loo et al., 2018; Saravanakumar et al., 2017). The exact antibacterial mechanism of silver nanoparticles is still not fully understood; however, several hypotheses are presented in Table 2:5 to explain the antibacterial activity of silver nanoparticles. These mechanisms take into account the morphological properties of the silver nanoparticles which allow them to adhere to or even penetrate through the bacterial cell walls or membranes and then directly affect the bacteria's intracellular components (Bruna et al., 2021; Dakal et al., 2016; Qing et al., 2018).

Table 2:2. Antibacterial Mechanism of Silver Nanoparticles

Antibacterial mechanism	**Resulting activity**
Adhesion of the cell membrane	Alters structure of the membrane and permeability
	Leakage of the cellular content and adenosine triphosphate
	Impairing of transport activity
Penetration inside the cell and nucleus	Mitochondrial dysfunction
	Destabilization and denaturing of proteins
	Destabilization of ribosomes
	Interaction with DNA
Cellular toxicity and generation of reactive oxygen species	Oxidising of proteins and lipids
	Oxidising of DNA base
Modulation of cell signalling	Alters phosphotyrosine profile

Source: (Dakal et al., 2016)

The antibacterial potential of silver nanoparticles has mainly been assessed using the agar well diffusion assay and the Kirby-Bauer disk diffusion assay. These tests have shown that the antibacterial activity is influenced by physicochemical parameters such as shape, size, surface charge and stability (Abbaszadegan et al., 2015; Chen et al., 2016; Raza et al., 2016). Studies have shown that smaller silver nanoparticles exhibit more significant antibacterial activity than larger nanoparticles. This is because of their superior surface area which results in good contact with the bacteria and enables the

nanoparticles to reach the nucleus of microbes (Lok et al., 2006). The antibacterial activity of different-sized nanoparticles was tested against various bacteria strains, and the results indicated that as the size of the silver nanoparticles decreased, the antibacterial activity increased (Korshed et al., 2019). Smaller nanoparticles have a higher surface area-to-volume ratio, which allows for greater interaction and binding with bacterial membranes. This interaction can cause damage to the membrane resulting in bacterial death. Additionally, the size of silver nanoparticles can also affect their ability to penetrate the bacterial cell wall. Smaller nanoparticles are more likely to penetrate deeper into the bacterial cells, leading to higher bactericidal activity. The shape of nanoparticles influences their interaction with bacteria, viruses and fungi. When the activity of different shaped nanoparticles was compared, spherical silver nanoparticles demonstrated superior antibacterial activity against *E. coli* and *P. aeruginosa* (Raza et al., 2016). As a result, nanoparticles with the right shape, size and surface properties are essential for effective use in a wide range of medical applications.

2.4 Imparting Antimicrobial Properties onto Textile Fabrics

2.4.1 Application of Plant Extracts onto Textile Fabrics

Plant extracts are a valuable source of antimicrobial agents with numerous medical applications. Plants have been used since ancient times to treat and prevent common ailments such as skin diseases, colds, diarrhoea and nausea (Cowan, 1999). Plants with antimicrobial properties against both gram-negative and gram-positive bacteria include cumin, ginger, pomegranate, thyme, cloves, guava, mulberry, sage, olives, hibiscus and rosemary. Extracts of various plant parts, such as peels, flowers, leaves and stems have been used and shown to have antibacterial properties against various bacterial strains (Hemeg et al., 2020; Mostafa et al., 2018). The antimicrobial activity of plant extracts

is attributable to the presence of phytochemicals such as alkaloids, phenols, tannins, quinones, terpenes and flavonoids. When these phytochemicals interact with bacteria, they either cause cell membrane rupture (Álvarez-Martínez et al., 2021), prevent bacterial adhesion (Famuyide et al., 2019) or inhibit biofilm formation (Maisetta et al., 2019), thus resulting in their antimicrobial properties. Due to the efficacy of these plant extracts against bacteria, they have been applied onto textile fabrics for the production of fabrics with antimicrobial properties.

Several techniques have been used for the application of plant extracts onto textile fabrics. The exhaust method has been used by several researchers because it produces high quality dyed or treated fabrics at a lower cost (Choudhury, 2017). This technique allows molecules to move from the solution to the fabrics until the molecule is exhausted. All of the material comes into contact with the extract or dye liquor and the fabric absorbs the dyes. As a result, the dye concentration in the bath gradually decreases. This is followed by rinsing to remove any excess dyestuff or extract on the fabric. This can also be followed by curing the fabric for fixation of the extract onto the fabric (M. Ashraf et al., 2021). Another method that is commonly used is the pad-dry-cure (see Figure 2:3) which has been successfully used in the development of bandages with antibacterial properties using tea tree and rosemary oils (Koyuturk & Soyastan, 2021). This technique has also been used in the application of plant extracts on cotton fabrics and the fabrics displayed excellent antimicrobial activity even after 10 to 40 washing cycles (El-Shafei et al., 2018; Ketema & Worku, 2020).

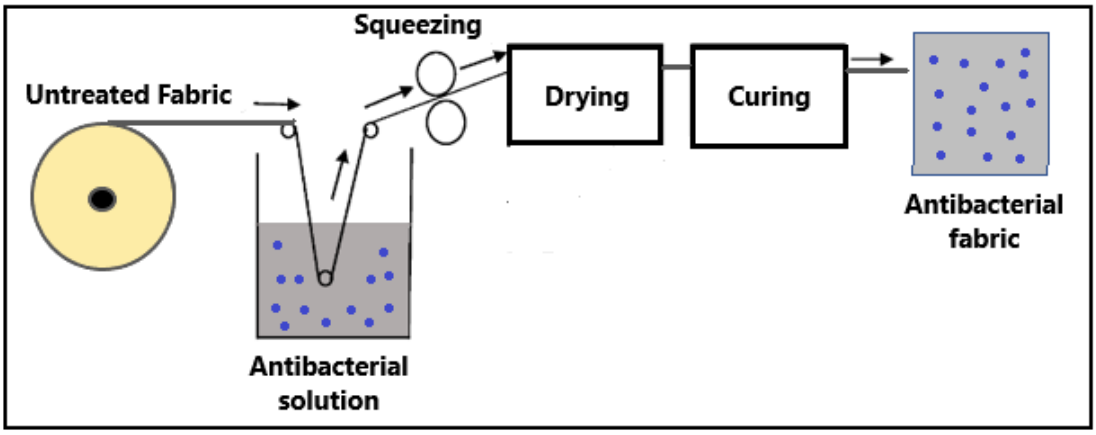

Figure 2:1. Antibacterial Finishing of Textile Fabric Using the Pad-Dry-Cure Technique (*Source* : Author elucidation based on: (Tania et al., 2021))

Most studies have shown that a crosslinking agent is required when applying extracts of fruits and other plants onto textile fabrics. The purpose of the crosslinking agent is to improve the fixation of the plant extracts onto the fabric and also improve the durability of the extracts on the fabrics. Chamomile, sage and green tea were applied onto textile fabrics and formaldehyde was used as the crosslinking agent between the extracts and the textile fabrics for increased fixation of the extracts on the textile fabrics (El-Shafei et al., 2018). Sodium bicarbonate has also been used as a crosslinking agent when lemon peel extracts were applied on cotton fabric (Qutaba et al., 2017).

Citric acid is another crosslinking agent that has been used in the application of stinging nettle plant leaf extract onto cotton fabric. In this study citric acid was used to crosslink cellulose in cotton fabric and the phenolic compounds isolated from stinging nettle plant leaves. The two carboxylic groups in citric acid were linked to the phenol and hydroxyl groups of the cellulose by covalent bonding (Ketema & Worku, 2020). Citric acid, a bio-based polycarboxylic acid found in fruits, has grown in popularity as a crosslinking agent due to its low cost and non-toxicity (W. Zhang et al., 2023). The use of citric acid as a crosslinking for dye application on cotton fabrics improves surface colour depth (K/S) values by approximately 160 %. It also improves light resistance

stability, rubbing fastness, washing fastness and antibacterial properties (Cai et al., 2021). It is therefore a recommended crosslinking agent in the application of plant extracts onto textile fabrics.

2.4.2 Methods of Applying Nanoparticles onto Textile Fabrics

There are various methods of applying nanoparticles onto textile fabrics such as impregnation, dipping, coating, printing and electrospinning. These are ex-situ synthesis techniques whereby the nanoparticles are first synthesized separately and then applied onto the textile fabrics. Chitosan-silver nanoparticles have been applied onto fine cotton fabric by immersion of the fabric in aqueous solution containing the nanoparticles along with a penetrant, antifoaming agent and an acidic buffer. The fabric was then passed through a padding mangle and then dried and cured (Arif et al., 2015). The same technique has been used in the application of magnesium oxide nanoparticles onto cotton fabrics (Dhineshbabu et al., 2014). In another study, the coating of silver nanoparticles was achieved by dipping the cotton fabric samples in nano-silver solution and then kept on a shaker for 1 hour at room temperature. The samples were then dried at 60 ℃ (Kumar, 2016). Nanoparticles have also been applied to textile fabrics by coating using electrospinning techniques. However the challenge with this application method is that the nanofiber layer delaminated easily from the textile surface (Heikkilä et al., 2007). Previous studies have shown that the most ideal ex-situ method of application of the nanoparticles onto textile fabrics is the pad-dry-cure method because it is a continuous process and it is simple, economical, consumes less energy and provides higher yields than other methods (Koyuturk & Soyastan, 2021).

Although ex-situ synthesis has been used widely by many researchers, there have been challenges such as the aggregation of nanoparticles, low adhesion affinity, non-uniform distribution and the procedure is time consuming which make the ex-situ process

difficult (Simoncic & Klemencic, 2015). There are weak adhesive forces between the nanoparticles and the fabric surface; therefore, the nanoparticles are rapidly released from the fabric resulting in unsatisfactory laundering durability due to the leaching out of the nanoparticles during washing (Huang et al., 2022). The use of a binding agent in the application of nanoparticles onto textile fabric has been explored by several researchers. In this method, the surface of the fabric is modified with a binder before silver nanoparticles are bonded to it. This improves the silver nanoparticles' adhesion to the cotton fabric (Hebeish et al., 2011; H. Liu et al., 2014; Xu et al., 2017). The drawbacks of these binders include the use of additional chemicals, as well as non-uniform deposition of silver nanoparticles on fabrics and a reduction in the antimicrobial activity of the nanoparticles (Jain et al., 2022). The in-situ route is thus proposed for the formation of stable and non-leaching nanoparticle-coated textile fabrics. The in-situ technique shown in Figure 2:4 involves the direct synthesis of nanoparticles onto textile fabrics in a one step process using synthesis methods such as chemical reduction, green synthesis or electrochemical reaction. $AgNO_3$ is added to the fabric then in the same container, the reducing agent is added resulting in the synthesis of the silver nanoparticles directly onto the fabric.

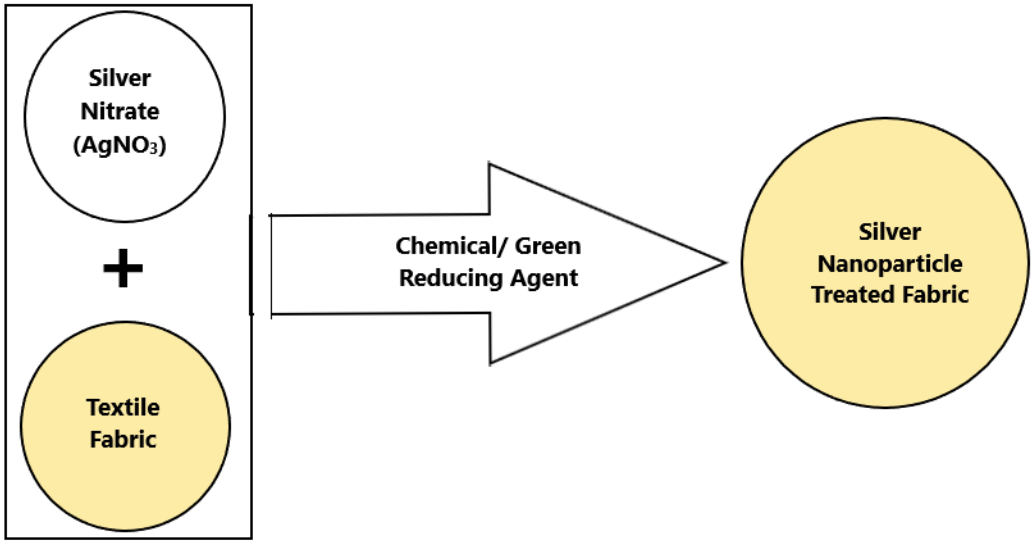

Figure 2:2. In-Situ Synthesis of Silver Nanoparticles onto Cotton Fabric by the Reduction Method (*Source*: Author elucidation based on Huang et al., 2022)

The in-situ synthesis of silver nanoparticles onto textile fabrics has been investigated by several researchers using silver nitrate as the precursor and plant extracts as the reducing agent. A comparison of the in-situ and ex-situ techniques for producing polyester/cellulosic fabrics with Ag-TiO_2 was conducted. According to the findings, fabrics coated with in-situ synthesis had smaller and more evenly distributed nanoparticles, a higher concentration of nanoparticles on the fabric surface and higher wash durability (Mahdieh et al., 2021). Other advantages of in-situ synthesis are that; there is reduced synthesis time because there is a one-step preparation and simultaneous deposition of nanomaterials on the textile substrate, there is improved nanoparticle stabilization efficiency and reduced agglomeration (Čuk et al., 2021; Harifi & Montazer, 2015; Huang et al., 2022; Jacob, 2022). Several factors influence the efficiency of in-situ synthesis of nanoparticles onto fabrics, including fabric surface properties, fabric composition and processing parameters. Surface properties of textile fabrics, such as surface roughness, hydrophilicity, surface charge, and fabric treatment, can all have a substantial impact on nanoparticle synthesis. These properties can

influence the adsorption of precursor agents onto the fabric surface, thereby influencing nanoparticle nucleation growth (Montes-Hernandez et al., 2021). Furthermore, the chemical composition of the fabric affects the functional groups present on the fabric surface, which can influence precursor agent adsorption and nanoparticle formation. That is the case in the in-situ synthesis of silver nanoparticles onto cotton fabric; the functional groups in cellulose also act as a reducing agent in the synthesis of silver nanoparticles (Pourreza et al., 2015). Processing parameters and reaction conditions such as pH, reaction temperature and time, drying temperature and time, incubation time and curing can all have an impact on the in-situ synthesis and durability of nanoparticles on fabric. These factors affect the coating efficiency, that is, the content and distribution of the nanoparticles deposited on the fabric surface, the nanoparticle size and subsequently affect the antibacterial activity of the treated fabrics (Abazari et al., 2023). The optimal reaction conditions should be chosen based on the type of precursor agent, the required properties of the nanoparticles, and the textile substrate. By optimizing these factors; it is possible to achieve efficient synthesis of stable nanoparticles onto textile fabrics.

2.4.3 Assessment of Antibacterial Properties of Textile Fabrics

Several tests have been done on multifunctional textiles to determine efficacy against gram-positive *Staphylococcus aureus* (*S. aureus*) and gram-negative *Escherichia coli* (*E. coli*) (Dhineshbabu et al., 2014; El-Nahhal et al., 2020; B. S. Kumar, 2016). Testing for antibacterial properties can be done qualitatively or quantitatively. Qualitative tests can be done by use of the Agar Disc Diffusion method based on International Testing Standards which has also been referred to as the fabric disc diffusion assay. In this technique, treated fabric discs are prepared for use in the assay instead of the antibiotic discs used in the disc diffusion method (Gulati et al., 2022). The fabric discs are placed

on inoculated agar surfaces and then incubated at suitable conditions. Thereafter the diameters of the zones of inhibition that appear around the antimicrobial discs are measured.

Researchers who have used the fabric disc diffusion assay have followed a similar general procedure to test for antibacterial activity against different bacterial strains (Gesese et al., 2022; Ibrahim et al., 2020; Jain et al., 2022). The steps in the procedure may differ from one test to another based on the antimicrobial substance and the bacterial of fungal strain used. The steps are as follows:

i. Agar plate preparation – a nutrient agar (solid growth medium) is first prepared and poured into a sterile petri dish to form a solid agar plate.
ii. Bacterial or fungal strain preparation and inoculation – the strains are grown in liquid broth culture until they reach a specific standard density of microbial cells. The microbial culture is then streaked evenly across the agar plate with a sterile cotton swab or inoculating loop, creating a thin, even layer of bacteria or fungi on the agar's surface.
iii. Impregnation of fabric discs – the fabric discs are impregnated with a solution containing the antimicrobial substance being tested. This substance can be an antifungal, antibiotic or any other antimicrobial agent.
iv. Placement of fabric discs – the impregnated fabric discs are then placed on the agar plate, gently pressing them down to ensure good contact with the agar surface.
v. Incubation – the agar plate is incubated at a specific temperature for a set period of time. This allows bacteria or fungi to grow, and if the impregnated substance is effective against them, it inhibits their growth and creates a clear zone around the fabric disc.

vi. Inhibition zone measurement – after incubation, the agar plate is examined and the zones of inhibition are measured. These zones are visible as clear areas around the fabric discs where microbial growth is completely inhibited due to the diffusion of the antimicrobial substance into the surrounding agar.

vii. Interpretation of data – the size of the inhibition zone in millimetres can be used to determine the potency and effectiveness of the tested antimicrobial substance against the microbial strain. The larger the zone of inhibition, the greater the antimicrobial agent's effectiveness against the tested strain.

The fabric disc diffusion assay is a simple and inexpensive way to assess the antimicrobial activity of substances. Researchers can determine a microbial strain's susceptibility or resistance to specific antimicrobial agents by comparing the size of the inhibition zones to known standards. However, the fabric disc diffusion assay has challenges in that it may not accurately reflect the actual conditions under which the textiles are used such as wearing or contact with bodily fluids as it is an in-vitro testing method (Balouiri et al., 2016; Mia et al., 2023). The results of the assay may also be influenced by factors such as fabric thickness, porosity, disc size, inoculum size and moisture content; as a result, it may not detect subtle differences in antimicrobial activity between fabrics or treatments. Additionally, some antimicrobial agents with low diffusion rates or high binding affinity to the fabric or agar may not be suitable for use with this technique and may give inaccurate results (Haase et al., 2017; Jain et al., 2022). It is therefore important to also consider quantitative antibacterial analysis of the treated fabrics. Quantitative testing provides precise and numeric results regarding the antibacterial properties of textile fabrics. This data quantifies the extent of bacterial inhibition or reduction provided by the antibacterial agent. The quantitative tests are generally more reliable and more accurate than the qualitative tests (Pinho et al., 2011).

Different standard testing methods have been used to quantitatively assess the antibacterial activity of antimicrobial-treated textile fabrics. Some of these methods are AATCC 100 – Test method for antibacterial finishes on textile materials; ISO 20743-Determination of antibacterial activity of textile products and JIS L 1902 – Textiles: Determination of antibacterial activity and efficacy of textile products. AATCC 100 is the most commonly used method because of it is inexpensive, sensitive and realistic (Ristic et al., 2011). The method measures the reduction of bacterial population on the fabric after a specified contact time. However, the protocol does not specify the exact concentration of bacteria to be tested but only states that it should be adjusted to appropriate dilution (Nicoloro et al., 2020). The ISO 20743 and JIS L 1902 are similar methods with some minor differences in the parameters and procedures. They measure the antibacterial activity of the fabric by comparing the number of viable bacteria recovered from the fabric with those recovered from a reference material. The antibacterial activity is expressed as a log reduction value or as a percentage reduction (Abramova et al., 2021; Agnhage et al., 2017). Although these methods are more complex, time-consuming and expensive to perform they have the advantage that they are more comprehensive and rigorous. Furthermore, the JIS L 1902 has been shown to be more sensitive to the quantity of antimicrobial agent than the AATCC 100 method, allowing it to distinguish the efficacy in serial dilutions of the antimicrobial agent (Pinho et al., 2011). These tests have all revealed various benefits and drawbacks. The most suitable method should be chosen based on the fabric sample being tested, the nature of the bacteria being tested, and the expected antibacterial results.

2.4.4 Assessment of Durability of Treated Fabrics

The end use of fabrics treated with silver nanoparticles may result in them going through conditions that may lead to the reduction of the treatment on the fabric.

Processes such as washing, exposure to light and rubbing may cause the treatment to be detached from the fabric, thus reducing the antibacterial properties. It is therefore important to ensure that there is good fixation of the antibacterial treatment on the fabric even after several uses. Researchers have explored several methods in an attempt to improve the durability of the treatment on the fabric such as fabric pre-treatment, use of binders and curing of the fabric.

The pre-treatment of cotton fabrics involves processes such as desizing, scouring and bleaching. Desizing grey fabric involves removing previously added starch, scouring uses alkali to remove oils, fats and waxes and bleaching uses oxidizing agents to improve the whiteness of the fabric (Harane & Adivarekar, 2017). A comparison has been made between untreated cotton and bleached cotton in the in-situ synthesis of silver nanoparticles. On both fabrics, very fine silver nanoparticles of approximately 20 nm were formed. However, morphology studies revealed that the untreated cotton fabric had a higher aggregation degree and a higher concentration of silver nanoparticles on the fabric. As a result, the untreated fabrics had higher antibacterial properties and a higher durability (Montes-Hernandez et al., 2021). A more recent study has shown that the additional process of mercerization increased the durability. Mercerization is a widely used alkali pre-treatment process in the textile industry for the improvement of the dyeability of the fabric by activating the cellulose, which is the main constituent of cotton (Holme, 2016). In this study, green synthesis of silver nanoparticles using *Azadirachta indica* leaf extract was done on both mercerized and un-mercerized cotton fabrics. Mercerization of the fabric resulted in a more uniform deposition of the silver nanoparticles at a higher concentration and also made the silver nanoparticle treatment wash resistant even up to 20 washes (Jain et al., 2022). Mercerization reduces the crystalline regions and increases the amorphous properties

of the cotton fibre, resulting in more pores and hydroxyl groups in the fibre, which could potentially increase the fixation and durability of nanoparticles on the fabric (Lin et al., 2022).

Another method that has been used to improve durability of finishes on textile fabrics is heat curing. The process of heat curing is used in textiles to improve the properties and durability of coatings and finishes applied on textile fabrics. The process entails exposing the treated fabric to a high temperature, approximately 120 ℃ to 220 ℃ for a set period of time in an oven or other specialized equipment. The curing temperature and the duration are determined by the type of finish used and the desired outcome. The effect of concentration, temperature of curing and reaction time on the antimicrobial properties of the fabric have been reported (Zhou et al., 2016), who padded a cotton fabric with 5,5-dimethylhydantoin (DMH) followed by nitrogen plasma treatment. Concentration and time were positively correlated to the antimicrobial efficacy while the optimal curing temperature was 120 ℃ and efficacy reduced at higher temperatures. Curing temperature is affected by the melting point of the coating; at curing temperatures higher than the melting point, the coating may get detached from the fabric, resulting in poor fixation and lower durability (Zhou & Kan, 2014).

To avoid any negative effects on the fabric's properties, the curing temperature should be carefully controlled. Excessive heat during the curing process can cause fabric damage such as discolouration, shrinkage, or loss of tensile strength. Damages to the fabric can compromise its overall performance and durability. Additionally, very high curing temperatures may lead to poor fabric handle as a result of the formation of extensive crosslinks (Poon & Kan, 2016). Curing of cotton fabric for 2 minutes at 160 ℃ resulted in excellent antibacterial activities up to 20 washes against *E. coli* and *S. aureus* (Abdel-Mohsen et al., 2012). Other researchers achieved optimal curing

temperatures of 110 ℃ for 60 minutes (Hebeish et al., 2011) and at 150 ℃ for 2 minutes (Fouda & Shaheen, 2017). These differences make it necessary to optimize the curing temperature to achieve desirable antibacterial properties and durability; while maintaining suitable fabric properties.

2.5 Characterisation of Treated Fabrics

The application of various treatments to textile fabrics is necessary to enhance their aesthetic appeal, improve comfort and performance and to add functional properties. However, these finishes can alter the physical and chemical properties of the fabrics, affecting their performance in their intended end use. Table 2.6 gives some of the tests and standards that have been used in the characterisation of multifunctional textiles. Properties such as tensile strength, wear resistance, tear resistance, abrasion resistance, UV protection, water absorption and air permeability have been shown to be affected by treating textile fabrics with various finishes (Chowdhury, 2018; Perera et al., 2013). Fabrics treated with chamomile, sage and green tea; with and without a crosslinking agent, had reduced tensile strength, elongation at break, abrasion resistance, water permeability, air permeability and stiffness of the fabric. However, the properties were still acceptable for their intended end use (El-Shafei et al., 2018).

Cotton fabrics coated with green synthesized silver nanoparticles had a higher tensile strength than the uncoated cotton fabrics due to the electrostatic interaction between the silver nanoparticle coating and the cotton fabric. As the amount of silver nanoparticles on the fabric increased, the tensile strength also increased (Balamurugan et al., 2017). The application of green synthesized silver nanoparticles on cotton fabrics also resulted in a decrease in air permeability and thermal conductivity with no effect on the change in breaking strength or the elongation of fabrics (Čuk et al., 2021).

Table 2:1. Tests and Standards for Characterisation of Multifunctional Textiles

Test	**Method/ Equipment used**	**Reference**
Water repellent property	Water Contact Angle (WCA) measurement	(Dhineshbabu et al., 2014) (Syafiuddin et al., 2020) (Shateri-Khalilabad et al., 2017)
Durability to washing	Wash fastness tests ISO 105:C06 AATCC 61 (2006)	(Dhineshbabu et al., 2014) (El-Nahhal et al., 2020) (Jain et al., 2022)
Stiffness in the bending length	AATCC 115:2005 Profile stiffness tester	(Mahmud et al., 2020)
Degradation temperature of fabrics	Thermogravimetric Analysis (TGA)	(Dhineshbabu et al., 2014) (Mahmud et al., 2020)
Flame retardancy	ASTM D6413	(Dhineshbabu et al., 2014)
Crease recovery angle	AATCC 66-2003	(Mahmud et al., 2020)
Surface morphology analysis of coated textile fabric	Scanning Electron Microscope	(B. S. Kumar, 2016) (Balamurugan et al., 2017) (Mahmud et al., 2020) (Montes-Hernandez et al., 2021)
Distribution of nanoparticles and other elements	Energy Dispersive X-ray Spectroscopy	(Syafiuddin et al., 2020) (Mahmud et al., 2020) (Shateri-Khalilabad et al., 2017)
Tensile strength	Strip method on tensile strength testing machine (IS EN ISO 29073)	(Balamurugan et al., 2017)
Absorbance and reflectance	UV-Vis	(Balamurugan et al., 2017)
Crystallinity of the sample	X-Ray Diffractometer	(Balamurugan et al., 2017) (Shateri-Khalilabad et al., 2017)
Air permeability	Air permeability tester (ISO 9273)	(Čuk et al., 2021)
Thermal conductivity	Lee's disc method	(Čuk et al., 2021)
Breaking strength and elongation	ISO 13934-1:1999	(Čuk et al., 2021)
Functional group analysis	Fourier Transform Infrared (FTIR)	(Mahmud et al., 2020)(Montes-Hernandez et al., 2021)
UV protective characteristics	AS/NZS 4399 : 1996	(Mahmud et al., 2020)

Other properties that have been shown to be affected by the application of extracts and nanoparticles on textile fabrics are crease recovery angle, colour strength, bending length (Mahmud et al., 2020), water absorption capacity and cotton woven fabric density (Syafiuddin et al., 2020). Tests have also been done to show the change in the morphology of the fabrics using the scanning electron microscope as well as the modification of the functional groups on the textile fabrics using the FTIR (Novoa et al., 2022). These tests are all necessary to determine the properties of the treated fabrics and their suitability for their applications.

When performing any characterisation on the fabric, it is important to consider the intended end-use of the fabric as well as the property requirements for that use. The requirements for hospital textiles are clearly stipulated in the EN 13795 series of standards. These textiles should be durable, breathable, soft, resistant to fluids, resistant to odour, have good fastness properties, easily washable and resistant to staining (Nocker, 2011). Durability of the fabrics is an important property due to the constant washing and heavy use of the hospital textiles. This can be assessed by testing the tensile strength of the fabric using the textile standard ISO 13934:2013 as well as the durability to different properties after several washes using the textile standard ISO 105:C06 or AATCC 61 (2006). Hospital clothing should allow airflow and moisture evaporation to help maintain comfort and reduce the risk of infections. Therefore, fabrics need to have good air permeability; this can be assessed using the air permeability tester and the standards ISO 9237 or D737 – 96 (Čuk et al., 2021). Furthermore, the clothing should be soft and comfortable to wear even for long hours, therefore cotton is a preferred fabric for that (Behera & Arora, 2009). However, the treatments on the cotton fabric may affect its softness and other properties. That is why it is important to check the properties of the treated fabric against the untreated fabric

and also against the required standard parameters for the end use. This will ensure that the textiles protect the wearer from any infectious microbes that may penetrate the fabric while also providing comfort.

2.6 Summary of Findings and Gaps from Literature

The literature survey highlighted several findings and gaps in the use of potato peels in the green synthesis of silver nanoparticles for the production of antibacterial finishes for textile fabrics. The main gaps and findings are explained in this section.

Although several methods of disposal of potato peel waste are available; there is need of exploring other potential uses of potato peels that get to utilize the full benefit of their active compounds and add value to the peels. Peels from different potato varieties contain different types and quantities of bioactive compounds in different varieties. Tests are required to determine the phytochemicals in each variety, quantitative testing is also necessary. Different plant extracts have been applied onto cotton fabrics as dyes and also for the impartation of antibacterial properties. Potato peels which potentially have antibacterial properties have so far not been used on textile fabrics. They could therefore be explored as antibacterial agents for textile fabrics. Tests will still need to be done to determine the antibacterial efficacy after application on the textile fabric because the efficacy may change after application.

Although studies have been done to confirm that potato peels generally consist of the bioactive compounds required for the green synthesis of nanoparticles, so far, they have only been used in the synthesis of zinc nanoparticles. There is therefore a gap in exploring the potato peel extracts for the green synthesis of silver nanoparticles. Synthesis parameters vary based on the extract used because all extracts have different types and concentrations of phytochemicals required for the reduction of Ag^{+} to Ag^{0}. Therefore, optimisation is necessary to determine the most suitable parameters.

The literature has shown the advantages of using direct in-situ synthesis of nanoparticles onto fabric in comparison with other methods such as ex-situ synthesis, aerosol deposition and electrospinning. The method is simple, less expensive and produces more durable nanoparticle treated fabrics. However, there is still need to optimise the process to determine the parameters that will provide the best durability while still providing suitable properties of the fabric. Treatment of the fabrics has an effect on their properties. Physical tests need to be done on the fabric to determine their properties after treatment as well as their suitability for their intended end use. These properties differ based on the quantity of nanoparticles deposited on the fabric, and therefore need to be assessed with every different treatment. The results need to be compared with standard requirements for the end-use, for example, with the required standards for hospital use.

CHAPTER THREE: MATERIALS AND METHODS

3.1 Materials used in the Study

The potatoes used in this study were the *Shangi* solanum tuberosum potatoes and harvested from a farm in Tulwop village in Uasin Gishu County, Kenya. The potatoes were planted during the rainy season and were harvested 3 months after the planting date. Hundred percent plain woven, bleached, mercerized and scoured cotton fabric was purchased from Rivatex East Africa Limited in Eldoret, Kenya and had the following characteristics: 72 ends/inch, 34 picks/inch, 28 Tex warp count, 128 g/m^2 and a thickness of 0.002 mm. Materials and reagents for extraction phytochemical screening: ferric chloride, potassium hydroxide, hydrochloric acid, sodium hydroxide, benzene, ammonia, ethanol (95%), methanol (99%), chloroform, acetic acid, sulphuric acid and Whatmann filter paper No. 1 were supplied by Centrihex Limited, Nairobi, Kenya. The standards for total flavonoid content and total phenolic content: pure gallic acid (99.5 %) and quercetin hydrate (99.5 %) were purchased from Loba Chemie Pvt Ltd, India and Gigma Aldrich respectively. Silver nitrate (99 %) was supplied by Science Lab, Nairobi, Kenya. Alamar blue was purchased from ThermoFisher Scientific (Waltham, MA, USA). Mueller Hinton agar, Mueller Hinton broth, gram-negative *E. coli* (ATCC 25922), gram-positive *methicillin resistant staphylococcus aureus* (*MRSA)* (33591), gram-positive *S. aureus* (ATCC 25923) and ampicillin (positive control) were purchased from Sigma-Aldrich (St. Louis, Mo, USA). All chemicals and reagents were of analystical grade and were used without further purification.

3.1.1 Preparation and Characterisation of Potato Peel and Potato Peel Powder

For control purposes, two sets of *Shangi* solanum tuberosum potatoes were used for this experiment. One set was collected from a farm in Tulwop village, Uasin Gishu County, Kenya; another set was purchased from the market in Eldoret town, Kenya. It

was important to have a set of potatoes planted under specific monitored conditions as the positive control, that is, the planting area (Tulwop); the planting time (from March to June); and the fertilizers used (NPK with nitrogen, phosphorus and potassium) and (DAP with diammonium phosphate). The potatoes from the market are the negative control because the planting conditions are not known. The potatoes were washed and then peeled using a ceramic peeler. The hand-peeling technique was used and it results in peels with some potato flesh on them. Although there is no way of standardizing the amount of flesh that remains with the peel, this technique was selected because it is the most preferred method by potato processing companies and potatoes peeled with this technique have similar characteristics (Javed et al., 2019). The peels were washed with distilled water, dried at 55°C for 12 hours and then ground to form a powder (Bhuvaneswari et al., 2017; Gebrechristos et al., 2020) as shown in Figure 3:1.

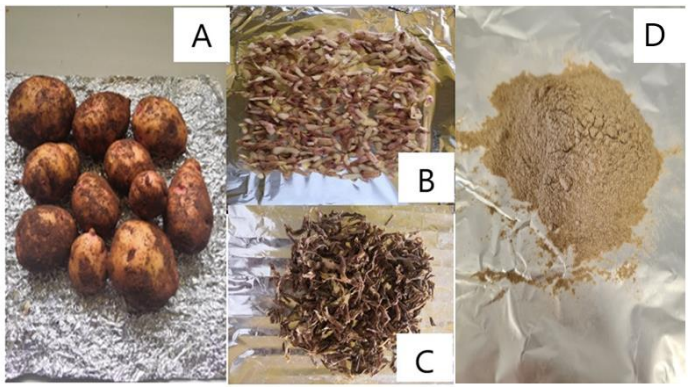

Figure 3:1. (A) *Shangi* Potatoes (B) Wet Potato Peels (C) Dry Potato Peels (D) Potato Peel Powder

The importance of using dried potato peels was demonstrated in a study conducted by (Alam & El-Nuby, 2019), in which phytochemical screening found a higher presence of bioactive compounds in dry potato peel samples compared to fresh ones. The removal of water from the peels through drying, results in peels with a higher

concentration of bioactive compounds. As a result, it is recommended that samples are dried before use.

Calculations were then made to determine the percentage potato peels attained from the potatoes as well as the moisture content of the potato peels using Equation 3.1 and Equation 3.2.

$$Percentage\ potato\ peels\ attained = \frac{W1}{W2} \times 100$$

Equation 3.1

Where: W1 is the weight of potato peels

W2 is the weight of unpeeled potatoes

$$Moisture\ content\ of\ potato\ peels\ (\%) = \frac{W1 - W4}{W1} \times 100$$

Equation 3.2

Where: W1 is the weight of potato peels before drying

W4 is the weight of potato peels after drying

3.1.2 Preparation of Potato Peel Extracts

Different extracts were prepared from the potato peels from the farm and those purchased from the market using ethanol and water as solvents.

3.1.2.1 Extraction Using Ethanol

The preparation of the potato peel extract using ethanol solvent was carried out according to the methods reported by (Gebrechristos et al., 2020; Helal et al., 2020). A total of 10 grams of potato peel powder was extracted overnight on a magnetic stirrer at room temperature with 100 ml of ethanol. The sample was then sonicated in a digital ultrasonic machine (Rico Scientific Industries, New Delhi) and then filtered through 0.45 µm pore size filter paper. The residue from filtration was re-extracted using the

same method. The filtrates were all combined and then evaporated at 50 ℃ in a rotary evaporator. The extracted dried powder was weighed to determine the extraction yield using Equation 3.3 and then kept at 4 ℃ until use; this is the refrigeration temperature and is suitable to avoid any negative influence of temperature. The growth of bacteria is slowed down at temperatures below 4 ℃ thus preserving the extracts until use.

$$Extraction\ yield = \frac{WPE}{WPP} \times 100$$

Equation 3.3

Where: WPE is the weight of the dry potato peel extract

WPP is the weight of the potato peel powder

3.1.2.2 Extraction Using Distilled Water

The preparation of aqueous potato peel extract from distilled water was carried out according to the methods used by (Gebrechristos et al., 2020; Helal et al., 2020) with modifications, as follows. 10 grams of potato peel powder was dispersed in 100 ml distilled water at 50 ℃ while stirring for 60 minutes using a magnetic stirrer to obtain a homogenous solution. The solution was sonicated in ultrasonic equipment at 50 ℃ for 20 minutes. The extracts were then chilled, filtered first with Whatman number one filter paper and then at a pore size of 0.45 µm. The residue was re-extracted and filtered under the same conditions. The different filtrates were combined and then freeze-dried using the SP Scientific BenchTop Pro freeze-dryer at -54.5 ℃ for 48 hours. The dried extracts were weighed to determine the extraction yield using Equation 3.3 and then stored at 4 ℃ until use.

3.1.3 Characterisation of the Potato Peel Extracts

3.1.3.1 Qualitative Phytochemical Screening of the Potato Peel Extracts

Phytochemical screening of both the aqueous extract and the ethanolic extract was done using several qualitative analysis techniques to determine the presence of secondary metabolites in the potato peel extracts. Tests were done to determine the presence of saponins, tannins, alkaloids, quinones, glycosides, steroids, flavonoids, phenols, anthraquinones, terpenoids, sterols and cardiac glycosides.

i. Test for saponins

The frothing test was used for testing for saponins. Approximately 10 ml of the potato peel extract was mixed with 5 ml of distilled water. The mixture was then shaken vigorously and then observed for changes. A persistent froth indicated the presence of saponins (Senthilkumar et al., 2018).

ii. Test for tannins

The ferric chloride test was used according to the method outlined in (Melkamu & Bitew, 2021). Briefly, 1 ml of the potato peel extract solution was mixed with 2 ml of distilled water and then 4 drops of ferric chloride solution were added to it. The formation of a blue-black colour confirmed the presence of tannins in the extracts.

iii. Test for alkaloids

The Hager's test was used to determine the existence of alkaloids in potato peel extract. The test was done according to the method described by (Kancherla et al., 2019) with modifications. 1 ml of solution of the potato peel extract was placed into a test tube and then 1 ml of Hager's reagent, that is, saturated ferric solution was added to it. The formation of a yellow-coloured precipitate confirmed the presence of alkaloids in the potato peel extracts.

iv. Test for quinones

The test for determining the presence of quinones in the potato peel extracts was done using the Alcoholic Potassium Hydroxide test. In this method 1 ml of the potato peel extract was mixed with three drops of alcoholic potassium hydroxide. The red to blue colour confirmed the presence of quinones in the extract (Shaikh & Patil, 2020).

v. Test for glycosides

A modified Bontrager's test method was used for testing the presence of glycosides in the extracts. 1 gram of the crude of the extract was placed in a test tube and then dissolved in 5 ml of dilute hydrochloric acid. 5 ml of 5% ferric chloride solution was then added and the mixture was shaken and then placed over a hot water bath. It was then allowed to boil for 10 minutes, cooled and then filtered. The resultant mixture was extracted again using benzene and an equal quantity of ammonia solution was added to the benzene extract. The appearance of a pink colour confirmed the presence of glycosides in the potato peel extracts (Shaikh & Patil, 2020).

vi. Test for flavonoids

For the determination of the presence of flavonoids, the alkaline reagent test was used (Abubakar & Haque, 2020). In this test 1 ml of extract was placed in a test tube then a few drops of sodium hydroxide solution were added and the mixture was shaken. The appearance of an intense yellow colour that turned to colourless after adding dilute acid indicated the presence of flavonoids in the potato peel extracts.

vii. Test for phenols

The Ferric Chloride test outlined in (Senthilkumar et al., 2018) was used to determine the presence of phenols in the extracts. Approximately 5 ml of the potato peel extract was mixed with a few drops of 5 % ferric chloride solution. The colour-change to dark green confirmed the presence of phenolic compounds in the extract.

viii. Test for anthraquinones

The Bontrager's test was used for determination of the presence of anthraquinones in the extract. Approximately 3 ml of the potato peel extract was mixed with 3 ml of benzene and then filtered. About 5 ml of 10 % ammonia solution was then added to the filtrate. The presence of a red, pink or violet colour after shaking, confirmed the presence of anthraquinones in the extract (Senthilkumar et al., 2018).

ix. Tests for terpenoids, sterols and steroids

The presence of terpenoids and steroids was determined using the Salkowski test. About 2 ml of chloroform was added to 5 ml of the potato peel extract. 3 ml of concentrated sulphuric acid was then added to form a layer. The formation of a reddish brown colour at the interface indicated the presence of terpenoids in the extract (Senthilkumar et al., 2018). The presence of steroids and sterols is shown by a red colour on the lower layer (Melkamu & Bitew, 2021; Shaikh & Patil, 2020).

x. Test for cardiac glycosides

The Keller-Killani test method was used to determine the presence of cardiac glycosides in the extract. 2 ml of the potato peel extract was treated with 0.5 ml of glacial acetic acid and 2-3 drops of 5% ferric chloride. 1 ml of concentrated sulphuric acid was added along the sides of the test tube. The formation of a blue colour in the acetic acid layer of the solution indicated the presence of cardiac glycosides (Kancherla et al., 2019).

3.1.3.2 Quantitative Analysis

Total Phenolic Content

The total phenolic content of the extracts was determined using the Folin and Ciocalteu reagent method using gallic acid as the standard as outlined by (Chandra et al., 2014). In this method 0.2 ml of potato peel extract was mixed with 0.2 ml of Folin-Ciocalteu's

reagent (1:10 in distilled water) and 0.6 ml distilled water. The mixture was made to stand for 5 minutes after which 1 ml of 7.5% sodium carbonate was added to it and then distilled water to make the volume up to 3 ml. The reaction was incubated in the dark at room temperature for 30 minutes. The absorbance of the blue colour from the different samples was measured at a wavelength of 765 nm using the Beckman Couter DU720 general purpose UV/Vis spectrophotometer against a prepared blank. All of the tests were done in triplicate and the phenolic content was calculated as gallic acid equivalents GAE/g of the potato peel powder using a standard calibration curve of gallic acid at different concentrations in the range of 5 – 30 mg/L.

Total Flavonoid Content

The total flavonoid content (TFC) of the extracts was determined using the aluminium chloride colorimetric complex forming assay according to the procedure used by Mohdaly et al., 2010 and Sulastri et al., 2018. Quercetin was used as the standard to make the calibration curve. Briefly, a stock solution of 100 µg/L was created by dissolving 0.01 g of quercetin in 100 ml of methanol. Standard solutions containing 5, 10, 20, 40 and 80 µg/mL were prepared by serial dilution. 1.5 ml of methanol, 0.1 ml of 10 % aluminium chloride, 0.1 ml of 1 M potassium acetate and 2.8 ml of distilled water were combined with 0.5 ml of each of the concentrations of standard solutions and 0.5 ml of each sample solution. The mixture was incubated for an hour at room temperature while being shaken periodically. Using a Beckham Coulter DU 720 UV-Vis Spectrometer (Beckham Coulter Inc, USA) set to a fixed wavelength of 420 nm, the absorbance of the reaction mixtures was measured against a prepared blank reagent. The quercetin standard absorbances were used to create a calibration curve, from which the TFC of the extracts; measured as the milligram quercetin equivalents per gram of

dry weight (mg QE/g DW) of the potato peel extracts was derived (Mohdaly et al., 2010; Sulastri et al., 2018).

3.1.3.3 Fourier Transform Infrared Spectroscopy (FTIR)

Dry aqueous potato peel extract was used for the identification of the active components of the extract using the FTIR. A KBr pellet was prepared from the dry extract and was characterised by a Jasco FT/IR-6600 type A equipped with a standard light source and a triglycine sulphate (TGS) detector. Spectrum was obtained at a resolution of 4 cm^{-1} and scans ranging from a wavelength of 400 cm^{-1} to 4000 cm^{-1}.

3.1.3.4 Thermal Analysis

Thermal analysis of the potato peel extracts was performed using thermogravimetric analysis (TGA). A simultaneous TGA/DSC analyser was used to investigate the thermal degradation of the potato peel extracts between room temperature and 800 ℃. Experiments were carried out with a sample size of 5 mg and at a heating rate of 10 ℃/ minute. Results for TGA analysis were presented graphically.

3.1.4 Antibacterial Tests of the Extracts

3.1.4.1 Agar Well Diffusion Assay

The agar well diffusion method was used to examine the antibacterial properties of the potato peel extracts according to the method described by (Balouiri et al., 2016; Gebrechristos et al., 2020). Gram-negative *E. coli* (ATCC 25922), and gram-positive MRSA (33591) and *S. aureus* (ATCC 25923) were used as references for the antibacterial assay of the potato peel extracts. *MRSA* is a prevalent, highly virulent infectious agent, causing high morbidity and mortality rates; it easily becomes resistant to new therapeutic agents (Raygada & Levine, 2009). *S. aureus* causes toxic shock, wound infections and other diseases and *E.coli* is responsible for a number of infectious diseases (Frickmann et al., 2019); therefore, it is important to determine the efficacy of

the extracts against these bacterial strains. Mueller Hinton agar (38 g) was dissolved in 1 litre sterile deionized water and then autoclaved at 121 ℃ for 30 minutes in a Huxley vertical type steam sterilizer HL340, supplied by Gemmy Industrial Corp, Taiwan. The media was cooled to a temperature of 50 ℃ under a laminar flow, poured into sterile petri-dishes and then left in the laminar flow until the nutrient agar solidified.

The suspensions of the bacteria were cultured in broth and then diluted until they met the 0.5 McFarland threshold for turbidity which is approximately 1 x 10^8 CFU/ml (CLSI, 2012). The turbidity was determined by testing the optical density of the suspension at 600 nm (OD600) using the UV-Vis; a 0.5 McFarland standard should have an OD600 between 0.07 and 0.1 (Daly et al., 2018). The Mueller Hinton agar plates with a diameter of 92.4 mm were then inoculated with bacterial strain of approximately 1 x 10^8 CFU/ml, under sterile conditions. Wells of approximately 6 mm diameter were made in the solidified agar and 50 µl of the potato peel extract was poured into each well. The petri dishes were kept at room temperature for about an hour to allow the extracts to diffuse onto the agar. They were then incubated in a Forma Scientific water jacketed incubator (model number 3164), at 37 ℃ for 24 hours after which the zone of inhibition was measured using a ruler in mm to determine the inhibitory effects of the extract. The samples that showed a distinct zone of inhibition were then used to calculate the minimum inhibitory concentration (MIC). All tests were carried out in triplicate.

3.1.4.2 Minimum Inhibitory Concentration (MIC) Assays

The minimum inhibitory concentration assay determines the minimum concentration of a specific antimicrobial agent required to inhibit the growth of bacteria. The MIC assay in this study was carried out using the broth microdilution method that was reported by (Tyavambiza et al., 2021). In the agar well diffusion test, samples displayed

a distinct zone of inhibition against *E. coli* and *S. aureus* but there was no zone of inhibition against MRSA. Therefore, MIC was determined against *E. coli* and *S. aureus*. 96 well plates were used for the assay; 50 µl of potato peel extract diluted in broth were added to the wells in decreasing concentrations, that is, 10 mg/ml, 5 mg/ml, 2.5 mg/ml, 1.25 mg/ml, 0.62 mg/ml and 0.31 mg/ml.

Microbial suspensions of the bacteria were cultured in broth and diluted to a 0.5 McFarland standard and then a volume of 50 µl of the suspension was added to each well containing broth and extract. The positive control used was ampicillin (10 mg/ml) a known antimicrobial agent and the negative control was deionized water with no antimicrobial treatment. Incubation of the well plates was done at 37 ℃ for 24 hours. Following incubation, 10 µl of alamarBlue™ dye was added to each of the wells after which the plate was incubated in the dark for 3 hours. In the presence of viable bacteria, the non-fluorescent alamarBlue™ dye (resazurin) was reduced to resofurin which emits a pink fluorescence, a colour change that can be observed visually. The colour change from blue to pink therefore indicated the existence of bacterial growth in the wells while a blue colour indicated the inhibition of bacterial growth (Henshaw, 2018). The MIC was concluded as the lowest concentration of the potato peel extract that was required to inhibit bacterial growth.

3.2 Green Synthesis of Silver Nanoparticles Using Potato Peel Extract

The green synthesis of silver nanoparticles involved the mixture of silver nitrate with potato peel extract for the reduction of the silver ions to silver nanoparticles according to the method described by Seifipour 2020. Briefly, 300 µl of 1mM silver nitrate solution was poured into an Eppendorf tube and brought to a temperature of 100 ℃. Potato peel extract was then added to it to make a volume of 400 µl and the mixture shaken in the dark on an Eppendorf, Themomixer Comfort (Merck Chemical (Pty) Ltd,

South Africa) at 500 rpm for 1 hour. Visually, the colour change of the mixture from colourless to a yellowish-brown colour indicated the formation of silver nanoparticles (H. M. M. Ibrahim, 2015; Rautela et al., 2019). The phytochemicals in plant extracts such as phenols and flavonoids act as reducing agents in the synthesis of silver nanoparticles. Plants differ in phytochemical composition (Mohammadi Bazargani et al., 2021), and thus in their ability to synthesize nanoparticles. As a result, it is critical to optimize the synthesis of nanoparticles from each plant extract.

3.2.1 Single Factor Varying of Parameters for Nanoparticle Synthesis

The effect of different parameters was studied by varying one parameter at a time while keeping the other parameters constant (Mahiuddin et al., 2020; Rao & Tang, 2017; Seifipour et al., 2020). This was done by observing the surface plasmon resonance (SPR) peaks of the solutions on the Beckham Coulter DU 720 UV-visible absorption spectrophotometer. A peak in the range of 400 - 500 nm indicated the presence of silver nanoparticles (J. M. Ashraf et al., 2016; De Leersnyder et al., 2020). For each of the parameters, the value with a peak that displayed higher intensity, that is a higher absorbance value and lower polydispersity observed by a narrower peak was selected for the next stage of experiments.

3.2.1.1 Concentration of Extract

The concentration of the extract affects the amount of phytochemicals available for the reduction of silver nitrate thus affecting the rate of synthesis of nanoparticles (H. M. M. Ibrahim, 2015). Potato peel extracts of different concentrations were prepared by serial dilution (100 %, 50 %, 25 %, 12.5 % and 6.25 %). Serial dilution was done by diluting 1 ml of the extract with distilled water at a ratio of 1:1 to form an extract of 50 % water and 50 % extract; the same method was repeated until the PPE was at a concentration of 6.25 %. The different PPE concentrations were then used for the green synthesis of

silver nanoparticles using the method outlined in the previous section. The temperature was kept constant at 100 ℃, and the solution thoroughly mixed at 500 rpm for 1 hour. The presence of silver nanoparticles was observed both visually and from the UV-vis spectra. The optimum extract concentration was used for the subsequent experiments.

3.2.1.2 Extract to Silver Nitrate Volume Ratio

Different volume ratios of the silver nitrate to potato peel extract were used to determine the effects of the silver nitrate ratio on the synthesis of silver nanoparticles as shown in Table 3.1 (Kaur et al., 2021; Mahiuddin et al., 2020). All other parameters were kept constant and the SPR peak was used to determine the optimum extract to silver nitrate ratio which was used for the next experiments.

Table 3:1.Potato Peel Extract to Silver Nitrate Volume Ratio

Potato peel extract to silver nitrate volume ratio	1 mM silver nitrate solution (µl)	Potato peel extract (µl)
1:1	200	200
1:2	133	267
1:3	100	300
1:4	80	320
1:5	67	333
1:6	57	343
1:7	50	350

3.2.1.3 Combined Effect of pH and Temperature

To evaluate the effect of pH on the green synthesis of silver nanoparticles, different pH values were used for the synthesis. The pH of the potato peel extracts was measured and found to be 5.8, which is acidic. Studies have shown that an alkaline extract is more suitable in the green synthesis of silver nanoparticles (Kredy, 2018; Velgosová et al., 2016). Therefore, values higher than 5.8 were varied to determine the effect of pH, that is; 6, 7, 8, 9, 10, 11 and 12. To adjust the pH to acidic values, 1M hydrochloric acid was used and 1M sodium hydroxide was used to adjust the pH to alkaline values. The mixture containing the silver nitrate and the potato peel extract at a volume of 400 µl

and in the optimum silver nitrate to PPE ratio determined in the previous section; was thoroughly mixed for 1 hour at different temperatures (100 ℃, 70 ℃, 50 ℃ and 25 ℃). The SPR peaks were observed on the UV-vis and the optimum pH and temperature were used for the next stage of experiments.

3.2.1.4 Effect of Stirring Speed

The rate of stirring is critical in the formation of silver nanoparticles. When the stirring rate is too slow or too fast, it can result in the formation of larger nanoparticles and agglomeration (Junaidi et al., 2016). The green synthesis of the silver nanoparticles was done at different speeds, that is, 0 rpm, 300 rpm, 500 rpm and 700 rpm to determine the effect of reaction speed on the synthesis of nanoparticles. The other parameters were constant and were based on the results obtained in preceding experiments. The SPR peaks were observed on the UV-Vis and the optimum stirring speed was used for the subsequent experiments.

3.2.1.5 Synthesis Time

The effect of synthesis time was studied by incubating the reaction mixture and recording the UV-visible absorption spectra at different time intervals, that is, 10 minutes, 30 minutes, 1 hour, 2 hours, 3 hours and 4 hours (Mahiuddin et al., 2020). The optimum values of the extract concentration, PPE to silver nitrate ratio, pH of PPE, reaction temperature and stirring speed obtained in previous experiments; were used in the synthesis of the nanoparticles.

3.2.2 Washing and Drying of Nanoparticles

The PPE-AgNPs were synthesised using the determined optimum conditions. The obtained nanoparticles were then centrifuged at 10000 rpm for 20 minutes to separate them from the solution (Liaqat et al., 2022) using the Centrifuge 5417R (Hamburg,

Germany). The separated nanoparticles formed a pellet at the bottom of a supernatant solution as shown in Figure 3:2.

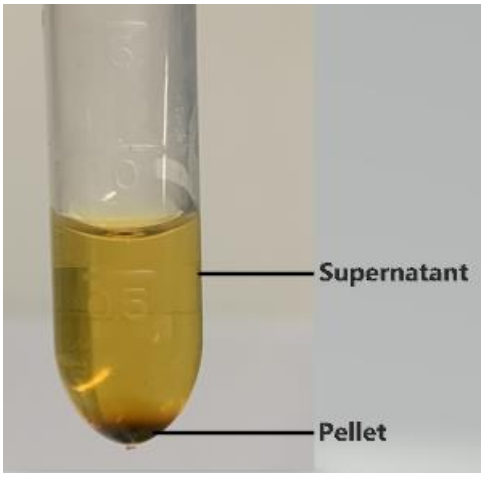

Figure 3:1. Separated Solution after Centrifugation

The pellet was resuspended in distilled water and centrifuged again to remove pollutants and any unreacted potato peel extract. The process was repeated three times for the formation of the washed silver nanoparticles, and the washed nanoparticles were then dried for 24 hours in an oven at 60 ℃ (Seifipour et al., 2020; Tyavambiza et al., 2021). The dried nanoparticles were stored in an air tight container in the dark for further analysis.

3.2.3 Characterisation of Nanoparticles

3.2.3.1 UV-Visible Spectroscopy

The POLARstar Omega microplate reader (BMG-Labtech, Ortenberg, Germany) UV-visible spectroscopy was used to confirm the presence of silver nanoparticles in solution by observing their surface plasmon resonance peaks. The samples were scanned at a wavelength range of 300 – 800 nm. A single peak in the 400 – 500 nm range indicated the presence of silver nanoparticles (J. M. Ashraf et al., 2016; Kredy, 2018).

3.2.3.2 Fourier Transform Infrared (FTIR)

FTIR analysis was performed to identify the bioactive compounds responsible for reducing silver ions to silver nanoparticles based on a previously reported method (Swidan et al., 2022). The dried silver nanoparticles were used to make a KBR pellet, which was then tested using a Jasco FT/IR-6600 type A equipped with a standard light source and triglycine sulfate (TGs) detector. The spectrum was obtained with a resolution of 4 cm^{-1} and scans ranging from 400 cm^{-1} to 4000 cm^{-1}. A comparison was made between the FTIR spectra of the green synthesized silver nanoparticles and that of the potato peel extract in order to identify potential biomolecules involved in the reduction of Ag^{+} to Ag^{0} nanoparticles (Liaqat et al., 2022).

3.2.3.3 Dynamic Light Scattering (DLS)

The DLS technique was used to determine the particle size distribution and zeta potential of the prepared silver nanoparticle suspension using the Zetasizer Nano ZS90 (Malvern, UK) with a size measurement from 0.3 nm to 5 microns using 90 degree scattering optics. A sample size of 1 ml was transferred into a cuvette and automatically equilibrated in the instrument for 2 minutes to measure the hydrodynamic diameter. The hydrodynamic diameter was determined by taking an arithmetic average of 5 runs. For the zeta potential analysis, 1 ml of the nanoparticle suspension was injected into a zeta cell and measured automatically (Clogston & Patri, 2011; Rao & Tang, 2017). All the information was recorded in triplicate.

3.2.3.4 X-Ray Diffraction (XRD)

The Rigaku Miniflex 600 x-ray diffractometer, which uses Cu-Kα radiation with a wavelength of 0.15406 mm and a scanning angle of 2θ from 0° to 100°, was used to reveal the crystallographic nature of the green synthesized silver nanoparticles. The

colloidal nanoparticles were deposited to form a thin film on a glass slide, allowed to dry, and then the XRD pattern was recorded (Almatroudi, 2020).

3.2.3.5 Scanning Electron Microscopy (SEM)

The Zeiss high resolution electron microscope equipped with energy dispersive spectroscopy was used to examine the morphological properties of the green synthesized nanoparticles. The samples were prepared by affixing the powdered nanoparticles to the sample holder with a conducting carbon strip and then placing them in the electron microscope's vacuum chamber. The SEM images were then captured at a voltage of 5.0 kV and magnification from 100 X to 100.00 K X (Khan et al., 2019; Rautela et al., 2019).

3.2.4 Antibacterial Efficacy of the Nanoparticles

3.2.4.1 Agar Well Diffusion Assay

The agar well diffusion method was used to assess the antibacterial activity of the biosynthesised silver nanoparticles according to the method described in previous studies (Balouiri et al., 2016; H. M. M. Ibrahim, 2015). Efficacy was tested against three different bacterial strains, that is, gram-negative *E. coli*, gram positive *S. aureus* and gram-positive MRSA as described in section 3.1.4.2. Ampicillin (10 mg/ml) was used as the positive control and distilled water as the negative control. The zone of inhibition was measured in millimetres and was used to assess the antibacterial efficacy of the green synthesized nanoparticles. Samples with a distinct zone of inhibition were used to determine the minimum inhibitory concentration (MIC). All tests were done in triplicate.

3.2.4.2 Minimum Inhibitory Concentration

The microdilution method outlined in a previous study (Tyavambiza et al., 2021), was used to determine the minimum inhibitory concentration of the green synthesized nanoparticles against *E.coli* and *S.aureus* as described in section 3.1.4.2. Deionized water was used as the negative control and ampicillin (10 mg/ml) was used as the positive control. The MIC was determined by the colour change on addition of alamarBlue™ to an incubated mixture of bacteria, broth and nanoparticle solution in different concentrations. The colour-change from blue to pink indicated the presence of bacterial growth in the wells, whereas blue indicated the inhibition of bacterial growth. The MIC was determined to be the lowest concentration of the silver nanoparticles required to inhibit bacterial growth.

3.3 Assessment of Antibacterial Efficacy of Treated Fabrics

3.3.1 Application of the Potato Peel Extract onto the Textile Fabric

The application of the potato peel extract was done in two stages based on methods used by (Ketema & Worku, 2020; Rajendran et al., 2011). First, the cotton fabric was treated with 6 % citric acid at 60 ℃ for 20 minutes. This served as the catalyst for the crosslinking of the potato peel extract and the cotton fabric. The fabric was then immersed in the prepared extract solution at 9 % of weight of fabric (o.w.f) and the mixture was brought to a boil over an 80 ℃ water bath for 30 minutes. The treated fabric was removed from the solution, allowed to cool, gently washed in cold water and then air dried. One set of the treated fabric was stored for further analysis and another set was washed according to ISO 105C10:2006 and then used to assess the durability of the treated samples to laundering.

3.3.2 In-Situ Synthesis of Silver Nanoparticles onto Textile Fabrics

Deposition of the silver nanoparticles onto the cotton fabric was done by a one-pot in-situ synthesis method with 1 mM silver nitrate solution as the precursor and potato peel extract as the reducing agent according to methods outlined by several researchers and based on the optimum conditions attained in the synthesis of the silver nanoparticles (Aladpoosh et al., 2014; H. Liu et al., 2014; Shaheen & Abd El Aty, 2018). Bleached, mercerized and scoured 100 % cotton fabric were first washed with non-ionic detergents at 60 ℃ for 40 minutes. The fabric was cut into pieces of approximately 300 mg and were placed in tubes containing 333 µl of 1 mM of silver nitrate solution. The mixture was heated on a stirrer to 50 ℃ and then 67 µl of potato peel extract; previously prepared to 25 % concentration and a pH of 12, were added to the mixture. The mixture was stirred at a speed of 500 rpm for 3 hours (See Figure 3:3).

Figure 3:1. Direct In-Situ Synthesis of Nanoparticles onto Cotton Fabric

When the reaction was complete, the fabrics were rinsed to remove any excess reagents on the fabric. The colour changes of the cotton fabrics from white to golden brown indicated the successful in-situ synthesis of the silver nanoparticles onto the fabric. The wet treated samples were dried in a drying cabinet at room temperature for 24 hours. The samples were then used for the fabric disc diffusion assay against *E. coli* and *S. aureus* to qualitatively determine the antibacterial properties of the treated fabrics.

3.3.3 Qualitative Efficacy Testing of the Treated Fabrics Against Bacteria

The agar disc diffusion assay was performed for the efficacy testing of the treated fabrics against bacteria according to the method outlined by (Jain et al., 2022). Briefly, a loop of bacterial cultures that had been grown overnight was uniformly streaked on nutrient agar plates, according to the method described in section 3.1.4.1. Treated and untreated fabrics were cut into 6 mm discs and placed in the centre of bacteria-streaked nutrient agar plates. The plates were then incubated at 37 ℃ for 16 – 18 hours. The zone of inhibition that appeared around the fabric discs after incubation was measured in millimetres. Discs impregnated in antibiotic were used as the positive control. All experiments were carried out in triplicates for each of the bacterial strains.

3.3.4 Experimental Design for In-Situ Synthesis of Nanoparticles onto Cotton Fabrics

A four-factor inscribed central composite design was used to identify the relationship existing between the response functions and the process variables in the in-situ synthesis of nanoparticles onto cotton fabrics. A rotatable design was used and the factors were tested at 5 levels with 20 runs and 3 replicas. The optimum reaction time in the green synthesis of silver nanoparticles using potato peel extract was found to be 3 hours. However, studies have shown that cotton aids in the in-situ synthesis of silver nanoparticles due to the presence of the hydroxyl groups in cellulose that act as reducing agents in the synthesis of silver. These groups also make the cotton fibre ideal for binding of metal ions onto the surface and may potentially reduce the reaction time (Haji et al., 2013; Tania et al., 2019). Therefore, the reaction time was varied from 1 hour to 3 hours. Earlier research has shown that curing of fabrics treated with silver nanoparticles can be done effectively at temperatures ranging from 110 ℃ to 180 ℃ and may be lower or higher depending on the curing time, the fabric used and the end

use (Fouda & Shaheen, 2017; Hebeish et al., 2011). In order to get the most suitable curing temperature, the values were varied from 80 ℃ to 180 ℃. The factors that were varied, their levels and their coding are shown in Table 3:2.

Table 3:1. Factors that were Varied in the Application of Nanoparticles onto Fabric

FACTOR	Coding	LOWER LIMIT	UPPER LIMIT
Reaction Time	X2	1 hour	3 hours
Curing Temperature	X3	80 ℃	180 ℃
Incubation Time	X4	0 hours	72 hours

The factors and levels for the application of the nanoparticles onto cotton fabric are shown in Table 3:3.

Table 3:2. Factors and Levels for the In-Situ Synthesis of Silver Nanoparticles onto Cotton Fabric

Factors		Levels				
		-α	Low	Medium	High	+α
Coding		-1.682	-1	0	1	1.682
Synthesis Time (hours)	X1	1	1.4	2	2.6	3
Incubation Time (hours)	X2	0	15	36	57	72
Curing Temperature (℃)	X3	80	100	130	160	180

Using the experimental design, the in-situ synthesis of the nanoparticles was done according to the method in section 3.3.2 with modifications in the reaction time, incubation time and curing time based on the values acquired in the experimental design in Appendix A. The reaction was carried out for periods ranging from 1 to 3 hours based on the experimental designed. When the reaction was complete, the fabrics were incubated in their solutions and in the dark for periods ranging from 0 to 72 hours, according to the experimental design shown in Appendix A. The cotton fabrics that had

been loaded with silver nanoparticles were then rinsed with distilled water to remove any excess reagents on the fabric. The wet treated samples were dried in a drying cabinet at room temperature for 24 hours. Following drying, the samples were cured for 5 minutes at temperatures ranging from 80 ℃ to 180 ℃, according to the experimental design shown in Appendix A. The wet treated samples were dried in a drying cabinet at room temperature for 24 hours. The samples were then used for the bacterial reduction assay against *E. coli* and *S. aureus*.

Experimental responses of antibacterial efficacy of the fabrics before washing and loss in antibacterial activity after washing were considered using regression analysis to predict the optimum and interaction effects. The untreated fabric was used as the negative control and fabric treated with ampicillin was used as the positive control.

3.3.5 Quantitative Antibacterial Testing of Treated Fabrics

Antibacterial testing was performed quantitatively using the ISO 20743:2021 method for the determination of antibacterial activity of textile products. The absorption method was used to determine the antibacterial effectiveness of the treated fabrics against gram-negative *E. coli* and gram-positive *S. aureus*. The treated and untreated fabrics were cut into sample sizes with a mass of approximately 0.4 g (test specimen). Six test specimens of the untreated fabric (control) and six test specimens of the treated fabrics were used. Three control samples and three antibacterial samples were used immediately after inoculation for zero time. The remaining six specimens were used for contact time after the incubation period. The samples were sterilized by autoclaving; then 0.2 ml of the bacterial suspension was soaked into several points on each test specimen. This was followed by shaking out in 20 ml of saline; five serial dilutions were then prepared repeatedly by adding 1 ml of the shake out bacteria into a test tube containing 9 ml of

nutrient broth and shaken well. Thereafter 1 ml of the last dilution was added to each petri dish followed by 15 ml of Mueller Hinton agar and then incubated at 37 ℃ for 24 hours. After incubation, the number of colonies on the petri dishes were counted. The antibacterial treatment's efficacy was determined by comparing the reduction in the number of bacteria on the treated sample to that of the control sample expressed as a percentage reduction as shown in Equation 3.4.

$$R\% = \left(\frac{B - A}{B}\right) X\ 100$$

Equation 3.4

Where: R% is the percentage reduction of bacteria; A is the number of bacteria recovered from the inoculated treated fabric samples after 24 hours incubation; B is the number of bacteria recovered from the inoculated control fabric samples after 24 hours incubation.

3.3.6 Durability to Washing

The fabric samples were washed according to ISO C10:2006 wash fastness standard procedure. Washing was done at 70 ℃ for 45 minutes with 100 steel balls, which is equivalent to 5 regular washes. This was followed by a 10 - minute hot rinsing in plain water at 40 ℃. Thereafter, the fabrics were air-dried in a conditioned lab overnight. The washing procedure was repeated to give an equivalent of 10 and 20 regular washes. Antibacterial tests against *E. coli* and *S. aureus* were performed on the treated and washed fabric samples. The results were used in comparison to the unwashed treated fabrics to determine the durability of the fabrics to washing. The reduction in antibacterial efficacy was expressed as a percentage and calculated using Equation 3.5.

$$L\ \% = R_2\ \% - R_1\ \%$$

Equation 3.5

Where: L % is the Percentage loss in bacterial activity, R_2 % is the percentage bacterial reduction before washing and R_1 % is the percentage bacterial reduction after washing.

3.3.7 Statistical Analysis

Statistical analysis was performed using Design Software and Minitab Software. A regression model was generated representing the relationship between the response variables and the parameters. Analysis of variance (ANOVA) was used to determine the significance of the independent variables, that is, incubation time, synthesis time and curing temperature on the dependant variables, that is, percentage bacterial reduction before washing and percentage loss in bacterial activity after washing. Significance was set at a level of 5 %. Interaction plots, variance inflation factors, lack-of-fit, the optimum values and other statistical data analysis were calculated using the software.

In-situ synthesis of the cotton fabrics was then performed using the optimum values for synthesis time, incubation time and curing temperature. Quantitative antibacterial testing was performed on the treated fabrics before and after 20 washes to determine the effect of using the optimum conditions. The treated fabrics were then characterised for their different physical properties.

3.4 Characterisation of the Physical and Chemical Properties of the Treated Fabric Samples

3.4.1 Scanning Electron Microscopy

Morphological analysis of the fabric was assessed using the Zeiss high resolution scanning electron microscope equipped with energy dispersive spectroscopy. Sample sizes of 5 mm X 5 mm of both the treated and untreated fabrics were prepared were prepared and mounted on the conductive carbon strip and then sputter coated with gold (Jain et al., 2022). The deposition of the silver nanoparticles on the samples was then observed as images displayed on the SEM.

3.4.2 Fourier Transform Infrared (FTIR)

The presence of chemical bonding between the untreated cotton fabric and fabric treated with silver nanoparticles was determined using a Jasco FT/IR-6600 type A equipped with a standard light source and a triglycine sulphate (TGS) detector. A KBr pellet was prepared from ground fabric pieces and potassium bromide. The analysis was performed with the prepared KBr pellet and the spectrum was obtained at a resolution of 4 cm^{-1} and scans ranging from a wavelength of 400 cm^{-1} to 4000 cm^{-1}.

3.4.3 Thermogravimetric Analysis (TGA)

Thermogravimetric analysis was performed on a Simultaneous TGA/DSC analyser under air atmosphere at a heating rate of 10 ℃/ minute, with temperatures ranging from room temperature to 800 ℃. Samples were cut into very small powder like pieces and then placed in an aluminium oxide pan. Approximately 10 mg of the sample was used in each pan.

3.4.4 Air Permeability

Air permeability of the fabric samples was measured based on ISO 9237 using the Air Permeability Tester at standard atmospheric testing conditions. Measurements were performed under constant air pressure of (Pa) for a 20 cm^2 fabric. Five samples from each fabric were measured and an average value was determined. The air permeability was expressed as the speed of airflow through a given area of fabric and the results are presented in mm/second.

3.4.5 Tensile Strength

The tensile properties of the untreated cotton fabric and the fabric treated with silver nanoparticles tested using a Testometric Micro 500 model universal tensile tester in accordance with ISO 13934:2013 Textiles – Tensile properties of fabrics. Samples were preconditioned to standard atmospheric conditions and then cut into rectangular strips for testing. The samples were clamped on the machine with the longer side parallel to the direction to be tested. Testing was done at a speed of 100 mm/min. The fabric sample was stretched at a constant rate until it broke and the maximum breakage force was recorded. Five samples were measured and an average value determined.

CHAPTER FOUR: RESULTS AND DISCUSSION

4.1 Characteristics of the Potato Peel Extracts

4.1.1 Yield of Extraction

The extraction yields of both the ethanol and water extracts of potato peels were calculated using Equation. A higher percentage yield of 7.52 % was obtained with the water extract compared to a percentage yield of 5.75 % with the ethanol extracts. The trend is similar to what was observed by (Samarin et al., 2012), who discovered that the percentage extraction yield was positively correlated to the polarity of the solvents. Water had the highest percentage yield of 11.2 % in their study; this was followed by methanol at 7.9 % with ethanol having the lowest yield at 5.6 %.

4.1.2 Phytochemical Screening

The phytochemical screening of the different extracts of potato peels showed the presence of several secondary metabolites such as saponins, alkaloids, flavonoids, tannins, quinones, steroids, terpenoids, sterols, cardiac glycosides and phenols as shown in Table 4:1. However, glycosides were not present in both extracts while anthraquinones were not detected in the aqueous extract but were moderately present in the ethanol extract. Flavonoids and phenols, which are the main focus of this study were revealed to be present in both the aqueous and the ethanol extracts. This confirms results obtained by (Alam & El-Nuby, 2019) which confirmed the presence of different phytochemicals in potato peel water extracts; namely saponins, flavonoids, alkaloids, tannins, sterols, cardiac glycosides and triterpenoids. Other researchers also confirmed the presence of phenols, glycoalkaloids, flavonoids and anthocyanins in potato peels extracted with different solvents (Ben Jeddou et al., 2021; Elkahoui et al., 2018; Silva-Beltrán et al., 2017). There was no difference in the phytochemicals present in the

potato peel extracts from the farm and those purchased from the market. This could be explained by results from earlier studies showing that the genetic type of a potato has more effect on the phytochemical content than the planting conditions and the location (Lombardo et al., 2013; Reddivari et al., 2007). Therefore, since all potatoes used in the study were *Shangi* potatoes, it is expected that the potato peel extracts would contain the same phytochemicals.

Table 4:1. Secondary Metabolites Identified in Solanum Tuberosum Potato Peel Extracts

Constituents	**Inference**			
	Aqueous Extract		**Ethanol Extract**	
	Farm PPE	**Market PPE**	**Farm PPE**	**Market PPE**
Saponins	+++	+++	+	+
Tannins	+	+	+	+
Alkaloids	+++	+++	++	++
Quinones	++	++	++	++
Glycosides	-	-	-	-
Steroids	+	+	++	++
Flavonoids	+++	+++	+++	+++
Phenols	++	++	++	++
Anthraquinones	-	-	++	++
Terpenoids	++	++	++	++
Sterols	+	+	++	++
Cardiac Glycosides	+	+	+++	+++

Note: +++ represents very high, ++ indicates moderate, + indicates low/traces, and – indicates absent.

4.1.3 Total Phenolic Content

The total phenolic content of solanum tuberosum potato peel extract was determined using the Folin-Ciocalteu method. A calibration curve was prepared for quantitative analysis and the linearity for gallic acid standard was established from the range of 5 mg/L to 30 mg/L which was fitted on the line $y = 0.0381x + 0.010x$ with $R^2 = 0.9967$ as shown in Figure 4:1.

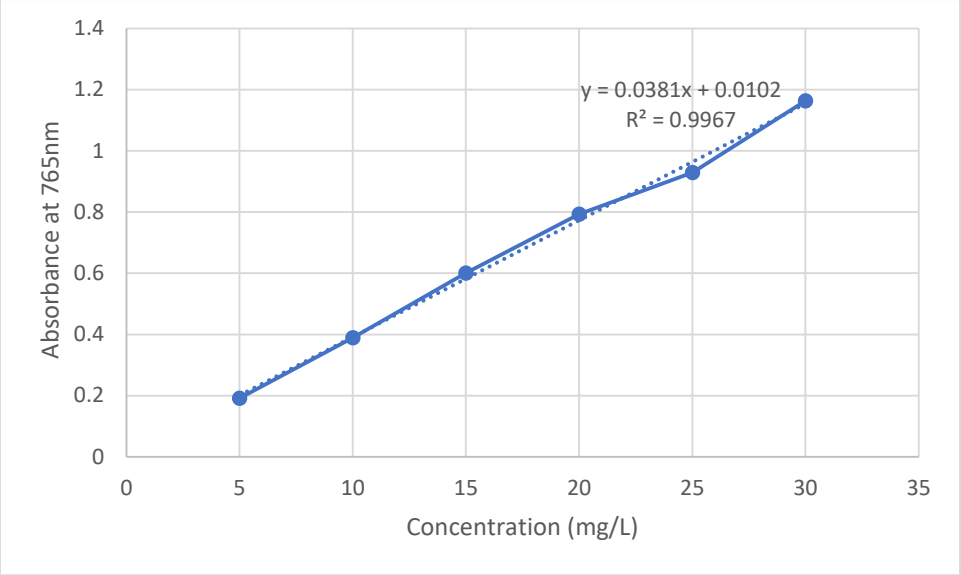

Figure 4:1. Gallic Acid Standard Calibration Curve

Calculations for the total phenolic content against gallic acid as the standard were then done by substitution using the linear Equation 4.1 from the gallic acid standard calibration curve.

$y = 0.0381x + 0.0102$ Equation 4.1

Where: x is the concentration of gallic acid and y is the absorbance.

Therefore: $x = (y - 0.0102) \div 0.0381$

Hence, the gallic acid equivalent for the aqueous extract with an absorbance of 0.449 is:

x = 11.517 mg GAE/g dry weight

The gallic acid equivalent for the ethanol extract with an absorbance of 0.315 is:

x = 8 mg GAE/g dry weight

The total phenolic content was higher for the aqueous extract with a value of 11.517 mg GAE/g DW as compared to a value of 8 mg GAE/g DW for the ethanol extract. An earlier study also revealed that the total phenolic content of potato peels was highest for ultrasonic water extracts when compared with ultrasonic extracts from methanol, acetone, ethanol and hexane (Samarin et al., 2012). Water is a polar solvent that can dissolve a wide range of substances and can therefore dissolve more substances than any other liquid.

4.1.4 Total Flavonoid Content

The aluminium chloride colorimetric method was used to determine the total flavonoid content of the extract using quercetin as the standard. The absorbance values that were obtained at various quercetin concentrations were used to create a calibration curve shown in Figure 4:2.

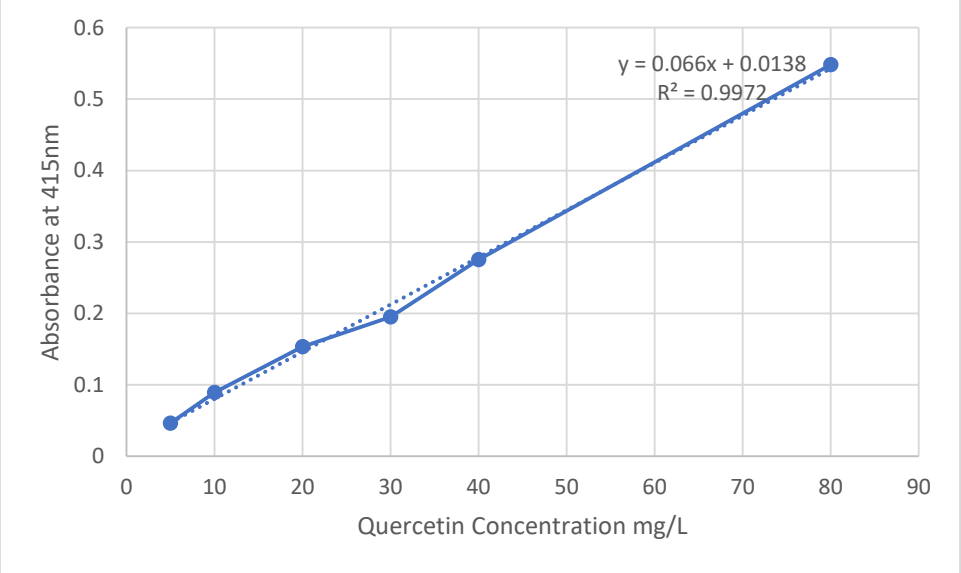

Figure 4:2. Quercetin Standard Calibration Curve

The total flavonoid content was then calculated against quercetin as the standard by substituting the linear equation (Equation 4.2) from the quercetin standard calibration curve.

$y = 0.066x + 0.0138$ Equation 4.2

Where: x is the concentration of quercetin and y is the absorbance.

Therefore: $x = (y - 0.0138) \div 0.066$

Hence, the quercetin equivalent for the ethanol extract with an absorbance of 0.202 is :

x = 2.85 mg QE/g dry weight

The quercetin equivalent for the water extract with an absorbance of 0.423 is:

x = 6.2 mg QE/g dry weight

The total flavonoid content was higher for the aqueous extract with a value of 6.2 mg QE/g dry weight as compared to a value of 2.85 mg QE/g dry weight for the ethanol extract which is agreement with results observed by (Samarin et al., 2012). Additionally, the total flavonoid content was lower than the total phenolic content for both extracts which supports the theory that flavonoids are also phenols and therefore contribute to the total phenolic content of the extracts (Mutha et al., 2021). This was also observed by several researchers including (Friedman et al., 2018; Mohdaly et al., 2010; Silva-Beltrán et al., 2017). Aside from the fact that water extracts have a higher total phenolic content, total flavonoid content and a higher yield than the ethanol extracts; the use of water as a solvent has numerous advantages as a green extraction solvent. Water is abundant in nature and thus economical; its non-toxicity, non-flammability, and low pollution in production make it popular as a green solvent. Therefore; based on the results and the advantages of using water as a solvent, the aqueous extracts were selected for further experiments in this study.

4.1.5 Fourier Transform Infrared Spectrum of Potato Peel Extract

The results from the FTIR characterisation of the potato peel extract are shown in Figure 4:3. The representative bands indicated the potential presence of the compounds shown in Table 4:2.

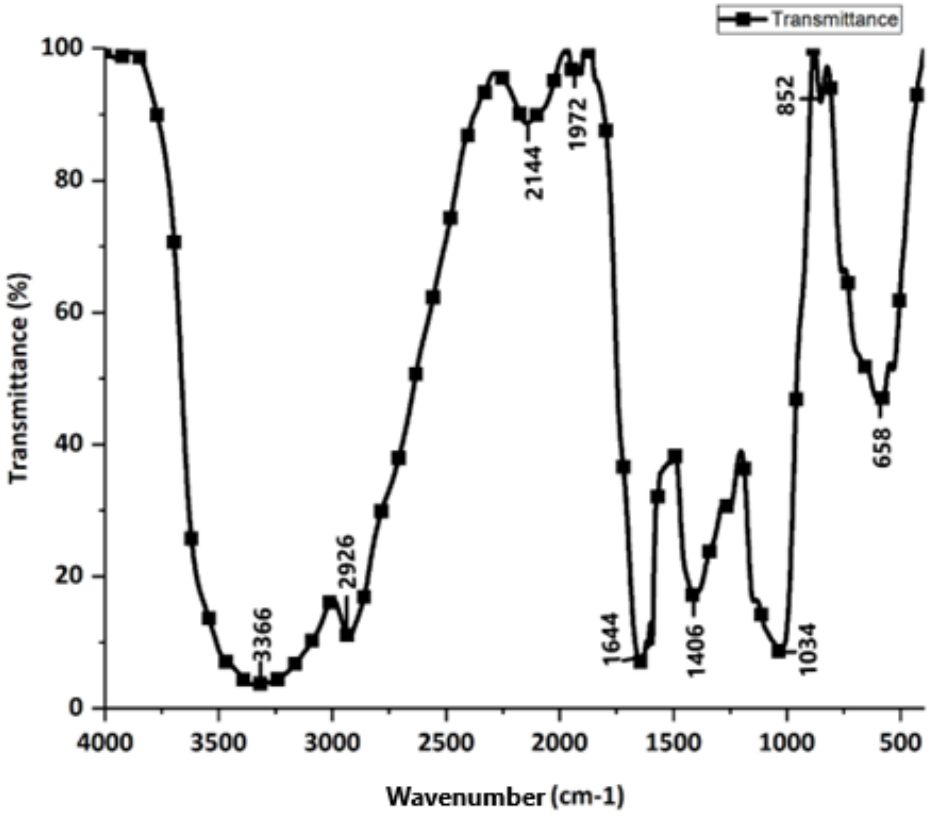

Figure 4:3. FTIR Spectrum for Potato Peel Extract

The peak at a wavelength of 3336 cm^{-1} is caused by the O-H stretching modes of the hydroxyl groups and is characteristics of cellulosic materials (Devi et al., 2018; Liang & McDonald, 2014). The absorption peak at 2926 cm^{-1} can be assigned to the stretching mode of aromatic C-H (El-Sakhawy et al., 2018). The peak at 1644 cm^{-1} is linked to aryl OH and can therefore indicate the presence of the phenyl group with conjugated systems such as ketoester, diketone and quinone. The same peak at 1644 cm^{-1} also indicates the existence of amides in the potato peels which can be linked to the proteins and lipids in the potato peels. The peak at 1406 cm^{-1} is the OH bend and is an indication

of the existence of phenols or tertiary alcohols in the potato peel extract (Nandiyanto et al., 2019). The absorption at 1032 cm^{-1} can be assigned to the C-O-C pyranose ring which is characteristic of saccharides thus indicating the occurrence of carbohydrates in the potato peels (El-Sakhawy et al., 2018). The weak absorption bands at 852 cm^{-1} to 658 cm^{-1} can be attributed to the tri and di distribution in the phenols (Devi et al., 2018). Overall, the FTIR spectra confirms the presence of carbohydrates, phenols, lipids and proteins in the potato peel powder.

Table 4:2. Characteristic IR Bands of Potato Peel Extracts

Wavenumber (cm^{-1})	**Band Assignment**	**Potential Compounds**
3336	O-H stretching	H-bonded hydroxyl groups
2926	Aromatic C-H bond	Methylene CH_2
2144	Aromatic C=C stretching mode	
1972	C=O bond	Carbonyls
1644	Combination of amide and aryl OH	Phenyl group and proteins
1406	OH bending	Phenols or tertiary alcohol
1032	C-O-C pyranose ring	Cellulose
852	Aromatic C-H	Aryl
658	OH, out of plane bending	Di and tri substitution in phenols

Source: ((Nandiyanto et al., 2019; El-Sakhawy et al., 2018; Devi et al., 2018)

With the major bonds being carbon or oxygen based, we can confirm that carbon and oxygen are the main elements in potato peels. This also supports elemental analysis studies conducted by (Bouhadjra et al., 2021) which revealed that the proportions of carbon and oxygen in potato peels were the highest when compared to other elements, thus confirming their organic nature. Additionally, it contains nitrogen and oxygen in lower quantities (Javed et al., 2019).

4.1.6 Antibacterial Activity of Potato Peel Extracts

4.1.6.1 Agar Well Diffusion

Antibacterial activity of the potato peel extracts was investigated against three bacterial strains, namely*; E. coli, S. aureus* and *MRSA* using disc diffusion method and the results are shown in Figure 4:4.

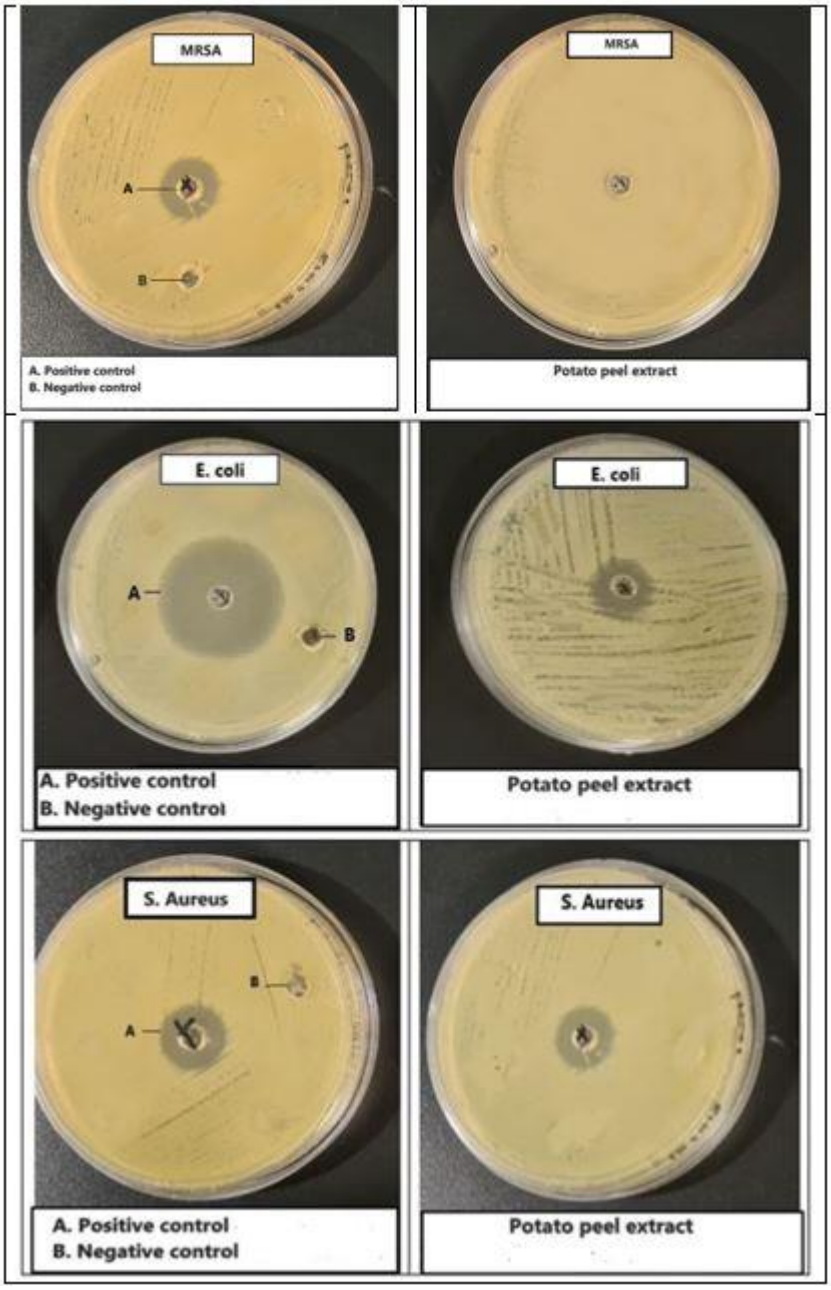

Figure 4:4. Test Results of Agar Well Diffusion of Potato Peel Extract Against *MRSA, E. coli* and *S. aureus*

Table 4:3 shows the results of the extract's antibacterial activity evaluation. The results revealed a distinct zone of inhibition against *E. coli* and *S. aureus*, but no distinct zone of inhibition against *MRSA. E. coli* had a larger zone of inhibition than *S. aureus*. In their study (Gebrechristos et al., 2020) confirmed the antibacterial activity of potato peel extracts against several bacteria strains including *E. coli* and *S. aureus*. The study revealed a clear zone of inhibition against *S. aureus* and a vague zone of inhibition against *E. coli*. Another study also confirmed the antibacterial efficacy of potato peel extracts against different bacterial strains; with a zone of inhibition of 7 mm and 2.5 mm against *S. aureus* and *E. coli* respectively (Helal et al., 2020).

Table 4:3. Zone of Inhibition of Potato Peel Extracts Against Selected Bacteria Strains

Bacterial Strain	Inhibition Zone (mm)
Staphylococcus aureus	5.60 ± 0.32
Escherichia coli	6.50 ± 0.09
Methicillin resistant staphylococcus aureus (MRSA)	0.00 ± 0.00

4.1.6.2 Minimum Inhibitory Concentration of the Potato Peel Extract

A microdilution minimum inhibitory concentration assay was used to accurately determine antimicrobial activity of the extracts against *S. aureus* and *E. coli*. When the concentration of potato peel extract fell below 5 mg/ml, the colour of alamarBlue™ dye changed from blue to pink, indicating the presence of bacteria (Henshaw, 2018). As a result, the minimum inhibitory concentration of potato peel extract for both *E. coli* and *S. aureus* was determined to be 5 mg/ml. The results are slightly higher for *Staphylococcus Aureus* and lower for *Escherichia coli* than those reported in an earlier study. They reported a positive antimicrobial response for *Escherichia coli*, *Staphylococcus aureus* and *salmonella enterica* with a minimum inhibitory concentration of 7.5 ± 2 mg/ml, 4.7 ± 1 mg/ml and 5.8 ± 2 mg/ml respectively but had

a negative response for *Listeria monocytogenes* and *Klebsiella pneumoniae* (Gebrechristos et al., 2020).

4.2 Formation of Silver Nanoparticles with Potato Peel Extract (PPE-AgNPs)

4.2.1 Visual Assessment of PPE-AgNPs

Silver nanoparticles have a strong absorption band and produce a specific colour in solution due to surface plasmon resonance (J. M. Ashraf et al., 2016). The colour change was used to track the formation of silver nanoparticles. The change in colour from a very light brown (Figure 4:5 A) to yellowish-brown in Figure 4:5 B confirmed the formation of silver nanoparticles (Ahmed et al., 2016). The mixture was had a very light and clear brown colour immediately after adding the potato peel extract to the silver nitrate solution. However, after 30 minutes, the colour changed to golden-brown, which intensified to a darker brown after 3 hours of reaction time (Figure 4:5 C).

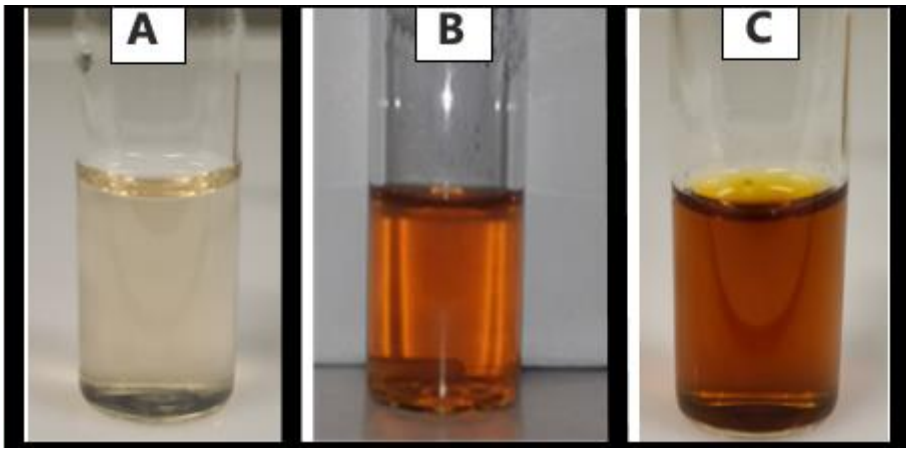

Figure 4:1. Visual Colour-Change of Synthesized Nanoparticles at (A) 0 minutes (B), 30 minutes and (C) 3 hours

The synthesis of silver nanoparticles was confirmed further by measuring the UV-Vis spectra at 300 – 800 nm. The PPE-AgNPs had a maximum absorbance (λmax) of around 420 nm, which is typical of silver nanoparticles. Silver nanoparticles have a

surface plasmon resonance (SPR) peak of around 400 – 500 nm (J. M. Ashraf et al., 2016; De Leersnyder et al., 2020). Lower wavelength SPR peaks indicate the formation of smaller nanoparticles while higher wavelength peaks indicate the formation of larger nanoparticles (Djuhana et al., 2016).

4.2.2 Effect of Synthesis Conditions on the Green Synthesis of Silver Nanoparticles

4.2.2.1 Effect of Extract Concentration

The effect of potato peel extract concentration on the green synthesis of nanoparticles was evaluated and the resultant UV-vis spectra is shown in Figure 4:6. The extract was used in the different concentrations provided at a silver nitrate to potato peel extract volume ratio of 1:5.

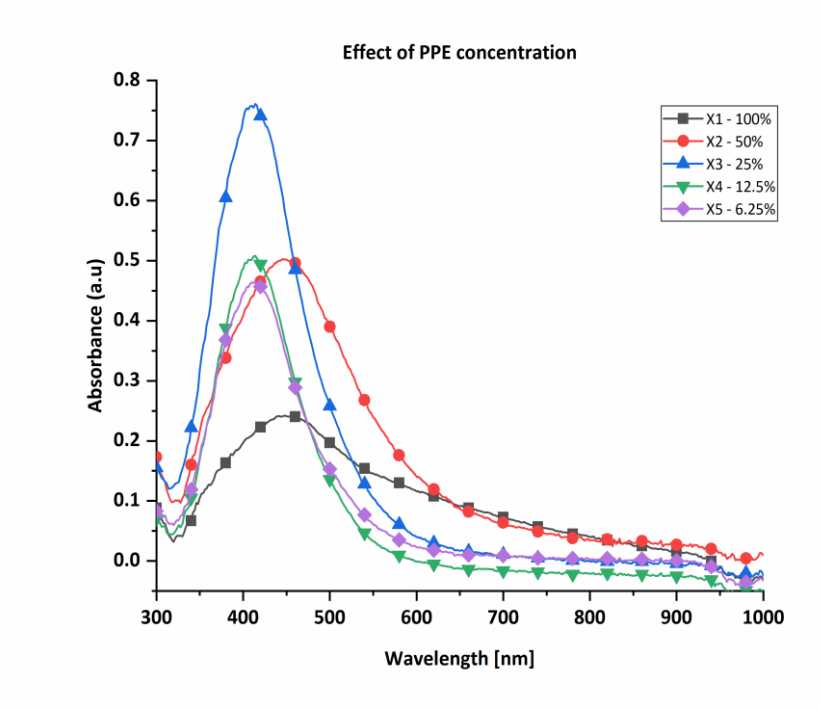

Figure 4:2. UV-Vis Absorption Spectra of Silver Nanoparticles Synthesized at Different Concentrations of Potato Peel Extract

As the plant concentration increased from 6.25 % to 25 % there was an increase in the absorbance of the UV-vis and the SPR peak was narrower. This was an indication of

the increased synthesis of nanoparticles, and the production of smaller nanoparticles with a uniform size distribution (Verma & Mehata, 2016). As the concentration increased, the phytochemical content also increased, thus increasing the reduction rate of the silver nitrate to silver nanoparticles (H. M. M. Ibrahim, 2015; Tyavambiza et al., 2021). However, at a concentration of 50 %, the SPR peak was broader which was an indication of polydispersity of the nanoparticles. This could be because the quantity of phytochemicals was too high and therefore the synthesis of nanoparticles was too rapid and led to aggregation of the nanoparticles and the formation of bulk silver (Kaur et al., 2021). The optimum extract concentration for the formation of smaller nanoparticles with a narrow size distribution was found to be 25 % and was therefore used in subsequent experiments.

4.2.2.2 Effect of PPE to $AgNO_3$ Volume Ratio

The effects of potato peel extract to silver nitrate volume ratio was studied by using different ratios for the synthesis, that is, 1:1, 1:2, 1:3, 1:4, 1:5, 1:6 and 1:7. The UV-vis spectra of the different reactions is shown in Figure 4:7.

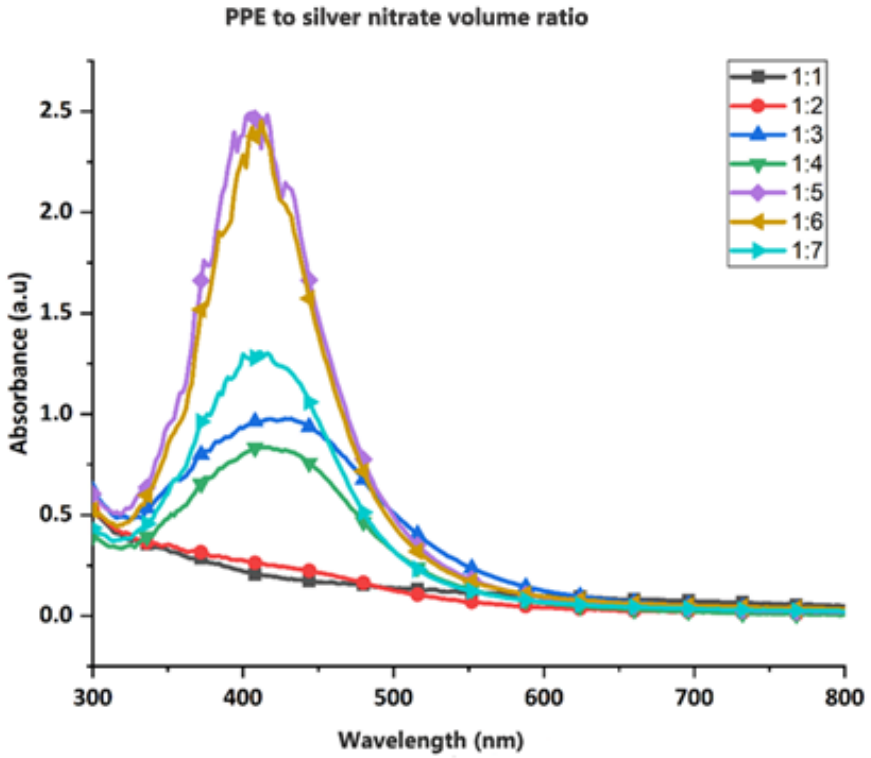

Figure 4:3. UV-Vis Absorption Spectra of Silver Nanoparticles Synthesized at Different Extract to Silver Nitrate Volume Ratios

From the observed UV-vis spectra, there was low reduction of Ag^{+} to Ag^{0} with little to no synthesis at volume ratios of 1:1 and 1:2 as shown by the broader SPR peak at a lower absorbance (Melkamu & Bitew, 2021). As the volume ratio of silver nitrate increased from 1:1 to 1:5 there was an increase in absorbance and intensity of the SPR peaks, thus higher amounts of nanoparticles were produced. The peaks became narrower due to the formation of smaller nanoparticles with a more uniform size distribution (Azarbani & Shiravand, 2020). This is in agreement with other studies that showed that for nanoparticle synthesis to occur, the volume ratio of silver nitrate should be higher than that of the extract. As the ratio increased to 1:6 the absorbance reduced and the peak became broader at a ratio of 1:7, indicating reduced synthesis and polydispersity. It is likely that as the volume ratio of the silver nitrate increases, there is insufficient potato peel extract for the reaction with silver ions, hence the reduced

synthesis (Mahiuddin et al., 2020). Therefore, 1:5 was used as the optimum volume ratio for further experiments.

4.2.2.3 Combined Effect of pH and Temperature

The UV-vis spectra of the nanoparticles synthesized at different pH at 99 ℃ is shown in Figure 4:8. The concentration of the nanoparticles formed in the solution increases as the pH of the extract becomes more alkaline, agreeing with previous studies that showed that alkaline conditions are more preferred for green synthesis of nanoparticles (Kaur et al., 2021; Kredy, 2018). Although all pHs showed nanoparticle synthesis at 99 ℃, synthesis was also done at other temperatures. Synthesis at lower temperatures is recommended in green chemistry because it simplifies the procedure, reduces the cost and is more energy efficient (Ahluwalia et al., 2004), therefore the goal was to determine the most suitable pH at lower temperatures.

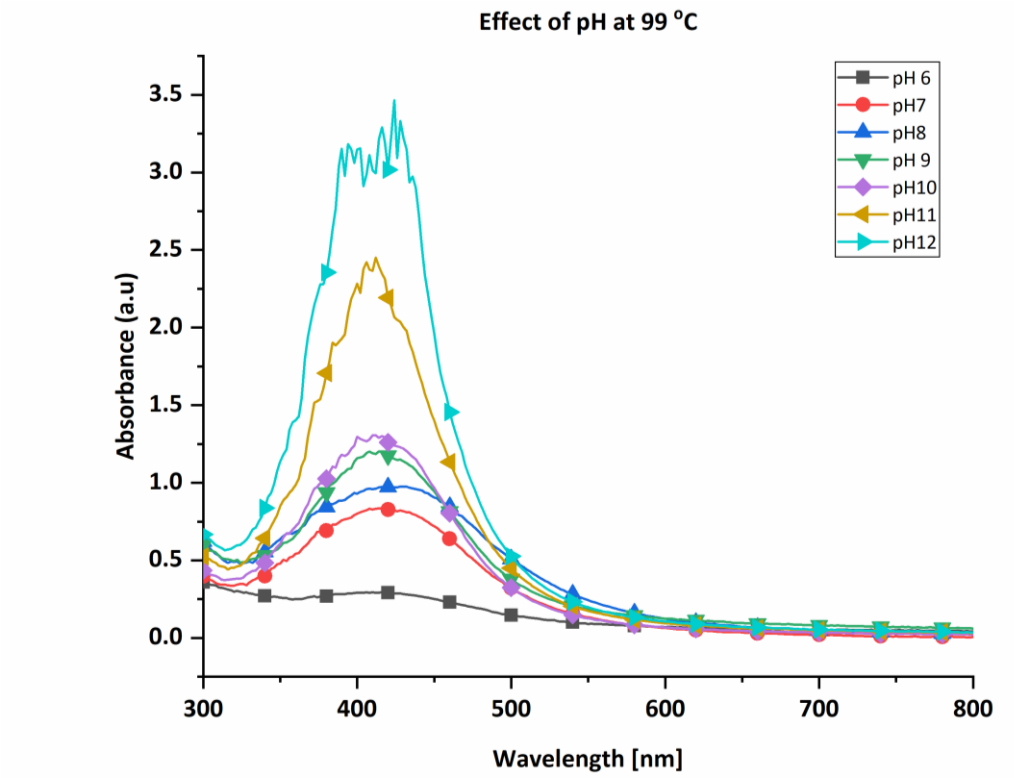

Figure 4:4. UV-Vis Absorption Spectra of Silver Nanoparticles Synthesized at Different pHs at 99 ℃

There are no substantial SPR peaks for pH 6 to pH 10 at temperatures of 70 ℃ (Figure 4:9), 50 ℃ (Figure 4:10) and 25 ℃ (Figure 4:11); however, SPR peaks can be seen for pH 11 and pH 12. A broad peak with low absorbance is observed for pH 11 at 50 ℃ but no peak is observed for the same pH at 25 ℃. Based on the intensity of the peaks, the optimum conditions were determined to be 50 ℃ and a pH of 12; these were used in subsequent experiments. Based on the intensity of the peaks, a temperature of 50 ℃ and a pH of 12 were determined to be the optimum conditions and were used in subsequent experiments.

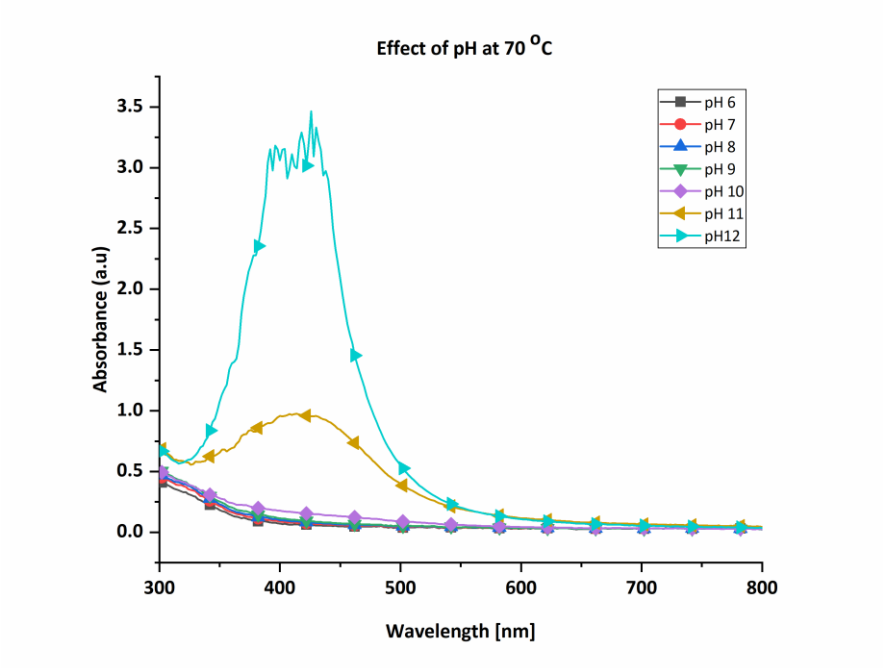

Figure 4:5. UV-Vis Absorption Spectra of Silver Nanoparticles Synthesized at Different pHs at 70 ℃

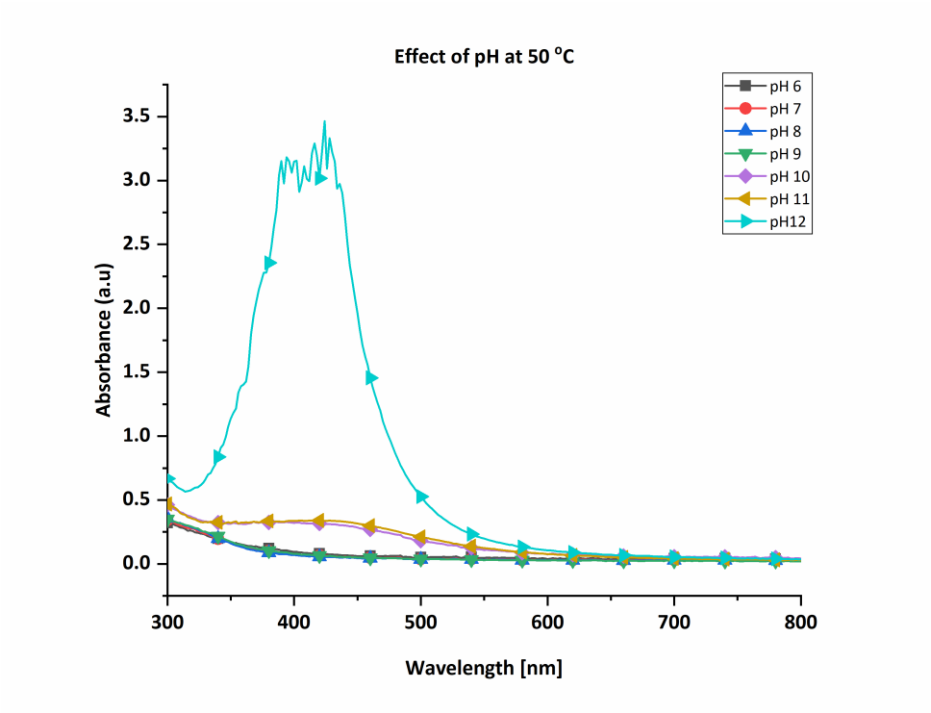

Figure 4:6. UV-Vis Absorption Spectra of Silver Nanoparticles Synthesized at Different pHs at 50 ℃

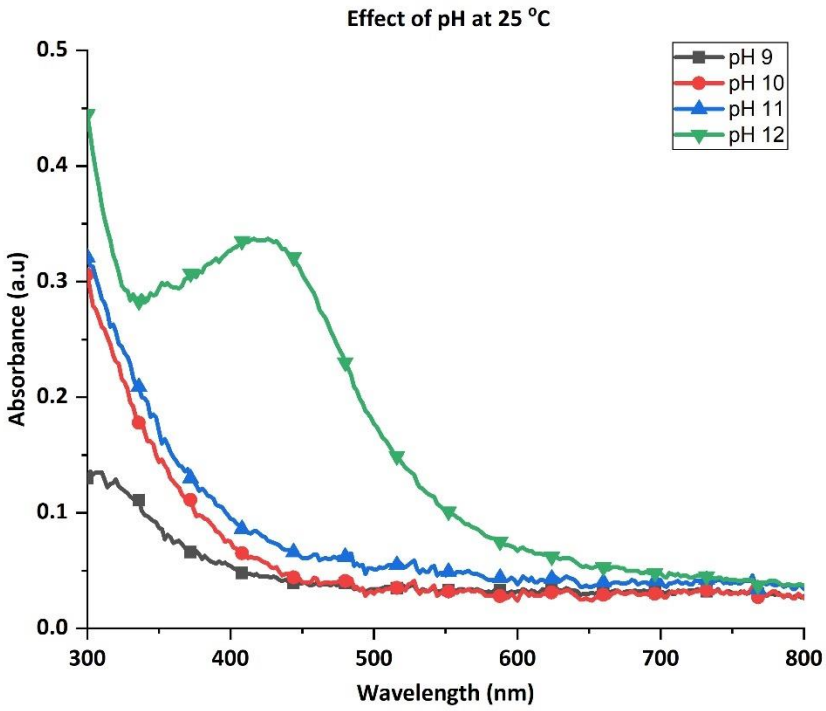

Figure 4:7. UV-Vis Absorption Spectra of Silver Nanoparticles Synthesized at Different pHs at 25 ℃

4.2.2.4 Effect of Stirring Speed

The effect of the stirring speed on the green synthesis of silver nanoparticles using potato peel extract is shown in the UV-vis spectra in Figure 4:12. As the reaction speed increased from 0 rpm to 300 rpm and then to 500 rpm, the absorbance increased showing an increase in the synthesis of nanoparticles. However, at a speed above 500 rpm the absorbance decreased and the peak became broader showing the formation of larger nanoparticles and polydispersity of the synthesized nanoparticles. When the synthesis speed is too low, there is reduced reaction and when the speed is too high there is more aggregation and larger nanoparticles are formed. This is agreement with previous studies where different stirring speeds were used and the optimum speed was found to be 500 rpm (Badri et al., 2015; Junaidi et al., 2016). Therefore, the stirring speed of 500 rpm was used for subsequent experiments.

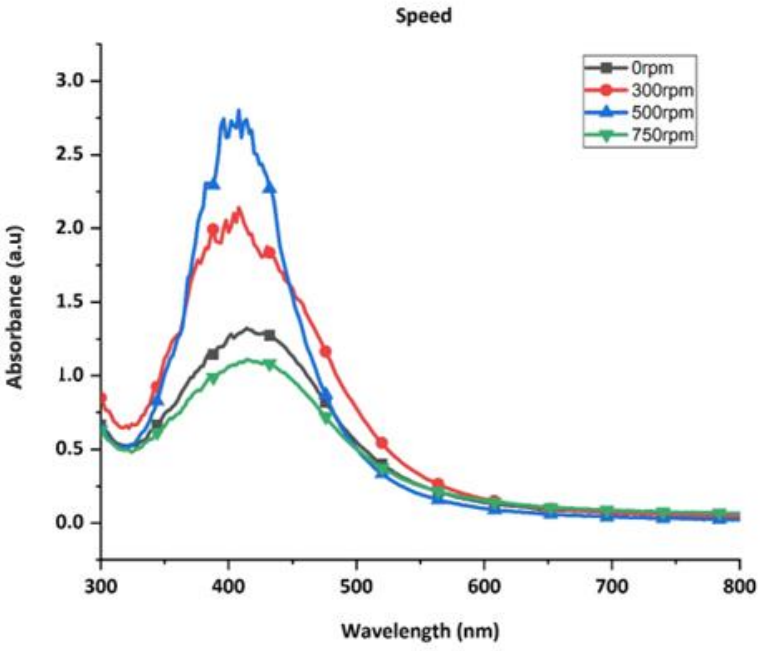

Figure 4:8. UV-Vis Absorption Spectra of Silver Nanoparticles Synthesized by Varying the Stirring Speed

4.2.2.5 Effect of Synthesis Time

The effect of synthesis time on the green synthesis of silver nanoparticles was investigated using UV-vis spectroscopy and SPR peaks as shown in Figure 4:13. The spectra show that the sharpness of the SPR peaks increases over time which confirms that rate of synthesis of nanoparticles is positively correlated with time and is in agreement with previous studies (Mahiuddin et al., 2020; Melkamu & Bitew, 2021). The nanoparticles start forming within 10 minutes of the silver nitrate reacting with the potato peel extract, with a slightly wider peak at a lower absorbance due to the slow conversion of silver ions to silver. As time passes, more silver ions are converted to silver nanoparticles, causing the peak to become sharper and the absorbance to rise at 30 minutes, 1 hour and 2 hours. Maximum absorbance is observed at 3 hours. However, the peak is much broader and at a much lower absorbance at 4 hours, indicating aggregation and the formation of larger nanoparticles. Therefore, a reaction time of 3 hours was found to be most suitable for the green synthesis of silver nanoparticles using potato peel extracts.

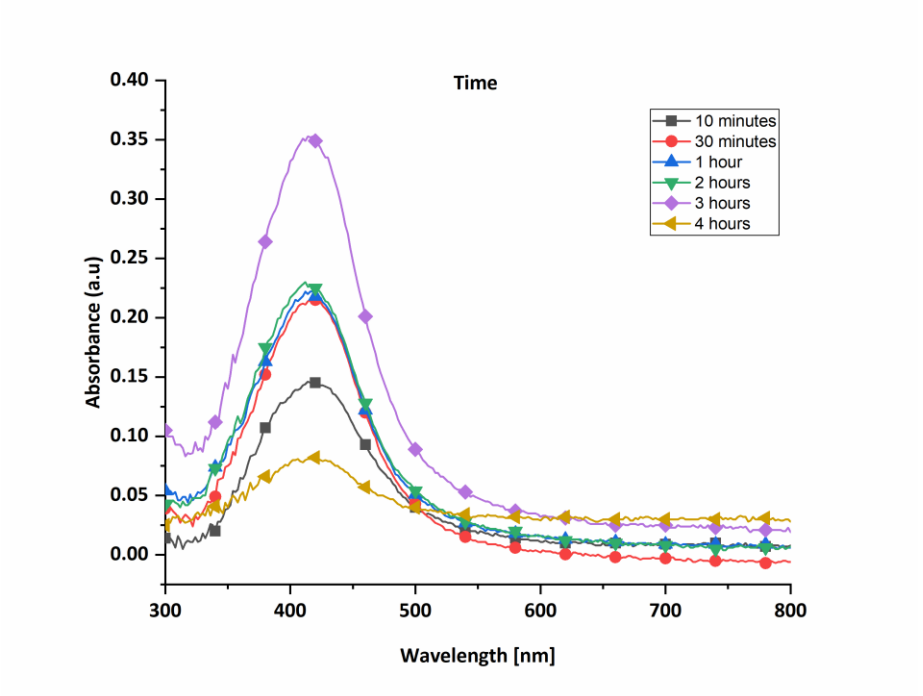

Figure 4:9. UV-Vis Spectra of Silver Nanoparticles Synthesized at Different Reaction Times

4.2.3 Characterisation of the Nanoparticle Synthesized Using Optimum Values

4.2.3.1 UV-Vis of PPE-AgNPs Synthesized Using Optimum Values

The nanoparticles were synthesized using the optimum values, that is: potato peel extract concentration – 25 %; pH – 12; temperature – 50 ℃; potato peel to silver nitrate volume ratio – 1:5; stirring speed – 500 rpm and time – 3 hours. Figure 4:14 shows the appearance of a single SPR peak at a wavelength of 418 nm.

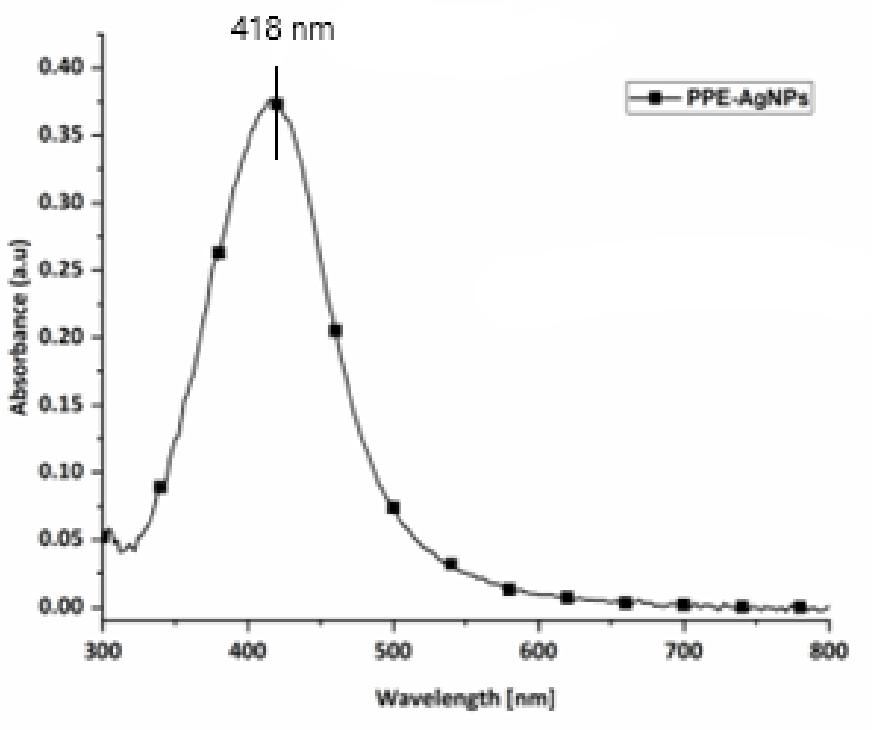

Figure 4:10. UV-Vis Spectrum of Silver Nanoparticles Green Synthesized with Potato Peel Extract

The peak is between 400 nm and 500 nm and thus confirms the formation of silver nanoparticles (Ashraf et al., 2016; Kredy, 2018).

4.2.3.2 Fourier Transform Infrared (FTIR) Spectroscopy

The surface chemistry composition of silver nanoparticles capped by the bioactive molecules in potato peel extracts was investigated using FTIR spectroscopy. The FTIR spectra of the green synthesised silver nanoparticles and potato peel extract are shown in Figure 4:15.

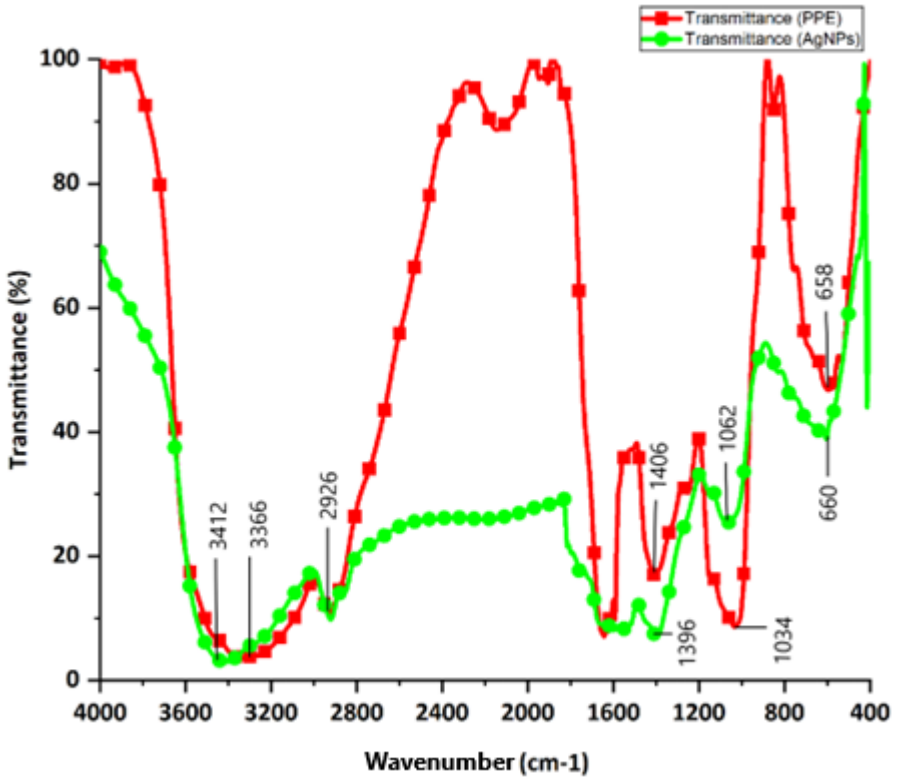

Figure 4:11. FTIR Spectra of Potato Peel Extract and Silver Nanoparticles

Potato peel extract displays the main absorbance peaks at 3366, 2926, 1644, 1406, 1034 and 658 which confirm the presence of carbohydrates, phenols, proteins and lipids in the extract (Devi et al., 2018). FTIR absorbance of the green synthesized silver nanoparticles have a high degree of similarity with those of the potato peel extract with a slight shift of the peaks with the nanoparticle peaks appearing at about 3412, 2922, 1636, 1396, 1062 and 600. The similarity of the peaks confirms the presence of the biomolecules found in potato peel extract are present in the nanoparticles while the shift in the FTIR peaks shows that the bioactive compounds found in PPE reduced the silver nitrate (Azarbani & Shiravand, 2020). The absorbance band at 3412 is due to the N-H stretching of amines or the OH stretching of the hydroxyl groups in alcohols and phenols (Liang & McDonald, 2014; Melkamu & Bitew, 2021). The peak at 2922 indicates the presence of C-H stretching groups in the nanoparticles (El-Sakhawy et al.,

2018). The bands at 1636 and 1396 arise from the C=O stretching in the carbonyl group or amides and the OH bend indicating the existence of phenols and tertiary alcohols respectively (Nandiyanto et al., 2019). The band at 1062 is related to the C-O-C pyranose ring and the band at 600 corresponds to the tri and di distribution in the phenols (El-Sakhawy et al., 2018; Melkamu & Bitew, 2021). The presence of the hydroxyl, carbonyl and amine groups in the green synthesized nanoparticles suggests that bioactive compounds like phenols, flavonoids and proteins are involved in the synthesis of silver nanoparticles as reducing, capping and stabilizing agents. The spectral analysis observed in this study was comparable to previous studies (Azarbani & Shiravand, 2020; Kaur et al., 2021; Melkamu & Bitew, 2021; Rao & Tang, 2017).

4.2.3.3 Dynamic Light Scattering (DLS)

The DLS was used to determine the size distribution of the prepared silver nanoparticles. Figure 4:16 depicts the nanoparticle size distribution which has an average hydrodynamic size of 50.18 nm which verifies the successful creation of silver nanoparticles, with studies obtaining nanoparticles in the 20 nm to 100 nm range using the DLS technique (Elamawi et al., 2018; Jang et al., 2015; Kaur et al., 2021). Nanoparticle dispersions are frequently polydisperse, which means that they contain particles of varying sizes and shapes rather than particles of single size and shape and therefore have differing polydispersity indexes. The PDI scale is from 0 to 1, with 0 representing monodisperse and 1 representing polydisperse nanoparticles. The results showed that the synthesized silver nanoparticles were poly-dispersed with a polydispersity index (PDI) of 0.282, which shows average polydispersity and is considered suitable (Jalab et al., 2021).

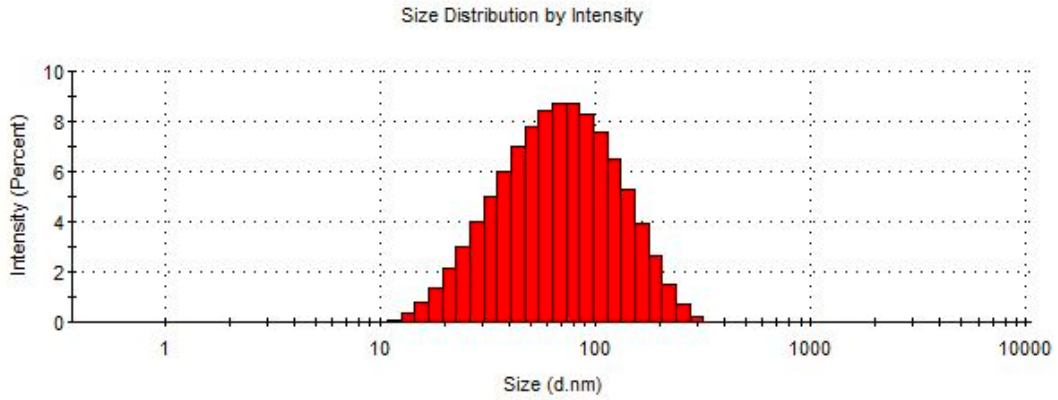

Figure 4:12. Size Distribution of PPE-AgNPs

The zeta potential shown in Figure 4:17 is – 33 mV and is sufficiently negative indicating moderate stability of the nanoparticles, their high dispersity as well as their good colloidal nature. This is due to the repulsive forces between the negatively charged silver nanoparticles which prevent aggregation and particle size increase thus improving the stability. (Erdogan et al., 2019; Samimi et al., 2018).

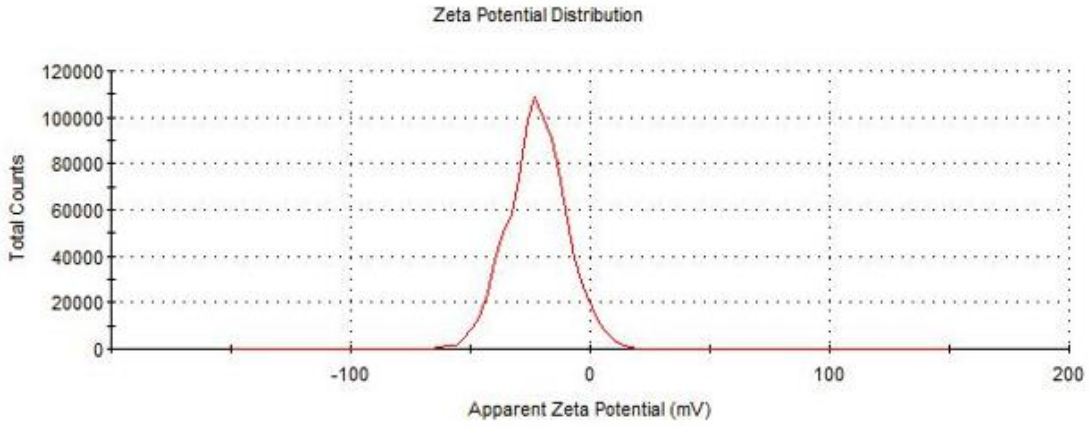

Figure 4:13. Zeta Potential of the Green Synthesised Silver Nanoparticles

4.2.3.4 X-Ray Diffractometer (XRD)

The XRD analysis was performed on the silver nanoparticles green synthesized using potato peel extracts to determine their crystallinity and the XRD pattern is shown in

Figure 4:18. Four distinct diffraction peaks, which correspond to the (111), (200), (220) and (311) diffraction planes were observed in the XRD pattern at the 2θ values of 38.09°, 44.31°, 64.39° and 77.51° respectively. This pattern indicated that the silver nanoparticles have a face-centred cubic structure (Holder & Schaak, 2019). This crystalline nature of green synthesized nanoparticles was also observed in other studies where plant extracts were used in the green synthesis of silver nanoparticles (J. M. Ashraf et al., 2016; Melkamu & Bitew, 2021).

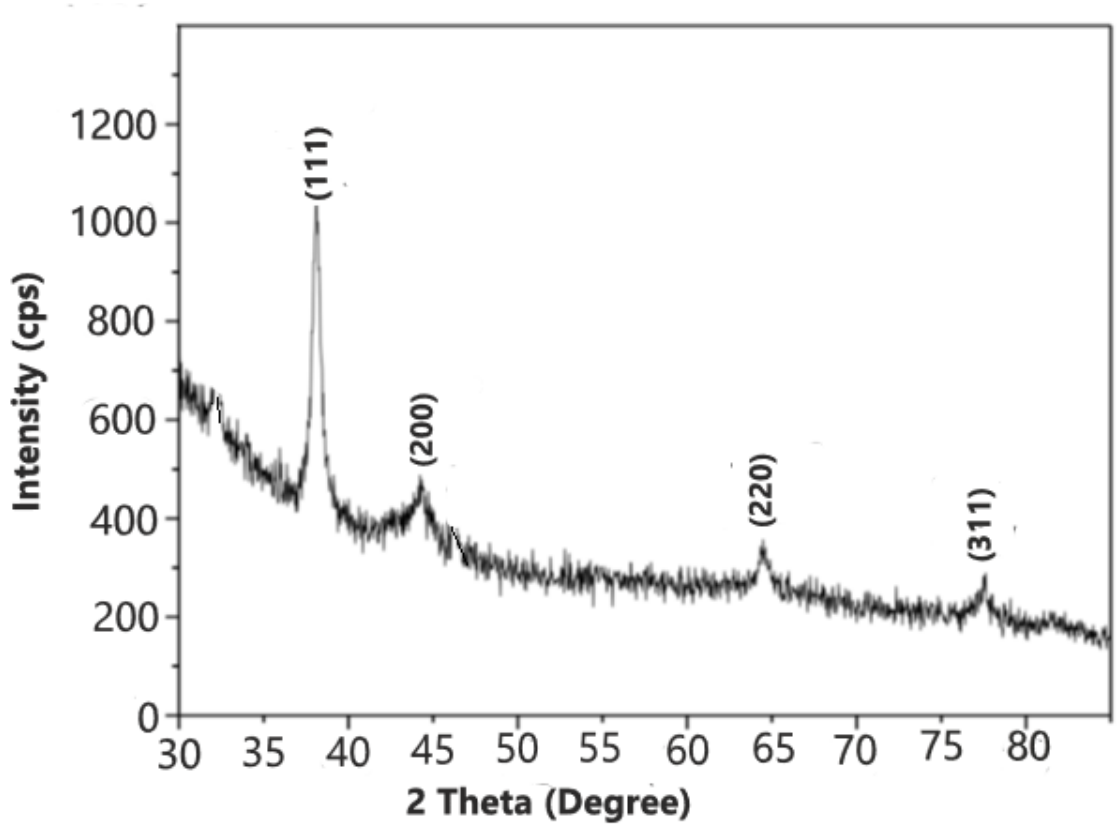

Figure 4:14. XRD Pattern of Green Synthesized Silver Nanoparticles from Potato Peel Extracts

4.2.3.5 Scanning Electron Microscopy

The morphology of the green synthesized silver nanoparticles was assessed using the scanning electron microscope and the image is shown in Figure 4:19. The obtained

silver nanoparticles were mostly spherical in shape, which is typical of green synthesized silver nanoparticles (Kaur et al., 2021; Mahiuddin et al., 2020; Rao & Tang, 2017). However, there were large particles/ clusters which were most likely formed by the agglomeration of smaller nanoparticles.

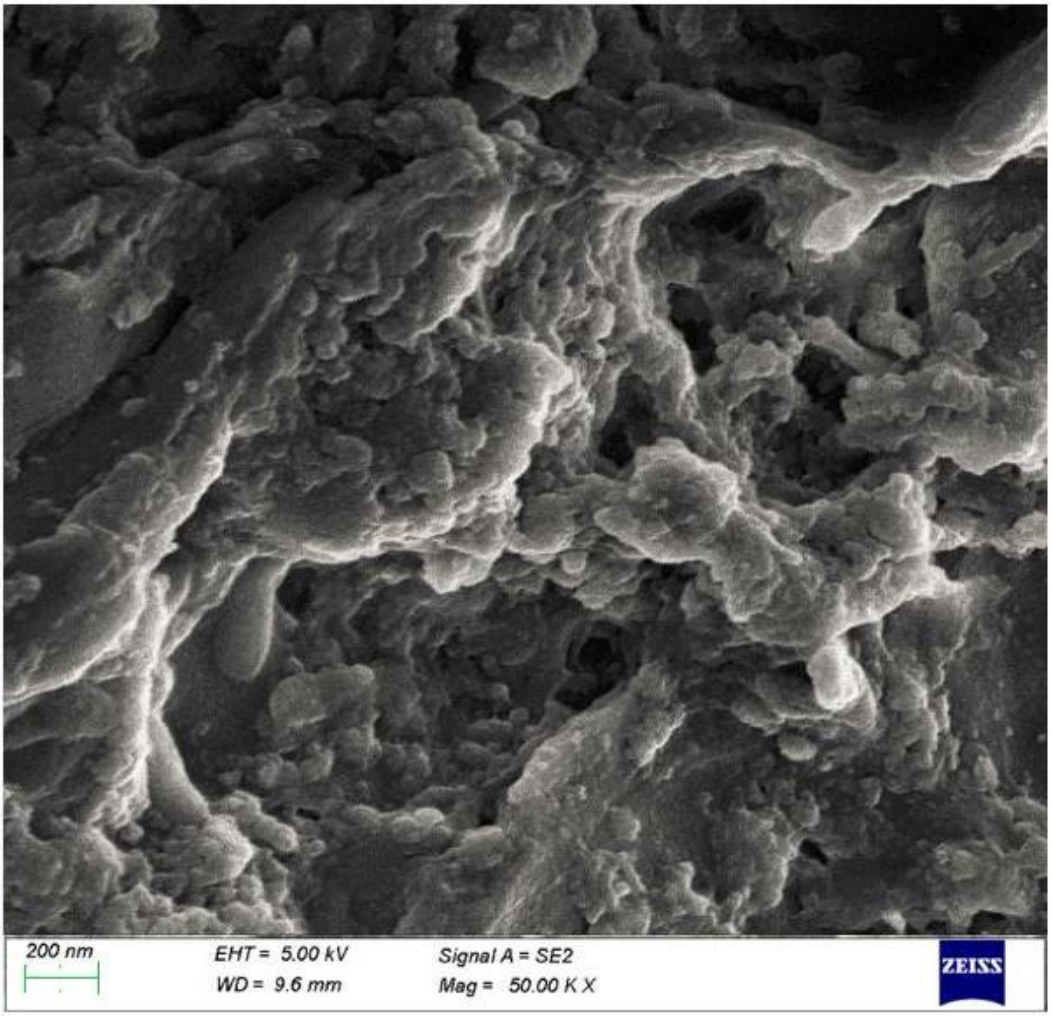

Figure 4:15. SEM Image of Green Synthesized Silver Nanoparticles

The EDX profile (Figure 4:20) revealed a strong signal peak at 3 keV, which is characteristic of silver nano crystallites (Jagtap & Bapat, 2013; Rao & Tang, 2017); indicating the presence of silver nanoparticles. The profile also contained carbon and oxygen but did not contain any nitrogen from the silver nitrate initially used thus

confirming the complete reduction of the silver nitrate to silver nanoparticles. Carbon and oxygen are most likely associated with organic compounds from potato peel extracts adsorbed on the surface of silver nanoparticles which play an important role as reducing agents and capping agents in the green synthesis of silver nanoparticles.

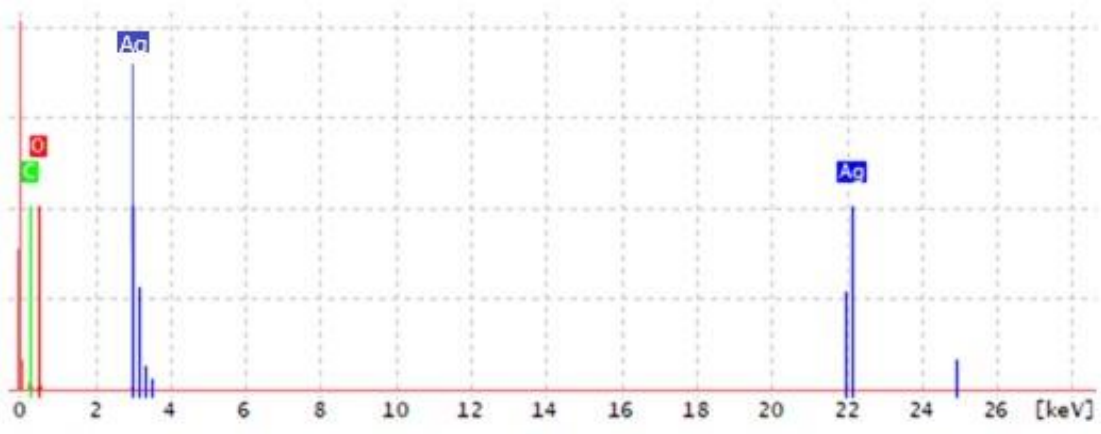

Figure 4:16. EDX spectra of green synthesized silver nanoparticles

4.2.4 Antibacterial Efficacy of the Green Synthesized Silver Nanoparticles

Using the agar well diffusion method, the antibacterial activity of the PPE-AgNPs was investigated against three bacterial strains, namely, *E. coli*, *S. aureus* and *MRSA* (Figure 4:21).

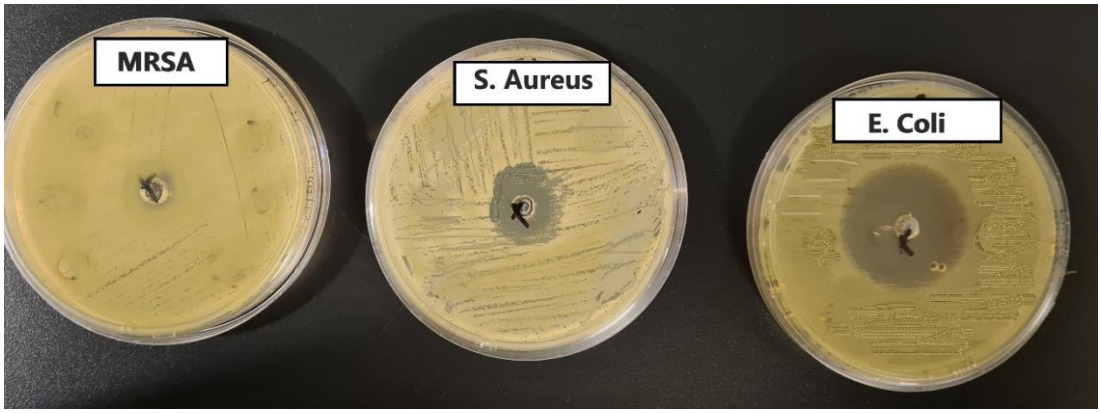

Figure 4:17. Test Results of Agar Well Diffusion of Silver Nanoparticles against *MRSA*, *E. coli* and *S. aureus*

The findings revealed the degree of susceptibility of the organisms studied. For each bacterial strain, the organisms displayed a different zone of inhibition. PPE-AgNPs had a higher zone of inhibition of 13 mm against gram-negative *E. coli* than a zone of inhibition of 9.3 mm against gram-positive *S. aureus* (Table 4:4). A similar result was also found for the green synthesis of silver nanoparticles using *Eriobotrya japonica* leaf extract (Rao & Tang, 2017).

Table 4:1. Zone of Inhibition of PPE-AgNPs on Tested Bacteria

Bacterial Strain	Inhibition Zone (mm) Mean ±SD
Staphylococcus aureus	9.30 ± 0.01
Escherichia coli	13.00 ± 0.02
Methicillin resistant staphylococcus aureus	0.00 ± 0.00

The powerful antibacterial properties of silver nanoparticles may be attributed to the released silver ions, which may interact with microorganisms by attaching to the surface of the bacteria cell membranes, penetrating into bacteria cells, and influencing membrane permeability and respiration (Rao & Tang, 2017). The antibacterial difference between gram-negative and gram-positive bacteria are due to the differences in their cell wall compositions. The cell membrane of gram-negative bacteria consists of a single layer of peptidoglycan, whereas the membrane of gram-positive bacteria contains multiple layers of peptidoglycan, making them more rigid and thus more resistant to antibacterial agents (Saravanakumar et al., 2017; Silhavy et al., 2010). The antibacterial activity of the green synthesized nanoparticles was greater than that of the extract alone; this is consistent with a previous study (Melkamu & Bitew, 2021). This shows that the process of synthesizing the silver nanoparticles using potato peel extract has enhanced or potentiated their antibacterial efficacy.

4.3 Antibacterial Efficacy of Treated Fabrics

4.3.1 Characterisation of the Cotton Fabric Treated with Potato Peel Extract

4.3.1.1 Visible Effects of PPE Treatment on Cotton Fabrics

The treated cotton fabric had a slight colour change from white to a very light brown colour as shown in Figure 4:22. The potato peel extract is brown in colour therefore, based on the physical attributes of dyes we can confirm that the colour change on the treated fabric is due to the adherence of the potato peel extract with the cotton fabric. Studies have also shown that potato peel contains anthocyanins which give them their dyeing potential (Ben Jeddou et al., 2021; Sampaio et al., 2021); this could explain the change in colour of the fabric upon application of the potato peel extract.

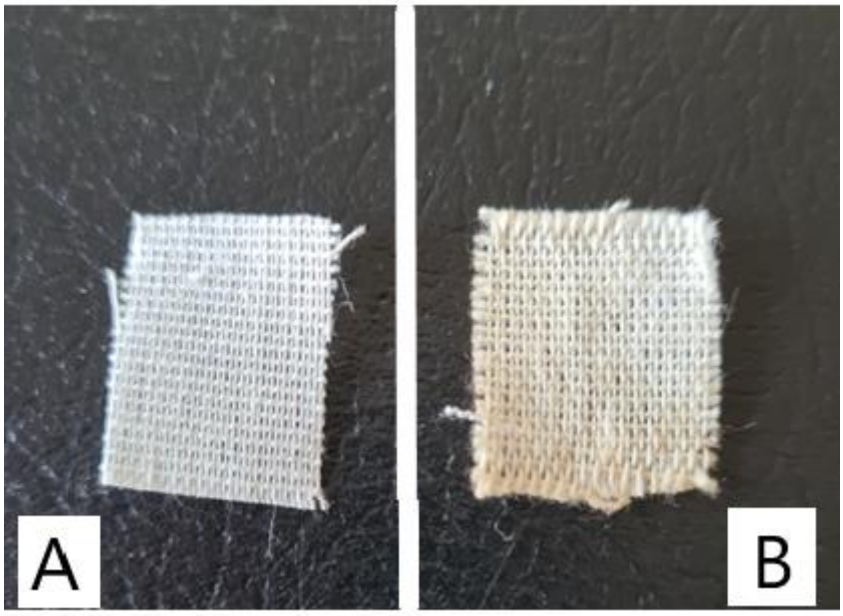

Figure 4:1. A - Untreated Cotton Fabric, B - Cotton Fabric Treated with Potato Peel Extract

4.3.1.2 FTIR Analysis of the Treated and Untreated Cotton Fabric

The existence of new functional groups was assessed through comparison of the FTIR spectra of the untreated cotton fabric and PPE treated cotton fabric as shown in Figure 4:23.

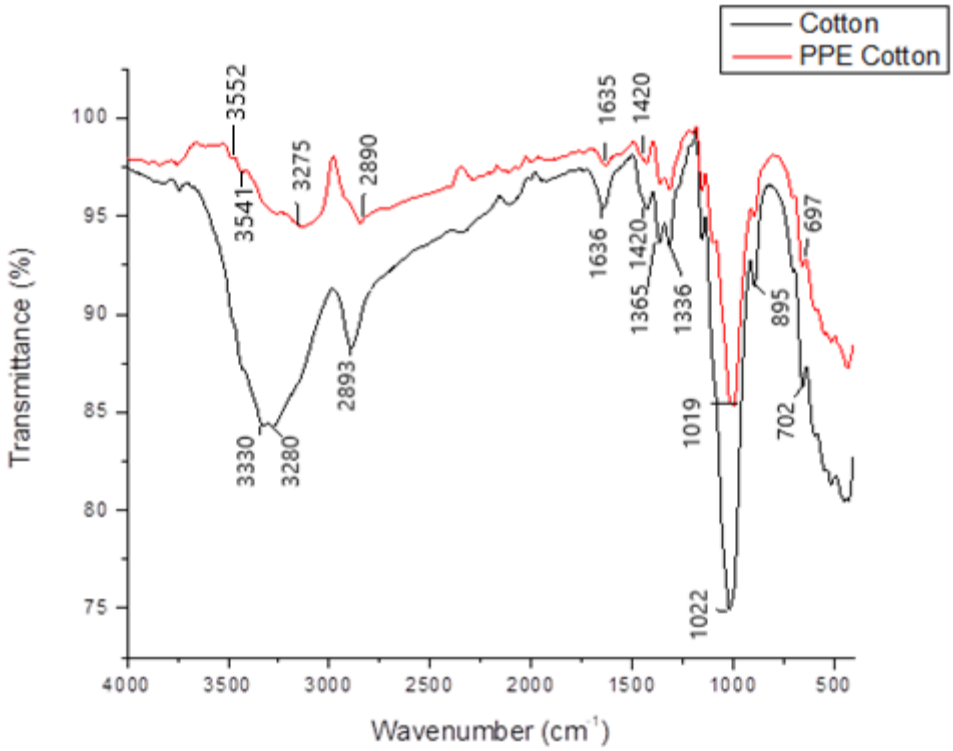

Figure 4:2. FTIR Spectra of Untreated Cotton Fabric (Cotton) and Cotton Fabric Treated with Potato Peel Extract (PPE Cotton)

The two FTIR spectra shown in Figure 4.23 are nearly identical, with only minor differences. This could be attributed to the PPE's partial interaction with the cotton fabric, as well as the fact that both PPE and the cotton fabric are cellulosic in nature. Cotton fabrics have a higher degree of polymerisation than potato peels, resulting in a higher peak intensity of the untreated cotton fabric than the PPE treated fabric. In the untreated cotton fabric, two peaks appear at 3330 cm^{-1} and 3280 cm^{-1} which are attributed to the H bonded OH stretching group (Devi et al., 2018; Liang & McDonald, 2014). The treated cotton fabric also showed the presence of the H bonded OH stretching group as indicated with a peak at 3275 cm^{-1}. Additional peaks at 3552 cm^{-1} and 3541 cm^{-1} which correspond to the stretching vibration of phenolic OH (Nandiyanto et al., 2019) are observed in the spectrum for the PPE treated cotton fabric due to the phenolic compounds in the potato peel extract. Peaks at 1636 cm^{-1},

1420 cm^{-1} and 1022 cm^{-1} for both treated and untreated fabrics corresponded to C=C stretching, CH bending of pyranose ring and C-O-C groups (Bouhadjra et al., 2021). Other information can be obtained in the region 895 cm^{-1} and 697 cm^{-1} with several peaks indicating the presence of aromatic C-H out of plane bend (Nandiyanto et al., 2019). The reduction in intensity of the peak at 3330 cm^{-1} and 3280 cm^{-1} representing the OH stretching is an indication of effective crosslinking. Also, the broadening of the peak indicates the confinement of nano molecules of water in the treated fabric formed by polar covalent bonding of oxygen and hydrogen. The shifts in certain peaks as well as the additional peaks confirm the modification of the cotton fabric due to the addition of potato peel extract.

4.3.1.3 Thermogravimetric Analysis Graphs of the Treated and Untreated Fabric Samples

The thermal decomposition of untreated cotton fabric and cotton fabric treated with potato peels (PPE cotton) is shown in the TGA curves in Figure 4:24. The decomposition occurred in three stages according to earlier described analysis (Charles et al., 2022; Suriyatem et al., 2019).

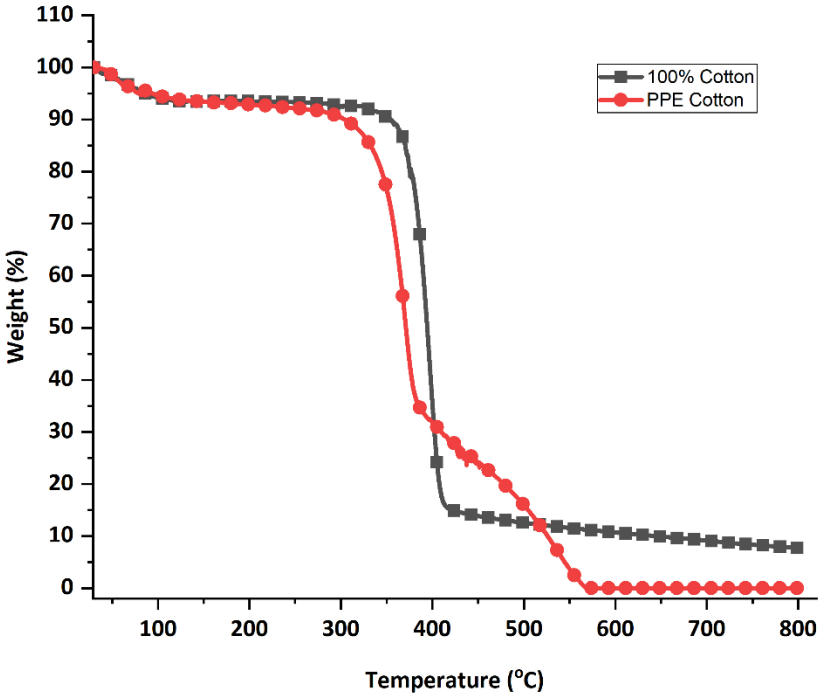

Figure 4:3. TGA Thermograms of Untreated Cotton Fabric and Fabric Treated with Potato Peel Extracts (PPE Cotton)

In the first stage from the room temperature to about 100 ℃, all samples showed an initial weight loss of approximately 5 % to 10 % due to the vaporization of the physically bound water molecules in the fabric. The fabric weight remained constant until the temperature range of 240 ℃ to 300 ℃ for PPE cotton and 250 ℃ to 360 ℃ for untreated cotton fabric where there was a weight loss of about 5 %. In the second stage a sharp weight loss from 90 % to 34 % is observed from 300 ℃ to 380 ℃ for PPE cotton. During the same stage a weight loss is also observed for untreated cotton from 90 % to 14 % at a temperature range of 360 ℃ to 390 ℃. This stage corresponds to the significant thermal decomposition and complete oxidation of the cotton fibre and is consistent with values of thermal degradation of cotton found in literature which range from 300 ℃ to 380 ℃ for untreated cotton fabric (Popescu et al., 2014).

The decomposition temperature for cotton fabric is heavily influenced by factors such as the morphology of the cellulose polymer, crystallinity or amorphousness of the sample, molecular mass and purity of the sample (Cuiffo et al., 2021). Samples with higher crystallinity have higher thermal stability because they have more ordered and compact molecular structures that are better able to resist thermal degradation than amorphous samples that have more disordered and loose molecular structures (Li et al., 2019; Santmartí & Lee, 2018). Potato peels are more amorphous than crystalline in nature (Osman, 2020) and have lower thermal stability, therefore addition of the peels to cotton fabric is expected to lower the thermal stability as observed in the TGA thermograms from 380 ℃ to 560 ℃. The last stage corresponds to the degradation of residual char formed during the thermal decomposition stage, which occurred with the complete oxidation of the samples (Charles et al., 2022). There was complete degradation of PPE cotton at 560 ℃ while the untreated cotton was still at 10 % weight. The TGA curve confirmed the addition of the potato peel extract onto the cotton fabrics due to the difference in the thermal stability of the fabric.

4.3.1.4 Antibacterial Efficacy of the Fabrics Treated with Potato Peel Extract

The disc diffusion assay was used to assess the antibacterial activity of cotton fabric treated with potato peel extract against *E.coli* and *S. aureus*. The results in Table 4:5 showed that the treated cotton fabrics displayed antibacterial activity against both *E. coli* and *S. aureus* with clear zones of inhibition. However, after washing the zone of inhibition reduced from 100 % to 58 % and from 100 % to 62 % for *S. aureus* and *E. coli* respectively.

Table 4:1. Inhibitory Zone of Treated and Untreated Cotton Fabrics on the Tested Bacteria

Fabric Samples	**Zone of Inhibition (mm) Mean ± SD**	
	S. Aureus	***E. Coli***
Untreated fabric (negative control)	0.00 ± 0.00	0.00 ± 0.00
Positive control	40.00 ± 0.02	30.00 ± 0.04
PPE treated fabric before washing	12.00 ± 0.01	8.00 ± 0.02
PPE treated fabric after washing	7.00 ± 0.00	5.00 ± 0.03

The quantitative reduction test results also confirmed the efficacy of the treated fabrics against both *E. coli* and *S. aureus*. Data indicated that the percentage reduction was found to be 72.10 % and 64.15 % for *E. coli* and *S. aureus* respectively. The treated fabric showed a gradual decrease in the antibacterial property after 20 washing cycles with a 54.74 % reduction in bacterial count for E. coli and a 51.23 % reduction in bacterial count for *S. aureus*. Similarly, plant extracts such as stinging nettle and *malva sylvetris* have shown good antibacterial properties even up to 10, 20, 30 and 40 washes (Ketema & Worku, 2020; Sadeghi-Kiakhani et al., 2022). The bacteria reduction was higher for gram-negative E. coli than for gram-positive *S. aureus*. The difference is likely due to the differences in their cell wall compositions. The cell membrane of gram-negative bacteria consists of a single layer of peptidoglycan, whereas the membrane of gram-positive bacteria contains multiple layers of peptidoglycan, making them more rigid and thus more resistant to antibacterial agents (Saravanakumar et al., 2017; Silhavy et al., 2010).

4.3.2 In-Situ Synthesis of Silver Nanoparticles onto Cotton Fabric using Potato Peel Extracts

4.3.2.1 Visible Effects of Silver Nanoparticles on Cotton Fabric

The visible effects of the silver nanoparticles on the cotton fabric are shown in Figure 4:25. colour of the cotton fabric changed from white to a brown colour after the in-situ

synthesis. This indicated the direct synthesis of silver nanoparticles onto the cotton fabric by reduction of Ag^{+} to Ag^{0} (Ahmed et al., 2016). The intensity of the colour reduced after 10 washes and reduced further after 20 washes, which showed the loss of silver nanoparticles after washing (Jain et al., 2022).

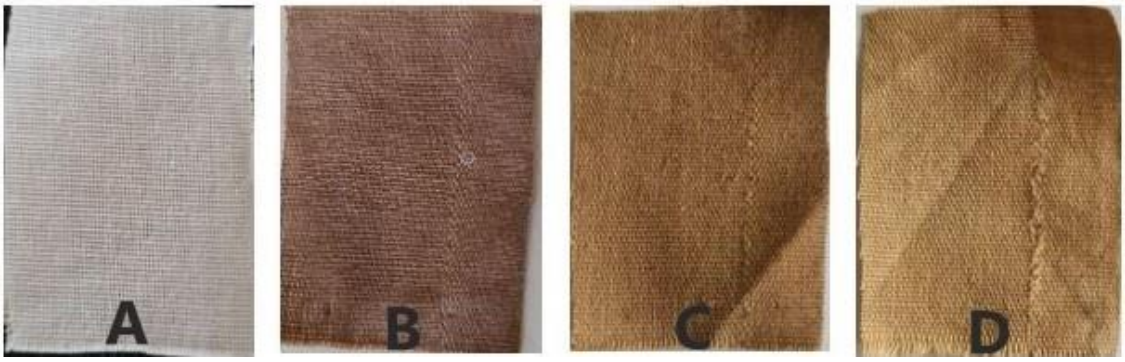

Figure 4:4. 100 % Cotton fabrics. A - Untreated, B - Treated with AgNps before Washing, B - Treated with AgNps after 10 Washes and C - Treated with AgNps after 20 Washes

4.3.2.2 Qualitative Antibacterial Analysis of PPE-AgNP Treated Cotton Fabrics

The antibacterial activities of the AgNP treated cotton fabrics were tested using the fabric disc diffusion assay against gram-positive *S. aureus* and gram-negative *E. coli*. The untreated cotton fabric served as the negative control, while the ampicillin – treated fabric antibiotic served as the positive control. Comparison was also made with the fabric treated with potato peel extract to determine the synergy of the potato peel extract and the silver nanoparticle in antibacterial activity. The results of the fabric diffusion assay are shown in Figure 4:26. The presence of an inhibition zone around the treated samples clearly indicates that they have antimicrobial activity as a result of the action of the treatment on the fabric. The uncoated negative control did not show any antibacterial activity. The zone of inhibition was larger for the AgNP treated fabric than the PPE treated fabric. This shows that the AgNP treated fabric has a better antibacterial effect against E. coli and S. aureus than the PPE treated fabric and also

confirms that the green synthesis of silver nanoparticles using potato peel extract is an improvement on the potential of potato peel extracts as antimicrobial agents. However, for both the PPE treated fabric and the AgNP treated fabric, the antibacterial activity reduced after washing.

Results from several studies have shown that nanoparticle coated fabrics possess antibacterial properties against E. coli and S. aureus (Balamurugan et al., 2017; Čuk et al., 2021); the antibacterial activities reduced after washing (Q. Zhou et al., 2022). Therefore, the results of this study are consistent with those of previous researches. The reduction of the antibacterial activity after washing shows the need for improving the in-situ synthesis in order to improve the durability of the silver nanoparticles on the cotton fabric.

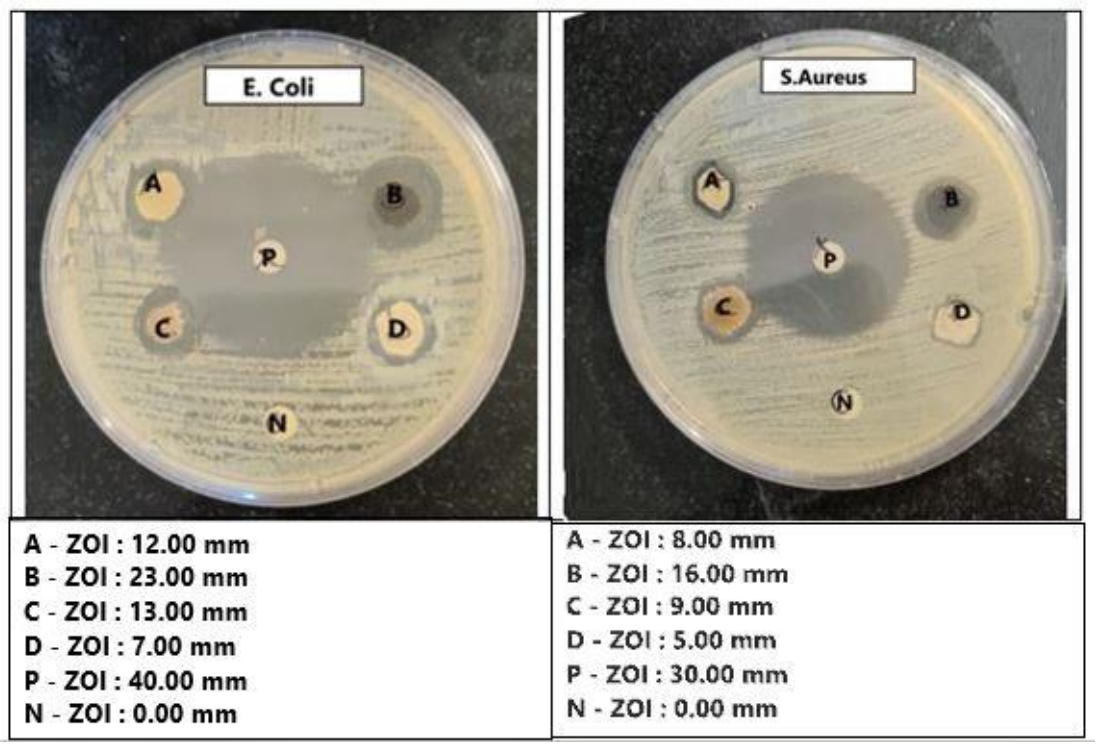

Figure 4:5. Antibacterial Efficacy of Different Fabrics against E. coli and S. Aureus. A - PPE Treated Fabrics before Washing, B - AgNPs treated fabric before washing, C - AgNPs Treated Fabric after Washing, D - PPE Treated Fabric after Washing, P - Ampicillin Disc (Positive control), N – Untreated Fabrics (Negative Control)

4.3.3 Influence of Process Parameters on the In-Situ Synthesis of Silver Nanoparticles on Cotton Fabrics

The antibacterial properties of the cotton fabrics treated with nanoparticles using the in-situ green synthesis method were characterised and optimized using statistical methods. Synthesis time (X_1), incubation time (X_2) and curing temperature (X_3) were considered as the input independent variables while antibacterial efficacy of the fabrics before washing (Y_1) and loss in antibacterial activity after washing (Y_2); were considered as the system's responses. The input independent variables were monitored in order to optimize the antibacterial properties of the treated fabrics against *E.coli* and *S. aureus*.

ANOVA was used to determine the adequacy of the regression equations against a significance level of 5 % for the bacterial count at different in-situ synthesis variables. R-squared values were also used to demonstrate how well the regression model (independent variables) predicted the observed data's outcome (dependent variables).

4.3.3.1 Antibacterial Properties of the Treated Fabrics Before Washing

The goal of the experimental design for percentage bacterial reduction for both *E. coli* and *S. aureus* was to maximise the response. That is, a higher percentage bacterial reduction meant that the antibacterial treatment had a higher efficacy against the tested bacterial strains. The percentages ranged from 0 % to 100 % with 0 % indicating that there was no efficacy while 100 % indicated that the antibacterial treatment was able to kill all bacteria on the surface.

The viable bacteria on the nutrient agar petri dishes were determined by counting the number of colony forming units per millilitre (CFU/ml). The control fabric exhibited

no antibacterial activity against both *S. aureus* and *E. coli*. Calculation of the percentage bacterial reduction was done against the negative control using Equation 3:4.

Results for E. Coli Percentage Reduction

The regression equation for the bacterial reduction of treated fabrics before washing against *E.coli* (Y_{EC1}) is shown in Equation 4.3. The model had a coefficient of determination (R^2) of 90.28 % and a p value of 0.000 %. This means that 90.28 % of the variation in Y_{EC1} can be explained by the input variables in the regression model. The adjusted R^2 for the unseen data set was 86.81 %. The high R^2 values suggest that the models adequately fit the data sets.

$$Y_{EC1} = 84.21 + 5.56\ X_1 + 0.2338X_2 + 0.0613X_3 - 0.003552X_2^2 - 0.0336X_1X_3$$

Equation 4:3

Table 4:6 displays the ANOVA, factor contributions, and Variance Inflation factors for percentage bacterial reduction (E.coli) before washing. According to the percentage contribution of the factors, the square of incubation time was the highest contributor for the model for *E. coli* bacterial reduction before washing with 67.47 %. In the in-situ synthesis of silver nanoparticles onto fabric, the incubation time refers to the amount of time the fabric is exposed to the silver nanoparticles solution during the synthesis process. In general, increasing the incubation time increases the antibacterial efficacy of the silver nanoparticles on the fabric because of the increase in the nanoparticles formed on the fabric (Wisnuwardhani et al., 2019); that could explain why it contributed the highest percentage to the regression model. Synthesis time contributed 11.98 %, incubation time contributed 5.21 %, the combined effect of curing temperature and synthesis time contributed 4.89 % and curing temperature contributed the least with a value of 0.72 %. The P values for the estimated coefficients, curvilinear and interaction

effects were less than 0.05, with the exception of curing temperature indicating that the model and all other factors were significant.

Table 4:2. ANOVA, Factor Contributions (FC%) and VIF for E. Coli Reduction before Washing

	ANOVA (P - value)	FC %	VIF
Regression model	0.000	90.28	
Linear	0.002	17.92	
Synthesis Time	0.001	11.98	1.00
Incubation Time	0.016	5.21	1.00
Curing Temperature	0.326	0.72	1.00
Square	0.000	67.47	
Incubation Time * Incubation Time	0.000	67.47	1.00
2-way Interaction	0.019	4.89	
Synthesis Time * Curing Temperature	0.019	4.89	1.00
Error		9.72	
Lack-of-Fit	0.000	9.69	
Pure Error		0.03	
Total		100	

Figure 4:27 shows the interaction effects of synthesis time and curing temperature. The graph shows that at a synthesis time of 1 hour, there was a higher mean of *E. coli* bacterial reduction at a curing temperature of 80 ℃ than at a curing temperature of 180 ℃. When synthesis time was increased to 3 hours, the mean of bacterial reduction of *E. coli* became less at a temperature of 180 ℃ than at a temperature of 80 ℃. Therefore, the combined effect showed that as the synthesis time increased and the curing time reduced, the mean of *E. coli* bacterial reduction increased.

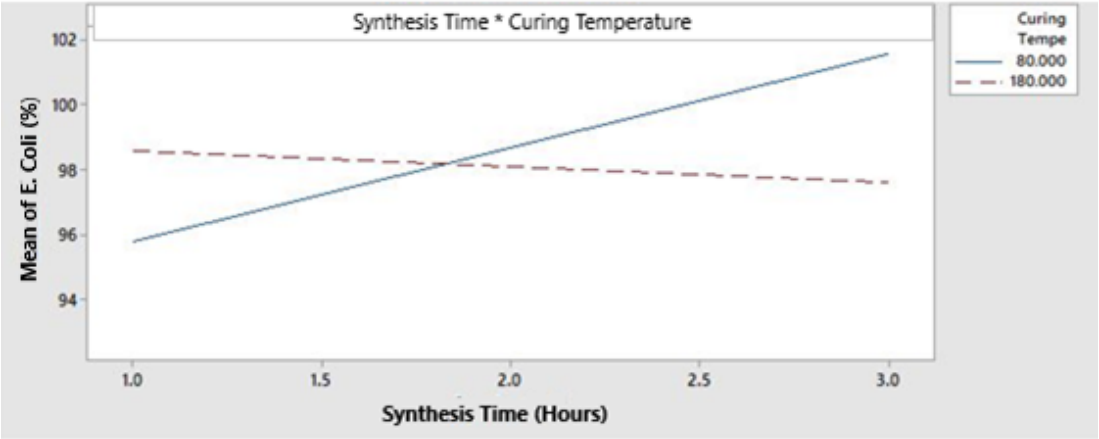

Figure 4:6. Combined Effect of Synthesis Time and Curing Temperature

The 3D surface plot graph in Figure 4:28 also shows the interaction between curing temperature and synthesis time and confirms that as the synthesis time increases and the curing temperature increases, there is an increase in the mean of *E. coli* bacterial reduction.

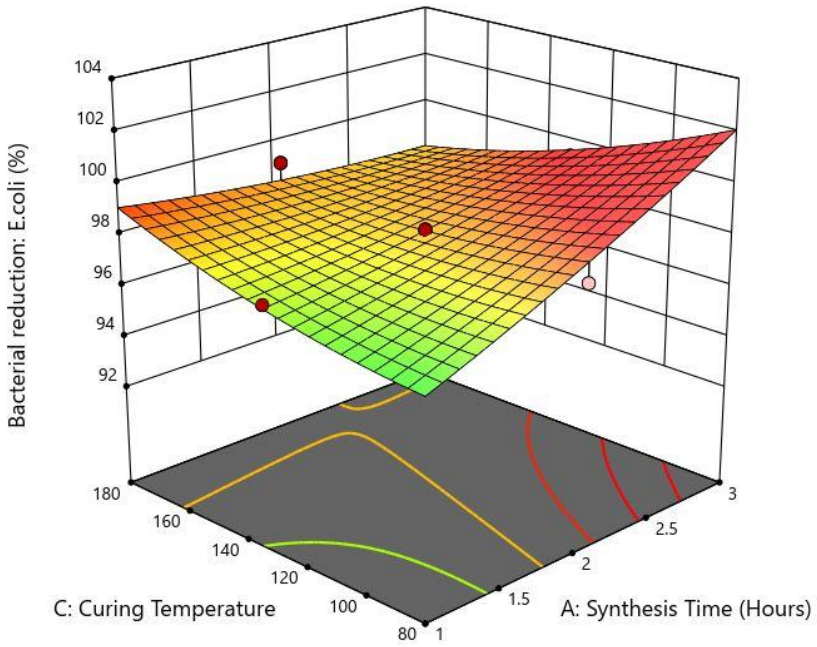

Figure 4:7. Response Surface 3D Plot Indicating the Interaction Between Synthesis Time and Curing Temperature on *E. Coli* Percentage Bacterial Reduction

The combined effect of synthesis time and incubation time in Figure 4:29 showed that at a curing temperature of 130 ℃, as the synthesis time increased and the incubation time increased, the percentage bacterial reduction increased until an incubation time of 31.5 hours, thereafter the percentage bacterial reduction reduced. Therefore, at that curing temperature, an incubation time of 31.5 hours and a synthesis time of 3 hours will result in optimum bacterial reduction.

The combined effect of curing temperature and incubation time in Figure 4:30 showed that at a synthesis time of 2 hours, as the curing temperature increased and the incubation time increased, the percentage bacterial reduction increased up to an incubation time of 36 hours, thereafter the percentage bacterial reduction reduced. Therefore, at a synthesis time of 2 hours, an incubation time of 36 hours and a curing temperature of 180 ℃ result in optimum bacterial reduction.

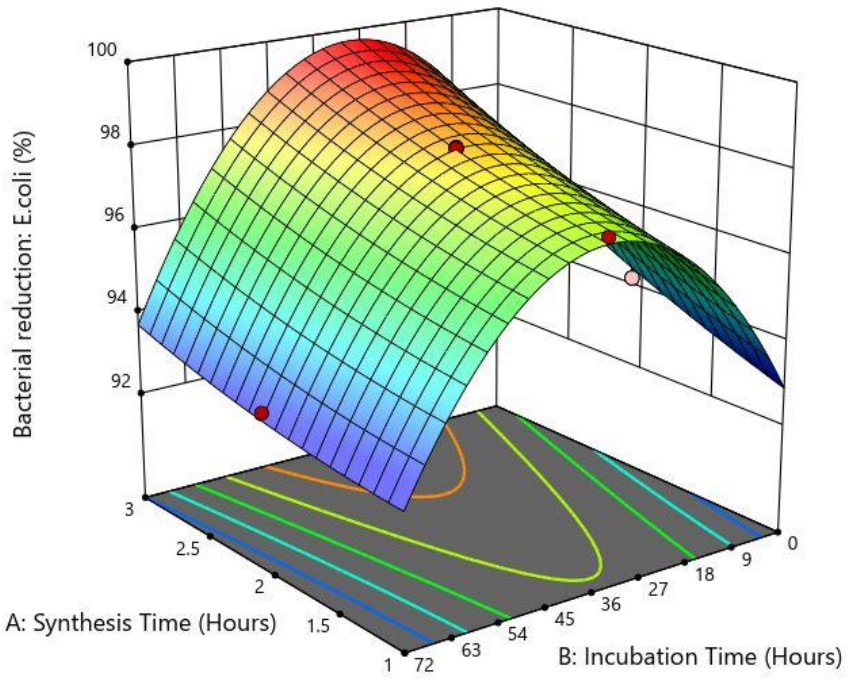

Figure 4:8. Response Surface 3D Plot Indicating the Interaction Between Synthesis Time and Incubation Time on *E. Coli* Percentage Bacterial Reduction

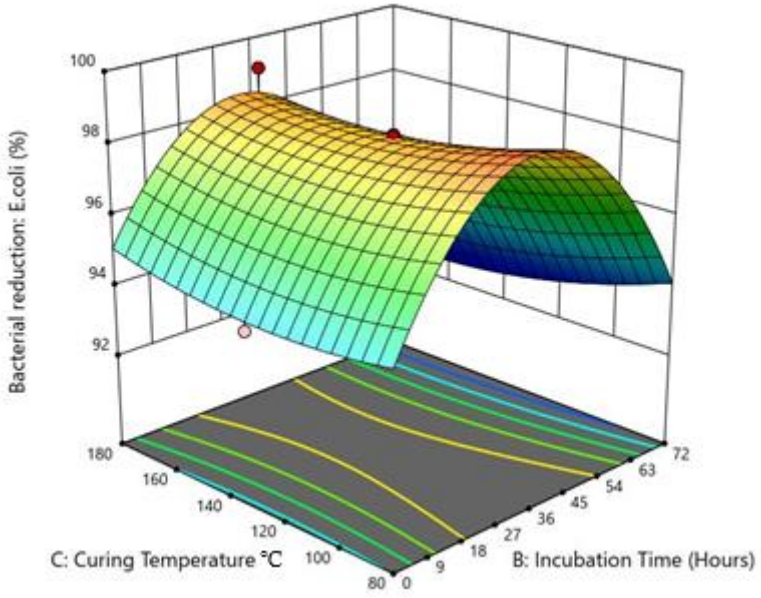

Figure 4:9. Response Surface 3D Plot Indicating the Interaction Between Curing Temperature and Incubation Time on *E. Coli* Percentage Bacterial Reduction

The optimal settings for a maximized percentage *E.coli* bacterial reduction were predicted from the regression model. The optimal settings obtained were: synthesis time of 3 hours, incubation time of 32.73 hours, curing temperature of 80 ℃ and a predicted *E. coli* percentage bacterial reduction of 99.94 %. The top five values closest to the predicted optimum settings for percentage *E. coli* bacterial reduction were also considered in case the optimum settings were not practicable and are shown in Table 4:7.

Table 4:3. Predicted Optimum Settings for Percentage *E. Coli* Bacterial Reduction

X_1	X_2	X_3	Predicted Y_{EC1}
3	36	130	99.5877
2.59	14.59	100.27	98.7125
2	36	80	98.6849
2	36	130	98.3919
2	36	180	98.0989

X_1 = Synthesis Time (hrs), X_2 = Incubation Time (hrs), X_3 = Curing Temperature (℃)

The optimum settings yielded a maximum synthesis time of 3 hours. As the synthesis time increased, the antibacterial efficacy increased as shown in Figure 4:31. An increase in synthesis time increases, more silver ions are reduced to silver nanoparticles. As a result, the concentration of nanoparticles on the fabric surface increases (Verbič et al., 2018). This increases the chance of the nanoparticles interacting with bacteria thus improving antibacterial efficacy. Longer synthesis time also allows for better silver nanoparticle dispersion and coverage on the fabric. This means that the nanoparticles are in contact with more areas of the fabric, resulting in improved antimicrobial activity. Adequate dispersion and coverage inhibit bacterial growth and colony formation thus enhancing antibacterial efficacy (Abazari et al., 2023).

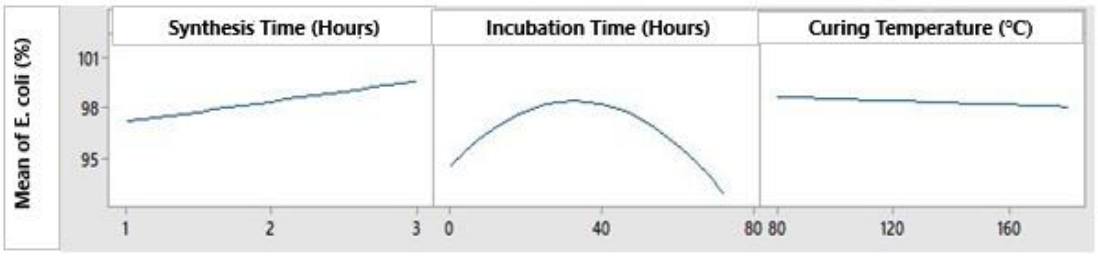

Figure 4:10. Settings and Sensitivity for Optimal Percentage *E. Coli* Bacterial Reduction

The optimum curing temperature was found to be 80 ℃. As the curing temperature increased, the antibacterial efficacy decreased. Higher temperatures can increase the size and the aggregation of the silver nanoparticles on the fabric surface. This can reduce the surface area and contact of the nanoparticles with the bacteria and decrease the antibacterial activity of the treated fabrics. Higher curing temperatures can also cause thermal damage to the stabilizing agents used to prevent silver nanoparticle agglomeration and oxidation. This can have an effect on the stability of the nanoparticles as well as the release of the silver ions, thus reducing the antibacterial activity of the fabrics. Previous studies agree that at very high temperatures the

antibacterial efficacy reduces (Pourali et al., 2013; C. E. Zhou et al., 2016). Lower curing temperatures can preserve the size, shape, distribution and stability of silver nanoparticles on the fabric surface, increasing the surface area and contact of the nanoparticles with bacteria and enhancing the fabric's antibacterial activity.

As the incubation time increased, there was an increase in antibacterial efficacy up to about 37 hours. Longer incubation times allow for more time for the reduction of silver ions in the solution, resulting in the formation of a greater quantity of silver nanoparticles on the fabric (Ribeiro et al., 2022). With the increased nanoparticles, there is more surface area available for interaction with bacteria, which improves the antimicrobial effect. Longer incubation times allow for more time for silver nanoparticles to attach to the fabric's surface. This attachment ensures more uniform distribution of nanoparticles and adhesion to the fibres, resulting in better contact between nanoparticles and bacteria.

Longer incubation time may result in the formation of larger silver nanoparticles. These are more stable and have lower tendency to aggregate, resulting in better antibacterial performance. The larger size enables more efficient silver ion release and better penetration into the bacterial cell membranes, resulting in increased antibacterial efficacy. After 37 hours of incubation time, the antibacterial efficacy reduced. This is because excessively long incubation times can cause nanoparticle aggregation or reduced dispersion, reducing their antimicrobial properties (Bélteky et al., 2021). Therefore, the optimum value for incubation time was found to be 32.73 hours.

Results for S. Aureus Percentage Bacterial Reduction

The regression equation for the bacterial reduction of treated fabrics before washing against *S. aureus* (Y_{SA1}) is shown in Equation 4.4. The model had a coefficient of

determination (R^2) of 87.99 % and a p value of 0.000 %. This means that 87.99 % of the variation in Y_{SA1} can be explained by the input variables in the regression model and also that the model is significant. The adjusted R^2 for the unseen data set was 82.44 % . The high R^2 values suggest that the models adequately fit the data sets.

$$Y_{SA1} = 81.85 + 6.51\ X_1 + 0.2808X_2 + 0.0494\ X_3 - 0.00300\ X_2^2 - 0.0454X_1X_2 - 0.0257X_1X_3$$

Equation 4.4

Table 4:8 displays the ANOVA, factor contributions, and Variance Inflation factors for percentage bacterial reduction (*S. aureus*) before washing. The highest factor contributor for the model for *S. aureus* bacterial reduction before washing was the square of incubation time with 50.14 % contribution and the least contributor was curing temperature with a contribution of 0.09 %. The antibacterial effectiveness of the silver nanoparticles is generally increased by increasing the incubation period due to an increase in the number of nanoparticles generated on the fabric (Wisnuwardhani et al., 2019). This explains why incubation time was the highest contributor to the regression model. Synthesis time contributed 19.25 %, incubation time contributed 11.13 %, the combined effect of synthesis time and incubation time contributed 7.38 % and the combined effect of synthesis time and curing temperature contributed 2.83 % to the regression model. The P values for the estimated coefficients, curvilinear and interaction effects were less than 0.05, with the exception of the combined effect of curing temperature and synthesis time as well as the curing temperature indicating that the model and all other factors were significant.

Table 4:4. ANOVA, Factor Contributions (%) and VIF for *S. aureus* Reduction before Washing

	ANOVA (P - value)	FC %	VIF
Regression model	0.000	87.99	
Linear	0.001	30.46	
Synthesis Time	0.001	19.25	1.00
Incubation Time	0.004	11.13	1.00
Curing Temperature	0.760	0.09	1.00
Square	0.000	50.14	
Incubation Time * Incubation Time	0.000	50.14	1.00
2-way Interaction	0.044	7.38	
Synthesis Time * Incubation Time	0.045	4.55	1.00
Synthesis Time * Curing Temperature	0.104	2.83	1.00
Error		12.01	
Lack-of-Fit	0.000	11.95	
Pure Error		0.06	
Total		100	

The interaction between different parameters was analysed and the results are shown in Figure 4:32. This shows that there was an interaction between synthesis time and incubation time and also between synthesis time and curing temperature.

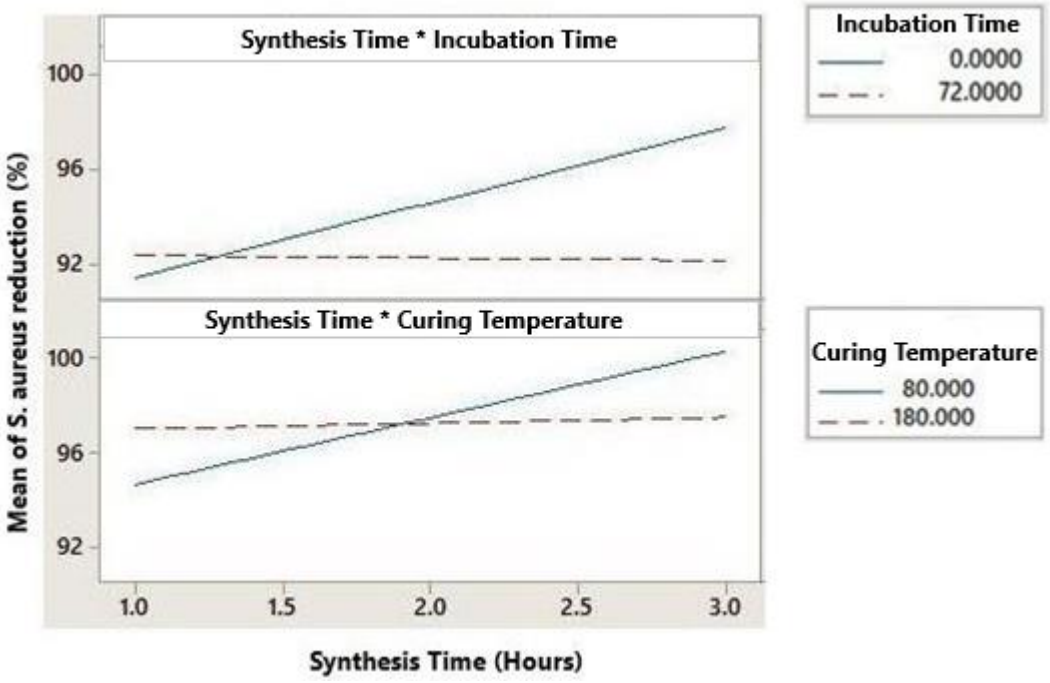

Figure 4:11. Combined Effects of Synthesis Time with Incubation Time and Curing Temperature

The combined effect of synthesis time and incubation time shows that at an incubation time of 0 hours, as the synthesis time increases there is no change in percentage bacterial reduction of *S. aureus*. However, at an incubation time of 72 hours, as the synthesis time increases, the percentage bacterial reduction of *S. aureus* increases. This is further explained in the 3D surface plot of incubation time and synthesis time against percentage bacterial reduction of *S. aureus* (Figure 4:33). At a curing temperature of 130 ℃, an increase in synthesis time and an increase in incubation time up to 36 hours results in an increase in percentage bacterial reduction for *S. aureus*. After 36 hours there is a decline in the percentage bacterial loss.

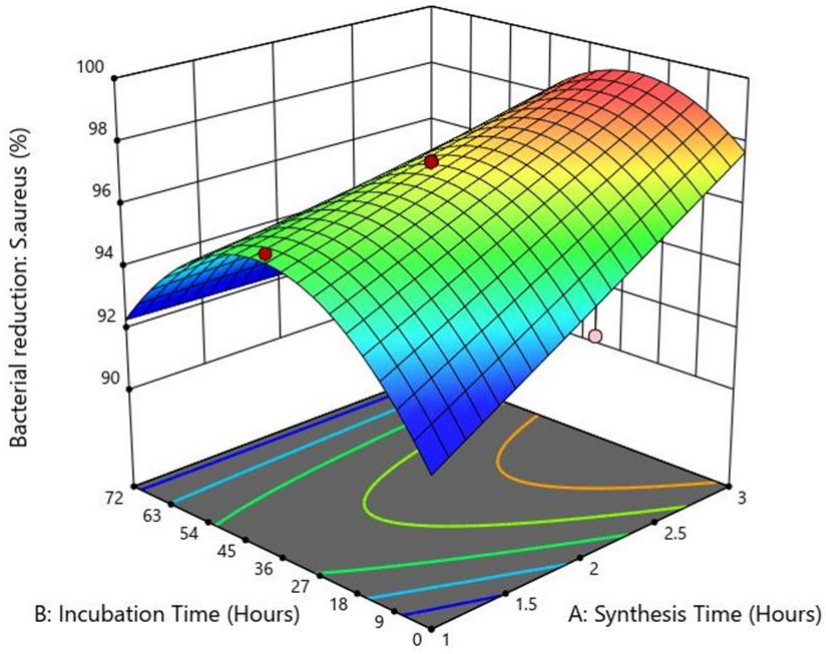

Figure 4:12. Response Surface 3D Plot Indicating the Interaction Between Incubation Time and Synthesis Time on *S. Aureus* Percentage Bacterial Reduction

The combined effect of synthesis time and curing temperature in Figure 4:34 shows that at a temperature of 80 ℃ there was an increase in percentage bacterial reduction for *S. aureus* as the synthesis time increased. However, at a temperature of 180 ℃ there was not much change in percentage bacterial reduction for *S. aureus*. This is further

explained in the 3D surface plot for synthesis time and curing temperature against percentage bacterial reduction for *S. aureus*. At an incubation time of 36 hours, an increase in synthesis time and an increase in curing temperature result in an increase in percentage bacterial reduction for *S. aureus*.

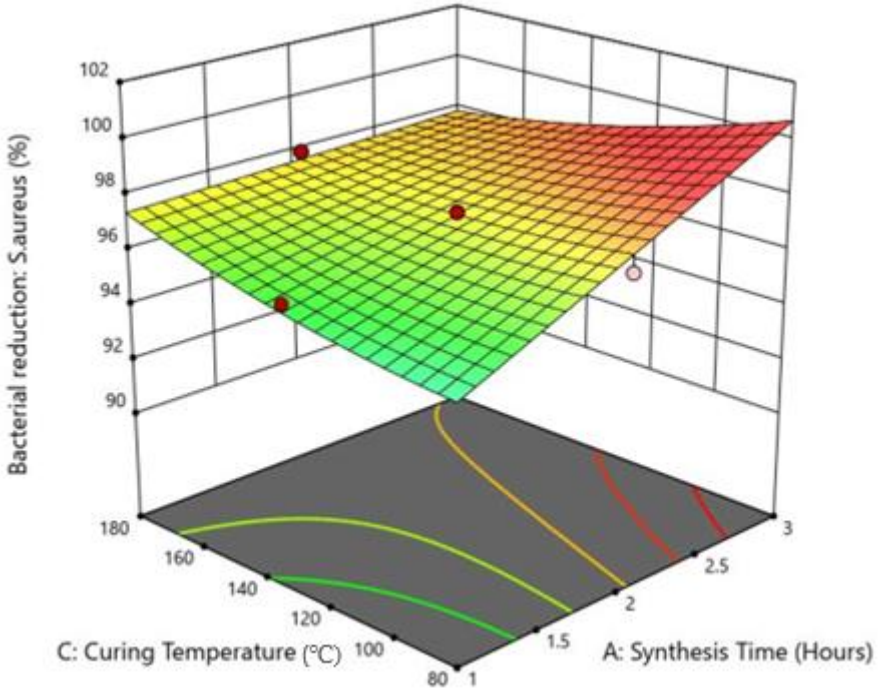

Figure 4:13. Response Surface 3D Plot Indicating the Interaction Between Curing Temperature and Synthesis Time on *S. Aureus* Percentage Bacterial Reduction

The regression model was used to predict the optimal settings for *S. aureus* percentage bacterial reduction. The optimal settings were found to be; synthesis time (X_1) of 3 hours, incubation time (X_2) of 23.27 hours and curing temperature (X_3) of 80 ℃, to obtain a predicted *S. aureus* percentage reduction (Y_{AS1}) of 99.398 %. The top five values closest to the predicted optimum settings for *S. aureus* percentage bacterial reduction (see Table 4:9) were also considered in case the optimum settings were not practicable.

Table 4:5. Values Closest to the Predicted Optimum Settings for *S. Aureus* Percentage Bacterial Reduction

X_1	X_2	X_3	Predicted Y_{AS1}
3	36	130	98.9596
2.595	14.594	100.27	98.7110
2.595	14.594	159.73	97.6766
2	36	80	97.5361
2	36	130	97.4316

X_1 = Synthesis Time (hrs), X_2 = Incubation Time (hrs), X_3 = Curing Temperature (°C)

The optimum settings yielded a synthesis time of 3 hours. The synthesis time was positively correlated to the antibacterial efficacy against *S. aureus* as shown in Figure 4:35. This is similar to the results obtained for *E. coli*; an increase in synthesis time results in the formation of more silver nanoparticles, increasing concentration of the nanoparticles on the fabric surfaces and therefore enhancing antibacterial efficacy. Longer synthesis time improves nanoparticle dispersion and coverage, inhibiting bacterial growth and formation. Similar results were observed in previous studies where the antibacterial efficacy increased with synthesis time (Abazari et al., 2023; Jain et al., 2022; Verbič et al., 2018).

The antibacterial efficacy increased with incubation time until it reached an optimum time of 23.27 hours beyond which the antibacterial efficacy reduced. Longer incubation times increase silver ion reduction, forming more silver nanoparticles on the fabric and improving antimicrobial effects (Ribeiro et al., 2022). This leads to better contact of the nanoparticles with bacteria. However, excessively long incubation can reduce antibacterial efficacy, as they can cause nanoparticle aggregation or reduced dispersion (Bélteky et al., 2021).

The optimum curing temperature for *S. aureus* antibacterial efficacy was found to be 80 °C. There was a slight decrease in the antibacterial efficacy as the curing temperature increased. Higher temperatures can increase silver nanoparticle size and aggregation on

fabric surfaces, reducing antibacterial activity. Additionally, higher curing temperatures can damage the stabilizing agents, affecting nanoparticle stability and the release of silver ions, further reducing fabric antibacterial activity (Pourali et al., 2013; Zhou et al., 2016).

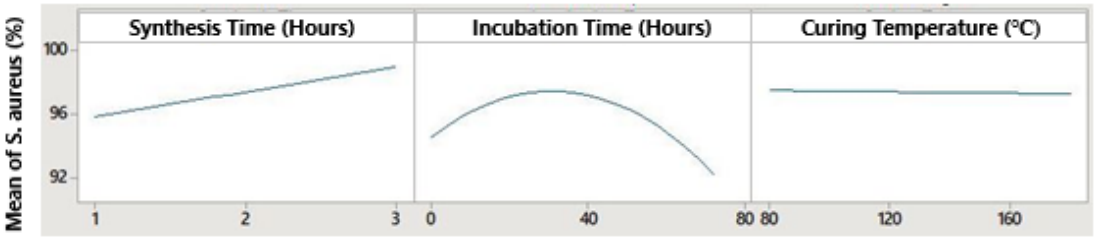

Figure 4:14. Settings and Sensitivity for Optimal *S. Aureus* Bacterial Reduction

4.3.3.2 Loss in Antibacterial Activity of the Treated Fabrics after Washing

The goal of the experimental design for percentage loss in antibacterial activity after 20 washes for both *E. coli* and *S. aureus* was to minimise the response. That is, a lower percentage loss in antibacterial activity meant that the antibacterial treatment was more durable against the tested bacterial strains. The percentages range from 0 % to 100 % with 0 % indicating that there was no loss in bacterial activity even after 20 washes and therefore the treatment was durable while 100 % indicated that there was complete loss in antibacterial treatment after 20 washes and therefore the treatment was not durable. The percentage loss in bacterial reduction was calculated as the difference between percentage bacterial reduction before and after washing.

Results for Loss in Antibacterial Activity on E. Coli

The regression equation for the percentage loss in antibacterial activity of treated fabrics after washing against *E. coli* (Y_{EC2}) is shown in Equation 4.5. The model had a coefficient of determination (R^2) of 82.89 % and a p value of 0.000 %. This means that 82.89 % of the variation in Y_{EC2} can be explained by the input variables in the regression

model and that the model is significant. The adjusted R^2 for the unseen data set was 79.86 %. The high R^2 values suggest that the models adequately fit the data sets.

$$Y_{EC2} = 3.061 - 0.02145X_2 - 0.005544X_3 + 0.000238X_2^2$$

Equation 4.5

Table 4:10 displays the ANOVA, factor contributions, and Variance Inflation factors for percentage loss in antibacterial activity for *E.coli* after washing. According to the percentage contribution of the factors, the curing temperature was the highest contributor for the model for *E. coli* percentage loss in antibacterial activity with 46.45 %. High curing temperature improves the stability and durability of treated textile fabrics against thermal and mechanical destruction (Billah, 2019; Dhiman & Chakraborty, 2017); therefore it contributed the most to the model. This was followed by the square of incubation time with a contribution of 21.86 %. Incubation time contributed 14.58 % while synthesis time was not included in the model. The P values for the estimated coefficients, curvilinear and interaction effects were less than 0.05, indicating that the model was significant.

Table 4:6. ANOVA, Factor Contributions (FC%) and VIF for *E. Coli* Percentage Loss in Antibacterial Activity

	ANOVA (P - value)	FC %	VIF
Regression model	0.000	82.89	
Linear	0.000	61.03	
Incubation Time	0.002	14.58	1.00
Curing Temperature	0.000	46.45	1.00
Square	0.000	21.86	
Incubation Time * Incubation Time	0.000	21.86	1.00
Error		17.11	
Lack-of-Fit	0.000	17.07	
Pure Error		0.04	
Total		100	

The combined effect of curing temperature and incubation time against the percentage loss in antibacterial activity on *E. coli* after washing is shown in the 3D plot in Figure 4:36. At a synthesis time of 2 hours, an increase in curing temperature results in a decrease in percentage loss in antibacterial activity which indicates an increase in durability of the antibacterial treatment to washing. As the incubation time increased, there was a decrease in percentage loss in antibacterial activity up to 40.5 hours indicating an increase in the durability of the antibacterial treatment to washing. After 40.5 hours there was an increase in percentage loss in antibacterial activity as the incubation time increased, indicating a reduction in durability of the antibacterial treatment to washing.

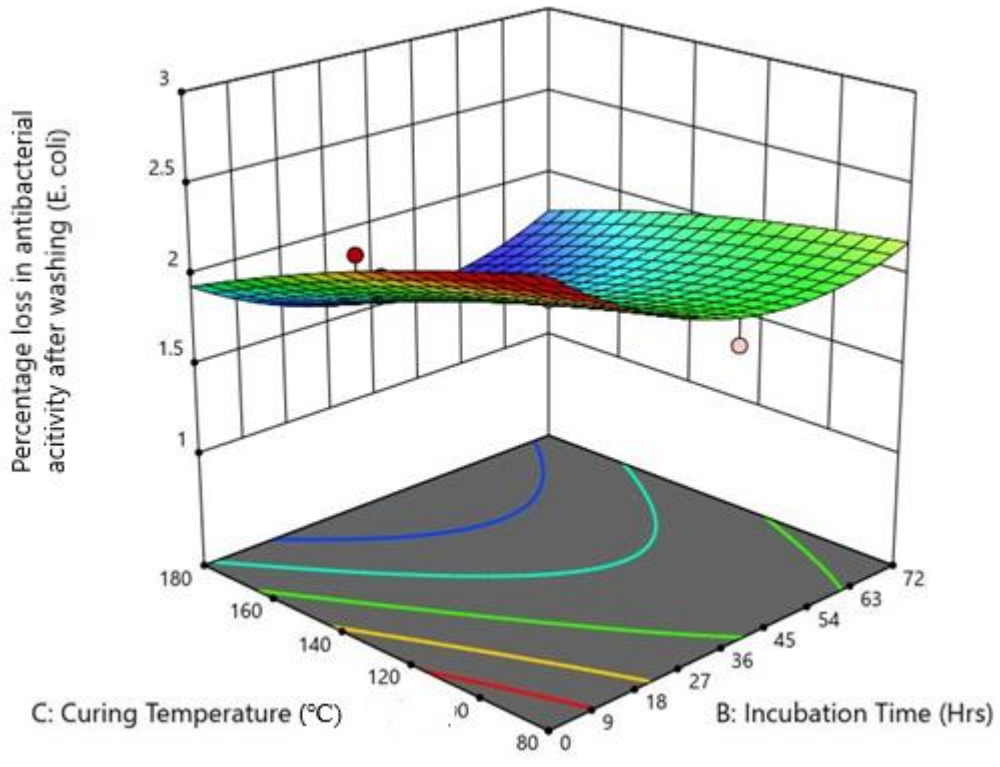

Figure 4:15. Response Surface 3D Plot Indicating the Interaction Between Curing Temperature and Incubation Time on *E. Coli* Percentage Loss in Antibacterial Activity after 20 Washes

The combined effect of incubation time and synthesis time against the percentage loss in antibacterial activity on *E. coli* after washing is shown in the 3D plot in Figure 4:37. At a curing temperature of 130 ℃, as the synthesis time increased, there was an increase in percentage loss in antibacterial activity which indicates a reduction in durability of the antibacterial treatment to washing. An increase in incubation time up to 40 hours resulted in a decrease in percentage loss in antibacterial activity, indicating an increase in durability of the antibacterial treatment. However, after an incubation time of 40 hours the percentage loss in antibacterial activity increased which indicated that the durability of the antibacterial treatment to washing decreased.

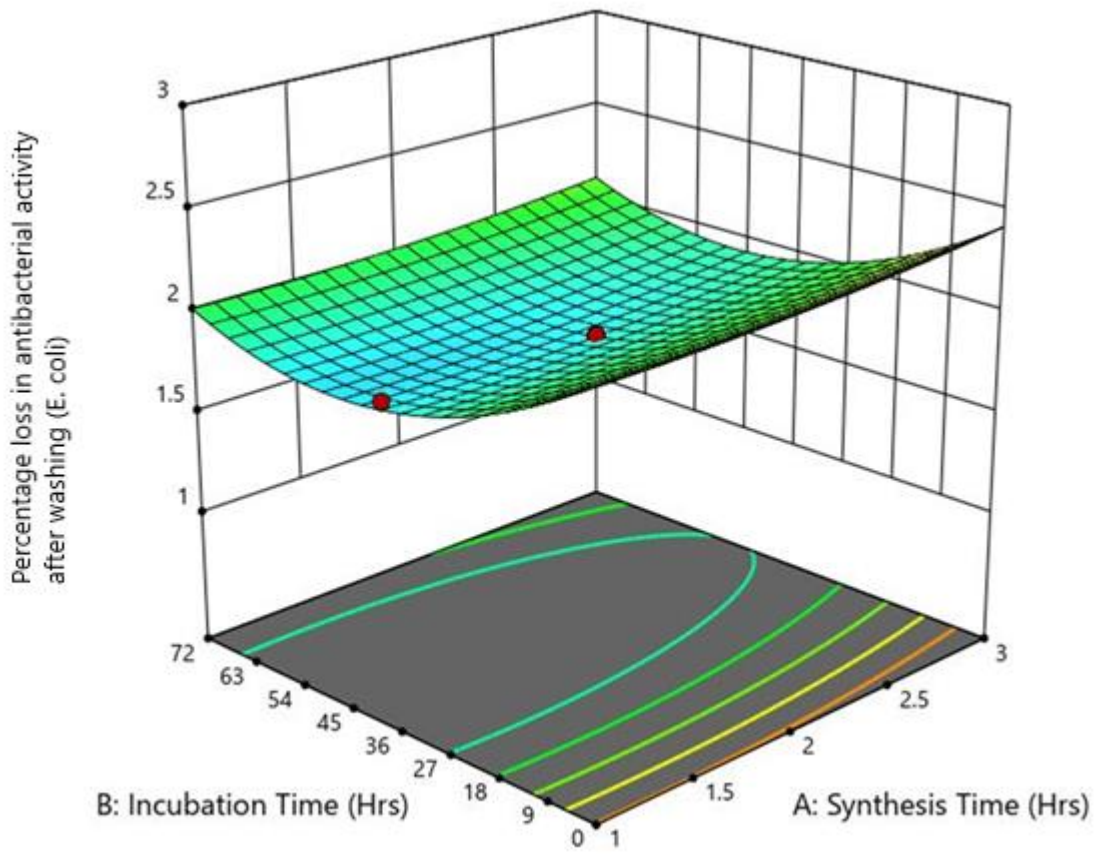

Figure 4:16. Response Surface Plot Indicating the Interaction Between Incubation Time and Synthesis Time on *E. Coli* Percentage Loss in Antibacterial Activity

The combined effect of curing temperature and synthesis time against the percentage loss in antibacterial activity on *E. coli* after washing is shown in the response surface 3D plot in Figure 4:38. At an incubation time of 36 hours, an increase in curing temperature and a decrease in synthesis time resulted in a reduction in the percentage loss in antibacterial activity which indicated an increase in durability of the antibacterial treatment to washing.

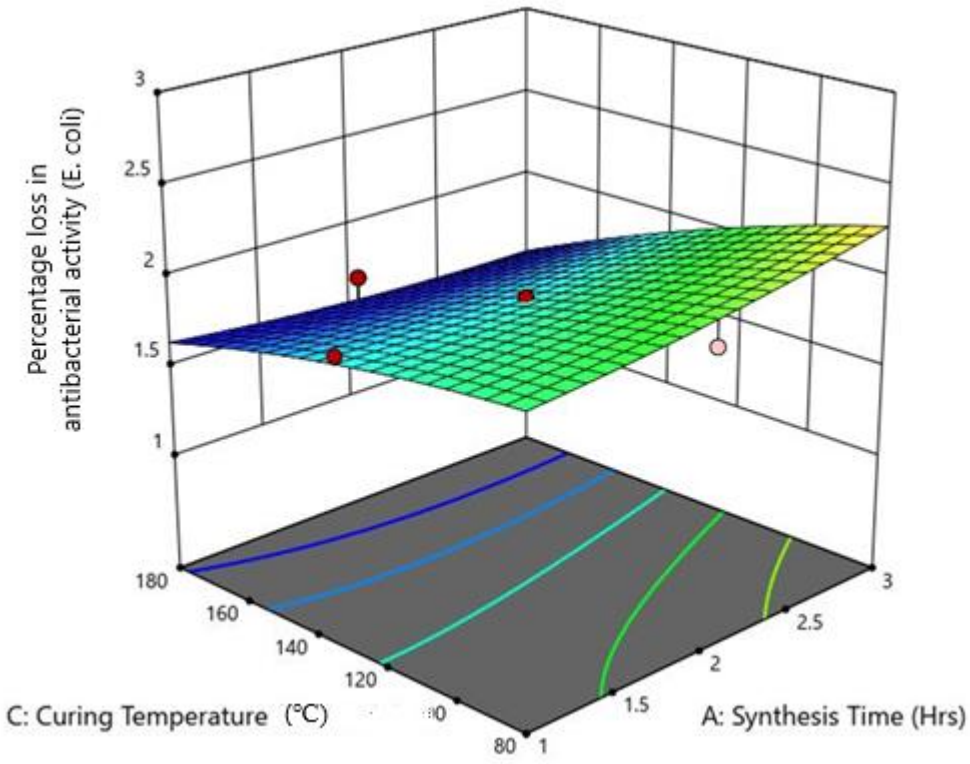

Figure 4:17. Response Surface 3D Plot Indicating the Interaction Between Curing Temperature and Synthesis Time on *E. coli* Percentage Loss in Antibacterial Activity

The optimal settings for a maximized percentage *E.coli* bacterial reduction were predicted from the regression model. The optimal settings obtained were: incubation time of 45.09 hours, curing temperature of 180 ℃ and a predicted *E. coli* percentage loss in antibacterial activity of 1.58029 %. The top five values closest to the predicted optimum settings for percentage *E. coli* bacterial reduction were also considered in case the optimum settings were not practicable and are shown in Table 4:11.

Table 4:7. Values Closest to the Predicted Optimum Settings for E. Coli Percentage Loss in Antibacterial Activity

X_2	X_3	Predicted Y_{EC2}
36	180	1.59983
57.4057	159.730	1.72895
36	130	1.87702
14.5943	159.730	1.91360
72	130	2.03025

X_2 = Incubation Time (hrs), X_3 = Curing Temperature (℃)

As the incubation time increased there was a decrease in the percentage loss of bacterial activity up to 32.73 hours (Figure 4:39) which meant that the durability of the silver nanoparticle finish on the fabric improved. Beyond 32.73 hours the loss in bacterial activity started to increase and the durability decreased. Longer incubation times provide additional time for the attachment of silver nanoparticles to the fabrics improving the adhesion of the nanoparticles to the fabric surface. This increased adhesion prevents nanoparticles from being washed away during subsequent laundering processes, ensuring that antimicrobial activity is maintained. However, excessively long incubation times can adversely reduce the antimicrobial properties. The optimum incubation time in this study was found to be 32.73 hours.

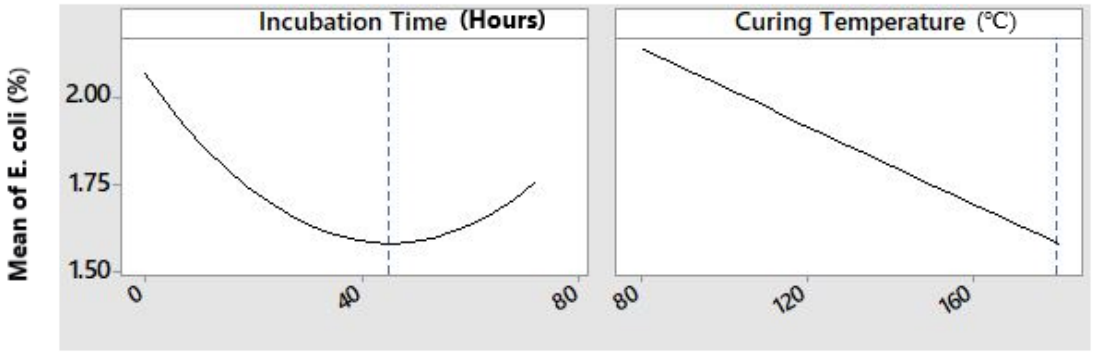

Figure 4:18. Main Effect Plots for Loss in *E. Coli* Bacterial Activity

The optimal curing temperature for minimum loss in *E. coli* bacterial activity was found to be 180 ℃. Higher curing temperatures can increase the stability and resistance of

silver nanoparticles on the fabric surface, which can prevent the agglomeration and oxidation of the nanoparticles and maintain their durability to washing . Earlier studies have also shown the importance of high curing temperatures in the durability of silver nanoparticles and their antibacterial efficacy even up to 20 washes (Abdel-Mohsen et al., 2012).

Results for Loss in S. Aureus Activity

The regression equation for the bacterial reduction of treated fabrics before washing against *S. aureus* (Y_{SA1}) is shown in Equation 13. The model had a coefficient of determination (R^2) of 85.07 % and a p value of 0.000 % . This means that 85.07 % of the variation in Y_{SA1} can be explained by the input variables in the regression model and that the model is significant. The adjusted R^2 for the unseen data set was 82.44 %. The high R^2 values suggest that the models adequately fit the data sets.

$$Y_{SA2} = - 0.292 – 0.02822X_2 + 0.0484X_3 + 0.000333X_2^2 – 0.000228X_3^2$$

Equation 4.6

The ANOVA, factor contributions, and variance inflation factors for percentage loss in antibacterial activity against *S. aureus* after washing are shown in Table 4:12. According to the percentage contribution of the factors, curing temperature contributed the highest with 47 % and incubation time contributed the least with 3.86 %. The square of curing temperature contributed 19.84 % while the square of incubation time contributed 14.37 % to the model. The P values for the estimated coefficients, curvilinear and interaction effects were all less than 0.05, indicating that the model is significant.

Table 4:8. ANOVA, Factor Contributions (FC%) and VIF for Percentage Loss in Antibacterial Activity Against *S. Aureus*

	ANOVA (P - value)	FC %	VIF
Regression model	0.000	85.07	
Linear	0.000	50.86	
Incubation Time	0.006	3.86	1.00
Curing Temperature	0.000	47.00	1.00
Square	0.000	34.21	
Incubation Time * Incubation Time	0.004	14.37	1.01
Curing Temperature * Curing Temperature	0.000	19.84	1.01
Error		14.93	
Lack-of-Fit	0.000	14.92	
Pure Error		0.01	
Total		100	

The combined effect of curing temperature and incubation time against the percentage loss in antibacterial activity on *S. aureus* after washing in shown in Figure 4:40. At a synthesis time of 2 hours, the loss in antibacterial activity increases as incubation time increases up to 40.5 hours indicating an increase in wash durability of the antibacterial treatment on the fabric. Thereafter, there is an increase in the loss in antibacterial activity on *S. aureus*, indicating a decrease in wash durability. During the same period, as curing temperature increases up to 130 ℃, there is an increase in the percentage loss in bacterial activity indicating a decrease in wash durability. Thereafter, the wash durability increases as the curing temperature increases, as shown by the reduction in percentage loss in antibacterial activity on *S. aureus*.

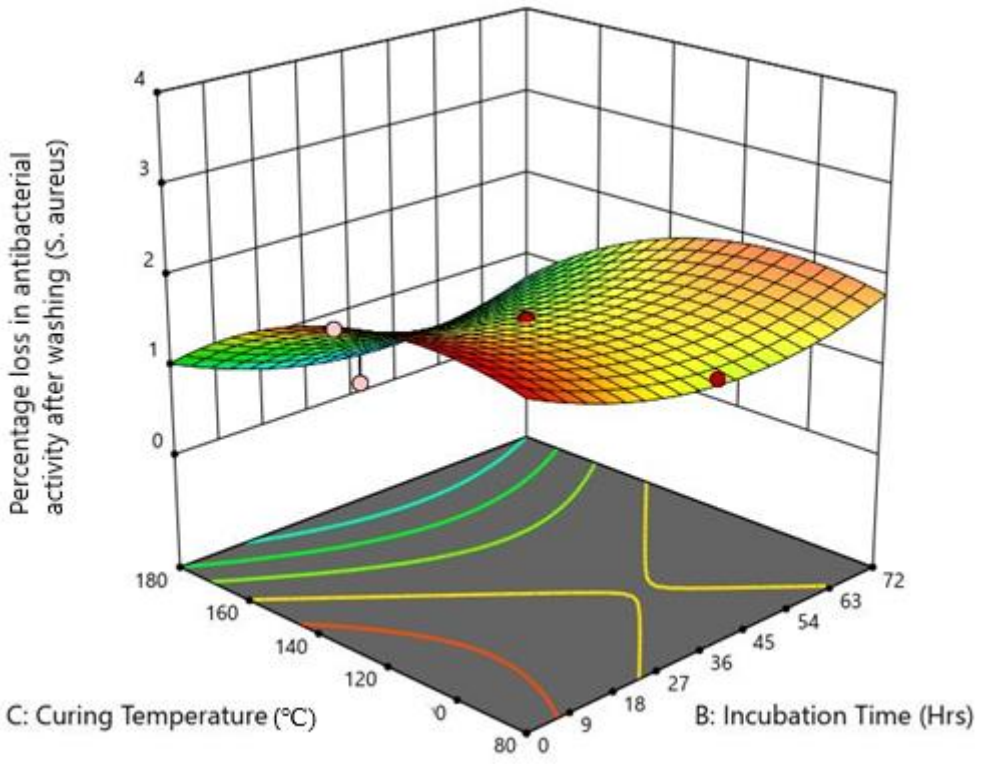

Figure 4:19. 3D Plot Indicating the Interaction Between Curing Temperature and Incubation Time on Percentage Loss in Antibacterial Activity against *S. Aureus*

The combined effect of curing time and synthesis time is shown in Figure 4:41. At a curing temperature of 130 ℃, the percentage loss in antibacterial activity increases as synthesis time increases indicating a decrease in wash durability of the antibacterial treatment on the fabric. During the same period, as incubation time increases up to 40.5 hours, there is a decrease in the percentage loss in antibacterial activity, indicating an increase in wash durability. Thereafter the percentage loss in bacterial activity increases as the incubation time increases, indicating a decrease in the durability of the antibacterial treatment to washing.

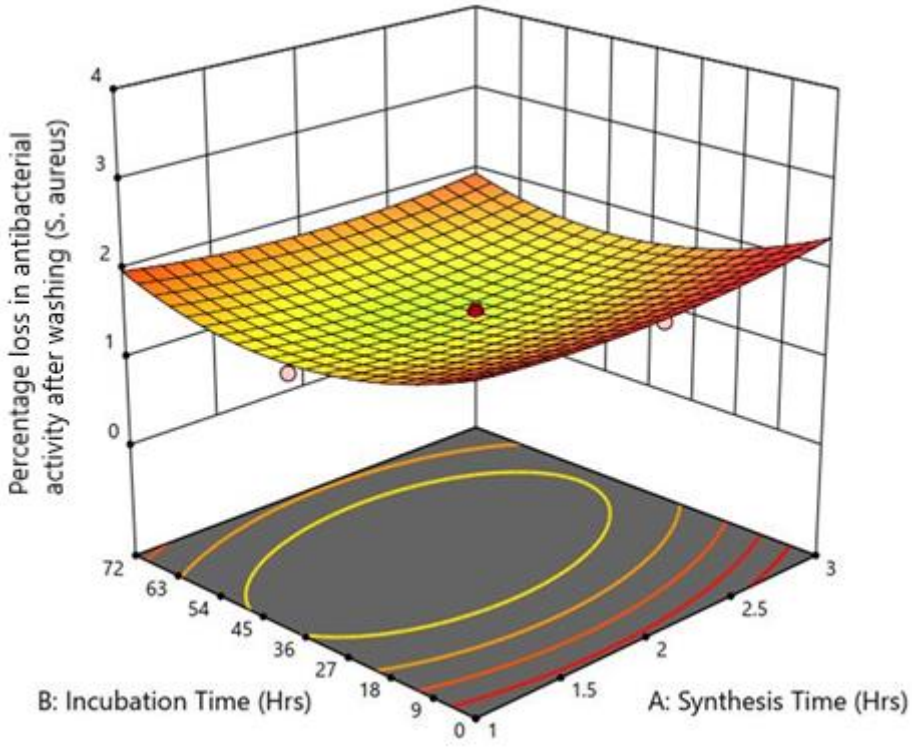

Figure 4:20. 3D Surface Plot Indicating the Interaction Between Incubation Time and Synthesis Time on Percentage Loss in Antibacterial Activity against *S. Aureus*

The combined effect of synthesis time and curing temperature at an incubation time of 36 hours, is shown in Figure 4:42. An increase in synthesis time and an increase in curing temperature up to 130 ℃ results in an increase in percentage loss in antibacterial activity on *S. aureus* indicating a decline in durability of the antibacterial treatment to washing. Thereafter, the percentage loss in antibacterial activity decreases as the curing temperature increases, indicating an increase in the durability of the antibacterial treatment to washing.

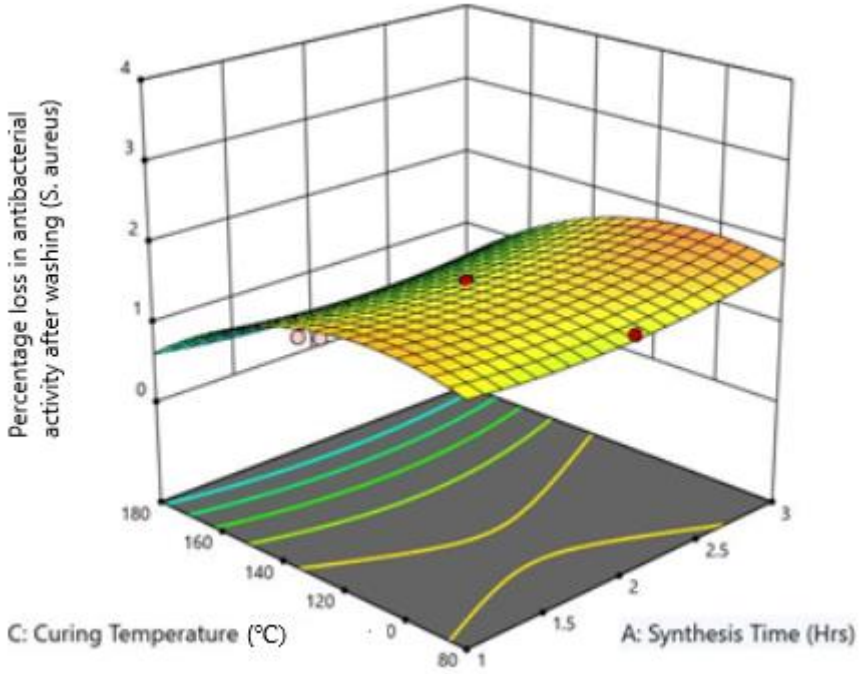

Figure 4:21. 3D Surface Plot Indicating the Interaction Between Curing Temperature and Synthesis Time on Percentage Loss in Antibacterial Activity against *S. Aureus*

A prediction of the optimal settings for a minimized percentage loss in antibacterial activity for *S. aureus* was made from the regression model. The optimal settings obtained were: incubation time of 42.1818 hours and a curing temperature of 180 °C for a predicted percentage loss in antibacterial activity of 0.451882 %. The values closest to the predicted optimum settings for the percentage loss in antibacterial activity against *S. aureus* were also considered in case the optimum settings were not practicable and are shown in Table 4:13.

Table 4:9. Values Closest to the Predicted Optimum Settings for Loss in Antibacterial Activity against S. Aureus

X_2	X_3	Predicted Y_{AS2}
36	180	0.465637
57.4057	159.730	1.11220
14.5943	159.730	1.29545
36	80	1.54092
36	130	1.57235

X_2 = Incubation Time (hrs), X_3 = Curing Temperature (°C)

The durability of silver nanoparticle finishes on cotton fabric improved with longer incubation times, up to 42 hours. Longer incubations improve the adhesion of nanoparticles to the fabric surface, preventing them from being washed away during the laundering processes. However, as shown in Figure 4:43, excessively long incubation times can reduce antimicrobial properties. After 42 hours the loss in antibacterial activity increased, indicating a reduction in durability of the silver nanoparticle antibacterial finish on the fabric.

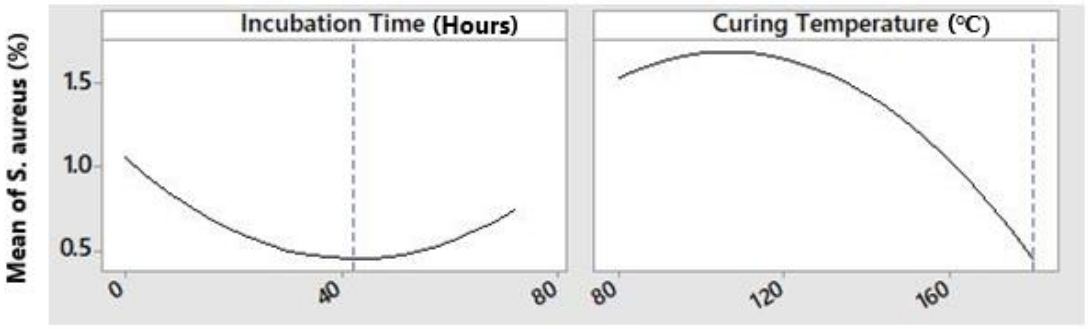

Figure 4:22. Main Effect Plots for *S. Aureus* Loss in Antibacterial Activity

The optimal curing temperature for minimizing *S. aureus* bacterial activity loss was found to be 180 ℃. As curing temperature increased from 80 ℃ to 100 ℃ the loss in antibacterial activity increased from 1.5 % to 2 %; thereafter the loss in antibacterial activity reduced indicating that there was improved durability of the silver nanoparticles on the cotton fabric. Higher curing temperatures enhance the silver nanoparticle stability and resistance, preventing agglomeration and oxidation on fabric surfaces, thus improving the durability of the treated fabrics to washing.

4.3.4 Antibacterial Efficacy of Fabrics Treated with Optimal Parameters

In the optimisation of the in-situ synthesis of silver nanoparticles onto cotton fabrics; maximum bacterial reduction was observed at a curing temperature of 80 ℃, an incubation time of 32.73 hours and a synthesis time of 3 hours. Maximum durability to

washing was observed at a curing temperature of 180 ℃, an incubation time of 42.18 hours and a synthesis time of 3 hours. Durability is a crucial factor to enable the enhanced use of the treated fabrics for a longer period of time and the endurance of the properties after several washes. Therefore, these parameters were used in the in-situ synthesis of silver nanoparticles onto cotton fabrics: incubation time of 42.18 hours, curing temperature of 180 ℃ and synthesis time of 3 hours. The treated fabric exhibited maximum antibacterial activity against gram negative *E. coli* compared to *S. aureus*; which is in agreement with earlier studies. The percentages of bacterial reduction at 0 washes and at 20 washes for both *E. coli* and *S. aureus* are shown in Table 4:14.

Table 4:10. The Antibacterial Activity of Untreated and Treated Cotton Fabrics before Washing and after 20 Washes

Sample	**Reduction of bacteria (%)**	
	E. coli	***S. aureus***
Silver nanoparticle treated cotton fabric before washing	100 %	99.68 %
Silver nanoparticle treated cotton fabric after 20 washes	99.52 %	99.01 %
Percentage loss in antibacterial activity after 20 washes	0.48 %	0.67 %

The results in Table 4:14 show that, when the optimum values were used for in-situ synthesis; there was an increase in the antibacterial efficacy of *E. coli* and *S. aureus*. There was also an improvement in the durability of the nanoparticle antibacterial finish on the fabric after 20 washes as shown by the lower percentage losses in antibacterial activity.

4.4 Characteristics of the Fabric Treated with Silver Nanoparticles

4.4.1 Morphology and Elemental Analysis

The changes in the surface morphology of the cotton fabrics caused by the in-situ synthesis of silver nanoparticles were investigated using the Scanning Electron

Microscope (SEM). The SEM images in Figure 4:44 revealed that the fibres of the untreated control cotton fabric (Figure 4:44 A) had a smooth longitudinal fibril structure with no contaminating particles on the surface. The cotton fibres treated with silver nanoparticles were coarser (Figures 4:44 B, C and D), due to the formation of a thin layer of nanoparticles around the fibres (marked with circles). The images demonstrated that the silver nanoparticles were spherical in nature and were distributed throughout the fibre surface. Some of the silver nanoparticles agglomerated therefore the images show a mix of small nanoparticles and larger aggregated particles; a trend that was previously reported by other researchers (Mahmud et al., 2020; Shateri-Khalilabad et al., 2017; Syafiuddin et al., 2020). Overall surface morphology showed that silver nanoparticles were successfully deposited onto the cotton fabric.

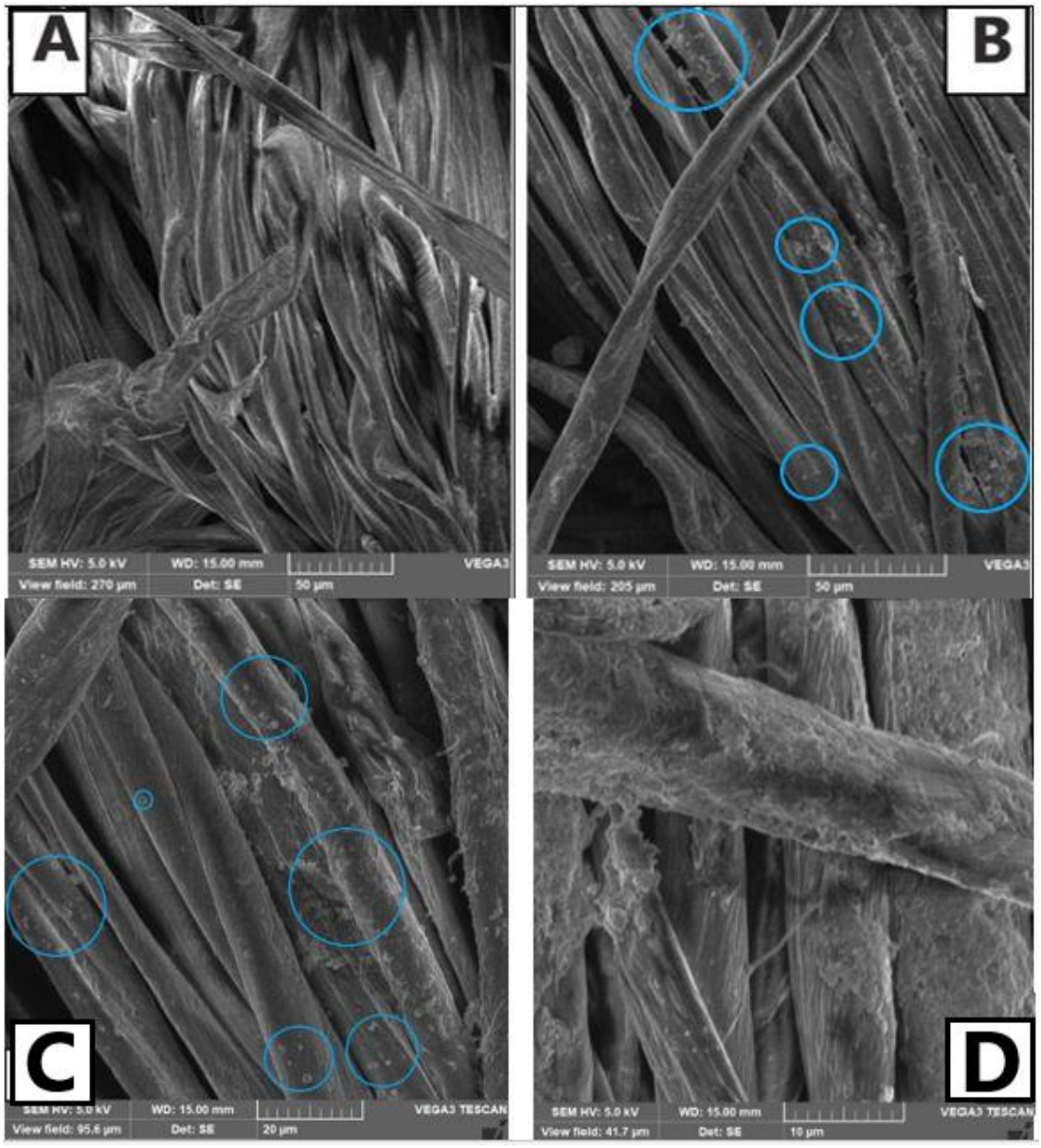

Figure 4:1. SEM Images of Cotton fabrics. A - Untreated Cotton Fabric, B - Treated Fabric at 1.02 k Magnification, C - Treated fabric at 2.18 k Magnification, D - Treated Fabric at 4.99 k Magnification.

The elemental profile of the silver nanoparticle treated fabric in Figure 4:45 revealed a clear peak at 3 keV which is characteristic of silver nanoparticles based on their surface plasmon resonance (Novoa et al., 2022); confirming the presence of silver nanoparticles. Furthermore, EDX elemental analysis revealed that the sample was primarily composed of carbon (46.15 %) and oxygen (48.69 %), which are constituent elements of cellulose, the main component of cotton fibres. Silver was present in trace

amounts (5.16 %) and confirmed the application of the silver nanoparticles on the cotton fabric. Trace amounts of silver nanoparticles were also observed by another research where the elemental analysis showed that there was 2.2 % silver on the treated cotton fabric with carbon and oxygen accounting for more than 90 % of the elemental composition (Novoa et al., 2022).

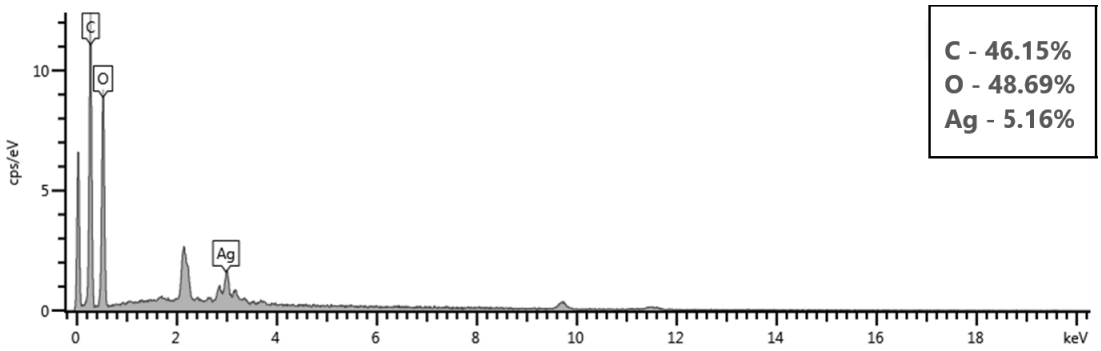

Figure 4:2. Elemental Analysis of the AgNP Treated Cotton Fabric

4.4.2 Functional Group Analysis

The functional group analysis of the cotton fabric before and after treatment with silver nanoparticles is shown in the FTIR spectra in Figure 4:46. The spectra show mainly the general characteristic peaks of cellulose, that is, 3330 cm^{-1} (H bonded O-H stretching), 2893 cm^{-1} (-CH stretching), 1636 cm^{-1} (C=C stretching) and 1022 cm^{-1} (C-O-C) for both the treated and untreated cotton fabrics. This demonstrates that the deposition of the green synthesized nanoparticles has no effect on the chemical structure of the cellulose fibre. It demonstrates that their interaction is only as a result of physical absorption and entrapment of the nanoparticles on the cotton fabric surface.

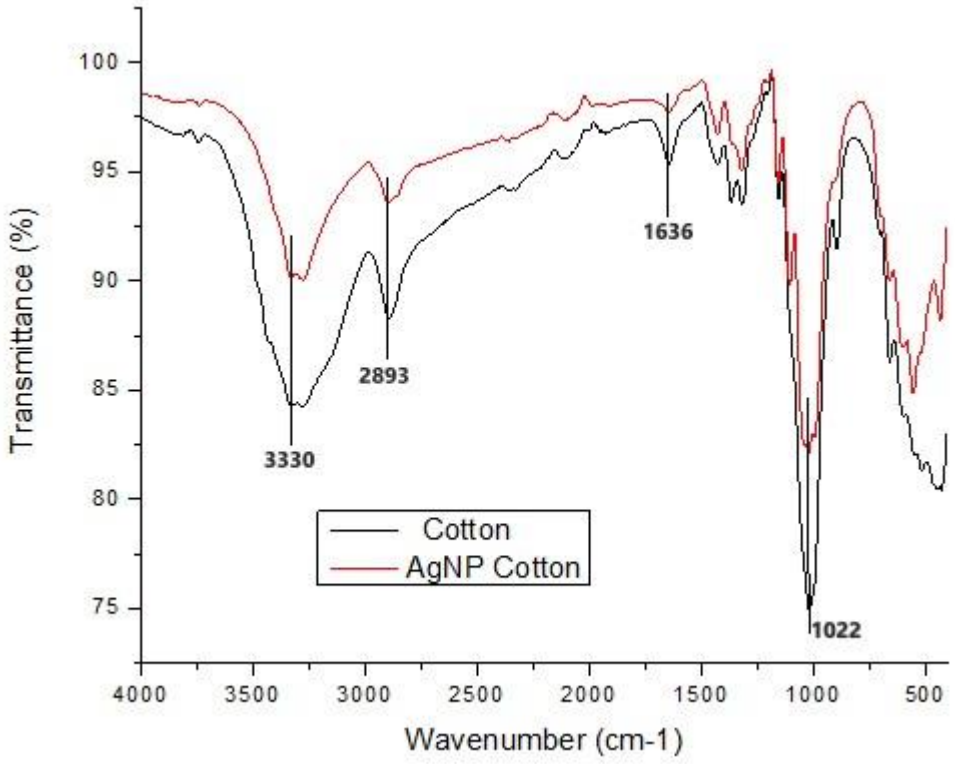

Figure 4:3. FTIR Spectra of Untreated Cotton Fabric and AgNP Treated Cotton Fabric

Similar results were observed in a study where silver nanoparticles were deposited on cotton fabric by in situ synthesis using ascorbic acid as a reducing agent. The results showed two spectra with no differences in peaks, indicating that the cellulose chemical structure was not altered by nano deposition (Tania et al., 2020). Another study where sodium alginate mediated silver nanoparticles were applied on cotton fabrics also found no new peaks on the treated fabric. However, there was an increase in peak intensity, particularly especially for C-H stretching, O-H stretching and C-O stretching, which was likely due to sodium alginate dominance (Mahmud et al., 2020). Silver nanoparticles bond with cellulosic materials through physisorption. This involves weak interactions between the nanoparticles and the fabric surface, such as, Vander Waals forces or electrostatic interaction (Salama et al., 2021). The process involves the silver nanoparticles adhering to fabric surface without significant chemical bonding and therefore does not alter the chemical structure of cotton (Huang et al., 2022).

4.4.3 Thermogravimetric Analysis

The thermogravimetric properties of the cotton fabric before and after adding the silver nanoparticles is shown in Figure 4:47.

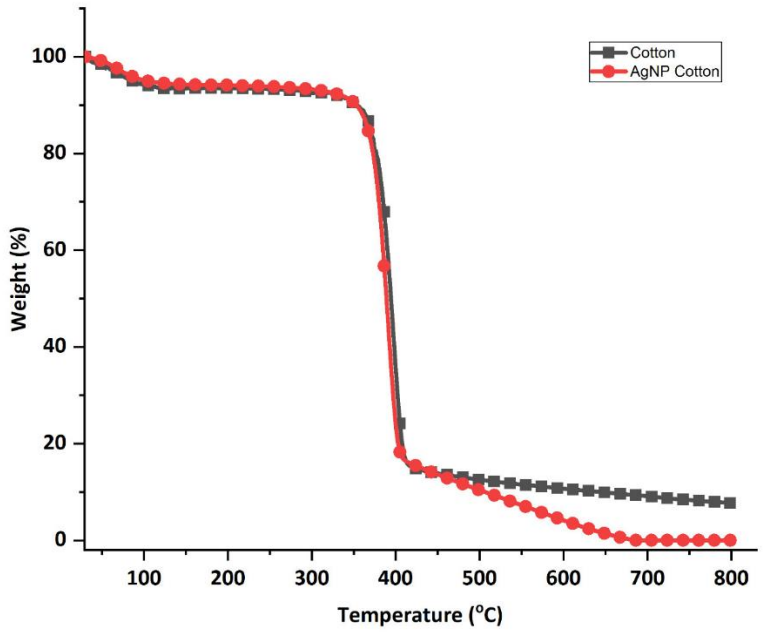

Figure 4:4. TGA Thermograms of Untreated Cotton Fabric and Fabric Treated with Silver Nanoparticles (AgNP Cotton)

There was no difference in weight loss for both fabric samples at the initial stage from room temperature to 100 ℃ and this is constant until around 350 ℃. The weight loss was approximately 5 % due to the removal of the moisture content in the fabrics 350 ℃. A sharp weight loss is observed for both fabric samples from about 350 ℃ to 400 ℃ for AgNP treated cotton fabric and from 350 ℃ to 410 ℃ for untreated cotton fabric, which can be attributed to the thermal decomposition of the cotton fabric (Krishnamoorthy et al., 2012). This weight loss continues until 700 ℃; however, the weight loss of the sample treated with silver nanoparticles is higher than the untreated sample. This is due to the interaction between the green synthesized silver nanoparticles and the cellulose molecules of the cotton fabric, which can alter the kinetics and thermal decomposition mechanism of the fabric (H. M. M. Ibrahim & Hassan, 2016). Previous

research has shown that silver nanoparticles can improve the thermal stability of cotton fabrics by forming a protective layer on the fabric surface, delaying thermal degradation and increasing char residue (Jagadeshvaran & Bose, 2023). However, other research suggests that silver nanoparticles can reduce the thermal stability of cotton fabrics by catalysing cellulose decomposition and decreasing the activation energy of thermal degradation (Nam et al., 2022). As a result, the effect of silver nanoparticles on the thermal stability of cotton fabrics may vary depending on factors such as nanoparticle size, shape, distribution and concentration as well as deposition method and cotton fabric type. Differences in thermal degradation of untreated and AgNP treated cotton fabrics were reported in earlier works (Abazari et al., 2023; H. Liu et al., 2014). In this current study the thermal stability of the fabric reduced upon addition of the silver nanoparticles, thus the char residue also reduced.

4.4.4 Air Permeability

There was a reduction in the air permeability on application of the silver nanoparticles onto the fabric. The average air permeability of the untreated cotton fabric was found to be about 6780.433 mm/s while that of the cotton fabric treated with silver nanoparticles was about 6181.966 mm/s. This reduction could be due to the nanoparticle's deposition on the yarn structure and the subsequent reduction in pore size. The fabric pore size is proportional to the fabric's air permeability (Ogulata, 2006; Onal & Yildirim, 2012). As a result, decreasing the pore size reduces the fabric's air permeability. The same trend of a reduction in air permeability was also observed by other researchers who deposited nanoparticles onto cotton fabric (Ali et al., 2018; Čuk et al., 2021; Noman et al., 2020). The air permeability of the treated fabric only reduced by 8.8 %; this is a small reduction from the untreated sample; implying that the

nanoparticle treated cotton fabrics will still provide acceptable comfort to the potential user.

4.4.5 Tensile Strength

The influence of the silver nanoparticle finish on cotton fabric properties was also investigated by measuring their mechanical properties in terms of tensile strength (MPa), as these parameters are directly affected by the fabric's continued use. The addition of silver nanoparticles increased the tensile strength (MPa) and reduced the percentage elongation at break (%) of the control samples. Tensile strength increased from 204.013 MPa for untreated cotton fabric to 301.14 MPa for silver nanoparticle treated cotton fabric. The elongation break reduced from 8.12 % to 7.27 %. This behaviour could be attributed to silver nanoparticle absorption on cotton fibres, which resulted in increased tensile strength of the treated fabric. In other similar studies, cotton fibres impregnated with silver nanoparticles demonstrated improved mechanical properties due to the binding of the silver nanoparticles to the hydroxyl group of the cotton fibres' cellulose chains through hydrogen bonding or Vander Waals forces (Gollapudi et al., 2020; H. M. M. Ibrahim & Hassan, 2016; Xu et al., 2017). Another factor which could have had an effect is the high temperature curing which could have improved the fixation of the silver nanoparticles on the cotton fabric thus improving the tensile strength. The reduction in the elongation at break can be explained by the fact that as the nanoparticles are added to the fabric it becomes less stretchable and more resistant to breaking or tearing under tension (Elmogahzy & Farag, 2018).

CHAPTER FIVE: CONCLUSIONS AND RECOMMENDATIONS

5.1 Conclusions

The aim of this study was to investigate the use of potato peels in the green synthesis of silver nanoparticles for the production of antibacterial finishes for textile fabrics. This involved the extraction and characterisation of potato peels, the green synthesis and characterisation of silver nanoparticles, the application of nanoparticles on the cotton fabrics and antibacterial efficacy testing as well as the characterisation of the treated fabrics. Several conclusions are drawn from the study.

Phytochemical screening of the aqueous and ethanolic extracts confirmed the presence of several secondary metabolites including phenols and flavonoids. Quantitative total phenolic and flavonoid content showed that the aqueous extracts had higher phenolic and flavonoid contents that the ethanolic extracts and were therefore more suitable for use. The potato peel extracts have good antibacterial properties against both gram-negative *E. coli* and gram-positive *S. aureus*. The presence of phytochemicals such as anthocyanins, phenolic compounds and flavonoids in the potato peel structure contributes to its antibacterial properties.

Silver nanoparticles can successfully be synthesized by the reduction of silver nitrate to silver ions using potato peel extracts with an average size of 50.18 nm. The synthesis is affected by different parameters namely; concentration of extract, extract to silver nitrate ratio, pH, temperature, stirring speed and synthesis time. This resulted in the formation of spherical nanoparticles which are crystalline nature.

The potato peel can effectively be used as an eco-friendly antibacterial agent for cotton fabrics against *S. aureus* and *E. coli* with a slight reduction in the efficacy after 20 regular washing cycles. Results of this study suggest that potato peel extracts can be

used for antibacterial activity in 100 % woven cotton fabrics. In-situ synthesis of silver nanoparticles onto cotton fabric was successful and resulted in fabrics with antibacterial properties against both gram-negative *E. coli* and gram-positive *S. aureus* even up to 20 washes. The efficacy was higher for fabrics treated with silver nanoparticles than those treated with potato peel extracts. Antibacterial properties and durability of the nanoparticles on the fabric were improved when the in-situ synthesis was performed at optimised synthesis time, incubation time and curing temperature.

There was a difference in the mechanical properties of the cotton fabric upon treatment with silver nanoparticles. The surface morphology showed a change from a smoother to a rougher surface indicating the presence of nanoparticles on the surface. There was a change in the thermal properties of the fabric on the treated fabric as well as an 8.8 % reduction in air permeability. The tensile strength increased by 32 % while the elongation at break reduced from 8.12 % to 7.27 %. However, FTIR analysis showed that the deposition of nanoparticles on the cotton fabric had no effect on the chemical structure of the cellulose fibre. This showed that although the silver nanoparticles were deposited on the fabric, there was no chemical interaction of the silver nanoparticles with the cellulose.

5.2 Recommendations

To maximise the green synthesis of silver nanoparticles using potato peel extracts and their potential as antibacterial finishes on textile fabrics, the following are recommended:

1. The use of Shangi potato peel aqueous extracts as antibacterial agents against *S. aureus* and *E. coli*.
2. The green synthesis of silver nanoparticles using potato peel extracts and their use as antibacterial agents against *S. aureus* and *E. coli*.

3. The application of potato peel extracts and silver nanoparticles on 100 % cotton fabric as antibacterial finishes against *E. coli* and *S. aureus*.
4. The use of optimised parameters for the in-situ synthesis of silver nanoparticles onto cotton fabric for improved antibacterial properties and improved durability of the antibacterial finish up to 20 washes.

More studies can be carried out to address the following limitations of this study:

- The study only focused on one variety of potatoes, that is, the *Shangi* potato. A follow up study should consider more potato varieties, to provide a better overview of the findings on phytochemical constituents and antibacterial properties of potato peel extracts.
- This study only focused on 100% woven cotton fabric, manufactured at Rivatex East Africa limited. Although cotton fabric is known to be susceptible to microbial attack this study has limitations in that the antibacterial efficacy of potato peels and silver nanoparticles on textiles based on other fibres was not considered. A follow-up study could look at textiles with different fibre types and construction.
- Efficacy testing can also be measured against other gram-negative and gram-positive strains of bacteria, fungi and viruses to assess the full potential of the potato peel extracts and the silver nanoparticles.
- Current tests were performed in-vivo, further tests can be done directly on hospital wear when in use to determine the effect of the different properties such as body sweat, body temperature and skin type on the antibacterial properties of the finishes.
- A wider range of curing temperature and synthesis time can be used for optimisation of the in-situ synthesis because the linear relationship exhibited in the study could not provide the optimal curing and synthesis time.

- Comparative studies between the green synthesized and commercial nanoparticles need to be done.
- Develop scientific model for bonding mechanism between nanoparticles and cotton fabric.
- Conduct multi-factor optimization studies for identifying optimal parameters for nanoparticle synthesis.
- An exploration of the capping element of the potato peel extracts in the green synthesis of nanoparticles.
- Fabrics used with conventional silver nanoparticles could be used for comparative study.

REFERENCES

Abazari, M., Badeleh, S. M., Khaleghi, F., Saeedi, M., & Haghi, F. (2023). Fabrication of silver nanoparticles-deposited fabrics as a potential candidate for the development of reusable facemasks and evaluation of their performance. *Scientific Reports*, *13*(1), 1–16. https://doi.org/10.1038/s41598-023-28858-9

Abbaszadegan, A., Ghahramani, Y., Gholami, A., Hemmateenejad, B., Dorostkar, S., Nabavizadeh, M., & Sharghi, H. (2015). The Effect of Charge at the Surface of Silver Nanoparticles on Antimicrobial Activity against Gram-Positive and Gram-Negative Bacteria: A Peliminary Study. *Journal of Nanomaterials*, 1–8. https://doi.org/http://dx.doi.org/10.1155/2015/720654

Abdel-Mohsen, A. M., Abdel-Rahman, R. M., Hrdina, R., Imramovsky, A., Burgert, L., & Aly, A. S. (2012). Antibacterial cotton fabrics treated with core – shell nanoparticles. *International Journal of Biological Macromolecules*, *50*, 1245–1253. https://doi.org/10.1016/j.ijbiomac.2012.03.018

Abramova, A. V., Abramov, V. O., Fedulov, I. S., Baranchikov, A. E., Kozlov, D. A., Veselova, V. O., Kameneva, S. V., Ivanov, V. K., & Cravotto, G. (2021). Strong antibacterial properties of cotton fabrics coated with ceria nanoparticles under high-power ultrasound. *Nanomaterials*, *11*(10). https://doi.org/10.3390/nano11102704

Abubakar, A. R., & Haque, M. (2020). Preparation of Medicinal Plants: Basic Extraction and Fractionation Procedures for Experimental Purposes. *Journal of Pharmacy and BioAllied Sciences*, *12*(1), 1–10. https://doi.org/10.4103/jpbs.JPBS_175_19: 10.4103/jpbs.JPBS_175_19

Afraz, N., Uddin, F., Syed, U., & Mahmood, A. (2019). Antimicrobial finishes for Textiles. *Fashion Technology and Textile Engineering*, *4*(5), 87–94. https://doi.org/10.19080/CTFTTE.2019.04.555646

Agnhage, T., Zhou, Y., Guan, J., Chen, G., Perwuelz, A., Behary, N., & Nierstrasz, V. (2017). Bioactive and multifunctional textile using plant-based madder dye: Characterization of UV protection ability and antibacterial activity. *Fibers and Polymers*, *18*(11), 2170–2175. https://doi.org/10.1007/s12221-017-7115-x

Ahamed, M., Alsalhi, M. S., & Siddiqui, M. K. J. (2010). Silver nanoparticle applications and human health. *Clinica Chimica Acta*, *411*(23–24), 1841–1848. https://doi.org/10.1016/j.cca.2010.08.016

Ahamed, M., Majeed Khan, M. A., Siddiqui, M. K. J., Alsalhi, M. S., & Alrokayan, S. A. (2011). Green synthesis, characterization and evaluation of biocompatibility of silver nanoparticles. *Physica E: Low-Dimensional Systems and Nanostructures*, *43*(6), 1266–1271. https://doi.org/10.1016/j.physe.2011.02.014

Ahmed, S., Saifullah, Ahmad, M., Swami, B. L., & Ikram, S. (2016). Green synthesis of silver nanoparticles using Azadirachta indica aqueous leaf extract. *Journal of Radiation Research and Applied Sciences*, *9*(1), 1–7. https://doi.org/10.1016/j.jrras.2015.06.006

Ajitha, B., Kumar Reddy, Y. A., Reddy, P. S., Jeon, H. J., & Ahn, C. W. (2016). Role of capping agents in controlling silver nanoparticles size, antibacterial activity and potential application as optical hydrogen peroxide sensor. *RSC Advances*, *6*(42), 36171–36179. https://doi.org/10.1039/c6ra03766f

Akhtar, I., Javad, S., Yousaf, Z., Iqbal, S., & Jabeen, K. (2019). Microwave assisted extraction of phytochemicals an efficient and modern approach for botanicals and pharmaceuticals. *Pakistan Journal of Pharmaceutical Sciences*, *32*(1), 223–230.

Akhtar, K., Khan, S. A., Khan, S. B., & Asiri, A. M. (2018). Scanning electron microscopy: Principle and applications in nanomaterials characterization. In *Handbook of Materials Characterization* (pp. 113–145). Springer International Publishing AG. https://doi.org/10.1007/978-3-319-92955-2_4

Akyol, H., Riciputi, Y., Capanoglu, E., Caboni, M. F., & Verardo, V. (2016). Phenolic compounds in the potato and its byproducts: An overview. *International Journal of Molecular Sciences*, *17*(6). https://doi.org/10.3390/ijms17060835

Al-Weshahy, A., & Venket Rao, A. (2009). Isolation and characterization of functional components from peel samples of six potatoes varieties growing in Ontario. *Food Research International*, *42*(8), 1062–1066. https://doi.org/10.1016/j.foodres.2009.05.011

Aladpoosh, R., Montazer, M., & Samadi, N. (2014). In situ green synthesis of silver nanoparticles on cotton fabric using Seidlitzia rosmarinus ashes. *Cellulose*, *21*(5), 3755–3766. https://doi.org/10.1007/s10570-014-0369-1

Alam, E. A., & El-Nuby, A. (2019). Phytochemical and Antinematodal Screening on Water Extracts of Some Plant. *International Journal Of Chemical and Pharmaceutical Sains*, *10*(4), 1–16.

Ali, A., Nguyen, N. H. A., Baheti, V., Ashraf, M., Militky, J., Mansoor, T., Noman, M. T., & Ahmad, S. (2018). Electrical conductivity and physiological comfort of silver coated cotton fabrics. *Journal of the Textile Institute*, *109*(5), 620–628. https://doi.org/10.1080/00405000.2017.1362148

Almadiy, A. A., & Nenaah, G. E. (2018). Ecofriendly Synthesis of Silver Nanoparticles Using Potato Steroidal Alkaloids and Their Activity Against Phytopathogenic Fungi. *Brazilian Archives of Biology and Technology*, *61*(0), 1–14. https://doi.org/10.1590/1678-4324-2018180013

Almatroudi, A. (2020). Silver nanoparticles: Synthesis, characterisation and biomedical applications. *Open Life Sciences*, *15*(1), 819–839. https://doi.org/10.1515/biol-2020-0094

Altemimi, A., Lakhssassi, N., Baharlouei, A., Watson, D. G., & Lightfoot, D. A. (2017). Phytochemicals: Extraction, isolation, and identification of bioactive compounds from plant extracts. *Plants*, *6*(4). https://doi.org/10.3390/plants6040042

Álvarez-Martínez, F. J., Rodríguez, J. C., Borrás-Rocher, F., Barrajón-Catalán, E., & Micol, V. (2021). The antimicrobial capacity of Cistus salviifolius and Punica granatum plant extracts against clinical pathogens is related to their polyphenolic composition. *Scientific Reports*, *11*(1), 1–12. https://doi.org/10.1038/s41598-020-80003-y

Amanpour, R., Abbasi-Maleki, S., Neyriz-Naghadehi, M., & Asadi-Samani, M. (2015). Antibacterial effects of Solanum tuberosum peel ethanol extract in vitro. *Journal of HerbMed Pharmacology*, *4*(2), 45–48.

Anand, K., Kaviyarasu, K., Muniyasamy, S., Roopan, S. M., Gengan, R. M., & Chuturgoon, A. A. (2017). Bio-Synthesis of Silver Nanoparticles Using Agroforestry Residue and Their Catalytic Degradation for Sustainable Waste Management. *Journal of Cluster Science*, *28*(4), 2279–2291. https://doi.org/10.1007/s10876-017-1212-2

Arapoglou, D., Varzakas, T., Vlyssides, A., & Israilides, C. (2010). Ethanol production from potato peel waste (PPW) Ethanol production from potato peel waste (PPW). *Waste Management*, *30*(10), 1898–1902. https://doi.org/10.1016/j.wasman.2010.04.017

Arif, D., Niazi, M. B. K., Ul-Haq, N., Anwar, M. N., & Hashmi, E. (2015). Preparation of antibacterial cotton fabric using chitosan-silver nanoparticles. *Fibers and Polymers*, *16*(7), 1519–1526. https://doi.org/10.1007/s12221-015-5245-6

Arikan, E. B., & Bilgen, H. D. (2019). Production of bioplastic from potato peel waste and investigation of its biodegradability. *Internation Advanced Researches and Engineering Journal*, *3*(2), 93–97. https://doi.org/10.35860/iarej.420633

Aschale, M., Tsegaye, F., & Amde, M. (2021). Potato peels as promising low-cost adsorbent for the removal of lead, cadmium, chromium and copper from wastewater. *Desalination and Water Treatment*, *222*, 405–415. https://doi.org/10.5004/dwt.2021.27108

Ashraf, J. M., Ansari, M. A., Khan, H. M., Alzohairy, M. A., & Choi, I. (2016). Green synthesis of silver nanoparticles and characterization of their inhibitory effects on AGEs formation using biophysical techniques. *Scientific Reports*, *6*(February), 1–10. https://doi.org/10.1038/srep20414

Ashraf, M., Rahman, H., & Rahman, M. (2021). Comparative Study on Antimicrobial Activity of Four Bangladeshi Medicinal Plants Used as Antimicrobial Finishes on Cotton Fabric. *Journal of Textile Science & Fashion Technology*, *8*(3), 6–11. https://doi.org/10.33552/jtsft.2021.08.000686

Asif, M., Yasmin, R., Asif, R., Ambreen, A., Mustafa, M., & Umbreen, S. (2022). Green Synthesis of Silver Nanoparticles (AgNPs), Structural Characterization, and their Antibacterial Potential. *Dose-Response*, *20*(1), 1–11. https://doi.org/10.1177/15593258221088709

Attia, E. M., Elazabawy, O. E., Hassan, N. S., & Hyba, A. M. (2020). Potato Peel Extract As An Eco-Friendly Corrosion Inhibitor For Carbon Steel In Formation Water. *International Journal of Advanced Research and Publications*, *4*(3), 51–56. www.ijarp.org

Azarbani, F., & Shiravand, S. (2020). Green synthesis of silver nanoparticles by Ferulago macrocarpa flowers extract and their antibacterial, antifungal and toxic effects. *Green Chemistry Letters and Reviews*, *13*(1), 41–49. https://doi.org/10.1080/17518253.2020.1726504

Azwanida, N. (2015). A Review on the Extraction Methods Use in Medicinal Plants, Principle, Strength and Limitation. *Medicinal & Aromatic Plants*, *04*(03), 3–8. https://doi.org/10.4172/2167-0412.1000196

Badri, W., Miladi, K., Eddabra, R., Fessi, H., & Elaissari, A. (2015). Elaboration of nanoparticles containing indomethacin: Argan oil for transdermal local and cosmetic application. *Journal of Nanomaterials*, *2015*. https://doi.org/10.1155/2015/935439

Baker, T. J., Tyler, C. R., & Galloway, T. S. (2013). Impacts of metal and metal oxide nanoparticles on marine organisms. *Environmental Pollution*, 1–15. https://doi.org/10.1016/j.envpol.2013.11.014

Balamurugan, M., Saravanan, S., & Soga, T. (2017). Coating of green-synthesized silver nanoparticles on cotton fabric. *Journal of Coatings Technology and Research*, *14*(3), 735–745. https://doi.org/10.1007/s11998-016-9894-1

Ballottin, D., Fulaz, S., Cabrini, F., Tsukamoto, J., Durán, N., Alves, O. L., & Tasic, L. (2017). Antimicrobial textiles: Biogenic silver nanoparticles against Candida and Xanthomonas. *Materials Science and Engineering C*, *75*, 582–589. https://doi.org/10.1016/j.msec.2017.02.110

Balouiri, M., Sadiki, M., & Ibnsouda, S. K. (2016). Methods for in vitro evaluating antimicrobial activity: A review. *Journal of Pharmaceutical Analysis*, *6*(2), 71–79. https://doi.org/10.1016/j.jpha.2015.11.005

Bamsaoud, S. F., Basuliman, M. M., Bin-Hameed, E. A., Balakhm, S. M., & Alkalali, A. S. (2021). The effect of volume and concentration of AgNO3aqueous solutions on silver nanoparticles synthesized using Ziziphus Spina-Christi leaf extract and their antibacterial activity. *Journal of Physics: Conference Series*, *1900*(1). https://doi.org/10.1088/1742-6596/1900/1/012005

Bandar, H., Hijazi, A., Rammal, H., Hachem, A., & Saad, Z. (2013). Techniques for the Extraction of Bioactive Compounds from Lebanese Urtica dioica. *American Journal of Phytomedicine and Clinical Therapeutics*, *1*(6), 507–513.

Bankar, A., Joshi, B., Kumar, A. R., & Zinjarde, S. (2010). Banana peel extract mediated novel route for the synthesis of silver nanoparticles. *Colloids and Surfaces A: Physicochemical and Engineering Aspects*, *368*(1–3), 58–63. https://doi.org/10.1016/j.colsurfa.2010.07.024

Behera, B. K., & Arora, H. (2009). Surgical gown: A critical review. *Journal of Industrial Textiles*, *38*(3), 205–231. https://doi.org/10.1177/1528083708091251

Bélteky, P., Rónavári, A., Zakupszky, D., Boka, E., Igaz, N., Szerencsés, B., Pfeiffer, I., Vágvölgyi, C., Kiricsi, M., & Kónya, Z. (2021). Are smaller nanoparticles always better? Understanding the biological effect of size-dependent silver nanoparticle aggregation under biorelevant conditions. *International Journal of Nanomedicine*, *16*(April), 3021–3040. https://doi.org/10.2147/IJN.S304138

Ben Jeddou, K., Kammoun, M., Hellström, J., Gutiérrez-Quequezana, L., Rokka, V. M., Gargouri-Bouzid, R., Ellouze-Chaabouni, S., & Nouri-Ellouz, O. (2021). Profiling beneficial phytochemicals in a potato somatic hybrid for tuber peels processing: phenolic acids and anthocyanins composition. *Food Science and Nutrition*, *9*(3), 1388–1398. https://doi.org/10.1002/fsn3.2100

Benavides-guerrero, R., Revelo-cuarán, Y. A., Osorio-mora, O., & Arango-bedoya, O. (2020). Ultrasound-assisted extraction of phenolic compounds from two varieties of an Andean native potato (Solanum phureja) and evaluation of their antioxidant activity. *Información Tecnológica*, *31*(5), 43–50.

Bhardwaj, B., Singh, P., Kumar, A., Kumar, S., & Budhwar, V. (2020). Eco-friendly greener synthesis of nanoparticles. *Advanced Pharmaceutical Bulletin*, *10*(4), 566–576. https://doi.org/10.34172/apb.2020.067

Bhattacharjee, S. (2016). DLS and zeta potential - What they are and what they are not? *Journal of Controlled Release*, *235*, 337–351. https://doi.org/10.1016/j.jconrel.2016.06.017

Bhuvaneswari, S., Subashini, G., & Subramaniyam, S. (2017). Green Synthesis of Zinc Oxide Nanoparticles Using Potato Peel and Degradation of Textile Mill Effluent By Photocatalytic Activity. *World Journal of Pharmaceutical Research*, *6*(6), 774–785. https://doi.org/10.20959/wjpr20176-8496

Billah, S. M. R. (2019). *Textile Coatings*. Springer Nature Switzerland. https://doi.org/10.1007/978-3-319-95987-0_30

Boryo, D. E. . (2013). The effect of microbes on textile material: a review on the way-out so far. *The International Journal Of Engineering And Science*, *2*(8), 9–13.

Bouhadjra, K., Lemlikchi, W., Ferhati, A., & Mignard, S. (2021). Enhancing removal efficiency of anionic dye (Cibacron blue) using waste potato peels powder. *Scientific Reports*, *11*(1), 1–10. https://doi.org/10.1038/s41598-020-79069-5

Bruna, T., Maldonado-Bravo, F., Jara, P., & Caro, N. (2021). Silver nanoparticles and their antibacterial applications. *International Journal of Molecular Sciences*, *22*(13). https://doi.org/10.3390/ijms22137202

Cai, X., Li, H., Zhang, L., & Yan, J. (2021). Dyeing Property Improvement of Madder with Polycarboxylic Acid for Cotton. *Polymers*, *13*(3289), 1–14. https://doi.org/https://doi.org/10.3390/ polym13193289

Carreira-Casais, A., Otero, P., Garcia-Perez, P., Garcia-Oliveira, P., Pereira, A. G., Carpena, M., Soria-Lopez, A., Simal-Gandara, J., & Prieto, M. A. (2021). Benefits and drawbacks of ultrasound-assisted extraction for the recovery of bioactive compounds from marine algae. *International Journal of Environmental Research and Public Health*, *18*(17). https://doi.org/10.3390/ijerph18179153

Carvalho, P. M., Felício, M. R., Santos, N. C., Gonçalves, S., & Domingues, M. M. (2018). Application of light scattering techniques to nanoparticle characterization and development. *Frontiers in Chemistry*, *6*(June), 1–17. https://doi.org/10.3389/fchem.2018.00237

Chandra, S., Khan, S., Avula, B., Lata, H., Yang, M. H., Elsohly, M. A., & Khan, I. A. (2014). Assessment of total phenolic and flavonoid content, antioxidant properties, and yield of aeroponically and conventionally grown leafy vegetables and fruit crops: A comparative study. *Evidence-Based Complementary and Alternative Medicine*, *2014*. https://doi.org/10.1155/2014/253875

Charles, A. L., Motsa, N., & Abdillah, A. A. (2022). A Comprehensive Characterization of Biodegradable Edible Films Based on Potato Peel Starch Plasticized with Glycerol. *Polymers*, *14*(17). https://doi.org/10.3390/polym14173462

Chen, J., Li, S., Luo, J., Wang, R., & Ding, W. (2016). Enhancement of the Antibacterial Activity of Silver Nanoparticles against Phytopathogenic Bacterium Ralstonia solanacearum by Stabilization. *Journal of Nanomaterials*, *2016*. https://doi.org/10.1155/2016/7135852

Choudhury, A. K. R. (2017). Introduction to finishing. *Principles of Textile Finishing*, 1–19. https://doi.org/10.1016/b978-0-08-100646-7.00001-1

Chowdhury, K. P. (2018). Effect of Special Finishes on the Functional Properties of Cotton Fabrics. *Journal of Textile Science and Technology*, *04*(02), 49–66. https://doi.org/10.4236/jtst.2018.42003

Clogston, J. D., & Patri, A. K. (2011). Zeta Potential Measurement. *Methods in Molecular Biology*, *697*, 63–70. https://doi.org/10.1007/978-1-60327-198-1_6

CLSI. (2012). *Methods for Dilution Antimicrobial Susceptibility Tests for Bacteria That Grow Aerobically ; Approved Standard — Ninth Edition* (Vol. 32, Issue 2). Clinical and Laboratory Standards Institute.

Cowan, M. M. (1999). Plant products as antimicrobial agents. *Clinical Microbiology Reviews*, *12*(4), 564–582. https://doi.org/10.3390/curroncol14040004

Cuiffo, M., Jung, H. J., Skocir, A., Schiros, T., Evans, E., Orlando, E., Lin, Y. C., Fang, Y., Rafailovich, M., Kim, T., & Halada, G. (2021). Thermochemical degradation of cotton fabric under mild conditions. *Fashion and Textiles*, *8*(1). https://doi.org/10.1186/s40691-021-00263-8

Čuk, N., Šala, M., & Gorjanc, M. (2021). Development of antibacterial and UV protective cotton fabrics using plant food waste and alien invasive plant extracts as reducing agents for the in-situ synthesis of silver nanoparticles. *Cellulose*, *28*(5), 3215–3233. https://doi.org/10.1007/s10570-021-03715-y

Da Silva, C. R., De Andrade Neto, J. B., De Sousa Campos, R., Figueiredo, N. S., Sampaio, L. S., Magalhães, H. I. F., Cavalcanti, B. C., Gaspar, D. M., De Andrade, G. M., Lima, I. S. P., De Barros Viana, G. S., De Moraes, M. O., Lobo, M. D. P., Grangeiro, T. B., & Nobre, H. V. (2014). Synergistic effect of the flavonoid catechin, quercetin, or epigallocatechin gallate with fluconazole induces apoptosis in Candida tropicalis resistant to fluconazole. *Antimicrobial Agents and Chemotherapy*, *58*(3), 1468–1478. https://doi.org/10.1128/AAC.00651-13

Dada, A. O., Adekola, F. A., Adeyemi, O. S., Bello, O. M., Olwaseun, A. C., Awakan, O. J., & Grace, F.-A. A. (2018). Exploring the Effect of Operational Factors and Characterization Imperative to the Synthesis of Silver Nanoparticles. In *Silver Nanoparticles - Fabrication, Characterization and Applications* (pp. 165–184). Intechopen. http://dx.doi.org/10.5772/intechopen.76947%0A167

Daimary, N., Eldiehy, K. S. H., Boruah, P., Deka, D., Bora, U., & Kakal, B. K. (2022). Potato peels as asustainable source for biochar, bio-oil and a green heterogeneous catalyst for biodiesel production. *Journal of Environmental Engineering*, *10*(1), 107108. https://doi.org/https://doi.org/10.1016/j.jece.2021.107108

Dakal, T. C., Kumar, A., Majumdar, R. S., & Yadav, V. (2016). Mechanistic basis of antimicrobial actions of silver nanoparticles. *Frontiers in Microbiology*, *7*(NOV), 1–17. https://doi.org/10.3389/fmicb.2016.01831

Daly, S. M., Sturge, C. R., & Greenberg, D. E. (2018). Inhibition of bacterial growth by peptide-conjugates morpholino oligomers. *Methods Mol Biol.*, *1565*, 115–122. https://doi.org/10.1007/978-1-4939-6817-6

Daraio, C., & Jin, S. (2011). Synthesis and Patterning Methods for nanostructures Useful for Biological Applications. In G. A. Silva & V. Parpura (Eds.), *Nanotechnology for Biology and Medicine* (pp. 27–44). Springer Science+Business Media. https://doi.org/10.1007/978-0-387-31296-5

De Leersnyder, I., Rijckaert, H., De Gelder, L., Van Driessche, I., & Vermeir, P. (2020). High variability in silver particle characteristics, silver concentrations, and production batches of commercially available products indicates the need for a more rigorous approach. *Nanomaterials*, *10*(7), 1–22. https://doi.org/10.3390/nano10071394

Devi, A., Kumar, V., & Deka, D. (2018). Evaluation of the effectiveness of potato peel extract as a natural antioxidant on biodiesel oxidation stability. *Industrial Crops & Products*, *123*(January), 454–460. https://doi.org/10.1016/j.indcrop.2018.07.022

Dhiman, G., & Chakraborty, J. N. (2017). Assessment of durable press performance of cotton finished with modified DMDHEU and citric acid. *Fashion and Textiles*, *4*(1), 1–18. https://doi.org/10.1186/s40691-017-0104-2

Dhineshbabu, N. R., Manivasakan, P., Karthik, A., & Rajendran, V. (2014). Hydrophobicity, flame retardancy and antibacterial properties of cotton fabrics functionalised with MgO/methyl silicate nanocomposites. *RSC Advances*, *4*(61), 32161–32173. https://doi.org/10.1039/c4ra03348e

Djuhana, D., Putra, M. H., Imawan, C., Fauzia, V., Harmoko, A., Handayani, W., & Ardani, H. (2016). Numerical study of the plasmonic resonance sensitivity silver nanoparticles coated polyvinyl alcohol (PVA) using Bohren-Huffman-Mie (BHMie) approximation. *AIP Conference Proceedings*, *1729*. https://doi.org/10.1063/1.4946926

Dorta, E., Lobo, M. G., & Gonzalez, M. (2012). Reutilization of mango byproducts: Study of the effect of extraction solvent and temperature on their antioxidant properties. *Journal of Food Science*, *77*(1), 80–88. https://doi.org/10.1111/j.1750-3841.2011.02477.x

Doughari, J. H. (2012). Phytochemicals: extraction methods, basic structures and mode of action as potential chemotherapeutic agents. *Phytochemicals - A Global Perspective of Their Role in Nutrition and Health*, 1–34. http://www.intechopen.com/books/phytochemicals-a-global-perspective-of-their-role-in-nutrition-and-health/phytochemicals-extraction-methods-basic-structures-and-mode-of-action-as-potential- chemotherapeutic-%0AInTech

Dung, T. T. N., Nam, V. N., Nhan, T. T., Ngoc, T. T. B., Minh, L. Q., Nga, B. T. T., Phan Le, V., & Quang, D. V. (2019). Silver nanoparticles as potential antiviral agents against African swine fever virus. *Materials Research Express*, *6*(12). https://doi.org/10.1088/2053-1591/ab6ad8

El-Nahhal, I. M., Salem, J., Anbar, R., Kodeh, F. S., & Elmanama, A. (2020). Preparation and antimicrobial activity of ZnO-NPs coated cotton/starch and their functionalized ZnO-Ag/cotton and Zn(II) curcumin/cotton materials. *Scientific Reports*, *10*(1), 1–10. https://doi.org/10.1038/s41598-020-61306-6

El-Sakhawy, M., Kamel, S., Salama, A., & Tohamy, H. A. S. (2018). Preparation and infrared study of cellulose based amphiphilic materials. *Cellulose Chemistry and Technology*, *52*(3–4), 193–200.

El-Shafei, A., Shaarawy, S., Motawe, F. H., & Refaei, R. (2018). Herbal extract as an ecofriendly antimicrobial finishing of cotton fabric. *Egyptian Journal of Chemistry*, *61*(2), 317–327. https://doi.org/10.21608/EJCHEM.2018.2621.1209

Elamawi, R. M., Al-Harbi, R. E., & Hendi, A. A. (2018). Biosynthesis and characterization of silver nanoparticles using Trichoderma longibrachiatum and their effect on phytopathogenic fungi. *Egyptian Journal of Biological Pest Control*, *28*(1), 1–11. https://doi.org/10.1186/s41938-018-0028-1

Elbagory, A. M., Cupido, C. N., Meyer, M., & Hussein, A. A. (2016). Large scale screening of southern African plant extracts for the green synthesis of gold nanoparticles using microtitre-plate method. *Molecules*, *21*(11). https://doi.org/10.3390/molecules21111498

Elkahoui, S., Bartley, G. E., Yokoyama, W. H., & Friedman, M. (2018). Dietary Supplementation of Potato Peel Powders Prepared from Conventional and Organic Russet and Non-organic Gold and Red Potatoes Reduces Weight Gain in Mice on a High-Fat Diet. *Journal of Agricultural and Food Chemistry*, *66*(24), 6064–6072. https://doi.org/10.1021/acs.jafc.8b01987

Elmogahzy, Y., & Farag, R. (2018). Tensile properties of cotton fibers: importance, research, and limitations. In *Handbook of Properties of Textile and Technical Fibres* (pp. 223–273). Elsevier Ltd. https://doi.org/10.1016/B978-0-08-101272-7.00007-9

Erdogan, O., Abbak, M., Demirbolat, G. M., Birtekocak, F., Aksel, M., Pasa, S., & Cevik, O. (2019). Green synthesis of silver nanoparticles via Cynara scolymus leaf extracts: The characterization, anticancer potential with photodynamic therapy in MCF7 cells. *PLoS ONE*, *14*(6), 1–15. https://doi.org/10.1371/journal.pone.0216496

Escuredo, O., Seijo-Rodríguez, A., Shantal Rodríguez-Flores, M., Meno, L., & Carmen Seijo, M. (2020). Changes in the morphological characteristics of potato plants attributed to seasonal variability. *Agriculture (Switzerland)*, *10*(4), 11–15. https://doi.org/10.3390/agriculture10040095

Ezekiel, R., Singh, N., Sharma, S., & Kaur, A. (2013). Beneficial phytochemicals in potato — a review. *Food Research International*, *50*, 487–496. https://doi.org/10.1016/j.foodres.2011.04.025

Famuyide, I. M., Aro, A. O., Fasina, F. O., Eloff, J. N., & Mcgaw, L. J. (2019). Antibacterial activity and mode of action of acetone leaf extracts of under-investigated Syzygium and Eugeia species on multi drug resisstant porcine diarrhoeagenic E. coli. *BMC Veterinary Research*, *15*(162), 1–14.

Fouda, A., & Shaheen, T. I. (2017). Silver Nanoparticles : Biosynthesis , Characterization and Application on Cotton Fabrics. *Microbiology Research Journal International*, *20*(1), 1–14. https://doi.org/10.9734/MRJI/2017/32961

Frickmann, H., Hahn, A., Berlec, S., Ulrich, J., Jansson, M., Schwarz, N. G., Warnke, P., & Podbielski, A. (2019). On the Etiological Relevance of Escherichia coli and Staphylococcus aureus in Superficial and Deep Infections-A Hypothesis-Forming, Retrospective Assessment. *European Journal of Microbiology and Immunology*, *9*(4), 124–130. https://doi.org/10.1556/1886.2019.00021

Friedman, M., Huang, V., Quiambao, Q., Noritake, S., Liu, J., Kwon, O., Chintalapati, S., Young, J., Levin, C. E., Tam, C., Cheng, L. W., & Land, K. M. (2018). Potato Peels and Their Bioactive Glycoalkaloids and Phenolic Compounds Inhibit the Growth of Pathogenic Trichomonads. *Journal of Agricultural and Food Chemistry*, *66*(30), 7942–7947. https://doi.org/10.1021/acs.jafc.8b01726

Friedman, M., & Levin, C. E. (2009). Analysis and Biological Activities of Potato Glycoalkaloids, Calystegine Alkaloids, Phenolic Compounds, and Anthocyanins. In *Advances in Potato Chemistry and Technology* (First Edit). Elsevier Ltd. https://doi.org/10.1016/b978-0-12-374349-7.00006-4

Fu, Z. F., Tu, Z. C., Zhang, L., Wang, H., Wen, Q. H., & Huang, T. (2016). Antioxidant activities and polyphenols of sweet potato (Ipomoea batatas L.) leaves extracted with solvents of various polarities. *Food Bioscience*, *15*, 11–18. https://doi.org/10.1016/j.fbio.2016.04.004

Gajic, I., Kabic, J., Kekic, D., Jovicevic, M., Milenkovic, M., Mitic Culafic, D., Trudic, A., Ranin, L., & Opavski, N. (2022). Antimicrobial Susceptibility Testing. *Antibiotics*, *11*(4), 1–26. https://doi.org/10.3390/antibiotics11040427

Gao, M., Wang, H., & Zhu, L. (2016). Quercetin Assists Fluconazole to Inhibit Biofilm Formations of Fluconazole-Resistant Candida Albicans in In Vitro and in Vivo Antifungal Managements of Vulvovaginal Candidiasis. *Cellular Physiology and Biochemistry*, *40*(3–4), 727–742. https://doi.org/10.1159/000453134

Gao, Y., Huang, Q., Su, Q., & Liu, R. (2014). Green synthesis of silver nanoparticles at room temperature using kiwifruit juice. *Spectroscopy Letters*, *47*(10), 790–795. https://doi.org/10.1080/00387010.2013.848898

Gao, Y. N., Wang, Y., Yue, T. N., Weng, Y. X., & Wang, M. (2021). Multifunctional cotton non-woven fabrics coated with silver nanoparticles and polymers for antibacterial, superhydrophobic and high performance microwave shielding. *Journal of Colloid and Interface Science*, *582*, 112–123. https://doi.org/10.1016/j.jcis.2020.08.037

Gebrechristos, H. Y., Ma, X., Xiao, F., He, Y., Zheng, S., Oyungerel, G., & Chen, W. (2020). Potato peel extracts as an antimicrobial and potential antioxidant in active edible film. *Food Science and Nutrition*, *8*(12), 6338–6345. https://doi.org/10.1002/fsn3.1119

Gesese, T. N., Workneh Fanta, S., Mersha, D. A., & Satheesh, N. (2022). Physical properties and antibacterial activity of cotton fabric treated with methanolic extracts of Solanum incanum fruits and red onion peels. *Journal of the Textile Institute*, *113*(2), 292–302. https://doi.org/10.1080/00405000.2020.1871183

Gollapudi, V. R., Mallavarapu, U., Seetha, J., Akepogu, P., Amara, V. R., Natarajan, H., & Anumakonda, V. (2020). In situ generation of silver and silver oxide nanoparticles on cotton fabrics using Tinospora cordifolia as bio reductant. *SN Applied Sciences*, *2*(3), 1–10. https://doi.org/10.1007/s42452-020-2331-1

Gonelimali, F. D., Lin, J., Miao, W., Xuan, J., Charles, F., Chen, M., & Hatab, S. R. (2018). Antimicrobial properties and mechanism of action of some plant extracts against food pathogens and spoilage microorganisms. *Frontiers in Microbiology*, *9*(JUL), 1–9. https://doi.org/10.3389/fmicb.2018.01639

Gopalasatheeskumar, K. (2018). Significant Role of Soxhlet Extraction Process in Phytochemical Research. *Mintage Journal of Pharmaceutical & Medical Sciences*, *7*(1), 43–47. www.mintagejournals.com43

Gour, A., & Jain, N. K. (2019). Advances in green synthesis of nanoparticles. *Artificial Cells, Nanomedicine and Biotechnology*, *47*(1), 844–851. https://doi.org/10.1080/21691401.2019.1577878

Gul, R., Jan, S. U., Faridullah, S., Sherani, S., & Jahan, N. (2017). Preliminary Phytochemical Screening, Quantitative Analysis of Alkaloids, and Antioxidant Activity of Crude Plant Extracts from Ephedra intermedia Indigenous to Balochistan. *Scientific World Journal*, *2017*(Figure 1). https://doi.org/10.1155/2017/5873648

Gulati, R., Sharma, S., & Sharma, R. K. (2022). Antimicrobial textile: recent developments and functional perspective. *Polymer Bulletin*, *79*(8), 5747–5771. https://doi.org/10.1007/s00289-021-03826-3

Haase, H., Jordan, L., Keitel, L., Keil, C., & Mahltig, B. (2017). Comparison of methods for determining the effectiveness of antibacterial functionalized textiles. *PLoS ONE*, *12*(11), 1–16. https://doi.org/10.1371/journal.pone.0188304

Haji, A., Barani, H., & Qavamnia, S. S. (2013). In situ synthesis of silver nanoparticles onto cotton fibres modified with plasma treatment and acrylic acid grafting. *Micro and Nano Letters*, *8*(6), 315–318. https://doi.org/10.1049/mnl.2013.0157

Hamouz, K., Lachman, J., Čepl, J., Dvořák, P., Pivec, V., & Prášilová, M. (2007). Site conditions and genotype influence polyphenol content in potatoes. *Horticultural Science*, *34*(4), 132–137. https://doi.org/10.17221/1894-hortsci

Harane, R. S., & Adivarekar, R. V. (2017). Sustainable processes for pre-treatment of cotton fabric. *Textiles and Clothing Sustainability*, *2*(1). https://doi.org/10.1186/s40689-016-0012-7

Harifi, T., & Montazer, M. (2015). A review on textile sonoprocessing: A special focus on sonosynthesis of nanomaterials on textile substrates. *Ultrasonics Sonochemistry*, *23*, 1–10. https://doi.org/10.1016/j.ultsonch.2014.08.022

Harish, V., Ansari, M. M., Tewari, D., Gaur, M., Yadav, A. B., García-Betancourt, M. L., Abdel-Haleem, F. M., Bechelany, M., & Barhoum, A. (2022). Nanoparticle and Nanostructure Synthesis and Controlled Growth Methods. *Nanomaterials*, *12*(18), 1–30. https://doi.org/10.3390/nano12183226

Hasan, K. M. F., Pervez, M. N., Talukder, M. E., Sultana, M. Z., Mahmud, S., Meraz, M. M., Bansal, V., & Genyang, C. (2019). A novel coloration of polyester fabric through green silver nanoparticles (G-AgNPs@PET). *Nanomaterials*, *9*(4), 1–13. https://doi.org/10.3390/nano9040569

Hebeish, A., El-naggar, M. E., Fouda, M. M. G., & Ramadan, M. A. (2011). Highly effective antibacterial textiles containing green synthesized silver nanoparticles. *Carbohydrate Polymers*, *86*(2), 936–940. https://doi.org/10.1016/j.carbpol.2011.05.048

Heikkilä, P., Sipilä, A., Peltola, M., Harlin, A., & Taipale, A. (2007). Electrospun PA-66 Coating on Textile Surfaces. *Textile Research Journal*, *77*(11), 864–870. https://doi.org/10.1177/0040517507078241

Helal, M. M., El-Adawy, T. A., El-Beltagy, A. E., El-Bedawey, A. ., & Youssef, S. M. (2020). Evaluation of Potato Peel Extract As a Source of Antioxidant and Antimicrobial Substances. *Menoufia Journal of Food and Dairy Sciences*, *5*(8), 79–90. https://doi.org/10.21608/mjfds.2020.113467

Hemeg, H. A., Moussa, I. M., Ibrahim, S., Dawoud, T. M., Alhaji, J. H., Mubarak, A. S., Kabli, S. A., Alsubki, R. A., Tawfik, A. M., & Marouf, S. A. (2020). Antimicrobial effect of different herbal plant extracts against different microbial population. *Saudi Journal of Biological Sciences*, *27*(12), 3221–3227. https://doi.org/10.1016/j.sjbs.2020.08.015

Henshaw, P. (2018). *Use of alamarBlue as an Indicator of Microbial Growth in Turbid Solutions for Antimicrobial Evaluation Submitted to the Graduate School of the* (Issue October) [University of Massachusetts Amherst]. https://doi.org/https://doi.org/10.7275/12222378 https://scholarworks.umass.edu/masters_theses_2/728

Hintzen, E., den Doelder, B. K., & Croall, M. (2018). *Appendix Sustainability Report 2017-2018: Lamb Westom / Meijer*. https://www.lambweston.eu/sustainability/appendix.html#waste

Holder, C. F., & Schaak, R. E. (2019). Tutorial on Powder X-ray Diffraction for Characterizing Nanoscale Materials. *ACS Nano*, *13*(7), 7359–7365. https://doi.org/10.1021/acsnano.9b05157

Holme, I. (2016). Coloration of technical textiles. In *Handbook of technical textiles* (pp. 231–234). Woodhead Publishing Limited.

Htwe, Y. Z. N., Chow, W. S., Suda, Y., & Mariatti, M. (2019). Effect of silver nitrate concentration on the production of silver nanoparticles by green method. *Materials Today: Proceedings*, *17*, 568–573. https://doi.org/10.1016/j.matpr.2019.06.336

Huang, C., Cai, Y., Chen, X., & Ke, Y. (2022). Silver-based nanocomposite for fabricating high performance value-added cotton. *Cellulose*, *29*(2), 723–750. https://doi.org/10.1007/s10570-021-04257-z

Huy, T. Q., Hien Thanh, N. T., Thuy, N. T., Chung, P. Van, Hung, P. N., Le, A. T., & Hong Hanh, N. T. (2017). Cytotoxicity and antiviral activity of electrochemical – synthesized silver nanoparticles against poliovirus. *Journal of Virological Methods*, *241*, 52–57. https://doi.org/10.1016/j.jviromet.2016.12.015

Ibrahim, H. M., Aly, A. A., Taha, G. M., & El-Alfy, E. A. (2020). Production of antibacterial cotton fabrics via green treatment with nontoxic natural biopolymer gelatin. *Egyptian Journal of Chemistry*, *63*(Part 2), 655–696. https://doi.org/10.21608/ejchem.2019.16972.2040

Ibrahim, H. M. M. (2015). Green synthesis and characterization of silver nanoparticles using banana peel extract and their antimicrobial activity against representative microorganisms. *Journal of Radiation Research and Applied Sciences*, *8*(3), 265–275. https://doi.org/10.1016/j.jrras.2015.01.007

Ibrahim, H. M. M., & Hassan, M. S. (2016). Characterization and antimicrobial properties of cotton fabric loaded with green synthesized silver nanoparticles. *Carbohydrate Polymers*, *151*, 841–850. https://doi.org/10.1016/j.carbpol.2016.05.041

Ibrahim, N. A. (2015). Nanomaterials for Antibacterial Textiles. In *Nanotechnology in Diagnosis, Treatment and Prophylaxis of Infectious Diseases*. Elsevier Inc. https://doi.org/10.1016/B978-0-12-801317-5.00012-8

Jacob, P. J. S. (2022). Cotton based cellulose nanocomposites: Synthesis and application. In *Cotton* (pp. 1–20). Intechopen. https://doi.org/http://dx.doi.org/10.5772/intechopen.106473

Jagadeshvaran, P. L., & Bose, S. (2023). Nano silver-deposited cotton textile core with carbon nanostructure-filled shell for suppression of electromagnetic radiation via absorption-reflection-absorption. *Materials Chemistry and Physics*, *293*(1 January), 126897. https://doi.org/10.1016/j.matchemphys.2022.126897

Jagtap, U. B., & Bapat, V. A. (2013). Green synthesis of silver nanoparticles using Artocarpus heterophyllus Lam. seed extract and its antibacterial activity. *Industrial Crops and Products*, *46*, 132–137. https://doi.org/10.1016/j.indcrop.2013.01.019

Jain, A., Kongkham, B., Puttaswamy, H., Butola, B. S., Malik, H. K., & Malik, A. (2022). Development of Wash-Durable Antimicrobial Cotton Fabrics by In Situ Green Synthesis of Silver Nanoparticles and Investigation of Their Antimicrobial Efficacy against Drug-Resistant Bacteria. *Antibiotics*, *11*(7). https://doi.org/10.3390/antibiotics11070864

Jalab, J., Abdelwahed, W., Kitaz, A., & Al-Kayali, R. (2021). Green synthesis of silver nanoparticles using aqueous extract of Acacia cyanophylla and its antibacterial activity. *Heliyon*, *7*(9), e08033. https://doi.org/10.1016/j.heliyon.2021.e08033

Jana, J., Ganguly, M., & Pal, T. (2016). Enlightening surface plasmon resonance effect of metal nanoparticles for practical spectroscopic application. *RSC Advances*, *6*(89), 86174–86211. https://doi.org/10.1039/c6ra14173k

Janardhanan, R., Karuppaiah, M., Hebalkar, N., & Rao, T. N. (2009). Synthesis and surface chemistry of nano silver particles. *Polyhedron*, *28*(12), 2522–2530. https://doi.org/10.1016/j.poly.2009.05.038

Jang, M. H., Lee, S., & Hwang, Y. S. (2015). Characterization of silver nanoparticles under environmentally relevant conditions using asymmetrical flow field-flow fractionation (AF4). *PLoS ONE*, *10*(11). https://doi.org/10.1371/journal.pone.0143149

Javed, A., Ahmad, A., Tahir, A., Shabbir, U., & Nouman, M. (2019). Potato peel waste — its nutraceutical , industrial and biotechnological applacations. *AIMS Agriculture and Food*, *4*(August), 807–823. https://doi.org/10.3934/agrfood.2019.3.807

Joly, N., Souidi, K., Depraetere, D., Wils, D., & Martin, P. (2020). Potato By-Products as a Source of Natural Chlorogenic Acids and Phenolic Compounds: Extraction, Characterization, and Antioxidant Capacity. *Molecules (Basel, Switzerland)*, *26*(1). https://doi.org/10.3390/molecules26010177

Junaidi, Yunus, M., Harsojo, Suharyadi, E., & Triyana, K. (2016). Effect of stirring rate on the synthesis silver nanowires using polyvinyl alcohol as a capping agent by polyol process. *International Journal on Advanced Science, Engineering and Information Technology*, *6*(3), 365–369. https://doi.org/10.18517/ijaseit.6.3.808

Junwei, L., Yunhai, M., Jin, T., Zichao, M., Lidong, W., & Jiangtao, Y. (2018). Mechanical properties and microstructure of potato peels. *International Journal of Food Properties*, *21*(1), 1395–1413. https://doi.org/10.1080/10942912.2018.1485031

Jyoti, K., Baunthiyal, M., & Singh, A. (2016). Characterization of silver nanoparticles synthesized using Urtica dioica Linn. leaves and their synergistic effects with antibiotics. *Journal of Radiation Research and Applied Sciences*, *9*(3), 217–227. https://doi.org/10.1016/j.jrras.2015.10.002

Kaguongo, W., Maingi, G., & Giencke, S. (2014). Post-harvest losses in potato value chains in Kenya. *Deutsche Gesellschaft Für Internationale Zusammenarbeit (GIZ) GmbH*.

Kancherla, N., Dhakshinamoothi, A., Chitra, K., & Komaram, R. B. (2019). Preliminary Analysis of Phytoconstituents and Evaluation of Anthelminthic Property of Cayratia auriculata (In Vitro). *Maedica*, *14*(4), 350–356. https://doi.org/10.26574/maedica.2019.14.4.350

Karthik, C., Suresh, S., Sneha Mirulalini, G., & Kavitha, S. (2020). A FTIR approach of green synthesized silver nanoparticles by Ocimum sanctum and Ocimum gratissimum on mung bean seeds. *Inorganic and Nano-Metal Chemistry*, *50*(8), 606–612. https://doi.org/10.1080/24701556.2020.1723025

Kaur, R., Avti, P., Kumar, V., & Kumar, R. (2021). Effect of various synthesis parameters on the stability of size controlled green synthesis of silver nanoparticles. *Nano Express*, *2*(2). https://doi.org/10.1088/2632-959X/abf42a

Ketema, A., & Worku, A. (2020). Antibacterial Finishing of Cotton Fabric Using Stinging Nettle (Urtica dioica L.) Plant Leaf Extract. *Journal of Chemistry*, *2020*. https://doi.org/10.1155/2020/4049273

Khan, M. J., Shameli, K., Sazili, A. Q., Selamat, J., & Kumari, S. (2019). Rapid green synthesis and characterization of silver nanoparticles arbitrated by curcumin in an alkaline medium. *Molecules*, *24*(4). https://doi.org/10.3390/molecules24040719

Kim, J., Soh, S. Y., Bae, H., & Nam, S. Y. (2019). Antioxidant and phenolic contents in potatoes (Solanum tuberosum L.) and micropropagated potatoes. *Applied Biological Chemistry*, *62*(1). https://doi.org/10.1186/s13765-019-0422-8

Kohli, D., Champawat, P. S., Mudgal, V. D., Jain, S. K., & Tiwari, B. K. (2021). Advances in peeling techniques for fresh produce. *Journal of Food Process Engineering*, *44*(10). https://doi.org/10.1111/jfpe.13826

Korshed, P., Li, L., Liu, Z., Mironov, A., & Wang, T. (2019). Size-dependent antibacterial activity for laser-generated silver nanoparticles. *Journal of Interdisciplinary Nanomedicine*, *4*(1), 24–33. https://doi.org/10.1002/jin2.54

Koyuturk, A., & Soyastan, D. D. (2021). Development of antibacterial medical textile materials applied with aromatic oil. *Emerging Materials Research*, *10*(2), 151–157. https://doi.org/https://doi.org/10.1680/jemmr.20.00338

Kredy, M. H. (2018). The effect of pH , Temperature on the green synthesis and biochemical activities of silver nanoparticles from Lawsonia inermis extract. *Journal of Pharmaceutical Sciences and Research*, *10*(8), 2022–2026.

Krishnamoorthy, K., Navaneethaiyer, U., Mohan, R., Lee, J., & Kim, S. J. (2012). Graphene oxide nanostructures modified multifunctional cotton fabrics. *Applied Nanoscience (Switzerland)*, *2*(2), 119–126. https://doi.org/10.1007/s13204-011-0045-9

Kulthong, K., Srisung, S., Boonpavanitchakul, K., & Kangwansupamonkon, W. (2010). Determination of silver nanoparticle release from antibacterial fabrics into artificial sweat. *Particle and Fibre Toxicology*, *7*(8), 1–9.

Kumar, B. S. (2016). Study on Antimicrobial Effectiveness of Silver Nano Coating over Cotton Fabric through Green Approach. *International Journal of Pharma Sciences and Research (IJPSR)*, *7*(9), 363–368.

Kumar, K. (2020). Nutraceutical potential and utilization aspects of food industry by-products and wastes. In *Food Industry Wastes*. INC. https://doi.org/10.1016/b978-0-12-817121-9.00005-x

Kumari, B., Tiwari, B. K., Hossain, M. B., Rai, D. K., & Brunton, N. P. (2017). Ultrasound-assisted extraction of polyphenols from potato peels: profiling and kinetic modelling. *International Journal of Food Science and Technology*, *52*(6), 1432–1439. https://doi.org/10.1111/ijfs.13404

Labulo, A. H., David, O. A., & Terna, A. D. (2022). Green synthesis and characterization of silver nanoparticles using Morinda lucida leaf extract and evaluation of its antioxidant and antimicrobial activity. *Chemical Papers*, *76*(12), 7313–7325. https://doi.org/10.1007/s11696-022-02392-w

Lara, H. H., Ayala-Nuñez, N. V., Ixtepan-Turrent, L., & Rodriguez-Padilla, C. (2010). Mode of antiviral action of silver nanoparticles against HIV-1. *Journal of Nanobiotechnology*, *8*, 1–10. https://doi.org/10.1186/1477-3155-8-1

Li, J., Wang, Y., Wang, X., & Wu, D. (2019). Crystalline characteristics, mechanical properties, thermal degradation kinetics and hydration behavior of biodegradable fibers melt-spun from polyoxymethylene/poly(L-lactic acid) blends. *Polymers*, *11*(11). https://doi.org/10.3390/polym11111753

Liang, S., & McDonald, A. G. (2014). Chemical and thermal characterization of potato peel waste and its fermentation residue as potential resources for biofuel and bioproducts production. *Journal of Agricultural and Food Chemistry*, *62*(33), 8421–8429. https://doi.org/10.1021/jf5019406

Liaqat, N., Jahan, N., Khalil-ur-Rahman, Anwar, T., & Qureshi, H. (2022). Green synthesized silver nanoparticles: Optimization, characterization, antimicrobial activity, and cytotoxicity study by hemolysis assay. *Frontiers in Chemistry*, *10*(August), 1–13. https://doi.org/10.3389/fchem.2022.952006

Lin, L., Jiang, T., Liang, Y., Zhu, W., Inamdar, U. Y., Pervez, M. N., Navik, R., Yang, X., Cai, Y., & Naddeo, V. (2022). Combination of Pre-and Post-Mercerization Processes for Cotton Fabric. *Materials*, *15*(6). https://doi.org/10.3390/ma15062092

Lin, L., Peng, X., Voirin, E., Donnio, B., Rastei, M. V., Vileno, B., & Gallani, J.-L. (2023). Influence of the Crystallinity of Silver Nanoparticles on Their Magnetic Properties. *Helvetica*, *106*(3).

Lin, P. C., Lin, S., Wang, P. C., & Sridhar, R. (2014). Techniques for physicochemical characterization of nanomaterials. *Biotechnology Advances*, *32*(4), 711–726. https://doi.org/10.1016/j.biotechadv.2013.11.006

Liu, H., Lee, Y. Y., Norsten, T. B., & Chong, K. (2014). In situ formation of anti-bacterial silver nanoparticles on cotton textiles. *Journal of Industrial Textiles*, *44*(2), 198–210. https://doi.org/10.1177/1528083713481833

Liu, T., Baek, D. R., Kim, J. S., Joo, S. W., & Lim, J. K. (2020). Green Synthesis of Silver Nanoparticles with Size Distribution Depending on Reducing Species in Glycerol at Ambient pH and Temperatures. *ACS Omega*, *5*(26), 16246–16254. https://doi.org/10.1021/acsomega.0c02066

Lok, C.-N., Ho, C.-M., Chen, R., He, Q.-Y., Yu, W.-Y., Sun, H., Tam, P. K.-H., Chiu, J.-F., & Che, C.-M. (2006). Proteomic analysis of the mode of antibacterial action of silver nanoparticles. *J. Proteome Res.*, *5*(4), 916–924. https://doi.org/10.1021/pr0504079.

Lombardo, S., Pandino, G., & Mauromicale, G. (2013). The influence of growing environment on the antioxidant and mineral content of "early" crop potato. *Journal of Food Composition and Analysis*, *32*(1), 28–35. https://doi.org/10.1016/j.jfca.2013.08.003

Loo, Y. Y., Rukayadi, Y., Nor-Khaizura, M. A. R., Kuan, C. H., Chieng, B. W., Nishibuchi, M., & Radu, S. (2018). In Vitro antimicrobial activity of green synthesized silver nanoparticles against selected Gram-negative foodborne pathogens. *Frontiers in Microbiology*, *9*(JUL), 1–7. https://doi.org/10.3389/fmicb.2018.01555

Lorenz, C., Windler, L., Goetz, N. Von, Lehmann, R. P., Schuppler, M., Hungerbühler, K., Heuberger, M., & Nowack, B. (2012). Chemosphere Characterization of silver release from commercially available functional (nano) textiles. *Chemosphere*, *89*(7), 817–824. https://doi.org/10.1016/j.chemosphere.2012.04.063

Mahdieh, Z. M., Shekarriz, S., & Taromi, F. A. (2021). The Effect of Silver Concentration on Ag-TiO2 Nanoparticles Coated Polyester/Cellulose Fabric by In situ and Ex situ Photo-reduction Method — A Comparative Study. *Fibers and Polymers*, *22*(1), 87–96. https://doi.org/10.1007/s12221-021-9049-6

Mahiuddin, M., Saha, P., & Ochiai, B. (2020). Green synthesis and catalytic activity of silver nanoparticles based on piper chaba stem extracts. *Nanomaterials*, *10*(9), 1–15. https://doi.org/10.3390/nano10091777

Mahmud, S., Pervez, N., Taher, M. A., Mohiuddin, K., & Liu, H. H. (2020). Multifunctional organic cotton fabric based on silver nanoparticles green synthesized from sodium alginate. *Textile Research Journal*, *90*(11–12), 1224–1236. https://doi.org/10.1177/0040517519887532

Maisetta, G., Batoni, G., Caboni, P., Esin, S., Rinaldi, A. C., & Zucca, P. (2019). Tannin profile, antioxidant properties, and antimicrobial activity of extracts from two Mediterranean species of parasitic plant Cytinus. *BMC Complementary and Alternative Medicine*, *19*(82), 1–11. https://doi.org/10.1186/s12906-019-2487-7

Martinez, J. S., Ayca, F., Maryam, S., Xiangyu, D., & Shulin, G. (2020). Recovering Valuable Bioactive Compounds from Potato Peels with Sequential Hydrothermal Extraction. *Waste and Biomass Valorization*, *0123456789*, 1–17. https://doi.org/10.1007/s12649-020-01063-9

Mathew, S. (2020). Phytonanotechnology: A historical perspective, current challenges, and prospects. In *Phytonanotechnology Challenges and Prospects* (pp. 1–15). Elsevier Inc. https://doi.org/https://doi.org/10.1016/B798-0-12-822348-2.00003-6

Melkamu, W. W., & Bitew, L. T. (2021). Green synthesis of silver nanoparticles using Hagenia abyssinica (Bruce) J.F. Gmel plant leaf extract and their antibacterial and anti-oxidant activities. *Heliyon*, *7*(11), e08459. https://doi.org/10.1016/j.heliyon.2021.e08459

Mia, R., Das, S., Banna, B. U., Ahmed, T., & Bakar, M. A. (2023). Enhancing antibacterial properties of organic cotton fabric using mahogany wood waste. *Case Studies in Chemical and Environmental Engineering*, *8*(April), 100387. https://doi.org/10.1016/j.cscee.2023.100387

Mihaylova, D., & Lante, A. (2019). Water an Eco-Friendly Crossroad in Green Extraction: An Overview. *The Open Biotechnology Journal*, *13*(1), 155–162. https://doi.org/10.2174/1874070701913010155

Miller, P. (2019, January 9). *Potato peels are the new green building material*. https://inhabitat.com/potato-peels-offer-a-sustainable-alternative-to-traditional-building-materials/

Mirjalili, M., Yaghmaei, N., & Mirjalili, M. (2013). Antibacterial properties of nano silver finish cellulose fabric. *Journal of Nanostructure in Chemistry*, *3*(1), 3–7. https://doi.org/10.1186/2193-8865-3-43

Mohamed, E. A. A., Muddathir, A. M., & Osman, M. A. (2020). Antimicrobial activity, phytochemical screening of crude extracts, and essential oils constituents of two Pulicaria spp. growing in Sudan. *Scientific Reports*, *10*(1), 1–8. https://doi.org/10.1038/s41598-020-74262-y

Mohammadi Bazargani, M., Falahati-Anbaran, M., & Rohloff, J. (2021). Comparative Analyses of Phytochemical Variation Within and Between Congeneric Species of Willow Herb, Epilobium hirsutum and E. parviflorum: Contribution of Environmental Factors. *Frontiers in Plant Science*, *11*(February), 1–16. https://doi.org/10.3389/fpls.2020.595190

Mohdaly, A. A. A., Sarhan, M. A., Smetanska, I., & Mahmoud, A. (2010). Antioxidant properties of various solvent extracts of potato peel, sugar beet pulp and sesame cake. *Journal of the Science of Food and Agriculture*, *90*(2), 218–226. https://doi.org/10.1002/jsfa.3796

Moldovan, B., Sincari, V., Perde-Schrepler, M., & David, L. (2018). Biosynthesis of silver nanoparticles using Ligustrum ovalifolium fruits and their cytotoxic effects. *Nanomaterials*, *8*(8). https://doi.org/10.3390/nano8080627

Mollick, M. M. R., Rana, D., Dash, S. K., Chattopadhyay, S., Bhowmick, B., Maity, D., Mondal, D., Pattanayak, S., Roy, S., Chakraborty, M., & Chattopadhyay, D. (2019). Studies on green synthesized silver nanoparticles using Abelmoschus esculentus (L.) pulp extract having anticancer (in vitro) and antimicrobial applications. *Arabian Journal of Chemistry*, *12*(8), 2572–2584. https://doi.org/10.1016/j.arabjc.2015.04.033

Montes-Hernandez, G., Di Girolamo, M., Sarret, G., Bureau, S., Fernandez-Martinez, A., Lelong, C., & Eymard Vernain, E. (2021). In Situ Formation of Silver Nanoparticles (Ag-NPs) onto Textile Fibers. *ACS Omega*, *6*(2), 1316–1327. https://doi.org/10.1021/acsomega.0c04814

Mori, Y., Ono, T., Miyahira, Y., Nguyen, V. Q., Matsui, T., & Ishihara, M. (2013). Antiviral activity of silver nanoparticle/chitosan composites against H1N1 influenza A virus. *Nanoscale Research Letters*, *8*(1), 93. https://doi.org/10.1186/1556-276x-8-93

Mostafa, A. A., Al-Askar, A. A., Almaary, K. S., Dawoud, T. M., Sholkamy, E. N., & Bakri, M. M. (2018). Antimicrobial activity of some plant extracts against bacterial strains causing food poisoning diseases. *Saudi Journal of Biological Sciences*, *25*(2), 361–366. https://doi.org/10.1016/j.sjbs.2017.02.004

Mourdikoudis, S., Pallares, R. M., & Thanh, N. T. K. (2018). Characterization techniques for nanoparticles: Comparison and complementarity upon studying nanoparticle properties. *Nanoscale*, *10*(27), 12871–12934. https://doi.org/10.1039/c8nr02278j

Mutha, R. E., Tatiya, A. U., & Surana, S. J. (2021). Flavonoids as natural phenolic compounds and their role in therapeutics: an overview. *Future Journal of Pharmaceutical Sciences*, *7*(1). https://doi.org/10.1186/s43094-020-00161-8

Nam, S., Baek, I. S., Hillyer, M. B., He, Z., Barnaby, J. Y., Condon, B. D., & Kim, M. S. (2022). Thermosensitive textiles made from silver nanoparticle-filled brown cotton fibers. *Nanoscale Advances*, *4*(18), 3725–3736. https://doi.org/10.1039/d2na00279e

Nandiyanto, A. B. D., Oktiani, R., & Ragadhita, R. (2019). How to read and interpret ftir spectroscope of organic material. *Indonesian Journal of Science and Technology*, *4*(1), 97–118. https://doi.org/10.17509/ijost.v4i1.15806

Neely, A. N., & Maley, M. P. (2000). Survival of enterococci and staphylococci on hospital fabric and plastic. *J. Clin. Microbiol.*, *38*(2), 724–726. https://www.ncbi.nlm.nih.gov/pmc/articles/PMC86187/pdf/jm000724.pdf

Nicoloro, J. M., Wen, J., Queiroz, S., Sun, Y., & Goodyear, N. (2020). A novel comprehensive efficacy test for textiles intended for use in the healthcare setting. *Journal of Microbiological Methods*, *173*(May), 105937. https://doi.org/10.1016/j.mimet.2020.105937

Nocker, W. (2011). Evaluation of occupational clothing for surgeons: Achieving comfort and avoiding physiological stress through suitable gowns. In *Handbook of Medical Textiles*. Woodhead Publishing Limited. https://doi.org/10.1533/9780857093691.4.443

Noman, M. T., Petru, M., Amor, N., & Louda, P. (2020). Thermophysiological comfort of zinc oxide nanoparticles coated woven fabrics. *Scientific Reports*, *10*(1), 1–12. https://doi.org/10.1038/s41598-020-78305-2

Novoa, C. C., Tortella, G., Seabra, A. B., Diez, M. C., & Rubilar, O. (2022). Cotton Textile with Antimicrobial Activity and Enhanced Durability Produced by L - Cysteine-Capped Silver nanoparticles. *Processes*, *10*(958), 1–10.

Ogulata, R. T. (2006). Air Permeability of Woven Fabrics. *Journal of Textile and Apparel, Technology and Management*, *5*(2), 1–10. https://doi.org/10.1177/004051754601601001

Onal, L., & Yildirim, M. (2012). Comfort properties of functional three-dimensional knitted spacer fabrics for home-textile applications. *Textile Research Journal*, *82*(17), 1751–1764. https://doi.org/10.1177/0040517512444331

Osman, A. I. (2020). Mass spectrometry study of lignocellulosic biomass combustion and pyrolysis with NOx removal. *Renewable Energy*, *146*(June), 484–496. https://doi.org/10.1016/j.renene.2019.06.155

Osman, A. I., Blewitt, J., Abu-dahrieh, J. K., Farrell, C., Al-muhtaseb, A. H., Harrison, J., Rooney, D. W., & Rooney, D. W. (2019). Production and characterisation of activated carbon and carbon nanotubes from potato peel waste and their application in heavy metal removal . *Environmental Science and Pollution Research*, *26*, 37228–37241.

Paleologou, I., Vasiliou, A., Grigorakis, S., & Makris, D. P. (2016). Optimisation of a green ultrasound-assisted extraction process for potato peel (Solanum tuberosum) polyphenols using bio-solvents and response surface methodology. *Biomass Conversion and Biorefinery*, *6*(3), 289–299. https://doi.org/10.1007/s13399-015-0181-7

Pandey, A., Tripathi, S., & Pandey, C. A. (2014). Concept of standardization, extraction and pre phytochemical screening strategies for herbal drug. *Journal of Pharmacognosy and Phytochemistry JPP*, *115*(25), 115–119.

Pant, D. R., Pant, N. D., Saru, D. B., Yadav, U. N., & Khanal, D. P. (2017). Phytochemical screening and study of antioxidant, antimicrobial, antidiabetic, anti-inflammatory and analgesic activities of extracts from stem wood of pterocarpus marsupium roxburgh. *Journal of Intercultural Ethnopharmacology*, *6*(2), 170–176. https://doi.org/10.5455/jice.20170403094055

Patra, J. K., & Baek, K. H. (2014). Green Nanobiotechnology: Factors Affecting Synthesis and Characterization Techniques. *Journal of Nanomaterials, 2014*. https://doi.org/10.1155/2014/417305

Pecora, R. (2000). Dynamic light scattering measurement of nanometer particles in liquids. *Journal of Nanoparticle Research*, *2*, 123–131.

Perera, S., Bhushan, B., Bandara, R., Rajapakse, G., Rajapakse, S., & Bandara, C. (2013). Morphological, antimicrobial, durability, and physical properties of untreated and treated textiles using silver-nanoparticles. *Colloids and Surfaces A: Physicochemical and Engineering Aspects*, *436*, 975–989. https://doi.org/10.1016/j.colsurfa.2013.08.038

Phongtongpasuk, S., & Poadang, S. (2015). Green Synthesis of Silver Nanoparticles Using Pomegranate Peel Extract. *Advanced Materials Research*, *1131*, 227–230. https://doi.org/10.4028/www.scientific.net/amr.1131.227

Pieter, L. (2020, March 11). *Winds of change: Which countries were the top 15 potato producers during 1961-2019? – Potato News Today*. https://www.potatonewstoday.com/2020/03/11/winds-of-change-which-countries-were-the-top-15-potato-producers-during-1961-2019/

Pinho, E., Magalhães, L., Henriques, M., & Oliveira, R. (2011). Antimicrobial activity assessment of textiles: Standard methods comparison. *Annals of Microbiology*, *61*(3), 493–498. https://doi.org/10.1007/s13213-010-0163-8

Poon, C., & Kan, C. (2016). Relationship between Curing Temperature and Low Stress Mechanical Properties of Titanium Dioxide Catalyzed Flame Retardant Finished Cotton Fabric. *Fibers and Polymers*, *17*(3), 380–388. https://doi.org/10.1007/s12221-016-5809-0

Popescu, V., Vasluianu, E., & Popescu, G. (2014). Quantitative analysis of the multifunctional finishing of cotton fabric with non-formaldehyde agents. *Carbohydrate Polymers*, *111*, 870–882. https://doi.org/10.1016/j.carbpol.2014.05.052

Poulikakos, L. D., Papadaskalopoulou, C., Hofko, B., Gschösser, F., Falchetto, A. C., Bueno, M., Arraigada, M., Sousa, J., Ruiz, R., Petit, C., Loizidou, M., & Partl, M. N. (2017). Resources , Conservation and Recycling Harvesting the unexplored potential of European waste materials for road construction. *"Resources, Conservation & Recycling," 116*, 32–44. https://doi.org/10.1016/j.resconrec.2016.09.008

Pourali, P., Baserisalehi, M., Afsharnezhad, S., Behravan, J., Ganjali, R., Bahador, N., & Arabzadeh, S. (2013). The effect of temperature on antibacterial activity of biosynthesized silver nanoparticles. *BioMetals*, *26*(1), 189–196. https://doi.org/10.1007/s10534-012-9606-y

Pourreza, N., Golmohammadi, H., Naghdi, T., & Yousefi, H. (2015). Green in-situ synthesized silver nanoparticles embedded in bacterial cellulose nanopaper as a bionanocomposite plasmonic sensor. *Biosensors and Bioelectronics*, *74*, 353–359.

Prabhu, S., & Poulose, E. K. (2012). Silver nanoparticles: mechanism of antimicrobial. *Int. Nano Lett.*, *2*, 32–41. http://www.inl-journal.com/content/pdf/2228-5326-2-32.pdf

Puupponen-Pimiä, R., Nohynek, L., & Meier, C. (2001). Antimicrobial properties of phenolic compounds from berries. *Journal of Applied Microbiology*, *90*(4), 494–507. https://doi.org/10.1046/j.1365-2672.2001.01271.x

Qidwai, A., Kumar, R., & Dikshit, A. (2018). Green synthesis of silver nanoparticles by seed of phoenix sylvestris L. and their role in the management of cosmetics embarrassment. *Green Chemistry Letters and Reviews*, *11*(2), 176–188. https://doi.org/10.1080/17518253.2018.1445301

Qing, Y., Cheng, L., Li, R., Liu, G., Zhang, Y., Tang, X., Wang, J., Liu, H., & Qin, Y. (2018). Potential antibacterial mechanism of silver nanoparticles and the optimization of orthopedic implants by advanced modification technologies. *International Journal of Nanomedicine*, *13*, 3311–3327. https://doi.org/10.2147/IJN.S165125

Quiroz, J. Q., Duran, A. M. N., Garcia, M. S., Gomez, G. L. C., & Camargo, J. J. R. (2019). Ultrasound-assisted extraction of bioactive compounds from annatto seeds, evaluation of their antimicrobial and antioxidant activity, and identification of main compounds by LC/ESI-MS analysis. *International Journal of Food Science*, *2019*, 5–7. https://doi.org/10.1155/2019/3721828

Qutaba, S., Malik, A., & Abbasi, R. (2017). Preparation of Anti-Microbial Finishes by Eco-Friendly Method from Peel of Citrus Fruit (Lemon) and Analyse Antimicrobial Activity. *ICTT-2017, November 2017*.

Raja, P. M. V, & Barron, A. R. (2022). Zeta potential analysis. In *Physical methods in chemistry and nano science* (p. 55842). LibreTexts. https://doi.org/10.1002/jctb.5000533702

Rajendran, R., Balakumar, C., Kalaivani, J., & Sivakumar, R. (2011). Dyeability and antimicrobial properties of cotton fabrics finished with Punica granatum extracts. *Journal of Textile and Apparel, Technology and Management*, *7*(2), 1–12.

Rao, B., & Tang, R. C. (2017). Green synthesis of silver nanoparticles with antibacterial activities using aqueous Eriobotrya japonica leaf extract. *Advances in Natural Sciences: Nanoscience and Nanotechnology*, *8*(1). https://doi.org/10.1088/2043-6254/aa5983

Rautela, A., Rani, J., & Debnath (Das), M. (2019). Green synthesis of silver nanoparticles from Tectona grandis seeds extract: characterization and mechanism of antimicrobial action on different microorganisms. *Journal of Analytical Science and Technology*, *10*(5), 1–10. https://doi.org/10.1186/s40543-018-0163-z

Raygada, J. L., & Levine, D. P. (2009). Methicillin-Resistant Staphylococcus aureus: A Growing Risk in the Hospital and in the Community. *American Health and Drug Benefits*, *2*(2), 86–95.

Raza, M. A., Kanwal, Z., Rauf, A., Sabri, A. N., Riaz, S., & Naseem, S. (2016). Size- and shape-dependent antibacterial studies of silver nanoparticles synthesized by wet chemical routes. *Nanomaterials*, *6*(4). https://doi.org/10.3390/nano6040074

Reddivari, L., Hale, A. L., & Miller, J. C. (2007). Genotype, location, and year influence antioxidant activity, carotenoid content, phenolic content, and composition in specialty potatoes. *Journal of Agricultural and Food Chemistry*, *55*(20), 8073–8079. https://doi.org/10.1021/jf071543w

Redfern, J., Kinninmonth, M., Burdass, D., & Verran, J. (2014). Using Soxhlet Ethanol Extraction to Produce and Test Plant Material (Essential Oils) for Their Antimicrobial Properties. *Journal of Microbiology & Biology Education*, *15*(1), 45–46.

Reed, R. B., Zaikova, T., Barber, A., Simonich, M., Lankone, R., Marco, M., Hristovski, K., Herckes, P., Passantino, L., Fairbrother, D. H., Tanguay, R., Ranville, J. F., Hutchison, J. E., & Westerhoff, P. K. (2016). Potential Environmental Impacts and Antimicrobial Efficacy of Silver- and Nanosilver-Containing Textiles Potential Environmental Impacts and Antimicrobial Efficacy of Silver- and Nanosilver- Containing Textiles School of Sustainable Engineering and the B. *Environmental Science and Technology*, 1–24. https://doi.org/10.1021/acs.est.5b06043

Restrepo, C. V., & Villa, C. C. (2021). Synthesis of silver nanoparticles, influence of capping agents, and dependence on size and shape. *Environmental Nanotechnology, Monitoring and Management*, *15*(December 2020), 100428. https://doi.org/10.1016/j.enmm.2021.100428

Reyes, L. F., Miller, J. C., & Cisneros-Zevallos, L. (2004). Environmental Conditions Influence the Content and Yield of Anthocyanins and Total Phenolics in Purple- and Red-flesh Potatoes during Tuber Development. *American Journal of Potato Research*, *81*(February), 187–193.

Ribeiro, A. I., Shvalya, V., Cvelbar, U., Silva, R., Marques-Oliveira, R., Remião, F., Felgueiras, H. P., Padrão, J., & Zille, A. (2022). Stabilization of Silver Nanoparticles on Polyester Fabric Using Organo-Matrices for Controlled Antimicrobial Performance. *Polymers*, *14*(6). https://doi.org/10.3390/polym14061138

Riciputi, Y., Diaz-de-Cerio, E., Akyol, H., Capanoglu, E., Cerretani, L., Caboni, M. F., & Verardo, V. (2018). Establishment of ultrasound-assisted extraction of phenolic compounds from industrial potato by-products using response surface methodology. *Food Chemistry*, *269*(July), 258–263. https://doi.org/10.1016/j.foodchem.2018.06.154

Ristic, T., Zemljic, L. F., Novak, M., Kuncic, M. K., Sonjak, S., Cimerman, N. G., & Strnad, S. (2011). Antimicrobial efficiency of functionalized cellulose fibres as potential medical textiles. In A. Mendez-Vilas (Ed.), *Science against microbial pathogens: communicating current research and technological advances* (pp. 36–51).

Rocha, M. F. G., Sales, J. A., da Rocha, M. G., Galdino, L. M., de Aguiar, L., Pereira-Neto, W. de A., de Aguiar Cordeiro, R., Castelo-Branco, D. de S. C. M., Sidrim, J. J. C., & Brilhante, R. S. N. (2019). Antifungal effects of the flavonoids kaempferol and quercetin: a possible alternative for the control of fungal biofilms. *Biofouling*, *35*(3), 320–328. https://doi.org/10.1080/08927014.2019.1604948

Rodríguez-Martínez, B., Gullón, B., & Yáñez, R. (2021). Identification and recovery of valuable bioactive compounds from potato peels: A comprehensive review. *Antioxidants*, *10*(10), 1–18. https://doi.org/10.3390/antiox10101630

Sadeghi-Kiakhani, M., Tehrani-Bagha, A. R., Miri, F. S., Hashemi, E., & Safi, M. (2022). Eco-Friendly Procedure for Rendering the Antibacterial and Antioxidant of Cotton Fabrics via Phyto-Synthesized AgNPs With Malva sylvestris (MS) Natural Colorant. *Frontiers in Bioengineering and Biotechnology*, *9*(January), 1–12. https://doi.org/10.3389/fbioe.2021.814374

Salama, A., Abouzeid, R. E., Owda, M. E., Cruz-Maya, I., & Guarino, V. (2021). Cellulose–silver composites materials: Preparation and applications. *Biomolecules*, *11*(11), 1–29. https://doi.org/10.3390/biom11111684

Salawu, S. O., Udi, E., Akindahunsi, A. A., Boligon, A. A., & Athayde, M. L. (2015). Antioxidant potential, phenolic profile and nutrient composition of flesh and peels from Nigerian white and purple skinned sweet potato (Ipomea batatas L.). *Asian Journal of Plant Science and Research*, *5*(5), 14–23.

Samaniego, I., Espin, S., Cuesta, X., Arias, V., Rubio, A., Llerena, W., Angos, I., & Carrillo, W. (2020). Analysis of Environmental Conditions Effect in the Phytochemical Composition of Potato (Solanum tuberosum) Cultivars. *Plants*, *9*(815), 1–13. https://doi.org/10.3390/plants9070815

Samarin, A. M., Poorazarang, H., Hematyar, N., & Elhamirad, A. (2012). Phenolics in potato peels: Extraction and utilization as natural antioxidants. *World Applied Sciences Journal*, *18*(2), 191–195. https://doi.org/10.5829/idosi.wasj.2012.18.02.1057

Samimi, S., Maghsoudnia, N., Eftekhari, R. B., & Dorkoosh, F. (2018). Lipid-Based Nanoparticles for Drug Delivery Systems. In *Characterization and Biology of Nanomaterials for Drug Delivery: Nanoscience and Nanotechnology in Drug Delivery*. Elsevier Inc. https://doi.org/10.1016/B978-0-12-814031-4.00003-9

Samotyja, U. (2019). Potato Peel as a Sustainable Resource of Natural Antioxidants for the Food Industry. *Potato Research*, *62*(4), 435–451. https://doi.org/10.1007/s11540-019-9419-2

Sampaio, S. L., Petropoulos, S. A., Dias, M. I., Pereira, C., Calhelha, R. C., Fernandes, Â., Leme, C. M. M., Alexopoulos, A., Santos-Buelga, C., Ferreira, I. C. F. R., & Barros, L. (2021). Phenolic composition and cell-based biological activities of ten coloured potato peels (Solanum tuberosum L.). *Food Chemistry*, *363*(June). https://doi.org/10.1016/j.foodchem.2021.130360

Sana, S. S., & Dogiparthi, L. K. (2018). Green synthesis of silver nanoparticles using Givotia moluccana leaf extract and evaluation of their antimicrobial activity. *Materials Letters*, *226*, 47–51. https://doi.org/10.1016/j.matlet.2018.05.009

Santmartí, A., & Lee, K.-Y. (2018). Crystallinity and Thermal Stability of Nanocellulose. *Nanocellulose and Sustainability*, *January*, 67–86. https://doi.org/10.1201/9781351262927-5

Saravanakumar, A., Peng, M. M., Ganesh, M., Jayaprakash, J., Mohankumar, M., & Jang, H. T. (2017). Low-cost and eco-friendly green synthesis of silver nanoparticles using Prunus japonica (Rosaceae) leaf extract and their antibacterial, antioxidant properties. *Artificial Cells, Nanomedicine and Biotechnology*, *45*(6), 1165–1171. https://doi.org/10.1080/21691401.2016.1203795

Scimeca, M., Bischetti, S., Lamsira, H. K., Bonfiglio, R., & Bonanno, E. (2018). Energy dispersive X-ray (EDX) microanalysis: A powerful tool in biomedical research and diagnosis. *European Journal of Histochemistry*, *62*(1), 89–99. https://doi.org/10.4081/ejh.2018.2841

Seifipour, R., Nozari, M., & Pishkar, L. (2020). Green Synthesis of Silver Nanoparticles using Tragopogon Collinus Leaf Extract and Study of Their Antibacterial Effects. *Journal of Inorganic and Organometallic Polymers and Materials*, *30*(8), 2926–2936. https://doi.org/10.1007/s10904-020-01441-9

Senthilkumar, R. P., Bhuvaneshwari, V., Malayaman, V., Ranjithkumar, R., & Sathiyavimal, S. (2018). Phytochemical Screening of Aqueous Leaf Extract of Sida acuta Burm. F. and its Antibacterial Activity. *Journal of Emerging Technologies and Innovative Research (JETIR)*, *5*(8), 474–478. www.jetir.org

Shafey, A. M. El. (2020). Green synthesis of metal and metal oxide nanoparticles from plant leaf extracts and their applications: A review. *Green Processing and Synthesis*, *9*(1), 304–339. https://doi.org/10.1515/gps-2020-0031

Shaheen, T. I., & Abd El Aty, A. A. (2018). In-situ green myco-synthesis of silver nanoparticles onto cotton fabrics for broad spectrum antimicrobial activity. *International Journal of Biological Macromolecules*, *118*, 2121–2130. https://doi.org/10.1016/j.ijbiomac.2018.07.062

Shaikh, J. R., & Patil, M. (2020). Qualitative tests for preliminary phytochemical screening: An overview. *International Journal of Chemical Studies*, *8*(2), 603–608. https://doi.org/10.22271/chemi.2020.v8.i2i.8834

Sharma, K., Guleria, S., & Razdan, V. K. (2020). Green synthesis of silver nanoparticles using Ocimum gratissimum leaf extract: characterization, antimicrobial activity and toxicity analysis. *Journal of Plant Biochemistry and Biotechnology*, *29*(2), 213–224. https://doi.org/10.1007/s13562-019-00522-2

Shateri-Khalilabad, M., Yazdanshenas, M. E., & Etemadifar, A. (2017). Fabricating multifunctional silver nanoparticles-coated cotton fabric. *Arabian Journal of Chemistry*, *10*, S2355–S2362. https://doi.org/10.1016/j.arabjc.2013.08.013

Silhavy, T. J., Kahne, D., & Walker, S. (2010). The Bacterial Cell Envelope1 T. J. Silhavy, D. Kahne and S. Walker, . *Cold Spring Harb Perspect Biol*, *2*, 1–16. https://www.ncbi.nlm.nih.gov/pmc/articles/PMC2857177/pdf/cshperspect-PRK-a000414.pdf

Silva-Beltrán, N. P., Chaidez-Quiroz, C., López-Cuevas, O., Ruiz-Cruz, S., López-Mata, M. A., Del-Toro-sánchez, C. L., Marquez-Rios, E., & Ornelas-Paz, J. D. J. (2017). Phenolic compounds of potato peel extracts: Their antioxidant activity and protection against human enteric viruses. *Journal of Microbiology and Biotechnology*, *27*(2), 234–241. https://doi.org/10.4014/jmb.1606.06007

Simoncic, B., & Klemencic, D. (2015). Preparation and performance of silver as an antimicrobial agent for textiles : A review. *Textile Research Journal*, 1–14. https://doi.org/10.1177/0040517515586157

Singh, A., Sabally, K., Kubow, S., Donnelly, D. J., Gariepy, Y., Orsat, V., & Raghavan, G. S. V. (2011). Microwave-assisted extraction of phenolic antioxidants from potato peels. *Molecules*, *16*(3), 2218–2232. https://doi.org/10.3390/molecules16032218

Sithara, R., Selvakumar, P., Arun, C., Anandan, S., & Sivashanmugam, P. (2017). Economical synthesis of silver nanoparticles using leaf extract of Acalypha hispida and its application in the detection of Mn(II) ions. *Journal of Advanced Research*, *8*(6), 561–568. https://doi.org/10.1016/j.jare.2017.07.001

Skiba, M. I., & Vorobyova, V. I. (2019). Synthesis of Silver Nanoparticles Using Orange Peel Extract Prepared by Plasmochemical Extraction Method and Degradation of Methylene Blue under Solar Irradiation. *Advances in Materials Science and Engineering*, *2019*. https://doi.org/10.1155/2019/8306015

Sophie, S. (2018). *Potato variety adoption and dis-adoption in Kenya* (Issue August).

Sotillo, D. R. D. E., & Hadley, M. (1998). Potato Peel Extract a Nonmutagenic Antioxidant with Potential Antimicrobial Activity. *Journal of Food Science*, *63*(5), 1–4.

Subramanian, K. ., Janavi, G. ., Marimuthu, S., Kannan, M., Raja, K., Haripriya, S., Jeya Sundara Sharmila, D., & Sathya Moorthy, P. (2013). Transmission Electron Microscope – Principle, Components and Applications. *A Textbook on Fundamentals and Applications of Nanotechnology*, *53*(9), 93–102.

Sulastri, E., Zubair, M. S., Anas, N. I., Abidin, S., Hardani, R., Yulianti, R., & Aliyah. (2018). Total phenolic, total flavonoid, quercetin content and antioxidant activity of standardized extract of moringa oleifera leaf from regions with different elevation. *Pharmacognosy Journal*, *10*(6), S104–S108. https://doi.org/10.5530/pj.2018.6s.20

Sun, Q., Cai, X., Li, J., Zheng, M., Chen, Z., & Yu, C. P. (2014). Green synthesis of silver nanoparticles using tea leaf extract and evaluation of their stability and antibacterial activity. *Colloids and Surfaces A: Physicochemical and Engineering Aspects*, *444*(March), 226–231. https://doi.org/10.1016/j.colsurfa.2013.12.065

Suriyatem, R., Auras, R. A., & Rachtanapun, P. (2019). Utilization of Carboxymethyl Cellulose from Durian Rind Agricultural Waste to Improve Physical Properties and Stability of Rice Starch-Based Film. *Journal of Polymers and the Environment*, *27*(2), 286–298. https://doi.org/10.1007/s10924-018-1343-z

Susarla, N. (2019). Benefits of Potato Peels. *ACTA Scientific Nutritional Health*, *3*(9), 147–153. https://doi.org/10.31080/ASNH.2019.03.0418

Swidan, N. S., Hashem, Y. A., Elkhatib, W. F., & Yassien, M. A. (2022). Antibiofilm activity of green synthesized silver nanoparticles against biofilm associated enterococcal urinary pathogens. *Scientific Reports*, *12*(1), 1–13. https://doi.org/10.1038/s41598-022-07831-y

Syafiuddin, A., Fulazzaky, M. A., Salmiati, S., & Roestamy, M. (2020). Sticky silver nanoparticles and surface coatings of different textile fabrics stabilised by Muntingia calabura leaf extract. *SN Applied Sciences*, *2*(4), 1–10. https://doi.org/10.1007/s42452-020-2534-5

Tan, J., Qiu, G., & Ting, Y. (2014). Osmotic membrane bioreactor (OMBR) for municipal wastewater treatment and the effects of silver nanoparticles on system performance. *Journal of Cleaner Production*, 1–6. https://doi.org/10.1016/j.jclepro.2014.03.037

Tania, I. S., Ali, M., & Arafat, M. T. (2021). Processing techniques of antimicrobial textiles. In *Antimicrobial Textiles from Natural Resources* (pp. 189–215). The Textile Institute Book Series. https://doi.org/10.1016/B978-0-12-821485-5.00002-0

Tania, I. S., Ali, M., & Azam, M. S. (2019). In-situ synthesis and characterization of silver nanoparticle decorated cotton knitted fabric for antibacterial activity and improved dyeing performance. *SN Applied Sciences*, *1*(1), 1–9. https://doi.org/10.1007/s42452-018-0068-x

Tania, I. S., Ali, M., & Bhuiyan, R. H. (2020). Experimental Study on Dyeing Performance and Antibacterial Activity of Silver Nanoparticle-Immobilized Cotton Woven Fabric. *Autex Research Journal*, *21*(1), 1–7. https://doi.org/10.2478/aut-2019-0074

Torres, M. D., & Domínguez, H. (2020). Valorisation of potato wastes. *International Journal of Food Science and Technology*, *55*(6), 2296–2304. https://doi.org/10.1111/ijfs.14228

Traiwatcharanon, P., Timsorn, K., & Wongchoosuk, C. (2015). Effect of pH on the Green Synthesis of Silver Nanoparticles through Reduction with *Pistiastratiotes L.* Extract. *Advanced Materials Research*, *1131*, 223–226. https://doi.org/10.4028/www.scientific.net/amr.1131.223

Trusheva, B., Trunkova, D., & Bankova, V. (2007). Different extraction methods of biologically active components from propolis; a preliminary study. *Chemistry Central Journal*, *1*(1), 1–4. https://doi.org/10.1186/1752-153X-1-13

Tyavambiza, C., Elbagory, A. M., Madiehe, A. M., Meyer, M., & Meyer, S. (2021). The antimicrobial and anti-inflammatory effects of silver nanoparticles synthesised from cotyledon orbiculata aqueous extract. *Nanomaterials*, *11*(5). https://doi.org/10.3390/nano11051343

Uddin, F. (2014). Environmental Concerns in Antimicrobial Finishing of Textiles. *International Journal of Textile Science*, *3*(1A), 15–20. https://doi.org/10.5923/s.textile.201401.03

V. K. Ahluwalia et al. (2004). Basic principles of green chemistry. In: new trends in green chemistry. *Green Chemistry and Technologies*, 6–14.

Vaitkevičienė, N. (2019). A comparative study on proximate and mineral composition of coloured potato peel and flesh. *Journal of the Science of Food and Agriculture*, *99*(14), 6227–6233. https://doi.org/10.1002/jsfa.9895

Varberg, T. D., & Skakuj, K. (2015). X-ray Diffraction of Intermetallic Compounds: A Physical Chemistry Laboratory Experiment. *Journal of Chemical Education*, *92*(6), 1095–1097. https://doi.org/10.1021/ed500804b

Velgosová, O., Mražíková, A., & Marcinčáková, R. (2016). Influence of pH on green synthesis of Ag nanoparticles. *Materials Letters*, *180*, 336–339. https://doi.org/10.1016/j.matlet.2016.04.045

Verbič, A., Šala, M., & Gorjanc, M. (2018). The influence of in situ synthesis parameters on the formation of ZnO nanoparticles and the UPF value of cotton fabric. *Tekstilec*, *61*(4), 280–288. https://doi.org/10.14502/Tekstilec2018.61.280-288

Verma, A., & Mehata, M. S. (2016). Controllable synthesis of silver nanoparticles using Neem leaves and their antimicrobial activity. *Journal of Radiation Research and Applied Sciences*, *9*(1), 109–115. https://doi.org/10.1016/j.jrras.2015.11.001

Wang, S., Lin, A. H. M., Han, Q., & Xu, Q. (2020). Evaluation of direct ultrasound-assisted extraction of phenolic compounds from potato peels. *Processes*, *8*(12), 1–14. https://doi.org/10.3390/pr8121665

Wisnuwardhani, H. A., Lukmayani, Y., Hazar, S., & Hoeruniswah, H. (2019). Optimization of Silver Nanoparticles Synthesis using Kawista (Limonia Acidissima Groff.) leaves ethanol extract. *Journal of Physics: Conference Series*, *1375*(1). https://doi.org/10.1088/1742-6596/1375/1/012077

Wolela, A. D. (2020). Fashion Technology & Textile Engineering Antibacterial Finishing of Cotton Textiles with Extract of Citrus Fruit Peels. *Fashion Technology and Textile Engineering*, *6*(1), 1–7. https://doi.org/10.19080/CTFTTE.2020.06.555676

Xu, Q. B., Xie, L. J., Diao, H., Li, F., Zhang, Y. Y., Fu, F. Y., & Liu, X. D. (2017). Antibacterial cotton fabric with enhanced durability prepared using silver nanoparticles and carboxymethyl chitosan. *Carbohydrate Polymers*, *177*, 187–193. https://doi.org/10.1016/j.carbpol.2017.08.129

Zhang, Q. W., Lin, L. G., & Ye, W. C. (2018). Techniques for extraction and isolation of natural products: A comprehensive review. *Chinese Medicine (United Kingdom)*, *13*(1), 1–26. https://doi.org/10.1186/s13020-018-0177-x

Zhang, W., Roy, S., Assadpour, E., Cong, X., & Jafari, S. M. (2023). Croos-linked biopolymeric films by citric acid for food packaging and preservation. *Advances in Colloid and Interface Science*, *314*, 102886. https://doi.org/https://doi.org/10.1016/j.cis.2023.102886

Zhang, X. F., Liu, Z. G., Shen, W., & Gurunathan, S. (2016). Silver nanoparticles: Synthesis, characterization, properties, applications, and therapeutic approaches. *International Journal of Molecular Sciences*, *17*(9). https://doi.org/10.3390/ijms17091534

Zhou, C.-E., & Kan, C.-W. (2014). Optimizing rechargeable antimicrobial performance of cotton fabric coated with 5 , 5-dimethylhydantoin (DMH). *Cellulose*, *22*(February), 879–886. https://doi.org/10.1007/s10570-014-0498-6

Zhou, C. E., Kan, C. W., Yuen, C. wah M., Matinlinna, J. P., Tsoi, J. K. hon, & Zhang, Q. (2016). Plasma treatment applied in the pad-dry-cure process for making rechargeable antimicrobial cotton fabric that inhibits S. Aureus. *Textile Research Journal*, *86*(20), 2202–2215. https://doi.org/10.1177/0040517515622147

Zhou, Q., Chen, J., Lu, Z., Tian, Q., & Shao, J. (2022). In Situ Synthesis of Silver Nanoparticles on Flame-Retardant Cotton Textiles Treated with Biological Phytic Acid and Antibacterial Activity. *Materials*, *15*(7). https://doi.org/10.3390/ma15072537

APPENDICES

Appendix A: Parameter Settings for In-Situ Synthesis

Run Number	Synthesis Time (Hours)	Incubation Time (Hours)	Curing Temperature (°C)
1	2	36	130
2	2	36	130
3	1.4	57.4	100.3
4	3	36	130
5	2.6	57.4	100.3
6	2	36	180
7	2	36	130
8	2	36	130
9	2	36	80
10	1.4	14.6	159.7
11	2	36	130
12	1.4	14.6	100.3
13	1.4	57.4	159.7
14	2.6	14.6	100.3
15	2.6	14.6	159.7
16	2	36	130
17	2	0	130
18	1	36	130
19	2.6	57.4	159.7
20	2	72	130

Appendix B: List of Publications

1. Mpofu, N.S., Mwasiagi, I.J., Nganyi, E.O., Kamalha, E. (2021). Antimicrobial and antiviral properties of metal nanoparticles and their potential use in textiles: A review, *Annals of the University of Oradea Fascicle of Textiles, leatherwork*, 22(2), 69-74, ISSN 1843 – 813X.
2. Mpofu, N.S., Mwasiagi, I.J., Mecha, C. A., Nganyi, E. O. (2023). Evaluation of solanum tuberosum potato peel waste for use as an eco-friendly antibacterial finish for cotton fabrics. *Research Journal of Textile and Apparel*. DOI: https://doi.org/10.1108/RJTA-05-2023-0052, ISSN 1560-6074

Appendix C: Plagiarism Similarity Index

SR309

ISO 9001:2019 Certified Institution

EDU 999 THESIS WRITING COURSE

PLAGIARISM AWARENESS CERTIFICATE

This certificate is awarded to

NONSIKELELO SHERON MPOFU

ENG/DPHIL/MT/3973/20

In recognition for passing the University's plagiarism

Awareness test for Thesis: **CHARACTERISATION AND EFFICACY TESTING OF MULTIFUNCTIONAL COTTON FABRICS BASED ON NANOPARTICLES GREEN SYNTHESIZED WITH SOLANUM TUBEROSUM POTATO PEELS** With a similarity index of 3% and striving to maintain academic integrity.

Awarded by:

Prof. Anne Syomwene Kisilu
CERM-ESA Project Leader Date: 2/10/2023

similarity index

By NONSIKELELO SHERON MPOFU NONSIKELELO SHERON MPOFU

WORD COUNT	54701	TIME SUBMITTED	02-OCT-2023 06:24PM
		PAPER ID	103172297

similarity index

ORIGINALITY REPORT

3%
SIMILARITY INDEX

PRIMARY SOURCES

1	www.science.gov Internet	350 words — 1%
2	etd.cput.ac.za Internet	237 words — 1%
3	ir.mu.ac.ke:8080 Internet	226 words — 1%
4	"Handbook of Renewable Materials for Coloration and Finishing", Wiley, 2018 Crossref	223 words — 1%
5	Shahid ul Islam, Gang Sun. "Biological Chemicals as Sustainable Materials to Synthesize Metal and Metal Oxide Nanoparticles for Textile Surface Functionalization", ACS Sustainable Chemistry & Engineering, 2022 Crossref	218 words — 1%
6	cris.brighton.ac.uk Internet	218 words — 1%

EXCLUDE QUOTES	ON	EXCLUDE SOURCES	< 1%
EXCLUDE BIBLIOGRAPHY	ON	EXCLUDE MATCHES	OFF